University of Cape Town

Fine-grinding Characterisation of PGM Ore Using HIGmill

Audrey Mabiza

A dissertation submitted to the Faculty of Engineering and the Built Environment, University of Cape Town, in fulfilment of the requirements for the degree of Master of Science in Chemical Engineering

2022

PLAGIARISM DECLARATION

I know the meaning of plagiarism and declare that all the work in the document, save for that which is properly acknowledged, is my own. This thesis/dissertation has been submitted to the Turnitin module (or equivalent similarity and originality checking software) and I confirm that my supervisor has seen my report and any concerns revealed by such have been resolved with my supervisor.

Signed by candidate

Audrey Mabiza

10 February 2022

ACKNOWLEDGEMENTS

First and foremost, I would like to give thanks to God for blessing me with this opportunity.

I would like to thank my supervisors Professor Aubrey Mainza and Dr Paul Bepswa for guiding me through this journey. I thank them for the wisdom they have imparted and the patience that they have shown me as we navigated this journey amidst a pandemic.

I am grateful for the Mandela Rhodes Foundation (MRF), who not only identified me as a young African leader but also sponsored my studies. When my studies were affected by the COVID-19 pandemic the MRF stepped in and for that I express my sincere gratitude.

Thank you to the management and staff of the Centre of Minerals Research laboratories: Shireen Govender for always ensuring I had everything I need to run my experiments, Kenneth Maseko for always helping me to troubleshoot the milling equipment and Monde Bekaphi who helped me with sample preparation and understanding the relevant procedures. A special thank you to a dear friend, Mathew Dzingai, who helped me throughout the experimental runs especially with the heavy lifting that the experiments required. I would also like to thank the team at the UCT Analytical lab who accommodated me and helped me when I was analysing samples with the Malvern Mastersizer. To Brian Chaponda and his team at Sibanye Stillwater, thank you for timeously assaying my flotation samples.

To my friends, thank you for being there and offering me pearls of wisdom when needed

To my parents: Louis and Virginia Mabiza, Justin and Priscilla Nyakunuhwa thank you for your unconditional support. To my siblings: Kuda, Rufaro, Taku, Noreen, Tererai and Natalie thank you for always cheering me on.

To my husband and friend Simbarashe Hebert Nyakunuhwa, thank you for always inspiring me and encouraging me to be my best. Thank you for your unconditional love and motivation. Thank you for planting the seed that started this journey.

Glory be to God for seeing me through this journey.

ABSTRACT

Historically, mineral processing industries use conventional tumbling mills to carry out milling operations However, the ore bodies that are currently being explored and mined are low-grade complex ores. These ore bodies often require fine grinding to liberate their valuable fine-grained minerals. Conventional mills have proven to be energy inefficient when they are used for fine grinding. Energy efficient technologies, such as stirred mills, are therefore being introduced to the minerals market for use in fine-grinding applications. The HIGmill is an example of a stirred mill that is used for fine grinding mineral ores.

This thesis reports the results obtained from the investigating of the influence of operating parameters on the HIGmill product size and specific energy when grinding UG2 platinum ore. The milling experiments were conducted using the HIG 5, which is a laboratory scale HIGmill. The operating variables tested were mill tip speed, solids concentration and grinding media size. Tip speeds tested in this study were between 300 rpm and 1050 rpm. The solids concentration tested was between 40% and 60%. Grinding media sizes used were 2 mm, 3.5 mm and 5 mm.

Using these parameters, a three-factorial design was used for the experiments. From the milling results, particle size distributions, stress intensity, specific energy and size specific energy were analysed for each variable tested. Signature plots were also produced for the milling results. Flotation tests were then carried out on the HIG 5 products to assess the downstream response of the HIGmill.

The milling results showed that the optimal tip speed was 600 rpm. The optimal solids concentration for the UG2 ore was 60%. For the feed top size of −1000 µm, using 5 mm grinding media was found to be energy intensive and it is recommended that 2 mm and 3.5 mm grinding media are considered when for the grinding the UG2 ore.

The flotation results highlighted that grinding finer increases the recovery potential of the ore from 73.2% to an average of 81%. It was also noted that grinding finer increases the chromite recoveries. Flotation kinetic models showed that there is no significant difference in the flotation kinetics of the HIGmill products.

TABLE OF CONTENTS

LIST OF FIGURES

LIST OF TABLES

LIST OF ABBREVIATIONS

PGM:	Platinum group metal
HIG:	High intensity grinding
UG2:	Upper ground 2
µm	Micrometres
rpm:	Revolutions per minute
PSD:	Particle size distribution
F80:	Size at which 80% of the feed material passes
P80:	Size at which 80% of the product material passes

1. INTRODUCTION

The intention of this thesis is to evaluate the response of platinum ore from South Africa's Upper Ground 2 (UG2 ore) reef to fine grinding using a high intensity grinding mill (HIGmill). The HIGmill is a vertical stirred fine-grinding technology adopted for the mining industry. UG2 platinum ore requires two or more milling stages to recover its valuable minerals using flotation downstream. For this thesis, the milled material was processed using froth flotation to assess the degree of grinding in the recovery. Froth flotation was chosen because it is the recovery method applied for the UG2 platinum ore at almost all plants processing this ore type.

This first chapter provides the background and the motivation for the work performed in the thesis. The problem statement, research objectives and the research limitations are presented as part of the introduction.

1.2 Background

The process of *comminution* is a primary step in mineral processing, where the ore is ground into finer particles. Comminution can be divided into three stages: blasting, crushing and grinding (Jankovic et al., 2006 ; Jeswiet & Szekeres, 2016). The main aims of these stages are to process the ore for handling in subsequent units and to liberate the valuable minerals for downstream processes, such as flotation and leaching, where the valuable minerals are separated out.

Comminution is energy intensive, and approximately 30% of concentrator energy is used in comminution processes (Ntsele & Allen, 2012). The characteristics of the ore, such as its mineral structure, mineral composition and ore hardness, are important in determining the energy consumed during comminution. Depletion of high grade and easy-to-process ores has led mining companies to start processing complex low-grade ores. Complex ores are generally difficult to process, and some contain fine-grained minerals that require finer grinding to reach the required degree of liberation (Jankovic et al., 2001). Efficient processing of complex and fine-grained minerals has become a major focus point for the mineral processing industry. The ores containing fine-grained minerals are usually classified among competent ores in terms of resistance to grinding, although some fine-grained ore types do not exhibit competent ore breakage characteristics.

The UG2 ore considered in this research is a fine-grained ore type but not competent in terms of breakage characterisation and therefore requires more energy when using conventional

grinding equipment (Cramer, 2001). Cramer (2001) stated that UG2 ore is fine-grained and requires fine grinding for “full liberation” to take place. UG2 ore has the unique breakage characteristic that the coarse rock breaks easily, but it is difficult to grind the sub 600 µm particles down to sub 150 µm.

Conventionally, tumbling mills such as semi-autogenous (SAG) mills and ball mills have been used for both coarse and fine grinding (80% passing the 75 µm sieve). However, the requirement to grind ore into finer particles so that more than the conventional 80% passes the 75 µm sieve has exposed the limitations of conventional circuits in producing a finer grind at reasonable energy utilisation levels. The application of tumbling mills to achieve such fine grinds has proven to be both energy intensive and energy inefficient. The mineral processing industry is therefore installing more energy-efficient technologies for fine grinding, and stirred mills are among the fine-grinding technologies that are being incorporated in comminution circuits (Hasan et al., 2016).

A *stirred mill* is a mill with a stationary grinding chamber fitted with an agitator (Lichter & Davey, 2006). Grinding media such as steel beads and ceramic beads are used in the mill to provide the forces and contact to break the ore particles. Stirred mills are widely used in the pharmaceutical and paint industries, and were introduced to the mineral processing industry in the late 1980s (Rule, 2010; Radziszewski & Moore, 2017). Currently, there are many stirred mills in the marketplace but the HIGmill is one of the new milling technologies being introduced (Lehto & Paz, 2013).

The HIGmill is a high-speed, vertical stirred mill that uses vane grinding discs and static shell stator rings to cause the media grinding motion (Erb et al., 2015). The vertical design of the mill allows gravity to ensure that there is constant contact between the grinding media and the ore particles (Roitto et al., 2013). The internal design of the HIGmill allows it to have up to 30 grinding chambers (Åstholm, 2015). The key operating variables of the HIGmill are throughput, grinding time, solids concentration, mill tip speed, media size, media material and media filling. It is important to understand the combination of parameters that is optimal for downstream efficiencies. The study evaluated the key operating parameters that affected stirred mill performance to determine the best combination to yield a fine grind that does not negatively impact downstream efficiencies.

With proven increased milling efficiencies, it is also valuable to investigate the response of the finely milled product to downstream processes. Recovery of platinum group elements in the UG2 ore is achieved by flotation, which is followed by the concentrates’ being treated with

pyrometallurgy processes (Ekmekçi et al., 2003). The standard reagent suite used to float the UG2 ore includes a depressant, a collector and a frother. Flotation of the UG2 ore can be problematic because of the chromite that reports to the flotation concentrate, as chromite affects the efficiency of the smelting process (Wesseldijk et al., 1999). In the study, the milled product was further processed using flotation, and the results were analysed to determine the milling conditions that give the best flotation results.

1.3 Problem Statement

The complex and fine-grained nature of current ore bodies means that the ore requires fine grinding to achieve sufficient mineral liberation. Obtaining a fine product with conventional milling technologies such as tumbling mills has proven to be energy intensive. The minerals processing industry needs new energy efficient technologies that are capable of fine-grinding complex ores.

1.4 Objectives

This thesis aimed to investigate the influence of milling operating parameters such as mill tip speed, solids concentration and grinding media size on the performance of the HIGmill (energy efficiency and grind PSD).

The objectives of the thesis were:

1. To investigate the influence of milling tip speed on product size and energy consumption
2. To investigate the influence of solids concentration on product size and energy consumption
3. To investigate the influence of grinding media size on product size and energy consumption
4. To determine the optimal fine grinding conditions for the UG2 ore
5. To determine the influence of fine grinding on flotation efficiencies.

1.5 Sustainable Development Goals

Figure 1-1: Sustainable development goals

This project aimed to directly address the following sustainable development goals:

- Sustainable development goal #9: Industry innovation and infrastructure

  The HIGmill is a novel vertical stirred mill with rotating grinding discs, and it has the potential to produce better efficiencies for the mining industry.

- Sustainable development goal #12. Ensuring sustainable consumption and production patterns

  The study demonstrates that using the HIGmill for fine-grinding purposes is more energy efficient than the current methods.

1.6 Limitations of Research

The research was limited to the use of a UG2 ore. The research was also limited to evaluating the performance of the HIGmill in terms of the grinding and flotation response of a UG2 ore. The HIGmill tests were performed under batch conditions and no continuous or classification effects were considered. The flotation tests were conducted using standard UG2 ore reagent doses and no reagent suite optimization was considered.

1.7 Thesis Structure

This thesis comprises five chapters, which are followed by a list of references and the appendices. This section provides an overview of each chapter in the thesis.

1.7.1 Chapter 1: Introduction

Chapter 1 provides the background for the work carried out in the research. The chapter then discusses the problem statement, research objectives and limitations of the work carried out.

1.7.2 Chapter 2: Literature Review

Chapter 2 reviews the relevant literature for the research work. The literature review highlights the stirred mills that are on the market and details similar studies conducted on various ores. The literature also takes a look at the flotation principles and reviews the flotation of UG2 ores. A hypothesis and relevant questions are then formulated based on the synthesised literature.

1.7.3 Chapter 3: Experimental Methods

Chapter 3 discusses the materials and methods that were used to test the hypothesis. The chapter details the equipment used and the procedures followed during the milling and the flotation experiments.

1.7.4 Chapter 4: Results and Discussion

Chapter 4 provides the results from the study and discusses the results. The results are interpreted and compared with previously published work.

1.7.5 Chapter 5: Conclusion and Recommendations

Chapter 5 concludes the work done in the study and describes the outcomes of the tested hypotheses. The key questions presented in earlier chapters are answered in this section. Chapter 5 also contains recommendations resulting from the research and it highlights areas that can be investigated in future studies.

2. LITERATURE REVIEW

This chapter critically reviews the literature that is relevant to the study, including previous studies conducted on similar equipment. The principles of comminution and the fundamentals of particle breakage are examined. The concept of fine grinding is introduced, with the stirred milling equipment that is relevant to fine grinding. The HIGmill is discussed, with the history of the equipment, and the operating parameters are reviewed. The flotation process is appraised in reference to the standard platinum group metals (PGMs) flotation process. The findings from the literature review are synthesised into a hypothesis for the study, and key questions are formulated.

2.1 Principles of Comminution

Many of the existing minerals are locked in gangue material and need to be unlocked through comminution processes (Wills, 1997).

2.1.1 Comminution

In the mineral processing industry, comminution is a process that aims to liberate valuable minerals so that the minerals can be separated from the gangue in downstream processes (Jankovic, Valery & La Rosa, 2001). Comminution starts at the mine with the *blasting* of ore (Jankovic et al., 2006). After the blasting process, the ore is further fragmented through crushing and grinding processes, where *crushing* uses compressive forces to break the rocks, and *grinding* further reduces the particle size so the mineral surfaces can be exposed for downstream processes (Jeswiet & Szekeres, 2016). The comminution in the scope of this thesis focuses on grinding and excludes blasting and crushing.

The main function of the comminution process is particle size reduction that results in the liberation of the valuable minerals from the gangue (Wills, 1997). For size reduction to take place, the structure of the minerals must be understood. Comminution theory assumes that material is brittle; however, some crystals exhibit elastic behaviour (Napier-Munn & Wills, 2006). There are three main types of elastic behaviour: linear-elastic, elastic-plastic and visco-elastic, and the correct amount of stress should be applied to the material to reach its elastic limit, resulting in breakage (Peukert, 2004). Other material properties that need to be considered for optimal breakage mechanisms to be applied include density, yield strength, hardness and fracture roughness (Peukert, 2004).

Apart from the material type, the grinding equipment must be considered. There are many types of equipment that are designed for size reduction. These include crushers, tumbling mills, vibratory mills and stirred mills (Lichter & Davey, 2006). Aspects of the equipment that need to be considered include equipment type, equipment size and equipment speed, as these parameters directly determine the stress intensity in the mill (Peukert, 2004). Comminution can thus be thought of as a process function that depends on equipment (the mill) and material, as illustrated in Figure 2-1.

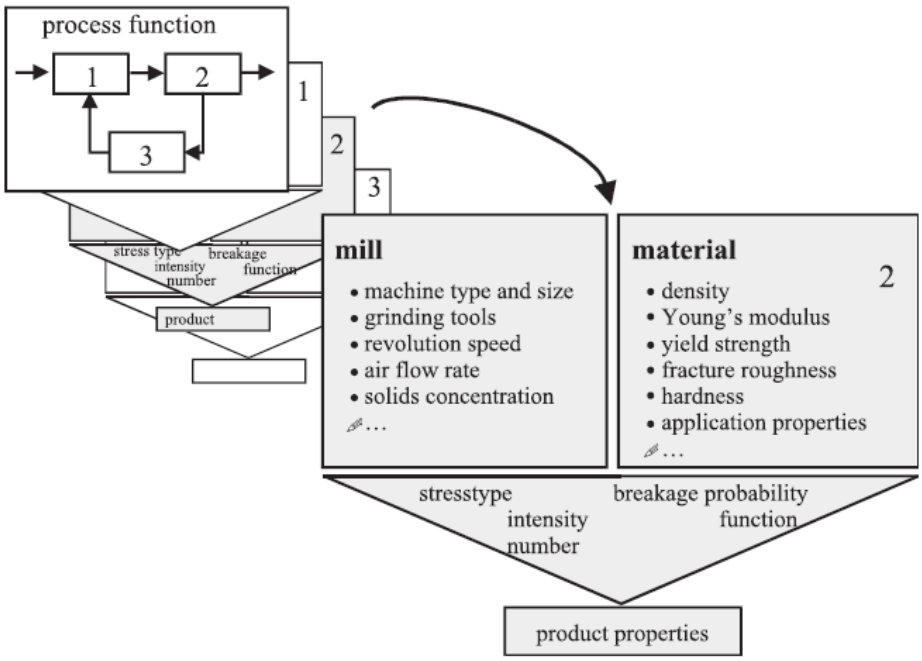

Figure 2-1: Comminution represented as a process function (Peukert, 2004)

2.1.2 Particle breakage

Particle breakage occurs as a result of stress applied to a particle, and it occurs through different mechanisms (Hogg & Cho, 2000). Particle breakage mechanisms can be differentiated in terms of the effect of the particle or of the forces that result in particle breakage (Pitchumani et al., 2004). Pitchumani et al. (2004) categorised the particle breakage mechanisms into three groups: body mechanisms, surface mechanisms and other mechanisms. However, Hasan et al. (2017) recently stated that the three main particle breakage mechanisms are fracture, cleavage and abrasion.

Cleavage occurs because of the slow application of intense stress (compression), producing fragments smaller than the parent particle (Hasan et al., 2017).

Fracture breakage is also known as *impact breakage* or shatter, and it involves the propagation of cracks in the parent particle that result in smaller particle fragments (Gao & Forssberg, 1995; Pitchumani et al., 2004; Hasan et al., 2017). Fracture results in a wide range of particle sizes, and fracture breakage can be the result of cleavage (King, 2001; Hasan et al., 2017).

Abrasion is a surface breakage mechanism that occurs when two particles move parallel to their plane of contact (Napier-Munn et al., 2005).

The breakage mechanisms are associated with each other, and they are influenced by the mill type, operating conditions and the material being ground (Hasan et al., 2017). However, the dominant particle breakage mechanisms for comminution differ with equipment type. For AG/SAG mills, the three dominant breakage mechanisms are abrasion, attrition and impact (Napier-Munn et al., 2005). In ball mills, the main breakage mechanism is impact breakage which occurs at the toe of the mill (Little et al., 2017). Many researchers have determined that the breakage mechanisms in stirred mills, regardless of orientation, are abrasion and attrition (Gao & Forssberg, 1995; Sinnott, Cleary & Morrison, 2006; Ye et al., 2010; Little et al., 2017). Comminution devices that have abrasion as the dominant breakage mechanism have a narrow product size distribution, as shown in Figure 2-3 (Gao & Forssberg, 1995).

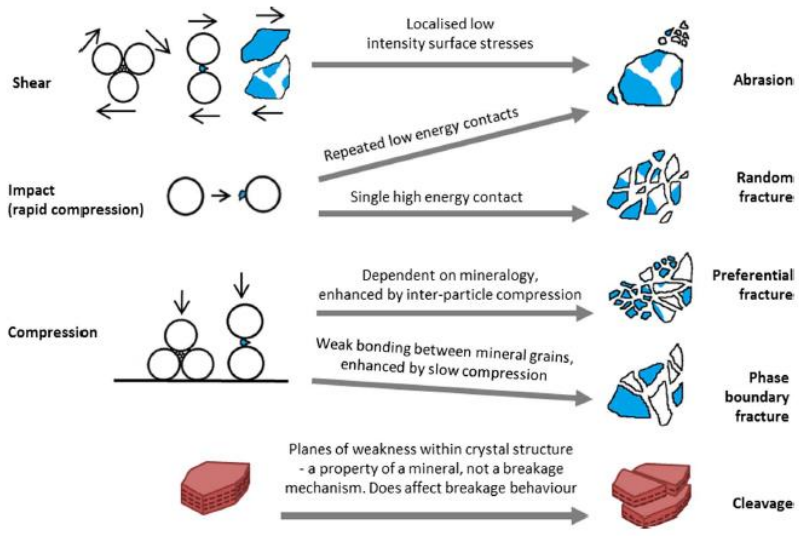

Figure 2-2: Particle breakage mechanisms, where circles represent grinding media (Little et al., 2017)

Many models have been developed to predict the size distribution of a milled product, and it was established that fine-grinding breakage kinetics follow a non-first-order model (Gao & Forssberg, 1995; Hasan et al., 2017).

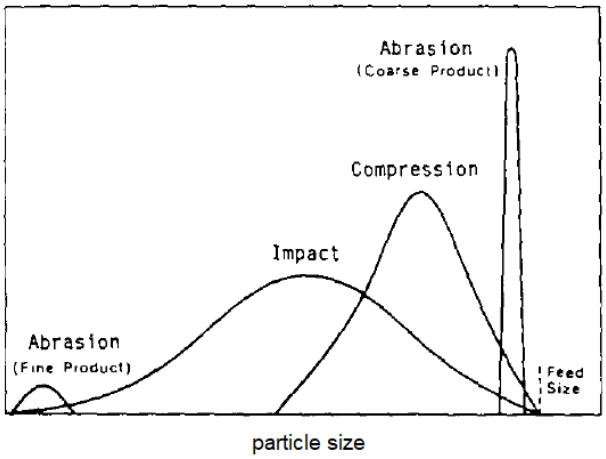

Figure 2-3: Resulting size distributions of the different breakage mechanisms (Gao & Forssberg, 1995)

The existing non-first-order models have two components: the breakage function and the distribution function (Hogg & Cho, 2000; Hasan et al., 2017). For fine grinding, the breakage and distribution functions are difficult to determine because of the sub sieve ranges (Hogg & Cho, 2000).

2.1.3 Energy consumption

Energy consumption in the mineral processing industry is becoming of increasing concern. Mining activities consume a great deal of energy, as shown in Figure 2-4, and 50% of the energy used in mining is used in comminution activities (Napier-Munn, 2012). In the United States of America (USA), comminution processes account for 3.8% of the total electricity consumption and 40% of USA mining energy use (De Bakker, 2014). Ballantyne et al. (2012) estimated that 9% of Australia's energy consumption is by comminution processes. If the existing comminution equipment in mineral processing plants is not upgraded to more energy efficient equipment, there will be an increase in mining energy consumption because of the complexity of the remaining ore bodies. For example, it is estimated that there will be a 16% increase in energy consumption by the Canadian copper mining industry between 2016 and 2025 (Jeswiet & Szekeres, 2016).

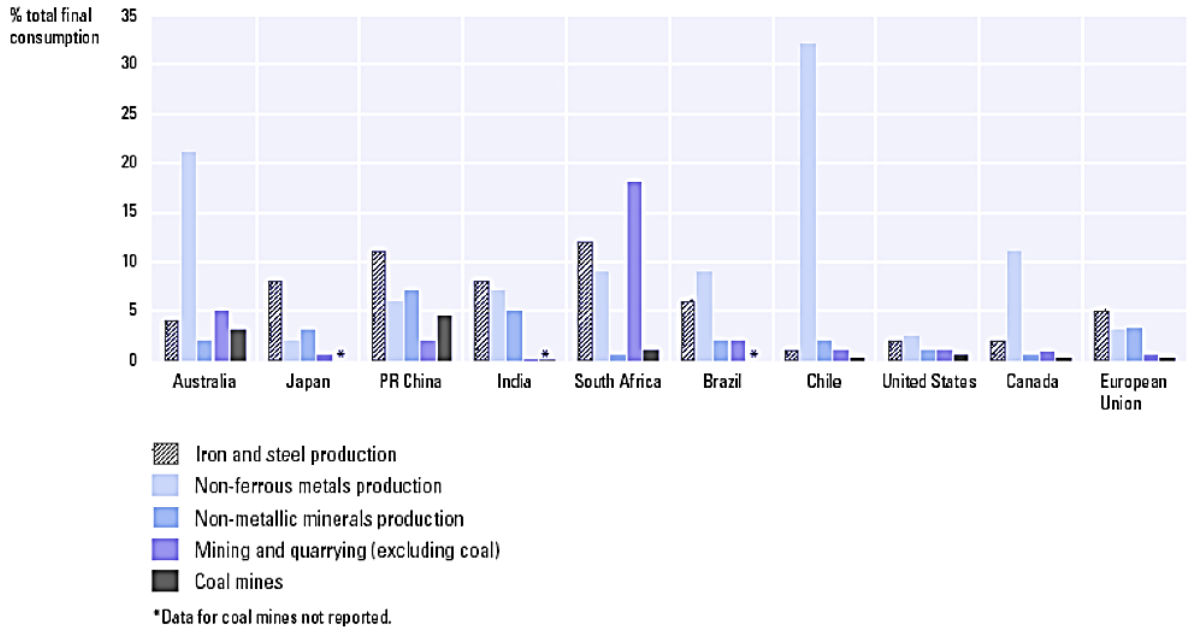

Figure 2-4: Percentage of total electricity consumption used by mining and minerals industries for selected countries and the EU (Napier-Munn, 2012)

Most of the energy that goes into grinding and grinding processes is converted to heat energy or is absorbed by the equipment, with only a small proportion of the energy going to particle breakage (Napier-Munn & Wills, 2006). For example, only 15% of the energy input into a ball mill goes to size reduction (Napier-Munn & Wills, 2006).

Many relationships have been established to determine milling energy consumption. Von Rittinger's theory states that the energy consumed by the size reduction is proportional to the new surface area produced, and it is given by Equation 1 (Napier-Munn & Wills, 2006).

Equation 1

$$E = K\frac{1}{D_2} - \frac{1}{D_1}$$

where E is the energy input, K is a constant, D_1 is the initial particle size and D_2 is the final particle size.

Kick recognised a similar relationship where the work required is proportional to the particle volume reduction (Napier-Munn & Wills, 2006).

Equation 2

$$W = \frac{10W_i}{\sqrt{P}} - \frac{10W_i}{\sqrt{F}}$$

where W_i is the work index (kW/t required to reduce the material from theoretical infinite size to 80% passing 100 µm), P is the diameter through which 80% of the product passes, and F is the diameter through which 80% of the feed passes (Napier-Munn & Wills, 2006).

These equations relate the energy consumed to the particle properties, which means that the relationships are applicable over a wide range of milling equipment, including stirred mills.

Over the last 20 years, it has been established that stirred mills are superior to ball mills in energy efficiency, so their use in the mining industry is increasing (Danielle et al., 2017). Stirred mills are approximately 50% more efficient than ball mills (Jeswiet & Szekeres, 2016). Rule (2009) conducted a study comparing the IsaMill and the ball mill at an Anglo-American plant, and his results showed that the IsaMill was more energy efficient than the ball mill.

2.2 Fine Grinding

2.2.1 Basics of fine grinding

Grinding can be classified into three; coarse grinding, intermediate grinding and fine grinding (De Bakker, 2014). The current mineral ore bodies are increasing in complexity; they have finer grain sizes and some have low grades, and they require fine grinding to achieve the necessary degrees of liberation (Jankovic et al., 2001). The definition of fine grinding differs between industries and between scholars (Jankovic, 2003). Gao & Holmes (2008) defined fine grinding and ultra-fine grinding as 80% passing through a 20 µm screen and 80% passing through 7 µm, respectively. However, Jankovic (2003) defined fine grinding as 80% passing through 30 µm and ultra-fine grinding as 80% passing through 10 µm, as shown in Figure 2-5.

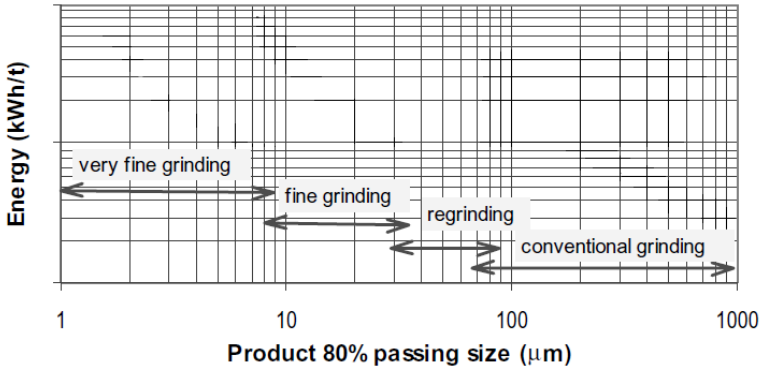

Figure 2-5: Classifications of the different grinding classification according to Jankovic (2003)

The mills that can be used for fine grinding fall into four categories: ball mills, stirred media mills, centrifugal mills and jet mills (Lichter & Davey, 2006). Ball mills and stirred mills make up the bulk of the fine-grinding equipment (Lichter & Davey, 2006). Lichter & Davey (2006) showed that stirred mills are replacing ball mills for fine-grinding applications because they are more energy efficient than tumbling mills (Figure 2-6). Jankovic (2003) made a similar observation.

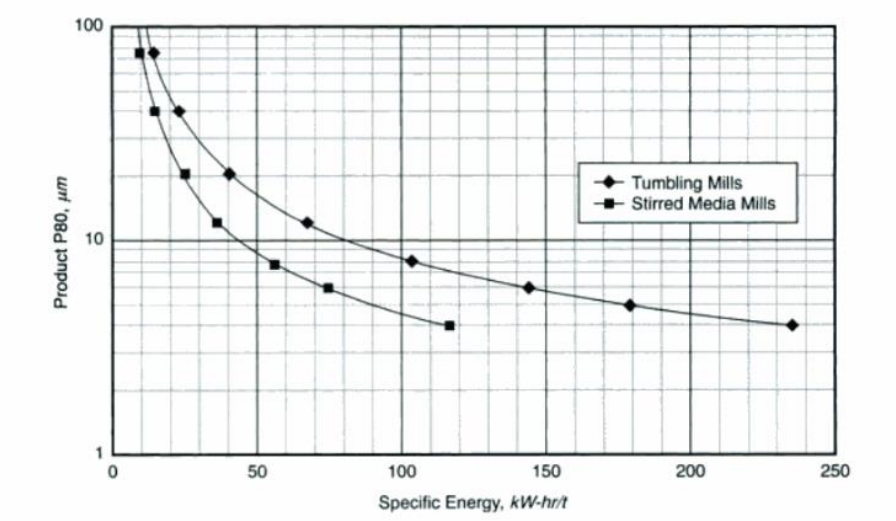

Figure 2-6: Relative performance of tumbling mills and stirred media mills (Lichter & Davey, 2006)

2.3 Stirred Mills

Stirred mills are mills that effect grinding by stirring together ore particles and grinding media. The first application of stirred milling technology in the minerals industry was in the late 1980s when the IsaMill was used in the lead and zinc industry by MIM (Xstrata Technology) (Rule, 2010). Since then, there has been an increase in the use of stirred mills in the minerals industry,

and there are currently many stirred mills on the market. *Table 2-1* highlights some of the different stirred mills available for the minerals processing industry.

A stirred mill consists of a chamber with a media agitator that can have spiral screws, pins or discs, and the media can be either fluidised or agitated (Lichter & Davey, 2006). When the media is fluidised, it forms a cavity near the shaft and is displaced near the wall. The role of the agitator is to stir the media, which causes particle breakage. There are many ways to classify stirred mills but agitator speed, mill orientation and mill geometry are the commonly used classifications. Jankovic et al. (2001) classified stirred mills in terms of orientation and speed. The two orientations of stirred mills are vertical, such as the Tower mill, and horizontal, such as the IsaMill. When classifying stirred mills in terms of their speed, the rotation rate of the stirrer tip is considered (Jankovic, Valery & La Rosa, 2001). High-speed mills operate at five times the speed of low-speed mills (15 mm/s) and they achieve a grind as fine as 5 µm (Jankovic et al., 2001). One of the advantages of stirred mills is that their performance is independent of their energy intensity (Lichter & Davey, 2006).

Particle breakage within stirred mills is determined by the shear and compression forces from the grinding media, the frequency with which stress events happen in the mill, and the intensity of the stress (Outotec, 2016). The dominant breakage mechanism in most stirred mills is attrition or shear type grinding (De Bakker, 2014). Attrition of particles in stirred media mills is caused by shear and compression stress, as illustrated in Figure 2-7.

Table 2-1: Stirred mills available for the minerals processing industry

Mill name	Manufacturer	Mill orientation	Agitator type	Feed size (F80) range (µm)	Product size (P80) range (µm)
Vertimill	Metso	Vertical	Helical Screw	100–300	15–100
Stirred Media Detritor (SMD)	Metso	Vertical	Impellers	15–100	6–7
Tower Mill	Kubota	Vertical	Helical Screw	100–300	15
ANI Metprotech Mill	ANI Metprotech	Vertical	Helical Screw	-	-
Knelson Deswick Mill/ VXP Mill	Deswik	Vertical	Impeller discs	300–400	-
HIGmill	Outotec	Vertical	Rotating grinding discs	>212	20
IsaMill	Mt Isa Mines & Netzsch GmbH	Horizontal	Rotating grinding discs	>300	7

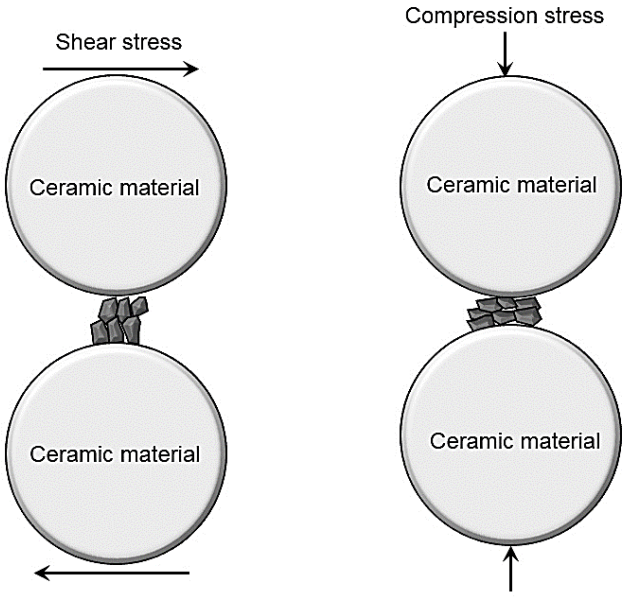

Figure 2-7: Stresses causing attrition grinding in stirred mills (Outotec, 2016)

2.3.1 Horizontal stirred mills

2.3.1.1 IsaMill

The IsaMill was developed by Mount Isa Mines Limited and NETZCH-Feinmahltechnik GmbH in 1990 (Jankovic, Valery & La Rosa, 2001), and the first IsaMill was put into operation at Mount Isa Mines (MIM) in 1994 (Jankovic, 2003).

The IsaMill is a high-speed horizontal mill with a static cylindrical body that is fitted with rotating grinding discs (Jankovic, Valery & La Rosa, 2001). The mill uses silica sand, slag and ceramic grinding media and operates at high power intensities in the order of 300 kW/m^3 (Ye et al., 2010). The IsaMill (Figure 2-8) is fitted with an internal classifier, and the feed passes through eight stages of grinding before classification (Glencore Technology, 2015).

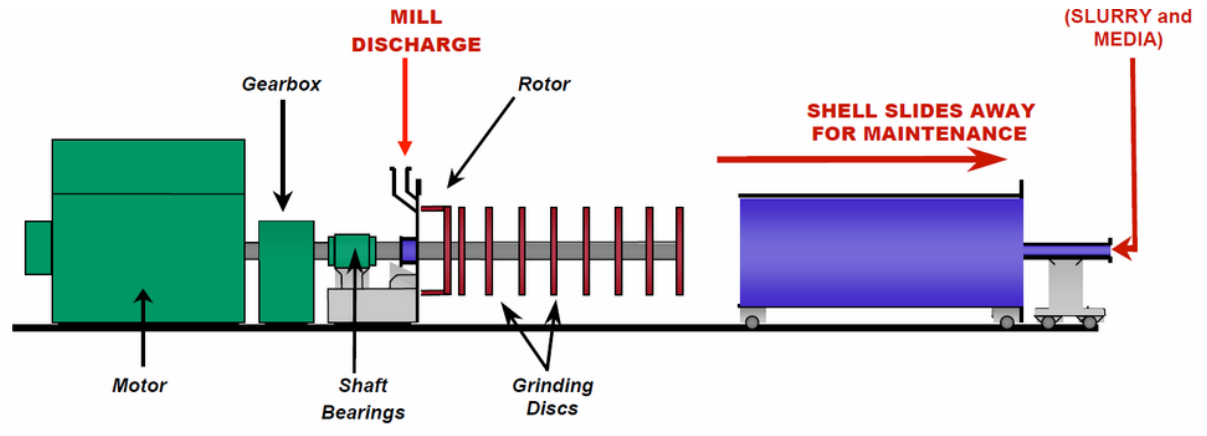

Figure 2-8: Schematic diagram of an IsaMill (Howling Pixel)

The IsaMill size ranges from 300 kW to 8000 kW. The discs rotate at up to 21 m/s (Glencore Technology, 2015). Typically, the media load of the mill is 60% and it can produce a P80 of 7 µm. The rotation of the shaft results in the grinding discs' agitating the media in a centrifugal motion towards the shell liner and, as the media reaches the liner, it is redirected to the mill shaft area (Anderson & Bandarian, 2019).

2.3.2 Vertical stirred mills

2.3.2.1 Tower mill/Vertimill

Nippon-Eirich currently owns the Tower mill, but it was invented by Iwasaki Iskoichi and introduced to industry by the Nichitsu Mining Industry Co. Ltd in 1953. Now, it is produced and marketed by Metso Minerals Ltd (Jankovic, 2008).

The Tower mill was the first low-speed vertical mill to be used in the minerals industry (Jankovic, 2003). The Vertimill has a static cylindrical shell that is fitted with a helical screw agitator. The helical screw agitator provides a lifting and rotating action that results in the grinding action in the mill. The mills also have a settling classifier and a pebble port, which is used to remove the grinding media. Figure 2-9 shows the schematics of the Tower mill and the Vertimill. There are over 250 Tower mills and 220 Vertimills installed in the industry (Rocha et al., 2018).

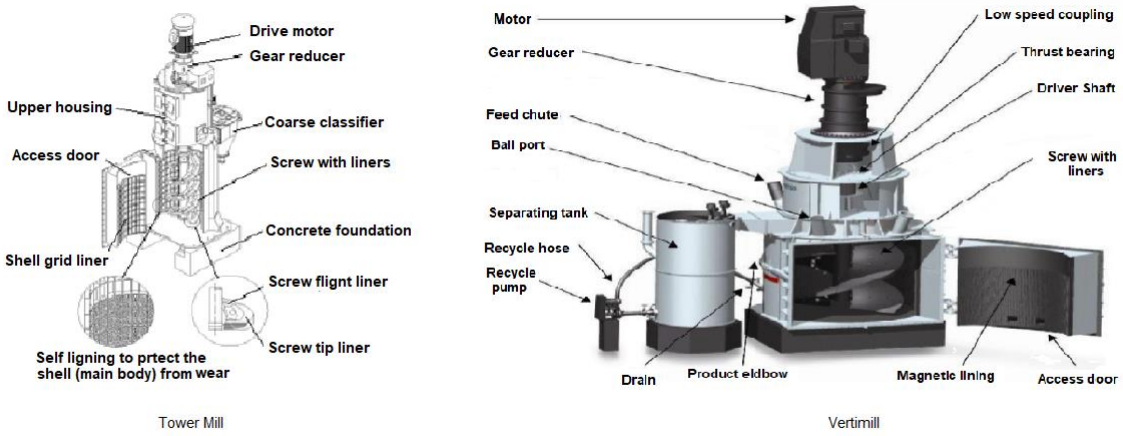

Figure 2-9: The Kubota Tower Mill and the Metso Vertimill (Rocha et al., 2018; Ntsele & Allen, 2012)

The Vertimill has been applied in many industries, including the gold and zinc industries (Rocha et al., 2018). The Vertimills come with an installed power between 11 kW and 3352 kW and have a typical tip speed of 3 m/s (Metso, 2018). Ceramic or steel media of sizes ranging from 6 mm to 40 mm can be used. The Vertimill is suitable for primary grinding, secondary grinding, regrinding, fine grinding and lime slacking. The size of media is chosen to suit the application. Depending on the application, the mill usually works in closed circuit with hydrocyclones and can achieve a product with 80% passing the size of 15 µm (Bergerman & Delboni, 2014).

2.3.2.2 Stirred Media Detritor

The Stirred Media Detritor (SMD) is currently produced and sold by Metso Minerals Ltd. The original design for the SMD was developed in the 1960s by ECC International under the name *SM mill* for their kaolin and calcium carbonate plants (Lofthouse & Johns, 2002). Around 1995, ECC International and Svedala Industries researched the use of the SM mill with metalliferous feeds. The SM mill for grinding metalliferous ores became known as the Svedala detritor, now the Metso SMD (Lofthouse & Johns, 2002).

The SMD is a fluidised media mill *(*Figure 2-10*)*. The mill design was adapted from the sand mills used in the pigment industry (Gao & Holmes, 2008). The SMD has an octagonal static body that is fitted with a multi-armed impellor, and there are also polyurethane screens at the top to retain the grinding media within the mill (Ntsele & Allen, 2012). The stirrers can rotate at a tip speed of 11 mm/s (Gao & Holmes, 2008).

Feed of 30–60% solids enters from the top of the mill and is directed to the bottom of the mill. The ceramic or silica grinding media of 1–3 mm in diameter is added from the media feed chute (Metso, 2019; Lichter & Davey, 2006). The feed size of the slurry is typically 15-100 µm

and the product can be is as fine as 80% passing 6 µm (Lichter & Davey, 2006). The SMD can therefore be used for fine and ultra-fine grinding. It is usually operated in open circuit.

Figure 2-10: Metso Stirred Media Detritor (SMD) Mill (Ntsele & Allen, 2012)

2.3.2.3 Knelson Deswik mill/VXP mill

The Knelson Deswik mill is a vertical stirred mill that was designed for fine grinding in the 1990s for the pigment industry and was later modified to be used in the minerals industry (Rahal, Erasmus & Major, 2011). The Knelson Deswik mill is now called the VXPmill and is produced by FLSmidth (Reddick et al., 2014).

The VXPmill (Figure 2-11) has modular disc impellers and was designed for slurries with an F80 of 300-400 µm. The mill is used for fine and ultra-fine grinding applications. It operates at tip speeds in the range of 10–12 m/s and is an intermediate between low-speed and high-speed mills (Rahal, Erasmus & Major, 2011). The mill works well in an open circuit. The grinding media type depends on the application but is usually beads with a diameter of 1.5–12 mm, and the mill can have a media load of 65–80% by volume (Rahal et al., 2011). The VXPmill comes in different sizes of installed power between 3.7 kW and 3000 kW, and the volumes are 3–1000 litres (Table 8-1). Slurry enters the bottom of the mill and exits through the top via the media retention screen (FLSmidth, 2018).

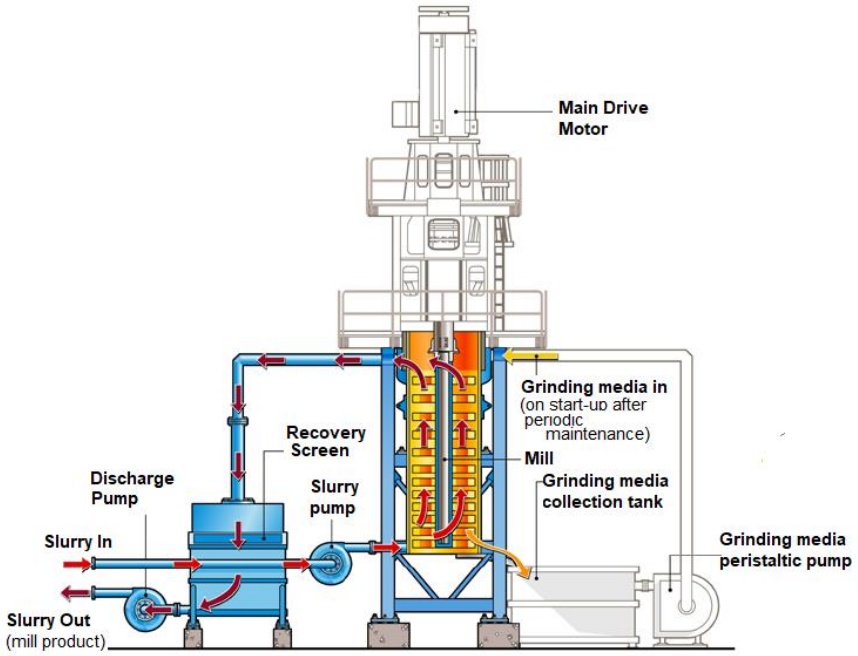

Figure 2-11: The FLSmidth VXPmill (FLSmidth, 2018)

2.3.2.4 HIGmill

The HIGmill was originally manufactured and sold by Swiss Tower Mills (STM), but it is currently marketed by Outotec (Erb et al., 2015). A schematic of the HIGmill is shown in Figure 2-12. The technology was previously used in the calcium carbonate industry (Lehto & Paz, 2013).

The HIGmill is a vertical mill with a static mill body, which consists of an agitator system that has rotating discs placed between stationary counter discs (Åstholm, 2015). There are 12 different HIGmill types, each with installed power that ranges between 132 kW and 5000 kW, with corresponding volumes between 400 L and 27,500 L (Lehto & Paz, 2013). The HIGmill has a variable speed drive with tip speeds of 4–8 m/s for the small mills and 8–12 m/s for the larger mills (Lehto & Paz, 2013).

The HIGmill is designed for regrinding and ultra-fine grinding. It has been applied to the regrinding of concentrates and fine grinding of precious metals (Junnola, 2013), and iron ore tertiary grinding. The mill works in open circuit. Grinding media can be in the form of steel balls or ceramic media, with a size range of 0.5–6 mm depending on the feed size (F80) and the required product size (P80). Ceramic media is used in the processing of sulphide ores in order to minimise galvanic interactions (Lehto et al., 2015). Of the installed HIGmills, the coarsest feed size is 212 µm and the mill produces a P80 of 20 µm (Åstholm, 2015).

The feed to the mill enters from the bottom and the product exits from the top of the mill. The slurry is transported upwards through the rotating discs and the space between the static counter discs and the wall (Lehto et al., 2015) (see Figure 2-12). Up to 30 discs can be installed in the mill, creating up to 30 grinding stages. The pump speed helps create a sharp size distribution curve in the mill by ensuring the fine particles are transported out of the mill faster. Gravitational forces help the coarse particles and the grinding media to be retained within the mill (Åstholm, 2015).

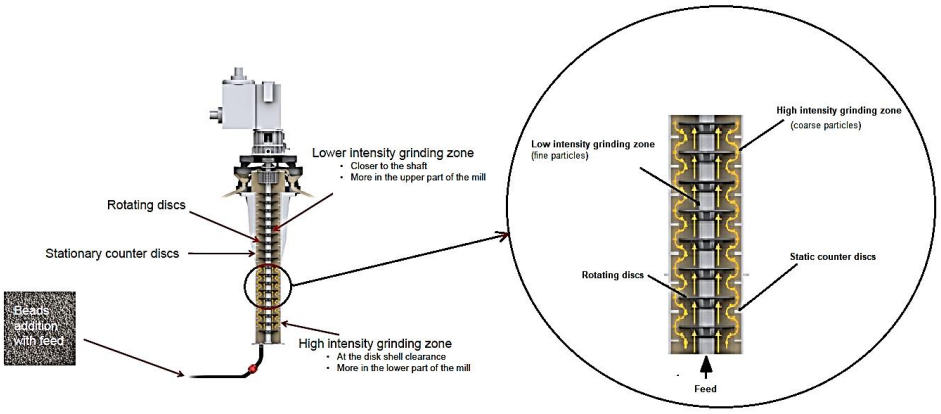

Figure 2-12: Outotec HIGmill (Åstholm, 2015)

2.4 Operating Parameters of Stirred Mills

Many parameters affect grinding in stirred mills. Kwade & Schwedes (2007) divided the parameters into four groups: operating parameters, operation mode, composition of suspension and mill geometry, as shown in Table 2-2. Jankovic (2003) defined the important parameters to be considered as mill design, grinding media, mill speed and slurry density. Most of the parameters identified by Jankovic (2003) fall under Kwade & Schwedes' (2007) definition of operating parameters. Many scholars have studied the different stirred mill parameters that affect fine grinding and they noted that the most important parameters are the stirrer tip speed, the solids concentration and the grinding media properties, such as size and material (Zheng et al., 1996; Jankovic, 2003; Gao & Holmes, 2008).

Table 2-2: Stirred mill parameters (Kwade & Schwedes, 2007)

Group	Parameters
Operating Parameters	Grinding or dispersing time, throughput, stirrer tip speed, grinding media size, grinding media material (density, elasticity and hardness), grinding media filling ratio
Operation Mode	One or multiple passage mode; pendulum or circuit operation
Composition of the Suspension	Solids concentration; type of solvent, additives or dispersing agents
Mill Geometry	Type of mill; size and dimensions of mill

2.4.1 Mill geometry

When considering mill geometry, factors such as the mill orientation, impeller design and the size of the mill are relevant. Aspects of the mill geometry have to suit the grinding application. There are different sizes of mills available for different duties.

Stirred mills come in two orientations: vertical and horizontal. The IsaMill is the only horizontal stirred mill mentioned above. A major factor to consider when choosing between a horizontal stirred mill and a vertical stirred mill is the footprint (Wills & Finch, 2016). Horizontal stirred mills have a larger footprint than vertical stirred mills; however, vertical stirred mills require more headroom than horizontal mills (Wills & Finch, 2016). Vertical stirred mills also have gravitational forces acting on their load and this affects their grinding (Cayirli & Serkan, 2017). The gravitational forces in the mill contribute to a settled load which negatively affects the grinding resulting in the vertical mill producing a coarser product than the horizontal mill for the same stress intensity as shown in Figure 2-13 (Cayirli & Serkan, 2017).

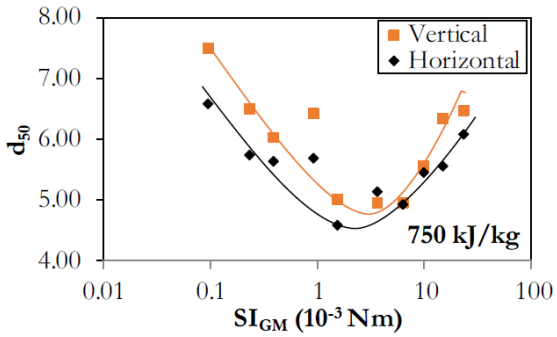

Figure 2-13: Grinding product size at 750 kJ/kg energy input for horizontal and vertical stirred mill (Cayirli & Gokcen, 2017)

There are several agitator designs available for stirred mills; however, the three commonly used agitators are helical screw, pin and disc impellers, as shown in Figure 2-14. Pin impellers and disc impellers are found in fluidised stirred mills, where they enable the suspension and

the grinding media to mix thoroughly (Hasan et al., 2016). Helical screw agitators are found in gravity-induced mills (low-speed mills) where the impeller allows the cascading and settling action of the media to promote particle breakage (Hasan et al., 2016).

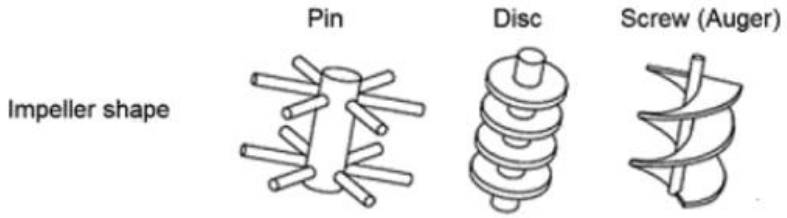

Figure 2-14: Three impeller designs common to stirred mills on the market (Wills & Finch, 2015)

2.4.2 Mill speed

When discussing the speed of a stirred media mill, the *speed* refers to the impeller tip speed, which is the tangential speed of the stirrer tip (Jankovic et al., 2001). The stirrer speed is an important parameter in stirred media mills because it affects the interaction between the media and the particles (Mankosa et al., 1989). The speed of the impeller affects the frequency and intensity of collisions between media and particles (Bel Fadhel & Frances, 2001).

Many studies have been conducted to study the comminution effect of stirred mill speeds. Various ranges of tip speeds have been tested throughout the studies conducted on stirred mills, some of which are highlighted in Table 2-3.

Stirred mills can operate at high speeds. Running them at high speeds increases the fineness of the product and the energy input but also leads to a decrease in the milling efficiency (Zheng et al., 1996; Weller et al., 2000; Bel Fadhel & Frances, 2001; Jankovic, 2003). Bel Fadhel & Frances (2001) ran several experiments with alumina hydrate using a stirred media mill and one of the parameters they tested was the stirrer speed (Figure 2-15). The experiments showed that increasing the impeller speed resulted in the particles reaching their limit of fineness faster. The authors also observed that the impeller speed has no effect on the comminution process when the specific energy is low and that, for higher specific energies, an increase in impeller speed decreases the mill efficiency. The findings of Bel Fadhel & Frances (2001) were similar to results obtained by Zheng et al, (1996), who concluded that increasing the impeller speed results in an increase in the product surface area and energy input; however, increasing impeller speed results in a decrease in energy efficiency.

Becker et al. (2001) conducted experiments on limestone and fused corundum and observed that, at high tip speeds, the time taken to achieve a certain level of product fineness is reduced.

Becker et al. (2001) concluded that increasing the mill tip speed increases the milling efficiency, contradicting the previously highlighted studies conducted by Bel Fadhel & Frances (2001) and Zheng et al. (1996).

He and Forssberg (2007) suggested that there is an optimum mill tip speed. If a mill operates below this optimum speed, the grinding media motion and resultant stress intensity are too low to cause adequate breakage events in the mill (He & Forssberg, 2007). However, if the mill is operated above the optimum, the energy imparted to the grinding media is wasted (for example, heat energy). The observations of He and Forssberg (2007) follow the results of experiments run by Yang et al. (2006) for their Discrete Element Method (DEM) models. These models showed that there is an optimum velocity for stirred mill operation and this optimum value varies with the operational conditions. This means that, when stirred mills are installed in their comminution circuits, adequate optimisation tests must be run to establish the optimum milling parameters for the installed stirred mill.

Table 2-3: Studies conducted on mill tip speed and mill speed ranges

Study	**Tip Speed Range (rpm)**	**Reference**
Effect of operating parameters in stirred ball mill grinding of coal	200–300	(Mankosa et al., 1986)
Effect of media size in stirred ball mill grinding	200–765	(Mankosa, Adel & Yoon, 1989)
Prediction of product size distributions for a stirred ball mill	805–2253	(Gao & Forssberg, 1995)
A study on grinding and energy input in stirred media mills	260–1000	(Zheng et al., 1996)
Wet batch grinding of alumina hydrate in a stirred bead mill	2130–4370	(Bel Fadhel & Frances, 2001)
Variables affecting the fine grinding of minerals using stirred mills	50–150	(Jankovic, 2003)
Influence of slurry rheology on stirred media milling of quartzite	1204–2255	(He & Forssberg, 2007)
Effects of disc rotation speed and media loading on particle flow and grinding performance in a horizontal stirred mill	400–1000	(Jayasundara et al., 2010)
Effect of operating variables on IsaMillTM performance using platinum bearing ores (MSc. Thesis)	1500–1800	(Chaponda, 2011)
Grinding of calcite suspensions in a stirred media mill: Effect of operational parameters on the product quality and the specific energy	1500–2500	(Ouattara & Frances, 2014)

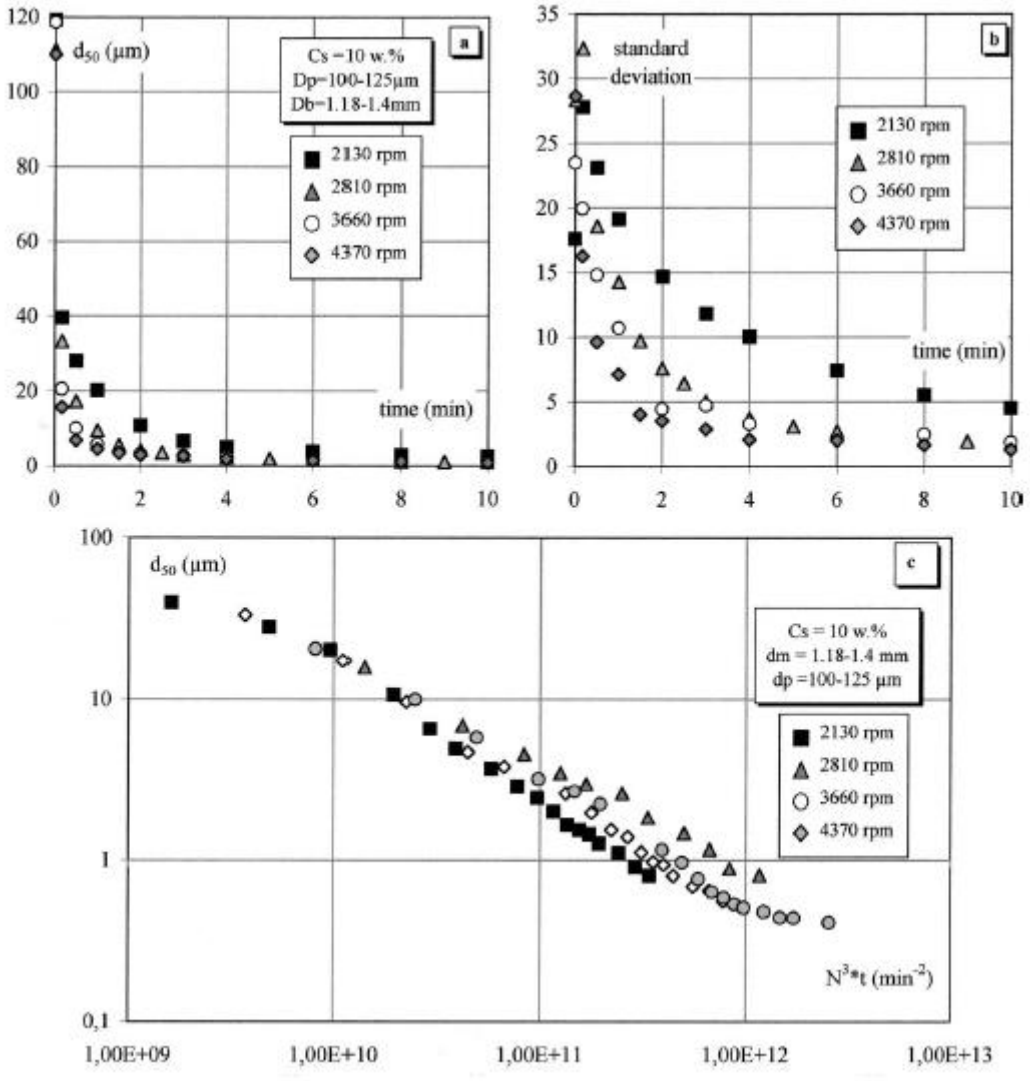

Figure 2-15: Effect of impeller speed on (a) median diameter, (b) size distribution standard deviation, and (c) specific energy (Bel Fadhel & Frances, 2001)

2.4.3 Solids concentration

Solids concentration is an important parameter when looking at wet grinding systems. (Ouattara & Frances, 2014). Solids concentration is the mass fraction of the slurry. At low solids concentrations, the probability of particles being trapped between grinding media is low, whereas, at high solids concentrations, the inter-particle distance is reduced, thereby increasing the probability of solid particles being trapped between grinding media (Kwade, 1999a). However, although high solids concentrations (slurry densities) result in higher probabilities of media-to-particle interactions, operating at high slurry concentrations affects the in-mill slurry rheology (Kwade, 1999b; Napier-Munn et al., 2005). At high solids concentrations, the viscosity of the slurry has to be considered and, in some cases, aids have

to be used to help the fluidity of the slurry (Mankosa et al., 1989; Bel Fadhel & Frances, 2001; Celep et al., 2011; Ouattara & Frances, 2014). Increasing the tip speed can counteract the viscosity effects of some of the slurries (Ouattara & Frances, 2014).

Napier-Munn et al. (2005) demonstrated that the relationship between solids concentration and viscosity is exponential. Studies conducted by He & Forssberg (2007) on slurry rheology using quartzite resonated with the findings of Napier-Munn et al. (2005), in that an increase in the solids concentration resulted in an exponential increase in the slurry viscosity. An increase in slurry viscosity negatively affects the breakage mechanisms in the mill because the viscous slurry dampens the action of the grinding media on the particles, which reduces the stress intensity of the grinding media (He, Wang & Forssberg, 2006). Figure 2-16 shows that relationship between the viscosity and the solids concentration.

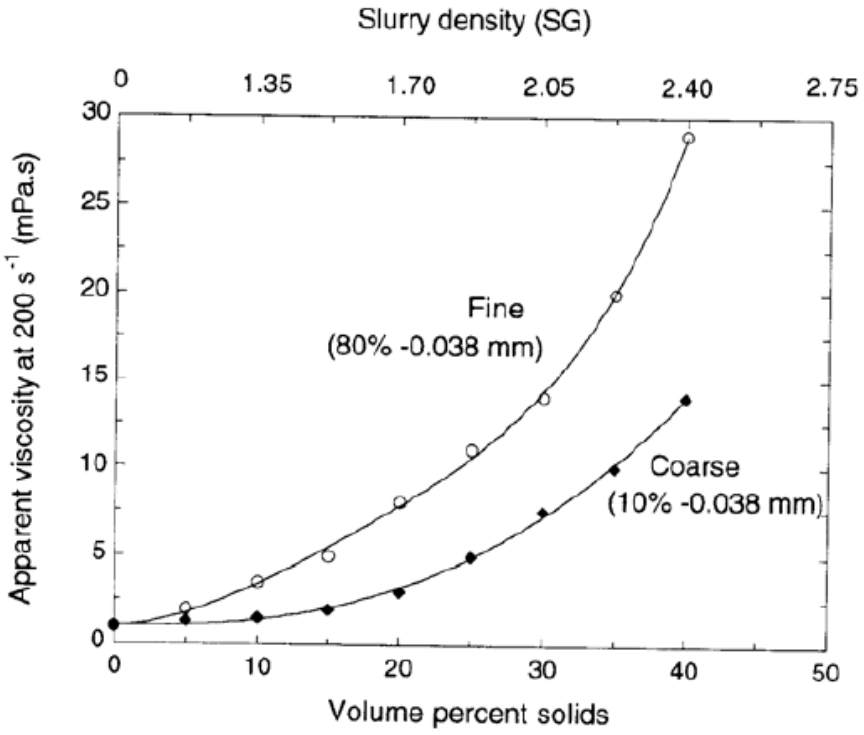

Figure 2-16: Relationship between apparent viscosity and slurry density (solids concentration) for a typical base metal ore (Napier-Munn et al., 2005)

In the pilot Tower mill and SAM mill, increasing the solids concentration resulted in an increase in grinding efficiency because, at high solids percentages, there was an increase in the particle breakage probability and a decrease in the power draw (Jankovic, 2003). These results contradict those obtained by Mankosa et al. (1989) for coal grinding using a pin stirred mill

because the earlier study showed that, at a high percentage of solids (60%), there was a coarser product distribution and a decrease in energy efficiency. The difference in the results may be attributed to the fact that, at 60% solids, the coal slurry viscosity increases but there was no negative viscosity effect with the ores tested by Jankovic (2003). Mankosa et al (1989) also noted that, within a certain range of solids concentrations (20%–50%), there was no significant impact on the PSD. Results obtained by Bel Fadhel & Frances (2001) from their experiments with black carbon agree with the findings of Mankosa et al (1989), in that the energy efficiency decreased with increasing solids concentration. Figure 2-17 shows a comparison of the results obtained by Jankovic (2003) and Mankosa et al. (1989).

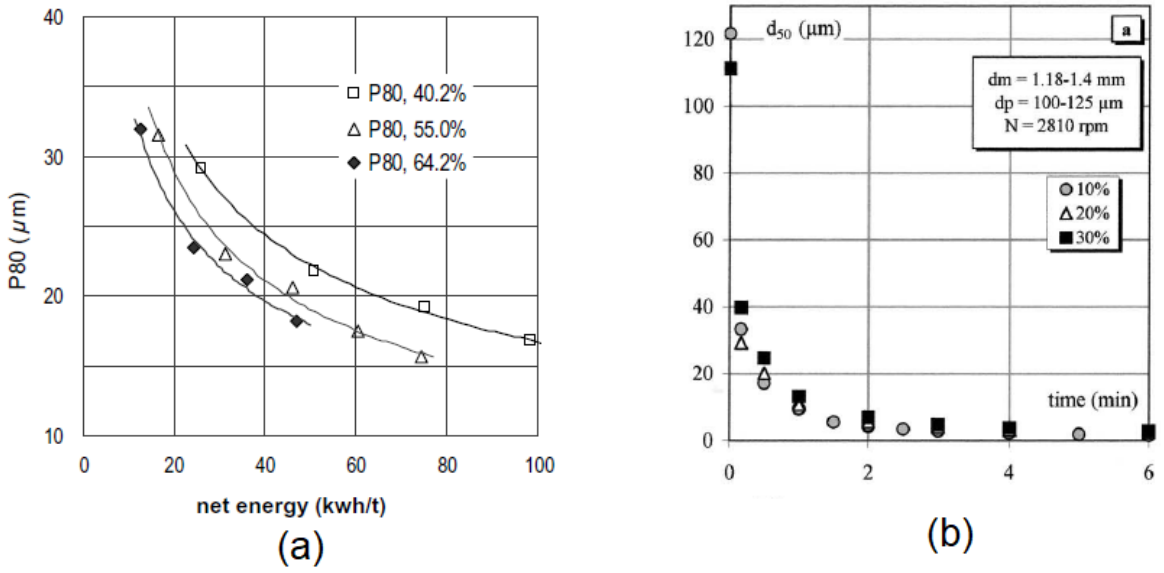

Figure 2-17: Comparison of the solids concentrations obtained by (a) Jankovic (2003) and (b) Mankosa et al. (1989)

The mentioned studies conducted with the solids concentration indicated that there is an optimum solids concentration for different milling parameter combinations. Zheng et al. (1996) showed that there is an optimum solids concentration for the milling of limestone, and the results obtained in their experiments are depicted in Figure 2-18. These results, along with the studies around mill tip speed, consolidate the fact that, before an operation instals a stirred mill in its process, it needs to adequately assess the optimal settings for the milling parameters.

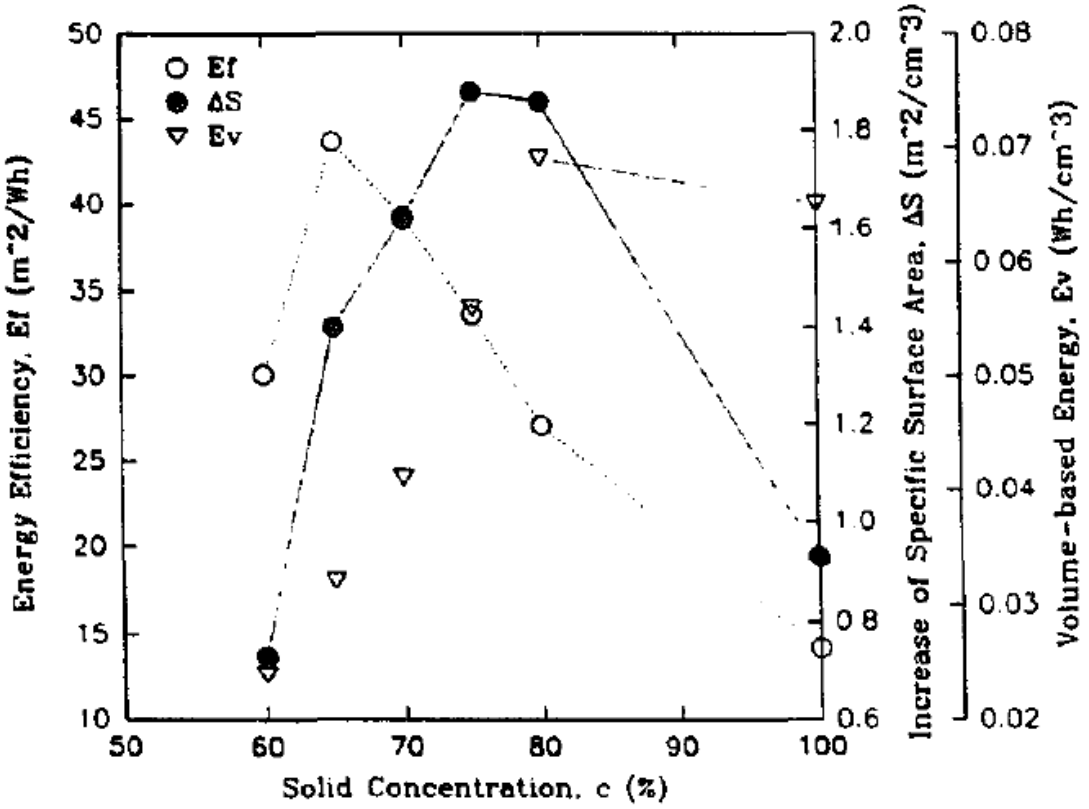

Figure 2-18: Effect of solid concentration. Conditions: D = 6.5 cm; T = I 1.8 cm; t = 15 mini N = 1000 rpm; R = 3; d = 2.05 mm; V= 150 cm "~.(Zheng et al., 1996)

2.4.4 Grinding media

The grinding media is one of the most key factors that affects the quality of fine grinding. Amongst the aspects of the grinding media that affect grinding are the grinding media type, size and filling (Lichter & Davey, 2006).

2.4.4.1 Grinding media type

Many materials are used to make grinding media and they can be grouped into two categories: ferrous and nonferrous materials (Lichter & Davey, 2006). Steel balls are an example of ferrous media, and ceramic beads and glass beads are examples of nonferrous media. The materials used as the grinding media have a great influence on the density of the grinding media.

Mankosa et al. (1986) experimented with two different grinding media materials (glass and steel) on coal and noted that steel beads were more efficient than glass beads (Figure 2-19) because the steel media achieved high energies faster than the glass media for the same energy inputs. However, Zheng et al. (1996) experimented with steel and glass media in grinding limestone and concluded that the glass beads were more energy efficient because

the denser steel media lost more heat through heat energy. Some operations use sand as their grinding media. Although sand may be cheaper than other types of grinding media, it is irregularly shaped and this may impact its efficiency: Lichter & Davey (2006) worked with ceramic and sand for grinding using the SMD and showed that the ceramic media was more efficient than the sand media (Figure 2-20).

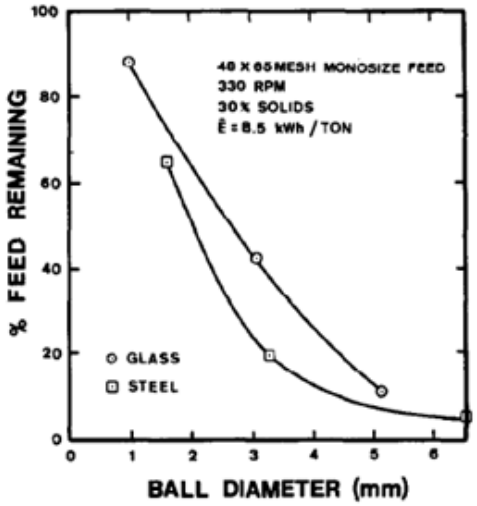

Figure 2-19: Comparison of glass beads and steel beads (Mankosa et al. 1986)

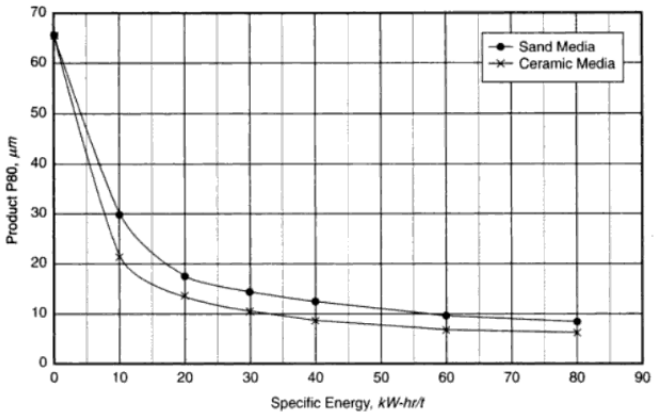

Figure 2-20: Comparison of the energy consumption of ceramic and sand grinding media (Lichter & Davey, 2006)

2.4.4.2 Grinding media density

Grinding media density is an important factor when considering the grinding media to be used in a stirred mill because the grinding media affects the comminution product. Using grinding media with high densities results in finer products (Zheng et al., 1996; He & Forssberg, 2007). Weber and Langlois (2010) demonstrated that the media density should be considered when

optimising stirred mills because the media size can be changed without affecting the grinding efficiency, as long as the media density is kept at an optimum. Zheng et al. (1996) demonstrated that, if the grinding media density is too high, it can result in energy losses and, therefore, decreased grinding media efficiency.

2.4.4.3 Grinding media size

Another factor that affects the grinding media's energy consumption is its size (De Bakker, 2014). Mankosa et al. (1986) established that the media size should be selected according to the mill's feed top size (F80). Jankovic (2003) explained this by noting that coarser feed top sizes require larger media sizes when conducting studies on grinding zinc concentrate, as shown in Figure 2-21.

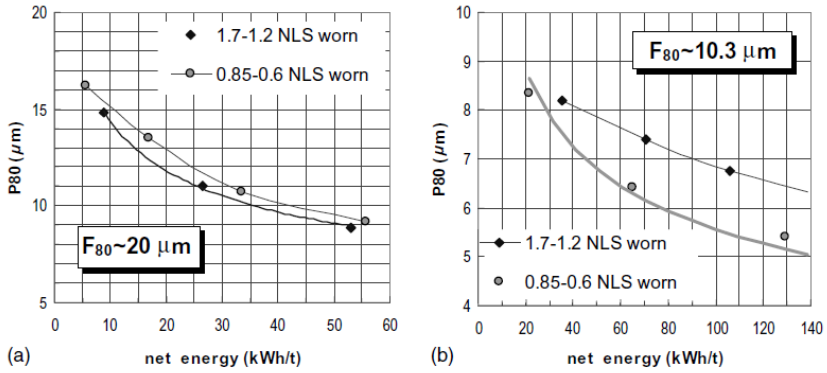

Figure 2-21: Effect of media sizes on F80 (Jankovic, 2003)

Yeu & Klein (2006) studied the effect of grinding media size on quartz particles of two different top sizes: 83 µm and 30 µm. Figure 2-22 shows that they found the grinding media size affected the coarser feed more than the finer feed. Figure 2-22 also shows that a smaller grinding media size resulted in lower specific breakage rates, which implies that the grinding media size affects the stress intensity (SI) and stress number (SN), which will be discussed later. Increasing the grinding media size resulted in an increased breakage rate, finer product size, a narrow product size distribution (PSD) and increased power usage. Yeu & Klein (2006) went on to establish that optimal ratios for top size and grinding media is between 20:1 and 200:1. Other scholars noted similar ratios of top size to ore using different ores, as shown in Table 2-4 (Mankosa, Adel & Yoon, 1986; Zheng, Harris & Somasundaran, 1996; He & Forssberg, 2007; Celep et al., 2011).

Mills operate with monosized grinding media in two instances: When the mill is first used and when all the grinding media is flushed out, a monosized media is added to the mill. Therefore,

it is essential to investigate grinding media with a varying size distribution. In the same experiments, Yeu & Klein (2006) also investigated the effect of a bimodal distribution of 0.5 mm and 2 mm grinding media (coarse media and fine media). In the experiments, Yeu & Klein (2006) noted that the presence of the fine media negatively impacted the milling efficiency because it resulted in the mill's not having enough stress intensity to cause particle breakage.

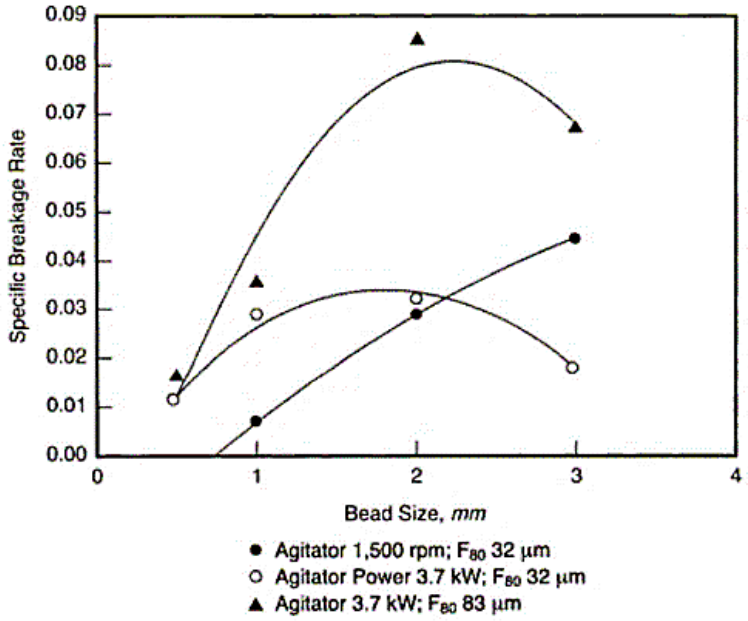

Figure 2-22: Effect of bead size on specific breakage rates (Yeu & Klein, 2006)

Table 2-4: Optimum grinding media to top size ratios for different mills and materials (Hasan, 2016)

Mill type	Effective ratio (media to top feed size)	Material	Reference
Pin Impeller	12:1	Limestone	(Zheng et al., 1996)
Pin Impeller	16:1	Gold/Silver Ore	(Celep et al., 2011)
Pin Impeller	20:1	Coal	(Mankosa et al., 1986)
Draiswerke Disk Impeller	150:1 to 200:1	Quartzite	(He & Forssberg, 2007)

2.4.4.4 Grinding media filling

Grinding media filling, also known as *grinding media load*, is a fourth key factor in stirred mills. Typically, the grinding media occupies 80% of the mill volume (Yeu & Klein, 2006; Rahal et al., 2011). In horizontal stirred mills, operating at high media loads results in a finer product because of the increase in the compressive forces on the ore particles (Yang et al., 2006). In vertical mills, the increase in the media load increases the effective mill grinding volume but does not affect the energy efficiency (Weller et al., 2000). Increasing the grinding media filling increases the milling up to a certain point, after which the energy efficiency of the mill decreases, which suggests that there is an optimum grinding media filling at which to operate

the stirred mill (Chaponda, 2011). Zheng et al. (1996) investigated the optimal media to slurry particle ratio by keeping the slurry concentration constant in a series of experiments where the media volume was changed. They found that the optimal ratio of media-to-particle volume is 2.8 (Figure 2-23). Zheng et al. (1996) then went on to establish the equation to determine the optimal ratio, as shown in Equation 3.

Equation 3

$$R = \frac{1-\epsilon_m}{\epsilon_m(1-\epsilon_p)}$$

where ϵ_m is the media packing porosity and ϵ_p is the particle packing porosity.

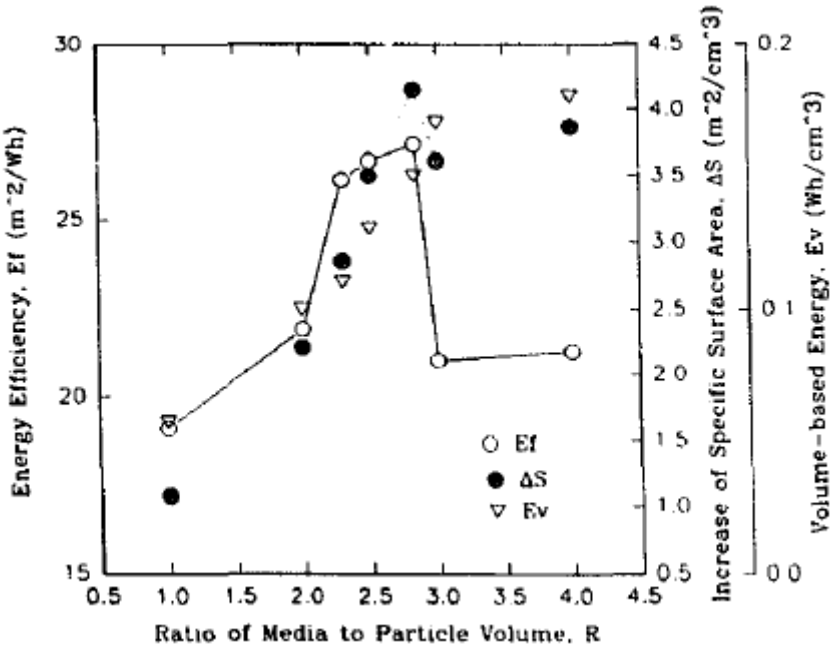

Figure 2-23: Effect of the ratio of media to particle volume (Zheng et al., 1996)

2.5 Stress Model

The stress model uses two approaches to help describe the physical processes occurring in mills: from the view of the product particle and from the view of the milling equipment (Kwade, 2003, 2006). The stress model states that the product quality and fineness are determined by three factors (Kwade, 2006):

1. the type of stress event including particle configuration (for example, compression and shear, impact).

2. how often each feed particle and its resulting fragments are stressed and thus, by the number of stress events of a feed particle, the stress number (SN_F); and
3. how high the specific energy or specific force at each stress event is and thus by the stress intensity at each stress event, the stress intensity (SI) (Kwade, 2006, p. 100).

The stress model looks at how the operating parameters affect the stress number and the stress intensity.

2.5.1 Stress intensity

Stress intensity is a measure of the specific energy required for breakage to occur at a specific stress event (Kwade, 1999b). Kwade developed the stress intensity approach (Kwade, 1999a,b, 2003; Kwade & Schwedes, 2002). The comminution process depends on the frequency of stress events and how high the stress intensity of each event is (Kwade, 1999b). The stress intensity is influenced by the circumferential stirrer speed, media density and media size (Kwade et al., 1996).

Many models have been developed to calculate the stress for different types of stirred mills. Kwade (1999a) developed the model for horizontal mills and it can be expressed using Equation 4.

Equation 4

$$SE \propto SE_{GM} = {d^3}_{GM}\, \rho_{GM}\, {v^2}_t$$

where SE_{GM} is the grinding media stress energy (Nm), d_{GM} is the grinding media diameter (m), ρ_{GM} is the grinding media density (kg/m^3), ρ is the slurry density (kg/m^3), and v_t is the stirrer tip speed (m/s).

Jankovic (2001) developed the stress intensity model for vertical stirred mills after noting that the gravitational force in the mill depends on the media height and mill design. The stress intensities for Tower mills and Pin mills are expressed by Equation 5 and Equation 6, respectively.

Equation 5

$$SI_{gm} = K D_m^2 \frac{(D - D_s)(\rho_{GM} - \rho)}{4\mu}$$

where SI_{gm} is the gravitational stress intensity of the grinding media (Nm), D_s is the screw diameter (m), D is the mill diameter, μ is the coefficient of friction, ρ_{GM} is the

grinding media density (kg/m^3), ρ is the slurry density (kg/m^3), and K is the ratio between vertical and horizontal media pressure.

Equation 6

$$SI_{gm} = D_m^2(\rho_{GM} - \rho)gh$$

where g is the gravitational constant (m/s^2), and h is the media height (m).

Becker et al. (2001) showed that, in limestone comminution, using a horizontal disc mill, each specific energy input results in a different stress intensity and product fineness, as shown in Figure 2-24. Figure 2-24 also shows that there is an optimum stress intensity, which decreases with decreases in the particle size because less energy is required to break the particle (Becker et al., 2001).

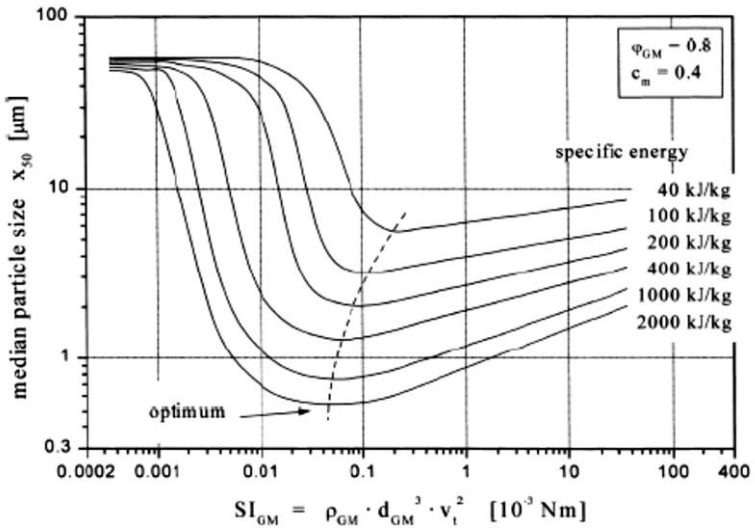

Figure 2-24: Product fineness as a function of stress intensity and specific energy (Becker et al., 2001)

Jankovic (2003) experimented with the effect of the energy inputs on zinc concentrate using a pin mill, and the results showed that the optimal stress intensity was not influenced by the energy input (Figure 2-25), which is contrary to the findings of Becker et al. (2001) for the horizontal mill. The difference in the results obtained with the two mill orientations can be attributed to the gravitational forces in vertical mills.

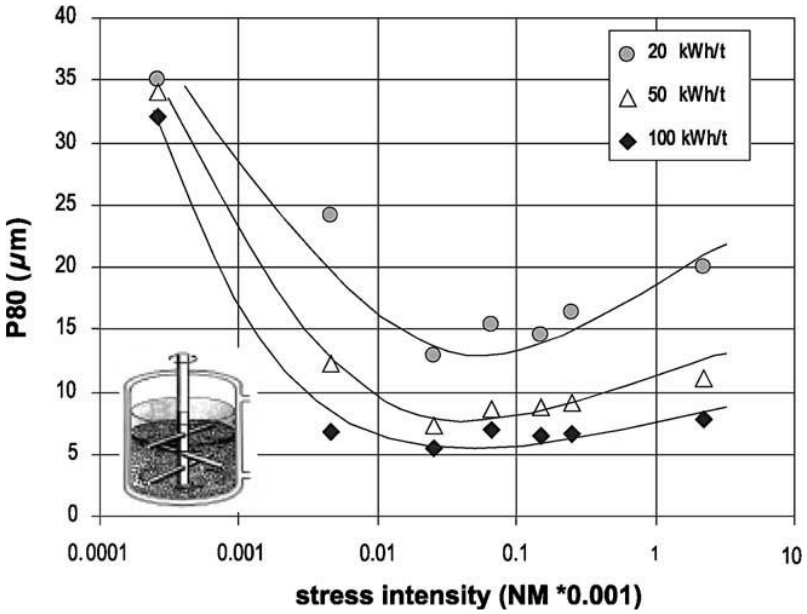

Figure 2-25: Product fineness as a function of stress intensity (Jankovic, 2003)

2.5.2 Stress number

The stress number can be described as the average number of stress events affecting the particles in the mill (Kwade, 1999b). The mill parameters that affect the stress number include the stirrer speed, the solids density and the media filling. In batch grinding, the stress number is determined by Equation 7 (Kwade & Schwedes, 2002):

Equation 7

$$SN = \frac{N_C P_S}{N_P}$$

where N_C is the number of media contacts, P_S is the probability that a particle is stressed during media contact, and N_P is the number of feed particles in the mill.

Equation 8

$$N_C \propto ntN_{GM}$$

where the number of media contacts is proportional to the number of stirrer revolutions (n), time (t) and the number of grinding media (N_{GM}), (Kwade & Schwedes, 2002).

Kwade & Schwedes (2002) investigated the effect of the stress number and stress intensity on limestone grinding. Their experiment showed that small media have a higher stress number, but the media size might not provide enough stress intensity for adequate breakage to take place, as shown in Figure 2-26.

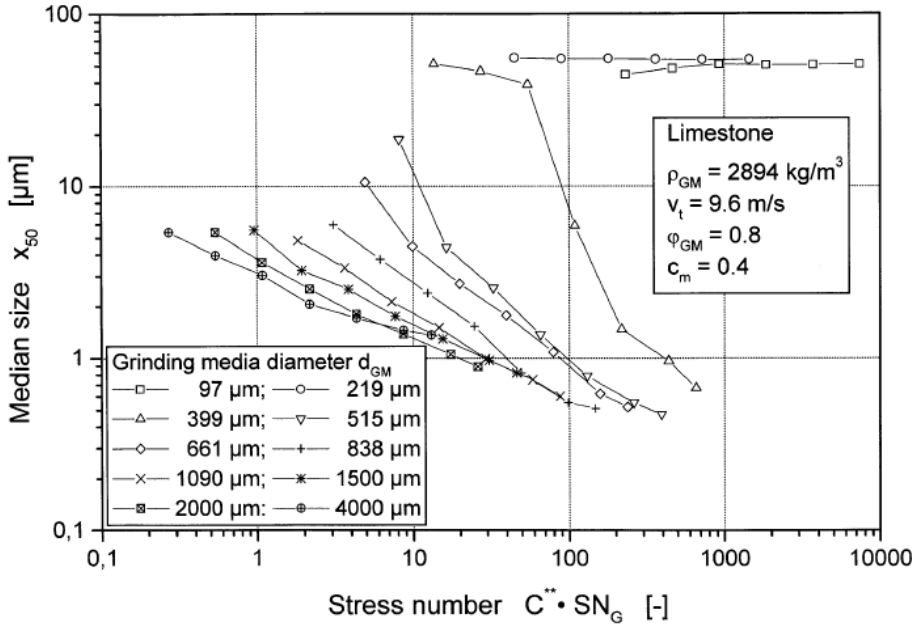

Figure 2-26: Relationship between the grinding media diameter, stress number and product size (Kwade & Schwedes, 2002)

2.5.3 Specific energy

Specific energy is a product of the stress intensity and the stress number (Kwade & Schwedes, 2002; Weber & Langlois, 2010). Specific energy describes the effect of parameters (i.e., mill size, circumferential stirrer speed, solids concentration, and grinding beads density) on the comminution result (Kwade et al., 1996). Specific energy can be calculated using Equation 9.

Equation 9

$$E_m(T) = \frac{E(T)}{m_p} = \frac{\int_0^T N(T)dT}{m_p} = \frac{\int_0^T (M_d(T) - M_{d,0})\omega_d dT}{m_p}$$

where E_m is the mechanical energy input, m_p is the mass of the ground product, N is the power input, T is the comminution time, M_d is the torque during comminution, $M_{d,0}$ is the no-load torque, and ω_d is the stirrer angular velocity.

The resultant specific energy of the comminution equipment is a good measure of the product of the stress number and the stress intensity (Kwade & Schwedes, 2002). Not all the energy that is applied to the mill results in particle breakage, so a factor has to be applied to the specific energy to give the effective specific energy. It is given by Equation 10.

Equation 10

$$E_{m,P} = v_E \cdot E_{m,M}$$

where, $E_{m,P}$ is the specific energy transferred to the particles, $E_{m,M}$ is the total specific energy consumption of the mill, and v_E is the energy transfer factor (Kwade, 2006).

2.6 Flotation

2.6.1 Flotation principles

Flotation is used in the mineral processing industry to separate valuable minerals from unwanted gangue (Napier-Munn & Wills, 2006). The process has three phases: solid, water and froth. There are two types of flotation: *direct flotation*, where the valuable minerals are recovered in the froth phase; and *reverse flotation*, where the valuable minerals are recovered in the pulp phase (Napier-Munn & Wills, 2006; Jaiswal, Tripathy & Banerjee, 2015). Direct flotation will be used for this research.

During flotation, mineral recovery happens via three mechanisms: true flotation, entrainment and entrapment (Napier-Munn & Wills, 2006). In *true flotation*, chemicals are used to induce hydrophobicity onto the mineral surface. The hydrophobic minerals then attach to the air bubbles. The air bubbles enter the froth zone, where the mineral is collected. *Entrainment* involves the recovery of the minerals in the water that is passed through the froth. *Entrapped* particles are trapped between the particles that attached to the bubbles. Figure 2-27 shows a conventional flotation cell.

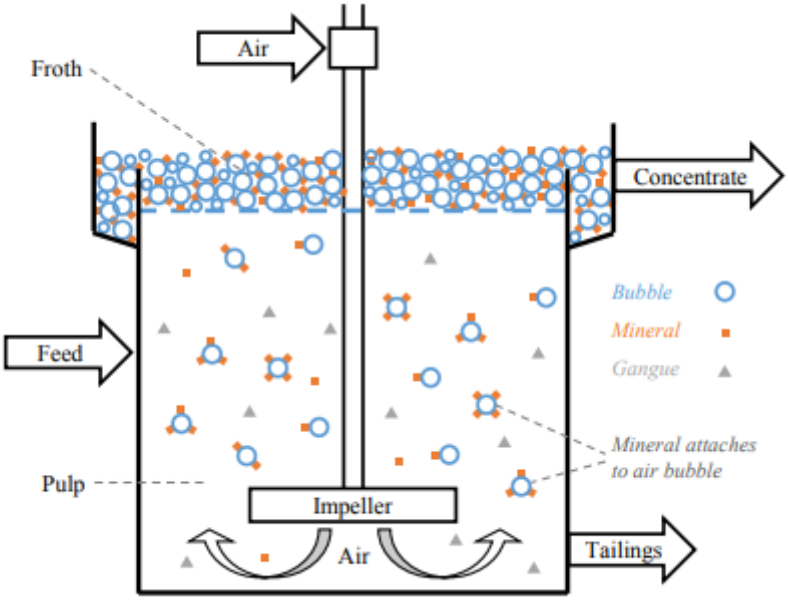

Figure 2-27: Flotation cell (Hu, 2014)

Many studies have investigated the effect of different particle sizes on flotation (Trahar & Warren, 1976; Feng & Aldrich, 1999; Pease et al., 2006). Figure 2-28 shows the recovery of different particle sizes.

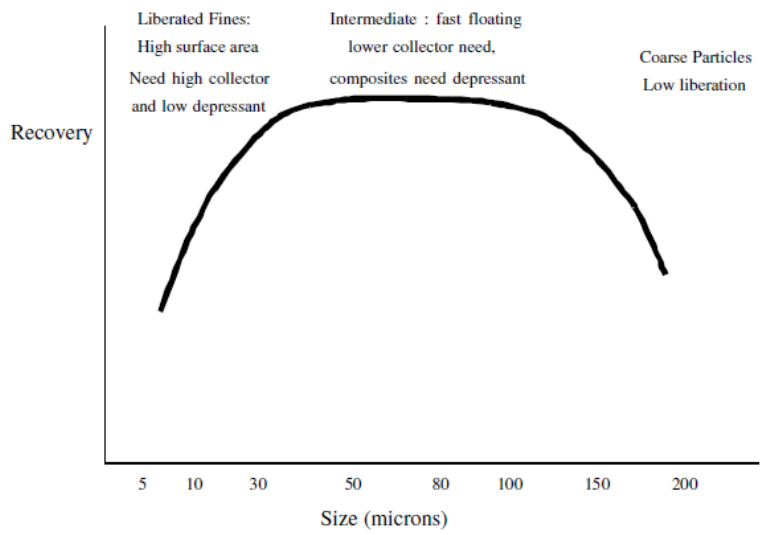

Figure 2-28: Recovery of different particle sizes (Pease et al., 2006)

Many scholars have concluded that very fine particles (<10 µm) can only be recovered by entrainment because they do not have enough energy to attach to the bubble (Subrahmanyam & Forssberg, 1990; Pease et al., 2006; Yianatos & Contreras, 2010).

2.6.2 Flotation reagents

The process of flotation depends on reagents to alter the mineral and gangue surface chemistry. Chemicals are used to render the gangue hydrophilic and the valuable minerals hydrophobic (Napier-Munn & Wills, 2006). Typically, three reagents are used during the flotation process: collectors, depressants and frothers.

2.6.2.1 Collectors

Collectors are organic surfactants that are used to render the valuable minerals hydrophobic (Napier-Munn & Wills, 2006). Collectors can be ionising or non-ionising compounds. The collector polar head adsorbs onto the mineral surface, leaving the non-polar tail exposed, as shown in Figure 2-29. Xanthate collectors are commonly used to float sulphide minerals (Napier-Munn & Wills, 2006). Once a collector has been added to the pulp, conditioning time should be allowed for adsorption to take place.

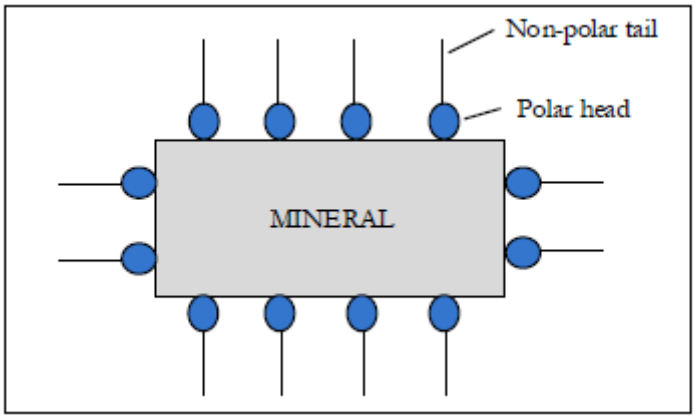

Figure 2-29: Collector adsorption on mineral surface (Napier-Munn & Wills, 2006)

2.6.2.2 Depressants

Depressants are used to make the gangue minerals hydrophilic (Napier-Munn & Wills, 2006). Many types of depressant are available for the flotation of sulphide minerals (Bradshaw, Harris & O'Connor, 1998). Sometimes slimes can act as a depressant by coating the mineral surface, and fine particles are particularly prone to slime coating (Parsonage, 1988).

2.6.2.3 Frothers

Frothers are non-ionic heteropolar organic reagents that stabilise the flotation bubbles by adsorbing on the air-water interface, as shown in Figure 2-30 (Napier-Munn & Wills, 2006). Frothers can reduce bubble coalescence, which in turn controls the bubble size (Laskowski, 2004). Frother dosage must be optimised to ensure the correct degree of bubble stability. Unstable bubbles burst easily and this results in the loss of the recovered mineral by drainage into the pulp phase (Napier-Munn & Wills, 2006). If the bubbles are too stable, water recovery increases and gangue materials are recovered in the froth phase (Napier-Munn & Wills, 2006).

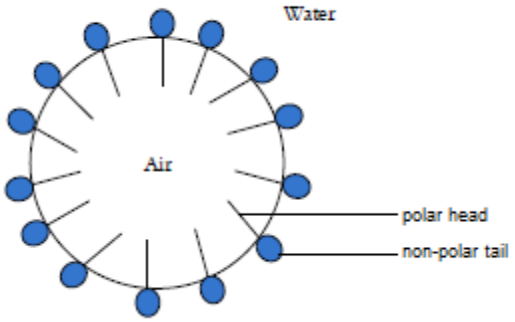

Figure 2-30: Frother adsorption onto the air-water interface

2.6.3 Flotation of UG2 ore

The UG2 ore reserve is a PGM ore body with a chromite layer. UG2 ore contains between 4-7 g/t of platinum group elements and has a chromite concentration of between 60% - 90% (Schouwstra et al., 2000). Typically, the PGMs and base metal sulphides are recovered from the UG2 ore by means of froth flotation. The chromite in the UG2 ore is believed to be recovered by entrainment. Entrainment is a process in flotation whereby liquid and suspended solids enters the froth layer resulting in unselective recovery of the gangue minerals. Chromite makes the processing of the UG2 ore difficult as it affects the smelting process by decreasing the smelter efficiency because chromite is stable at high temperatures (Becker et al., 2008). Ideally, UG2 concentrates that are sent to the smelter are expected to have a chromite content of less than 3% (Wesseldijk et al., 1999)

Flotation circuits that are designed the UG2 ore are usually designed to target the flotation of base metal sulphides (Harris, 2001). To reduce the amount of chromite recovered in the flotation circuit, the UG2 flotation circuits usually have a complex layout. The layout to treat the UG2 ore consists of a rougher and cleaner circuit with long residence times to reduce the degree of entrainment (Harris, 2001). The reagents used for the flotation of UG2 ore consists of a collector, a depressant and frother. In some flotation circuits an activator is also used to increase the adsorption of the collectors on to the sulphide mineral surface (Wesseldijk et al., 1999).

2.6.4 Flotation efficiencies

2.6.4.1 Water and solids recovery

Solids recovery is defined as the solids that are collected in the concentrate during batch flotation. *Water recovery* is defined as the water collected in the concentrate during the flotation process. Water recovery considers only the water that makes up the slurry and does not include the water that is added during the flotation process.

2.6.4.2 Recovery models

2.6.4.2.1 Klimpel model

The Klimpel model assumes that the maximum recovery is less than 100%. The model is represented in Equation 11 (Ramlall & Loveday, 2015).

Equation 11

$$R = R_{max}\left(1 - \frac{1}{k_\tau}\left(1 - e^{k_\tau}\right)\right)$$

where R is the model recovery at a time τ (min), R_{max} is the theoretical maximum recovery (%) and k_τ is the first-order kinetic rate constant (min^{-1}).

2.6.4.2.2 Kelsall model

The Kelsall model is a first-order kinetic model that assumes the maximum recovery is 100% and it considers both fast-floating and slow-floating particles (Bu et al., 2017). The Kelsall model is given by Equation 12:

Equation 12

$$R = R_{fast}\left(1 - e^{-k_{fast}\tau}\right) + R_{slow}\left(1 - e^{-k_{slow}\tau}\right)$$

$$R_{fast} + R_{slow} = 100\%$$

where R_{fast} is the recovery of the fast-floating particles, R_{slow} is the recovery of the slow-floating particles (%), k_{fast} is the rate constant for the fast-floating particles (min^{-1}), k_{slow} is the rate constant for the slow-floating particles (min^{-1}) and τ is the time (min).

2.7 Conclusion

The fine-grained nature and complexity of the ores that are currently being processed in industries has led to a drive to add fine-grinding technologies to existing grinding circuits and incorporate fine-grinding technologies into new circuits. The increased demand for stirred mills is also a result of their efficiency compared to tumbling mills when it comes to fine-grinding applications.

The common stirred milling equipment consists of the IsaMill, the SMD, the Knelson Deswick mill, the Vertimill and the HIGmill. Stirred mills have numerous parameters that can be optimised to achieve the required comminution result. Of the many parameters that are available for optimisation, the critical stirred mill parameters are mill tip speed, grinding media size and solids concentration. Numerous studies have been conducted on these parameters and it has been shown that there are ideal parameter settings that are required to achieve the optimal grinding result. Achieving the optimal comminution targets allows for the optimisation of the downstream processes, such as flotation.

It is important to understand the effect of different milling parameters on the ore and it is also important to investigate the resultant downstream response in order to identify the optimal set of parameters that leads to increased downstream efficiencies.

2.8 Hypothesis

Based on the background presented in the literature review, the following hypotheses were proposed for this work:

1. To get a finer product, there should be an increase in energy intensity because smaller particles need a higher stress intensity for particle breakage to occur.
2. Fine grinding will result in improved recoveries for the complex and hard ores because the fine grinding will result in increased mineral liberation.

2.9 Key Questions

In order to assess out the hypotheses, the following key questions were developed:

1. What is the effect of media size, solids concentration and tip speed on specific energy?
2. What is the effect of media size, solids concentration and tip speed on particle size distribution?

3. What is the effect of fine grinding on flotation recoveries?

3. EXPERIMENTAL APPARATUS AND METHODOLOGY

This chapter provides descriptions of the key equipment used in the experimental work: The main equipment in this study was a HIGmill and the flotation tests were performed using a 5 L Leeds cell. The chapter describes the materials and the methods used for the experimental work that was conducted to test the hypotheses formulated for this thesis.

The study was aimed at evaluating the performance of the HIGmill under different design and operating conditions when grinding UG2 platinum ore. The variables considered in the study included grinding media size, slurry solids concentration and stirrer speed. Since the work was carried out to assess whether the HIGmill could produce a product suitable for flotation in the UG2 platinum ore process flowsheet, the flotation response was evaluated by performing batch flotation tests.

3.1 Description of Apparatus

3.1.1 HIGmill

The HIGmill is a vertical stirred mill with a top-mounted motor to drive the agitator. The mill agitator is fitted with grinding discs that provide the momentum to the grinding media for particle grinding to occur. Slurry enters the stationary mill chamber from the bottom of the mill and exits from the top of the mill. Due to the size of the grinding media and the size of the particles, the main mode of grinding in the mill is attrition grinding. As the slurry flows upwards, particle classification occurs simultaneously with the grinding process because the coarse product remains on the periphery and the finer product flows upwards to exit the mill.

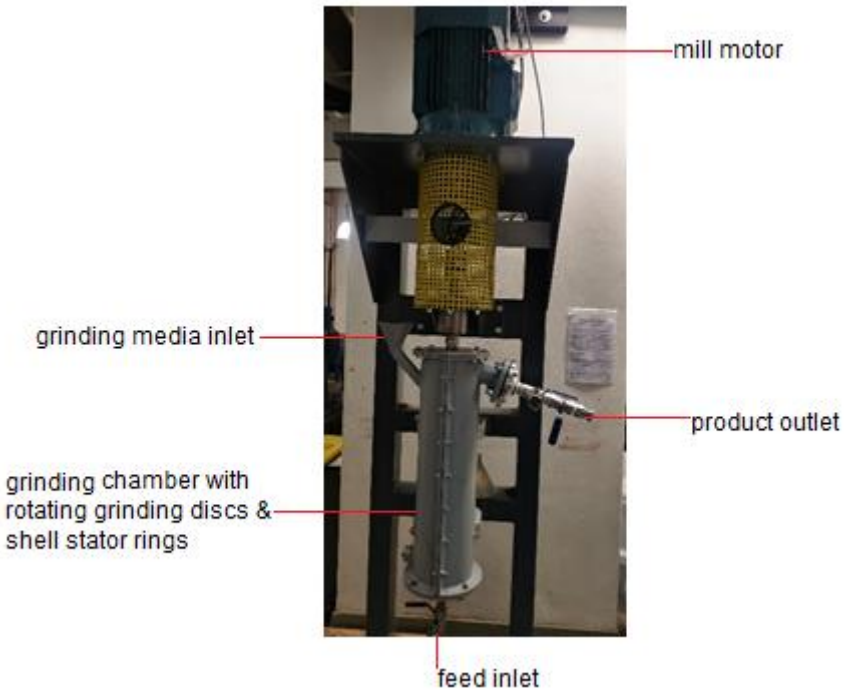

Figure 3-1: UCT HIGmill

3.1.1.1 HIGmill set up

The HIGmill model used in the experimental work was a HIG 5 mill, which is a 6.5 L model with a 5 kW motor. The grinding chamber has a diameter of 143 mm and is fitted with nine grinding discs with a diameter of 110 mm, a minimum speed of 350 rpm and a maximum speed of 1200 rpm. The discs impart the motion to the grinding media and ore particles for grinding to take place. The mill has a grinding media inlet where grinding media is added to the mill. A schematic of the mill setup is shown in Figure 3-2.

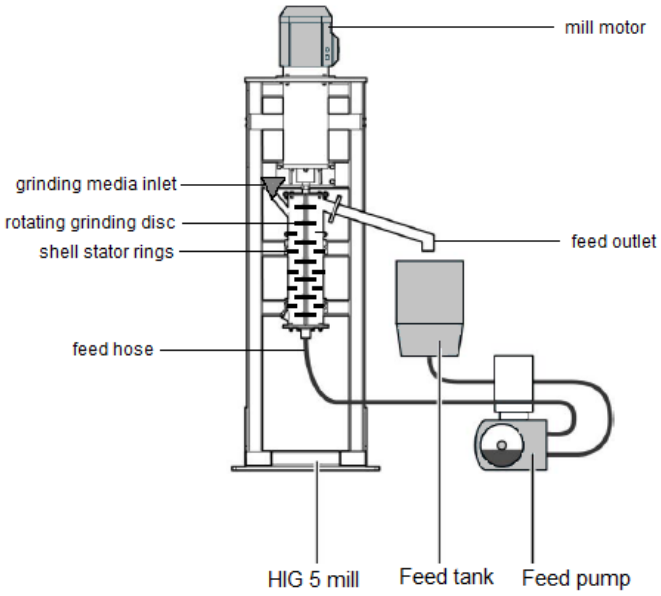

Figure 3-2: Test work setup

3.1.1.2 Mill control cabinet

The settings for the mill are entered and adjusted from a control cabinet. The control panel displays the mill speed, mill power and mill torque. There is a USB slot where a computer can be connected to log the experimental data for data analysis.

3.1.1.3 Mill auxiliary equipment

The mill auxiliary equipment includes the mill feed tank and the mill feed pump. The feed tank is an agitated feed tank with baffles, and the agitator is mounted on top. The agitation setup is to ensure that the feed suspension is well mixed. The feed pump inlet is connected to the feed tank and the outlet is connected to the mill. The feed tank conveys the slurry into the mill via the feed pipe.

3.1.2 Flotation cell

The flotation tests were carried out to establish the flotation response from the different grind levels produced by the HIGmill. The UCT 3 L Barker flotation cell was used for the batch flotation tests. This cell is made of clear Perspex, which enables monitoring of the froth height. The cell has an air regulator that allows the air flow rate in the cell to be varied. There is also an impeller attached at the top of the cell to allow the cell contents to be agitated.

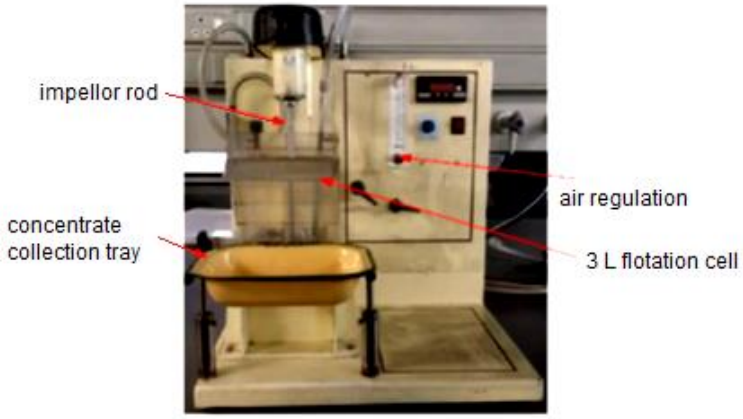

Figure 3-3: UCT 3 L Barker flotation cell

3.1.3 Ore type

The ore used in the scope of work was Upper Group 2 (UG2) chromitite ore. South Africa is the largest producer of platinum group elements in the world. The main ore bodies for Southern Africa are UG2 (~60%), Merensky (~24%), Platreef (11%) and the Great Dyke (~5%) (Mudd, 2010). The UG2 reef accounts for the majority of the PGM ore reefs, and the strategies to maximise the recoveries in this ore body require explanation. The ore has a pegmatoidal feldspathic pyroxenite and chromitite mineral composition (Becker et al., 2008). The 4E-PGE grade of UG2 ore is between 3 g/t and 6 g/t, with a high chromite content between 49% and 80% (Little, 2016). The high chromite content of the ore affects downstream smelting processes because the chromite decreases the smelter efficiency due to its high stability at high temperatures (Becker et al., 2008). When using conventional grinding equipment, comminuting UG2 platinum ore is more energy intensive than comminuting other ores because it is considered a hard ore (Cramer, 2001). The UG2 ore is also fine-grained, with a PGM particle size of <10 µm, and therefore requires finer grinding for adequate liberation to occur. Table 3-1 lists the properties of the UG2 platinum ore.

Table 3-1: Characteristics of UG2 ore (Ramlall, 2013)

Upper Group 2 (UG2) chromitite ore	
Rock type	chromite
PGE content	4–10 ppm
Ni content	700 ppm
Cu content	180 ppm
BMS content	<1%
BMS grain size	30 µm
PGM grain size	up to 10 µm
Density	4 g/m^3

3.1.4 Media type

The grinding media used was Keramax Z grinding media supplied by Magotteaux. Keramax Z is ceramic and designed for use in the IsaMill, HIGmill and the VXP. Table 3-2 lists its specifications. Three grinding media diameter sizes were used for the scope of the thesis: 2 mm, 3.5 mm, and 5 mm.

Table 3-2: Grinding media specifications.

Keramax Z Grinding media	
Available mm	0.5–6
Chemical components	Al_2O_3, ZrO_2, Others
Specific density (g/cm^3)	>3.9
Bulk density (t/m^3)	2.3
Hardness (Vickers, Hv10)	1500
Sphericity (%)	99
Colour	white
Typical application	IsaMill, HIGmill, VXP

3.2 Test Methodology

The test work carried out compromised of comminution only tests to understand the relationship between energy and product size for the different media sizes. The second set of tests involved comminuting the particles under carefully selected grinding conditions and subjected the ground product to batch flotation tests to assess the flotation response of the comminuted product.

3.2.1 Design of experiments

The milling experiments for the flotation test work had a three-factorial design to ensure that all the interactions between the various factors were studied. Each factor was studied at three levels. Thus, the total number of experiments carried out was 27, as shown in Figure 3-4. All the experiments were repeated to assess their reproducibility. Table 8-3 in the Appendix shows the test work matrix that is depicted in Figure 3-4. Additional milling experiments were conducted to assess the effect of the media volume fill and the effect of varying the grinding media size distribution (monosized media and variable sized media).

The three factors that were investigated in the test work were grinding media size, solids concentration and mill speed. The grinding media sizes investigated were 2 mm, 3.5 mm and 5 mm because these are the most commonly used sizes for fine grinding. The solids concentrations tested were between 40% and 60% because these are the solids concentration ranges used in studies conducted with stirred media mills (Mankosa, Adel & Yoon, 1989; Jankovic, 2003). The HIG5mill has a minimum speed of 350 rpm and a maximum speed of

1200 rpm. The test work was done at the low speed of 350 rpm, a midpoint at 700 rpm and the high point at 1050 rpm.

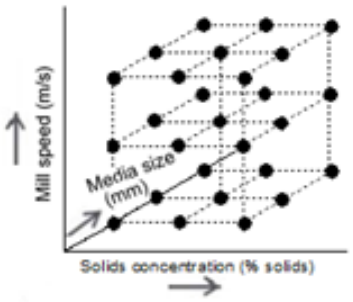

solids concentration [% solids]	tip speed [rpm]	grinding media size [mm]
40	350	2
50	700	3.5
60	1050	5

Figure 3-4: Factorial design with 3 factors and 3 levels showing the levels of each variable.

3.2.2 Sample preparation

A sample of UG2 platinum ore was obtained from one of the mines in South Africa. Four drums of sample from the primary mill product were shipped (in slurry form) to the University of Cape Town (UCT). Before carrying out any test work, the ore was homogenised to ensure that each test was carried out on a sub-sample with similar composition and other characteristics, such as particle size distribution. The procedure for homogenisation involved drying the sample from each drum separately and splitting the dried ore. Before splitting the ore, it was screened using a 1000 µm sieve to ensure a uniform top size.

The dried ore was split using a 10-way rotary splitter to obtain 10 bags. The 10 bags of ore were further split to obtain 100 bags. In the final splitting iteration, the homogenised samples were split using a rotary splitter and packed into 3-kg bags in preparation for the tests. To check that the blending procedure had resulted in homogenous samples, the particle size distributions (PSDs) of three random samples were analysed. Figure 3-5 shows the feed PSD obtained for the UG2 ore. The PSDs were also used to establish the ore top size. The PSDs obtained from the random samples shows that the blending and homogenisation process yielded samples with similar PSDs.

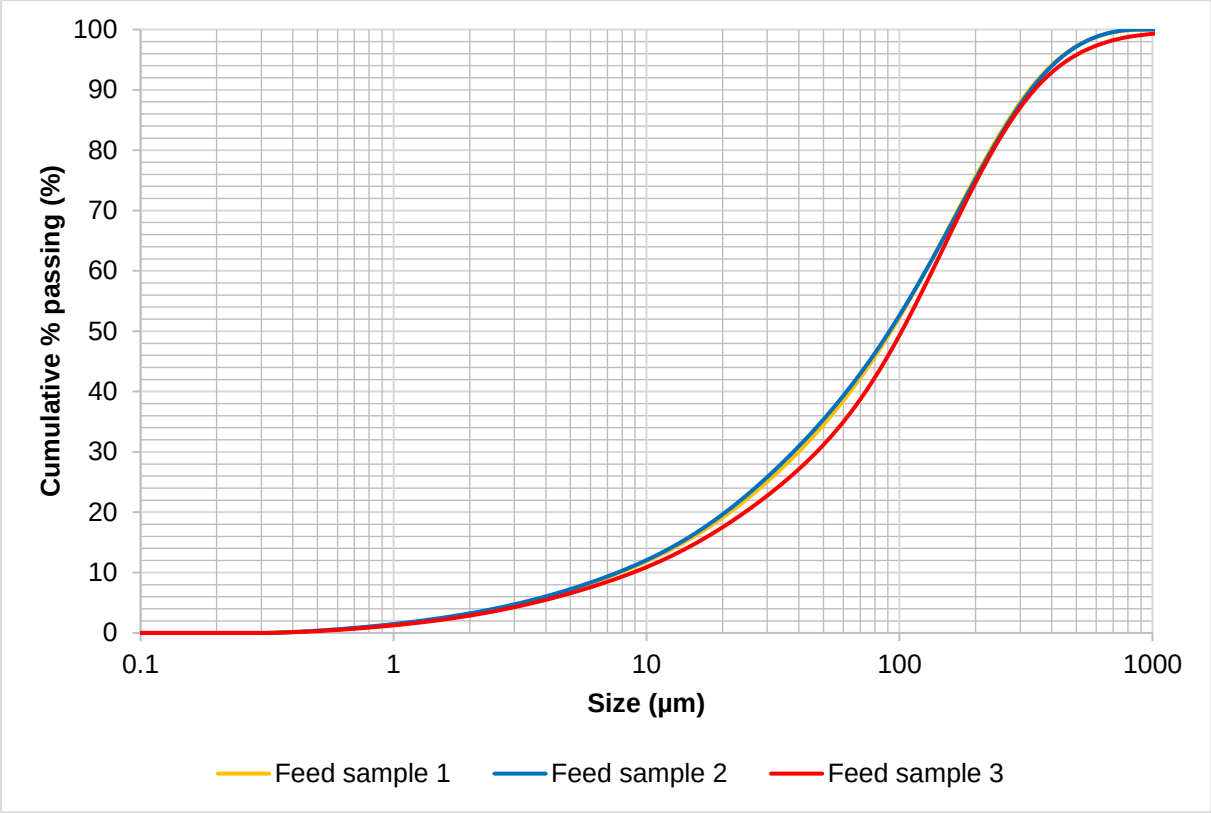

Figure 3-5: Particle size distributions of blended UG2 ore samples

3.2.3 Media preparation

The grinding media was conditioned before carrying out the tests to simulate the grinding media that would be used in large-scale operations. Media conditioning was done by charging the mill with the required volume of media and water. The mill was run at test work midpoint parameters (700 rpm tip speed) for an hour. After it was dried and weighed to ensure its mass had not changed, the conditioned media was used for the test work.

3.3 Experimental Setup

3.3.1 Test methods

The various tests that can be run using the HIG5 are batch tests, semi-continuous tests and continuous tests.

3.3.1.1 Batch test

The batch test is a small sample test where the mode has a fixed speed for a set time. In this test, the sample mass is 3–9 kg.

For the small sample test, grinding media, ore and water are added to the mill. The water and ore quantities required are guided by the solids concentration required by the test matrix (Figure 3-4). The mill is then started up and the stirrer speed set. After grinding for the set time, the mill contents are emptied into a bucket. The slurry and media are separated using a sieve, and the clean media is dried and weighed. The slurry is agitated in a tank with baffles, and the tank product is pumped into a product tank. A sample cut is taken using a sample cutter and the samples are taken for PSD analysis.

3.3.1.2 Semi-continuous test

This test requires a sample mass of 30–50 kg at a flow rate of 120–240 L/hr. The test requires two mixing tanks. Grinding media is added to the mill, the mill is started up and the speed is set. The feed tank pump is then started, and feed enters the mill for grinding. The mill product exits via the mill product outlet and is fed into a product tank. In the semi-continuous test, the product of the first test is used as the feed of the second test. It should be noted that, at the beginning of the second stage, the mill will contain some product from the first stage so the mill should be emptied of the product before the start of the next milling stage. The specific grinding energy (SGE) is the sum of the SGE over the passes. Limitations of the semi-continuous test are that there is a possibility of mixing the feed of the current stage with the product from the previous stage.

For the first pass in the semi-continuous test, the grinding media is added to the mill. The mill is started, and the stirrer tip speed is adjusted according to the test matrix. Water is then poured into the mill to impart motion to the beads. The feed slurry is prepared using 50 kg of ore. To prepare the slurry, the required volume of water is added to an agitated feed tank, then the required ore is added to make up a slurry of the specified solids concentration. Once the feed has been prepared, the feed pump is started, and the slurry is fed into the mill. Since the mill is filled with water before the slurry is pumped into the mill, this water needs to be displaced before any samples and recordings of mill parameters can be taken. To ensure that the water has been displaced, the density should be measured until it reaches a steady state. When a sample is taken, the power, torque and mill speed should be noted from the control panel. One reading is taken at the start of the pass, and a second reading is taken in the middle of the pass. The readings are averaged to give a representative figure for the parameters.

3.3.1.3 Continuous test

The continuous test requires 100–150 kg of dry solids at a flow rate of 240 L/hr. The pump is set to give 1–2 minutes of residence time. The test requires the feed tank and reception tank

the material to be passed through the mill once and mill settings are changed during the test run. Samples are collected within the run.

3.3.1.4 Experimental test method

For the purposes of these experiments, the batch test was used. The feed and the products from these tests were analysed using a Malvern Mastersizer 2000. This equipment uses both the Fraunhofer model and the Mie theory to predict how the light is scattered by spherical particles (Malvern Instruments, 2007). Using the Fraunhofer model and Mie theory, it calculates the size of the particles that create a light pattern because each particle has a distinctive scatter pattern (Malvern Instruments, 2007).

3.3.2 Milling procedure

3.3.2.1 Mill calibration

The HIG5mill was calibrated before commencing the test work to ensure that its parameters were within specifications and that the measurements taken during the test work would match what was expected by the equipment manufacturers. Calibration tests were carried out using water and 4 mm MTX Magotteaux grinding media. The calibration tests were run using three different media fillings: 30%, 45% and 60%. For each media filling, three different water flow rates were used: 60 l/h, 120 l/h, and 240 l/h. During each grinding media filling and water flow rate test, the mill motor speed was varied (from the control box) using 10% increments and the corresponding frequency (Hz), VSD motor power (W), measured torque (Nm) and motor power (W) were recorded. The motor power was calculated using the torque arm model from Bonds Model according to Equation 13.

Equation 13

$$P = \frac{2\pi TN}{60}$$

Where P is the motor power, T is the recorded torque in Nm and N is the motor speed in rpm.

The calibration showed that the mill motor power and the shaft speed are not affected by a change in the water flow rate. Figure 3-6 shows the calibration curve obtained for a test conducted at a media fill of 30%. The curves for the tests conducted at 45% and 60% media fill are shown in the Appendix.

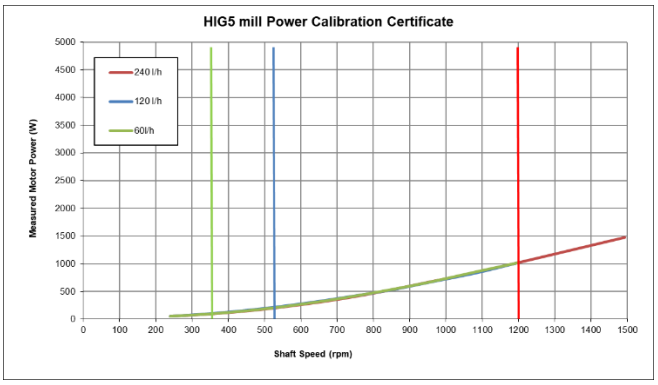

Figure 3-6: HIG mill calibration certificate (30% media fill)

3.3.2.2 Mill power

The mill power draw is an important parameter to measure throughout the experiments. The recorded power draw is used to calculate the specific energy consumption of the mill. For the specific energy consumption calculations, the net power draw is used. The net power is the difference between the gross power draw and the no-load power draw. The no-load power of the mill, which is the power when the mill is running without media or slurry, needs to be determined. The no-load power draw is obtained by calculating the power draw when the mill is empty for different stirrer speeds. The no-load power for the stirrer speeds tested is given in Table 3-3.

Table 3-3: Average no-load power for the different stirrer speeds

Tip speed [rpm]	Frequency [Hz]	Power [kW]			Average power [kW]
		5 min	10 min	15 min	
305	10	0.16	0.16	0.16	0.16
453	15	0.16	0.16	0.16	0.16
601	20	0.17	0.17	0.17	0.17
748	25	0.19	0.19	0.19	0.19
898	30	0.22	0.22	0.22	0.22
1049	35	0.26	0.26	0.26	0.26

3.3.2.3 Mill speed

The stirrer speed was adjusted by changing the mill frequency from the control panel of the mill. The output mill speed is given in revolutions per minute (rpm). Calibration tests were performed to discover the mill frequency inputs required to determine the desired stirrer speeds in rpm. Figure 3-7 shows the results obtained from the mill speed calibration tests carried out.

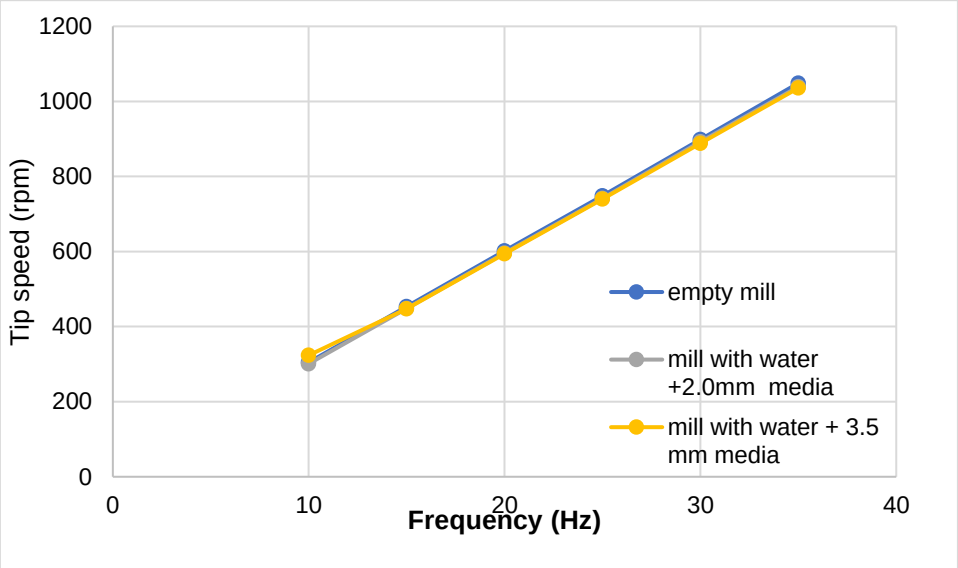

Figure 3-7: Mill speed calibration

3.3.2.4 Media load

The recommended media load for the HIGmill is 60% so the media load was kept at 60% for the main experiments. The mass of the media required was calculated by using the net media volume and a void space of 0.4, which is the widely used void space for the ceramic media. Additional experiments were also conducted to see the effect of media load on the grind, as shown in the test matrix in Table 8-3. The additional media fillings tested were 40%, 50% and 70%.

3.3.2.5 Experimental run

The mill was then filled with grinding media (grinding media filling was dictated by the test matrix). Dry ore and water were then added to the mill. The required frequency (determined by the frequency curve) for the desired mill speed was then input on the mill control box. The mill was then started and run for 3 minutes. The milling grinding time was determined by grind curve experiments conducted prior to the test work. The power draw, stirrer speed and mill torque were monitored and recorded throughout the experiment to give information on the stability conditions of each test run.

3.3.3 Flotation procedure

For the tests involving flotation, 3 kg of ore was milled under the desired grind conditions. The HIGmill product was transferred into the 3-L Barker flotation cell and synthetic plant water (SPW) was added to the 2 cm froth height mark. To minimise the particle loss during the transfer from the mill to the flotation cell, the mill product was transferred in slurry form and the

SPW used to make it up to the 2 cm froth height was used to rinse the container. The impeller was run at 1200 rpm. After running the impeller for more than a minute (to ensure the cell contents were in suspension), a 50 ml feed sample was collected using a syringe. A depressant, Sendep 30F, was added at 20 g/t and then a collector, SIBX, was added 2 minutes after the depressant addition at 100 g/t. The conditioning time after the addition of the reagents was 2 minutes, after which a frother, Dow 200, was added at 20 g/t and conditioned for 1 minute. Air was then introduced at 7.5 L/min.

Froth was collected in pre-weighed concentrate trays every 15 seconds, ensuring that the froth height stayed at 2 cm by adding SPW water when needed. After 2, 4, 6 and 8 minutes of froth collection, concentrates C1, C2, C3 and C4 were collected, respectively. Once the C4 sample was collected, the air was switched off, and two 50-ml tailings, T1 and T2, were collected. The air and impeller were switched off. The bulk tails sample was collected. Each flotation test was repeated to increase confidence in the results obtained. A schematic of the procedure for the batch flotation process is depicted in Figure 3-8.

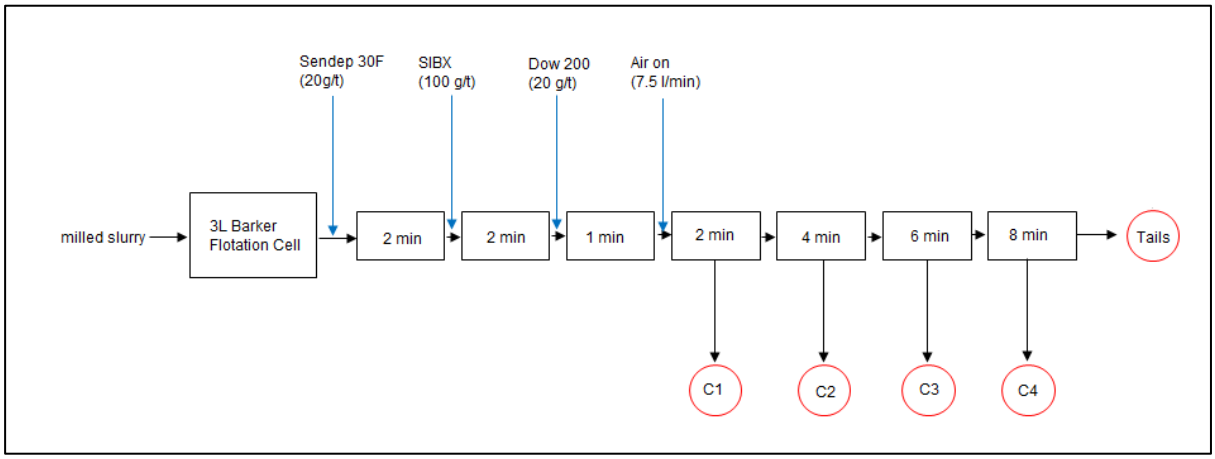

Figure 3-8: Batch flotation procedure

The feed, concentrate and tailings samples collected were then filtered using pre-weighed filter paper for mass pull calculations. The samples were oven dried at 80 °C to prevent oxidation of the sulphides. Dried samples were weighed, and the masses recorded. The samples were rolled out into powder form and bagged in labelled bags to be sent for analysis at the analytical laboratory.

3.3.4 Sample processing

3.3.4.1 Milling sample

From the milling test work, a representative sample was taken for Malvern analysis of the PSD of the sample.

3.3.4.2 Flotation sample

The samples collected from the flotation test work were sent to the Lonmin analytical laboratory, where they were analysed for 4E and base metals.

4. ASSESSMENT OF MILLING PERFORMANCE

This chapter reports the results obtained from the experimental work conducted using the HIGmill to assess the influence of some operating variables on grinding and flotation performance. The variables that were tested on the HIGmill were the stirrer tip speed, the solids concentration, the grinding media size, and the media filling.

4.1 Methods Applied to Analyse the Comminution Data

There are many ways to assess the milling performance of grinding equipment. The milling results in this study were evaluated in terms of PSD per variable, power, signature plots, and size specific energy performance. The stress intensity as also analysed for the experiments run in the scope of work.

The various methods used to analyse and interpret the results obtained from milling the UG2 ore are described the following sections.

4.1.1 Particle size distribution per variable

The PSD was analysed to see the fineness of grind that was achieved in each experimental run. The PSD analyses were carried out using the Malvern Mastersizer. PSD data from the Malvern Mastersizer was used to generate the PSD curves that are presented in the results section. The P80 was also studied to determine the fineness of grind achieved under the different milling conditions. The P80 is the particle size at which 80% of the material will pass when screened (Van Schoor & Sandenbergh, 2012).

4.1.2 Power

Mill parameters have an effect on the power draw of the mill. The power consumption of the mill is an important parameter to monitor as it is used to determine the efficiency of the equipment. In the analysis, the net power was considered.

4.1.3 Signature plots

Signature plots are used to depict the relationship between the product size and the energy input. Signature plots are shown in the results section to depict the relationships observed between the milling energy and the product size (P80).

4.1.4 Size specific energy

The specific energy consumption was calculated using the mill net power draw, the grinding time and the quantity of the ore used in the milling test. In this study, the specific energy and the P80 were used in signature plots to measure the milling energy efficiency. However, using the P80 is limiting when comparing energy efficiency across different mills as some mills, such as the SAG mill, do not have parallel product size distributions in a log-log space (Amelunxen & Meadows, 2011; Ballantyne & Giblett, 2019). Ballantyne & Giblett (2019) proposed the size specific energy (SSE) method as an alternative as it does not have the limitations associated with using the P80.

The SSE method involves evaluating the milling energy efficiency by measuring the energy consumed in the generation of fines (Ballantyne & Giblett, 2019). Since the requirement in this study involved evaluating how much sub 20 µm material was produced, the size specific energy was assessed using the -20 µm production rate. According to Rittinger's law of comminution, energy input is proportional to the generation of new surfaces (Ballantyne et al., 2015). To apply this law, the generation of −20 µm material was used as a proxy for the surface area. The effect of the operating variables on the size specific energy was also analysed to determine the efficiency of the HIGmill.

4.1.5 Stress intensity

Kwade (1999a) described stress intensity as a measure of the specific energy required for breakage to occur in a specific stress event. The concept of stress intensity was described in Section 2.5 and will be applied in this chapter. The effect of gravitational forces on the stress intensity was not considered in this study because the high stirrer speeds used in the experiments resulted in high centrifugal forces that were more dominant than the gravitational forces (Jankovic, 2003).

The stress intensity model was applied to the UG2 ore, and the results are presented in this section. The equation applied to the experimental data was Equation 4.

Equation 14

$$SE \propto SE_{GM} = {d^3}_{GM}\, \rho_{GM}\, {v^2}_t$$

where SE_{GM} is the grinding media stress energy (Nm), d_{GM} is the grinding media diameter (m), ρ_{GM} is the grinding media density (kg/m^3), ρ is the slurry density (kg/m^3), and v_t is the stirrer tip speed (m/s).

Applying the stress intensity model helps to select the optimal operating conditions.

4.1.6 Stirrer tip speed

The tip speed is an important variable in stirred mills because the energy transfer from the media to the particles being broken is facilitated by the rotation of the stirrer. Therefore, a wide range of stirrer speeds was considered in the tests performed. The stirrer tip speeds investigated in this study varied between 350 rpm and 1050 rpm. The tip speed range that was used to carry out the experimental work in this thesis was informed by the ranges of the tip speeds that were used in past studies, as highlighted by Table 2-3 in the literature review. The selection of the mill speed range was also determined by the laboratory equipment because the HIG5mill operated at between 350 rpm and 1200 rpm with a recommended nominal speed of 520 rpm (STM Minerals, 2019).

4.1.6.1 Effect of tip speed on PSD and P80

Stirrer tip speed affects the fineness of the mill product. This was studied using 5 mm grinding media at 50% solids concentration. The 5 mm grinding media was chosen over 3.5 mm grinding media because it performed similarly to 3.5 mm grinding media, and more data points for the mill tip speed were generated for this grinding media size. The 50% solids concentration was chosen because it was the central point for the solids concentration data. Figure 4-1 shows that increasing the tip speed of the stirrer results in a finer product. The same trend was observed when using 3.5 mm and 2 mm grinding media as shown in the Appendix. This is due to the increase in the shear rate, which causes the grinding action. Wang & Forssberg (2000) noted that increasing stirrer speed in the wet grinding and dry grinding of dolomite not only resulted in a finer product but also gave a narrow particle size distribution. The resultant finer product is because high tip speeds increased interaction frequency and intensity between the media and the dolomite particles Wang & Forssberg (2000). Ouattara & Frances (2014) conducted similar studies on a calcite suspension and noted that the increase in stirrer tip speed resulted in a finer product for the same grinding time. Figure 4-3 shows the results obtained from Ouattara & Frances (2014). The results observed with a particular grinding media size were consistent across the different solids concentrations tested, and the relevant PSD plots can be found in the Appendix.

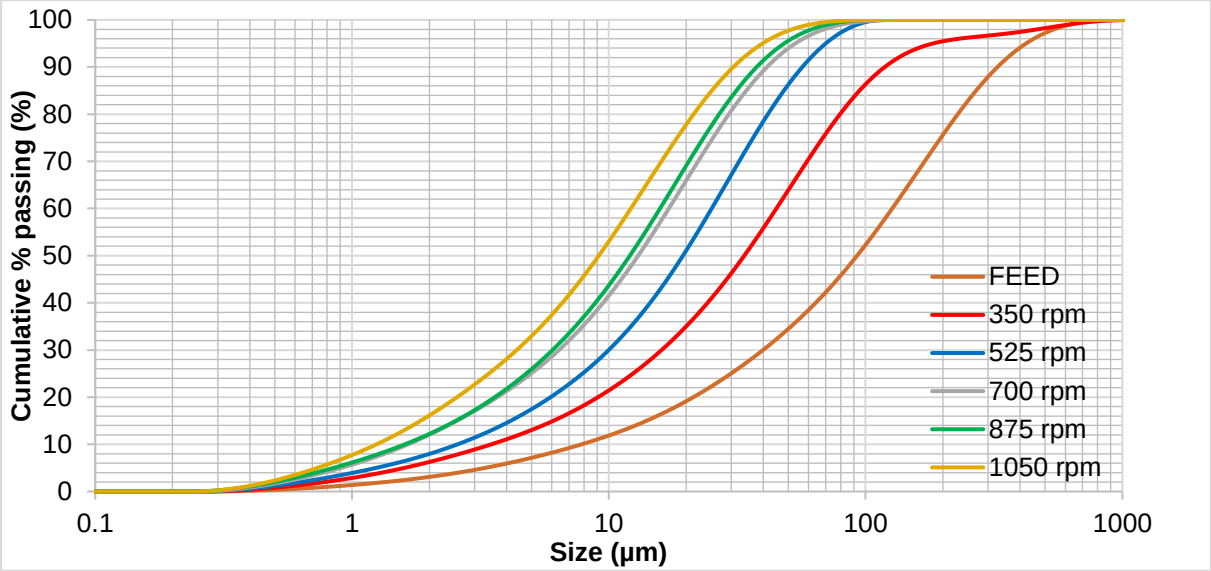

Figure 4-1: Effect of mill speed on product PSD at 3 min grinding time, 50% solids concentration, and a grinding media size of 5 mm

The effect of the tip speed on the P80 was analysed using 5 mm grinding media at a solids concentration of 50%. The increase in tip speed from 350 rpm to 1050 rpm resulted in a decrease in the P80 from 79.6 µm to 21.3 µm, as shown in Figure 4-2(a). The trend is similar to what Santosh et al. (2020) obtained when they conducted experiments with a PGE ore and the NETZSCH laboratory vertical stirred mill, as shown in Figure 4-2(b). In both studies, a sharp decrease in P80 was obtained from stirrer speed in the region of 350 to 600 rpm, after which a gradient change in P80 with stirrer tip speed was exhibited. This is because there is an optimum tip speed for certain milling conditions and, as the optimum tip speed is approached, there is an increase in the kinetic energy of the grinding media, which results in high stress intensities and higher particle breakage rates (Hasan, 2016; Santosh et al., 2020). After the optimum tip speed has been reached, there is minimal change in the product P80 and, if a change in P80 needs to be realised, other milling parameters, such as grinding media size, should be changed.

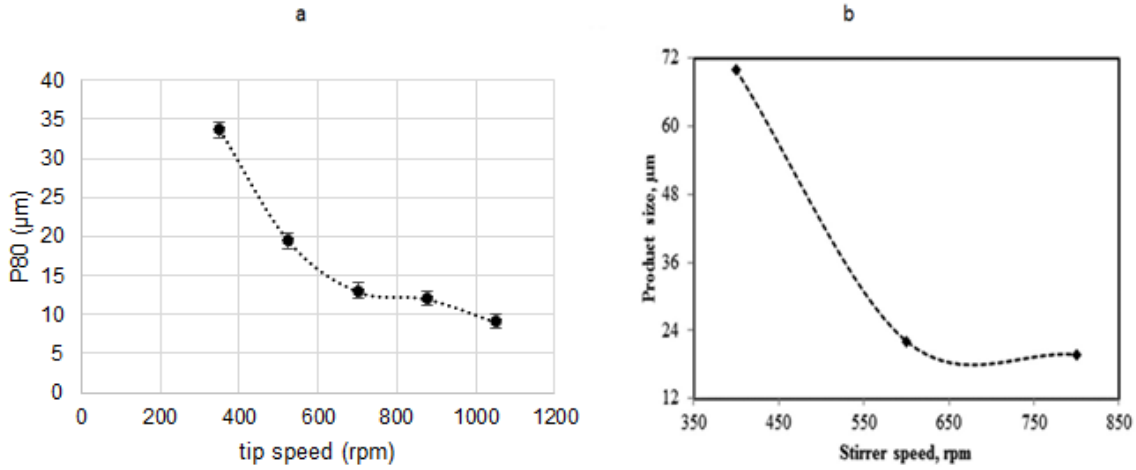

Figure 4-2: Effect of tip speed on P80 (a) HIGmill using 5mm grinding media (b) NETZSCH mill (Santosh et al., 2020)

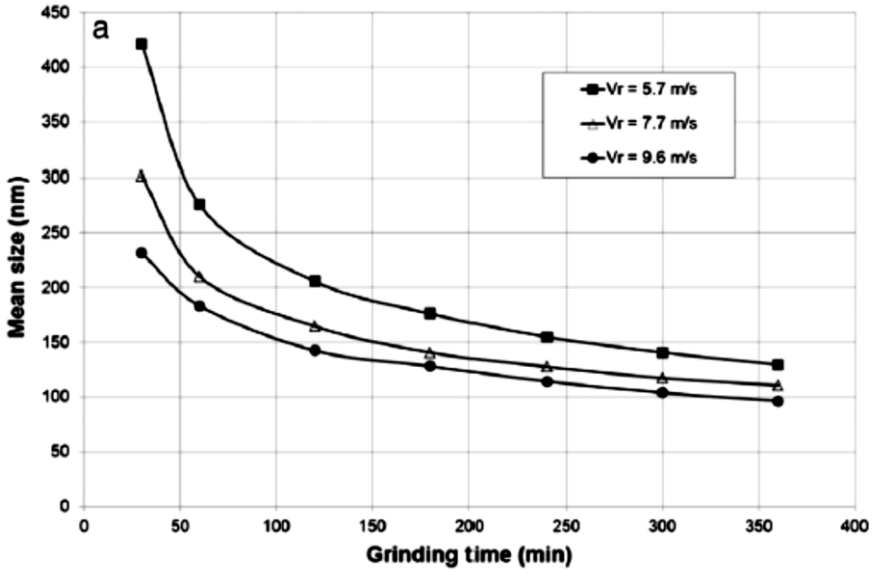

Figure 4-3: Effect of stirrer tip speed on grinding result (Ouattara & Frances, 2014)

4.1.6.2 Effect of tip speed on power draw

Figure 4-4 shows the effect of the tip speed on the power draw for the experiments performed using the HIGmill on the UG2 platinum ore. The effect of the tip speed on power was investigated using 5 mm grinding media at a 50% concentration of solids. Power draw increased from 0.5 kW to 4.3 kW with an increase of tip speed from 350 rpm to 1050 rpm. Zheng et al. (1996) made similar observations when they increased stirrer speed from 400 rpm to 1500 rpm; they also noted that an increase in stirrer speed resulted in an increase in volume-based power draw from 0.02 Wh/cm^3 to 0.19 Wh/cm^3.

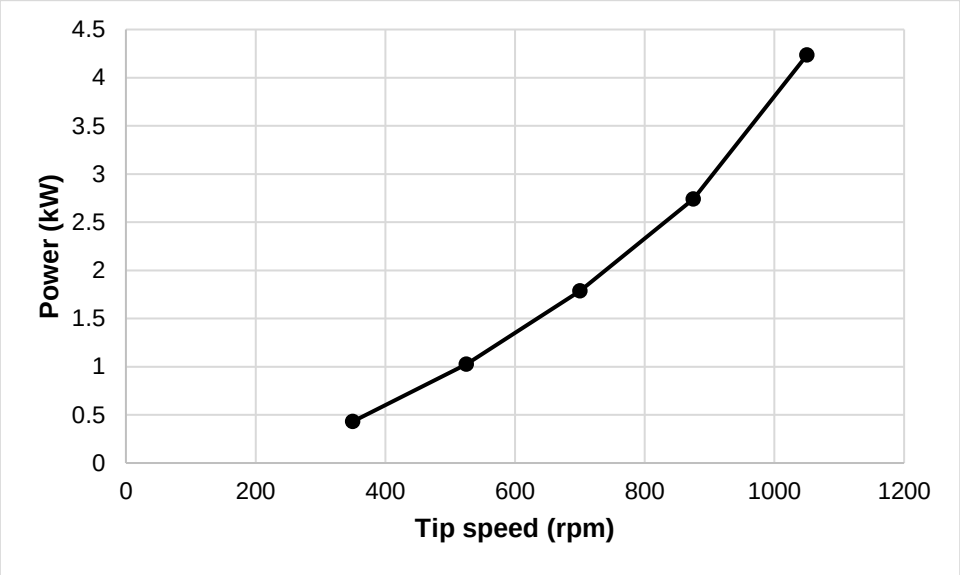

Figure 4-4: Effect of tip speed on power for 5 mm grinding media at a 50% concentration of solids

4.1.6.3 Signature plots

Specific energy is a function of the mill power draw, the grinding time, and the product quantity. The specific energy increased with the increase in stirrer tip speed for the range of tip speeds tested. The trends observed in this work are in agreement with the findings of Jayasundara et al. (2010), who reported an increase in energy consumption with an increase in impeller speed. The relationship between stirrer tip speed and energy consumption is similar to that of power and, since the specific energy is a function of power and the quantity of ore, and the grind time was kept constant for the experiments. Figure 4-5 shows the signature plots for the effect of tip speed on the specific energy and the resultant P80 for 5 mm grinding media. Increasing the tip speed results in a finer product and a higher energy consumption. The line of best fit was used to determine the most efficient tip speed, and it was observed that a tip speed of 700 rpm gave a finer product at lower energy consumption.

Similar signature plots were generated for 2 mm grinding media as shown in Figure 4-6 and 3.5 mm grinding media as shown in the Appendix, and they also showed that increase in the tip speed resulted in an increase in the specific energy. It was also observed that the specific energy at a speed of 1050 rpm for 5 mm grinding media (11.23 kWh/t) was over double that observed for 2 mm grinding media at 1050 rpm (5.12 kWh/t). Lisso, (2012) conducted tested to evaluate the effect the tip speed on the energy consumption and also noted that the increase in tip speed increased the energy consumption. When experimenting using the IsaMill to grind

a UG2 ore, Chaponda, (2011) noted that there was an optimum stirrer speed to operate the IsaMill which was in accordance with the findings of (Yang et al., 2006).

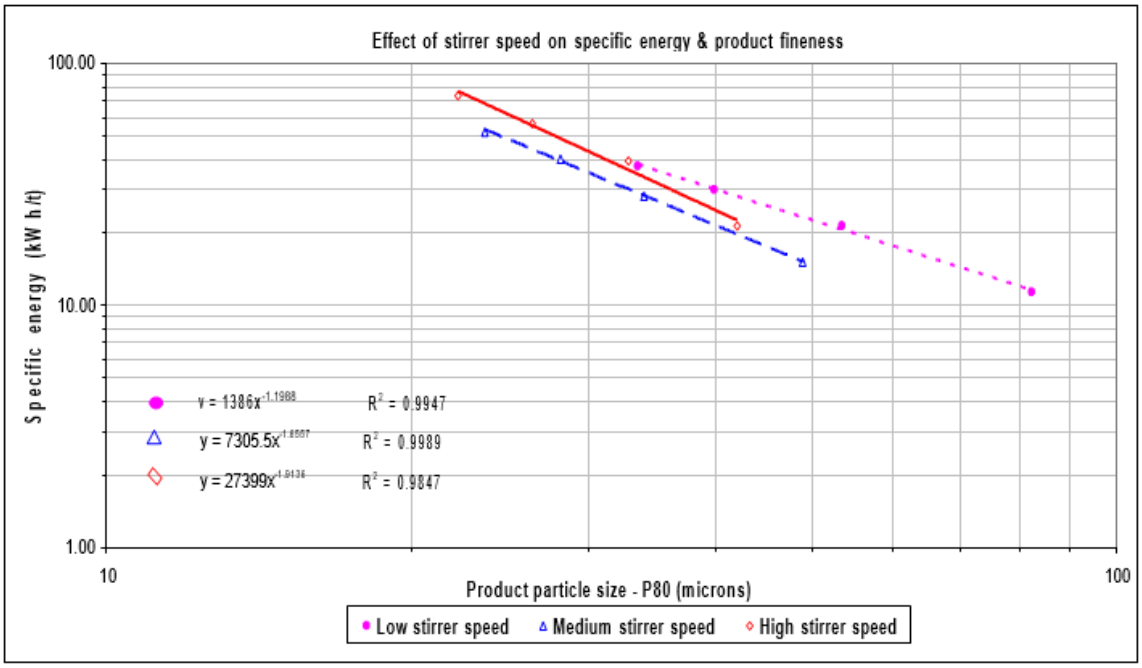

Figure 4-7 shows the results obtained by Chaponda, (2011) which show the optimum stirrer speed was the high speed.

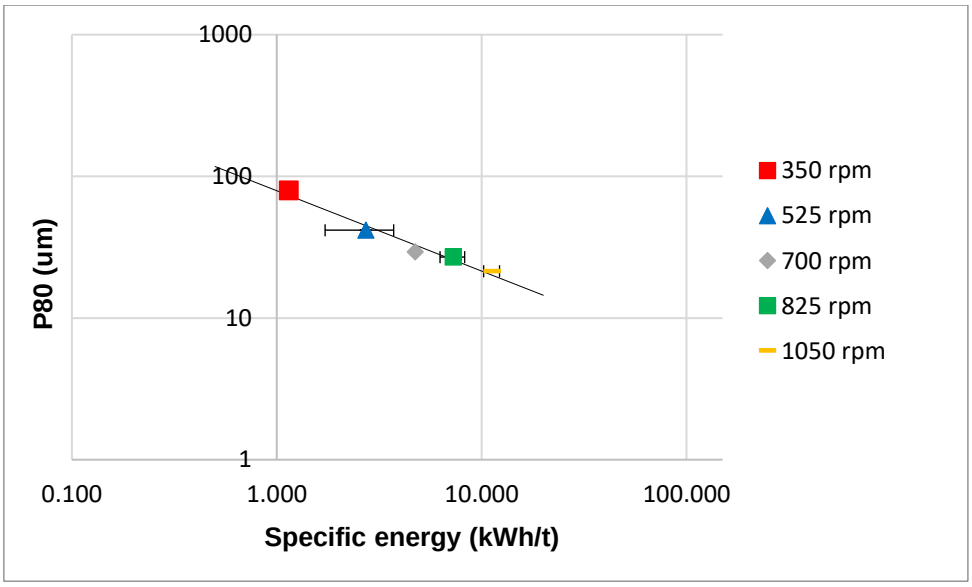

Figure 4-5: Signature plot showing the effect of tip speed on the specific energy using 5 mm grinding media at solids concentration of 50%

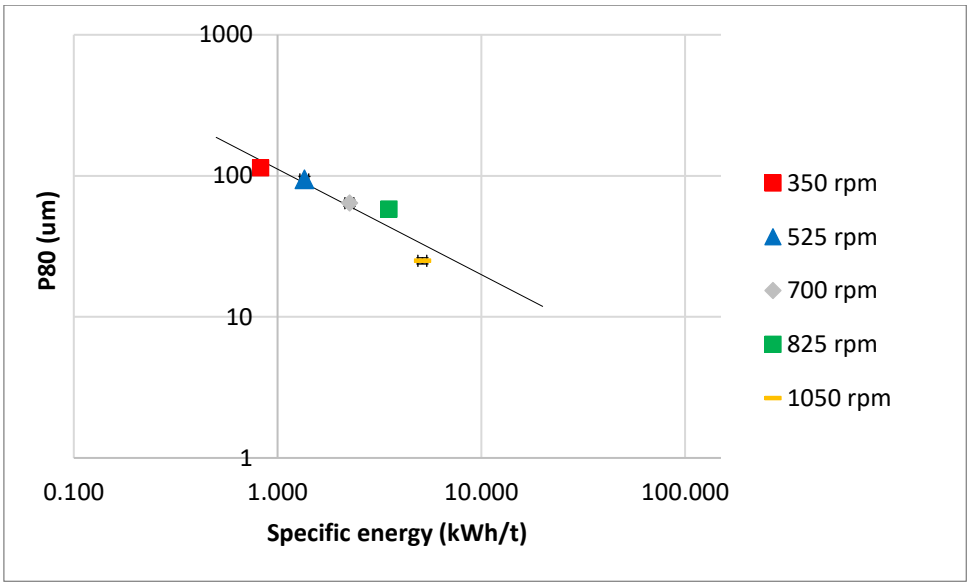

Figure 4-6: Signature plot showing the effect of tip speed on the specific energy using 2 mm grinding media at solids concentration of 50%

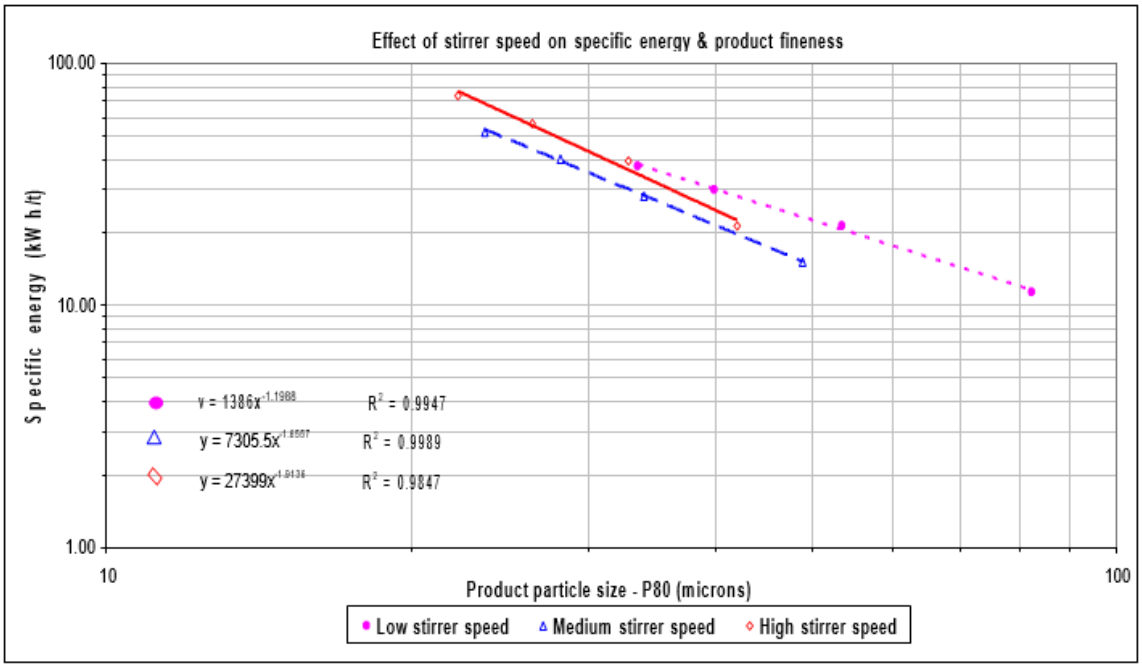

Figure 4-7: Effect of stirrer tip speed on specific energy and product fineness (Chaponda, 2011)

4.1.6.4 Effect of tip speed on size specific energy consumption

The energy required to produce new −20 µm was calculated for experiments performed at different tip speeds. A line of best fit was plotted for the data to show the expected percentage passing 20 µm for a given energy input. Figure 4-8 shows that the tip speed of 700 rpm was

the most efficient tip speed because it produced a higher fraction of sub 20 µm material. Speeds of 300 rpm and1050 rpm produced less sub 20 µm product than predicted by the line of best fit. Similar trends were observed using the 5 mm grinding media at 50% and 60% solids concentrations.

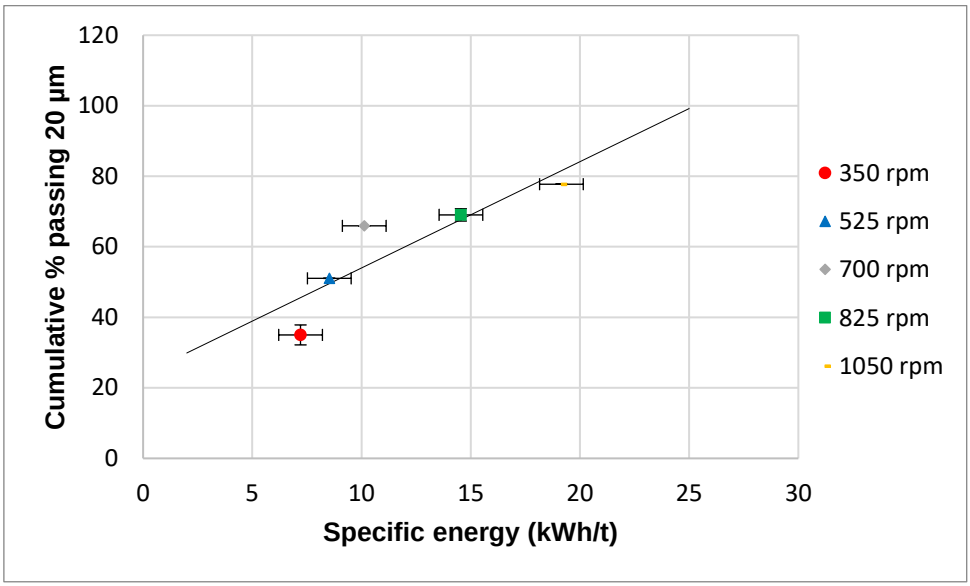

Figure 4-8: Size specific energy of different tip speed at 5 mm grinding media and solids concentration of 50%

4.1.7 Solids concentration

The solids concentration is an important parameter in fine grinding as it has an impact on both energy consumption and product fineness (Zheng et al., 1996). Operating a stirred mill at its optimum solids concentration allows the mill to be energy efficient and it also can result in an increase in mill throughput (Hasan, 2016). The solids concentration was investigated by varying the solids concentration between 40% and 60% at the different grinding media sizes. The range of solids concentrations used in the study was informed by stirred mill studies conducted by other scholars (Zheng et al., 1996; Jankovic, 2003; Gao & Holmes, 2008; Chaponda, 2011; Lisso, 2012)

4.1.7.1 Effect of solids concentration on PSD and P80

Solids concentration is known to influence the product size in wet grinding comminution equipment because in-mill rheology is affected by the solids concentration (He et al., 2006). If the solids concentration is too high, the mill rheology is altered and the resultant high slurry viscosity results in a decrease in media velocity (He et al., 2006). Ouattara & Frances (2014)

experimented with calcite and established that the lower calcite solids concentration also resulted in a finer grind.

The PSD results from the experiments show that there is an interaction between the grinding media size and solids concentration. The effect of the solids concentration was tested using 2 mm, 3.5 mm and 5 mm grinding media at a tip speed of 700 rpm. The tip speed of 700 rpm was selected because it is the centre point for the tip speeds tested in the experiments. Figure 4-9 shows the particle size produced from the feed size after batch grinding at three different solids concentrations with 5 mm grinding media. The high solids concentration of 60% gave a coarser product but there was no significant difference between the product fineness obtained at solids concentrations of 40% and 50%. This aligns with the observations of Ouattara & Frances (2014). Although the solids concentration of 60% did obtain a coarser product, it was not significantly different from the PSDs resulting from the solids concentrations of 40% and 50%. This is reflected in the P80 values (28. 3 µm, 29.3 µm, 30.9 µm, respectively) that were obtained at these solids concentrations. These observations are consistent with those obtained with 3.5 mm grinding media (centre point grinding media) at 700 rpm. For the 2 mm grinding media, a similar trend was noted, except that, at the P80 mark, the graphs showed significantly different P80 values. This indicates that grinding media size has an influence on the distribution of the product. Repeats of the experiments run with the solids concentration can be found in the Appendix.

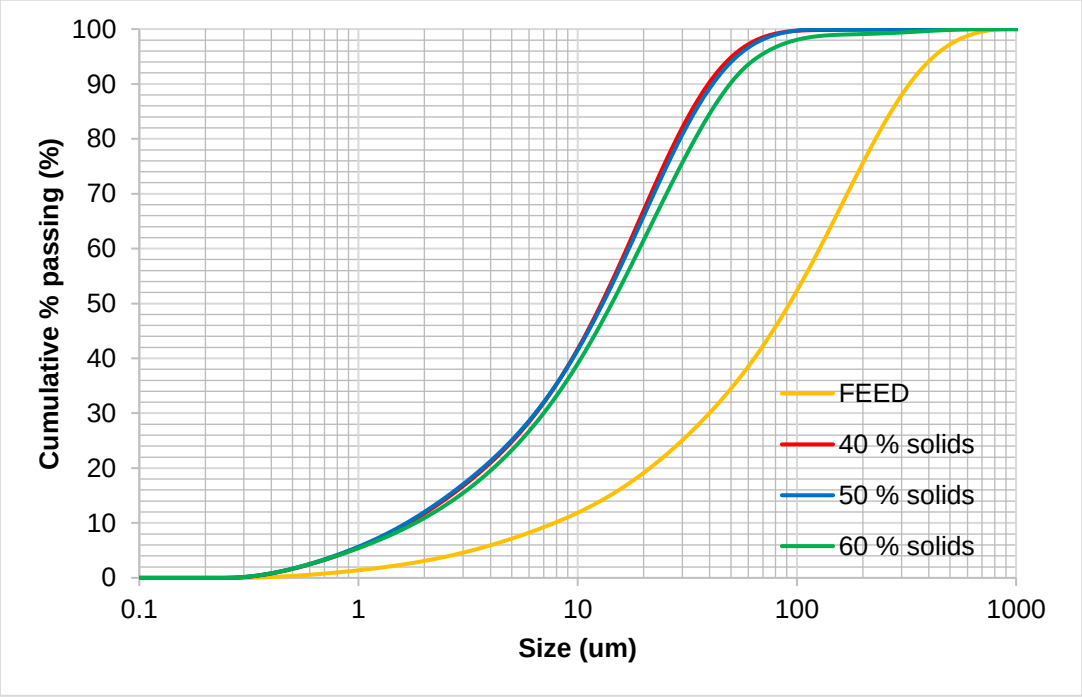

Figure 4-9: Effect of solids concentration on PSD for 5 mm grinding media at 700 rpm.

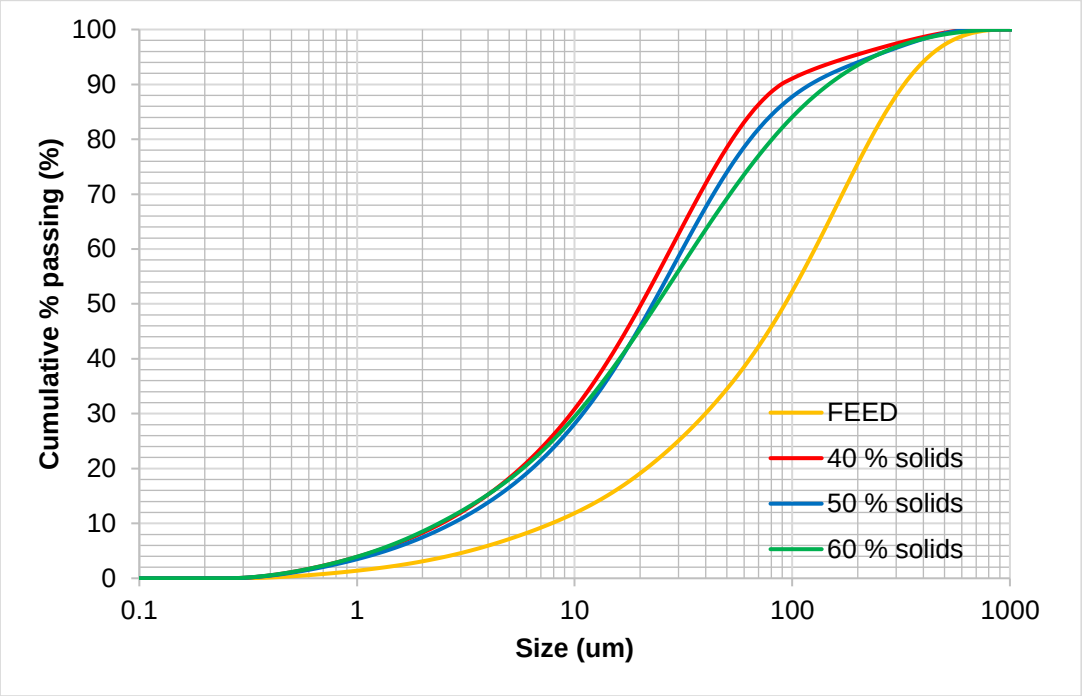

Figure 4-10: Effect of solids concentration on PSD for 2 mm grinding media at 700 rpm.

4.1.7.2 Effect of solids concentration on power draw

The solids concentration has an effect on the slurry viscosity (Kwade, 1999b; Napier-Munn et al., 2005). As the solids concentration increases, the viscosity increases exponentially (Napier-Munn et al., 2005). In continuous comminution circuits, the viscosity influences the mill power draw. However, in the batch experiments conducted, the solids concentration had little effect on the power draw. This indicates that it was the slurry transportation coupled with the solids concentration that impacted the power draw of the mill for the continuous tests. Table 4-1 shows the recorded mill power at 40%, 50% and 60% solids concentration at the different speeds run with the 5 mm grinding media. The table shows that there is no difference between the power draw for different solids concentrations at the same tip speed. The effect of the solids concentration was noted for the 2 mm and the 3 mm grinding media, and these results can be found in the Appendix.

Table 4-1 Recorded mil power at the different solids concentration

Tip Speed	Solids Concentration	Power
350	40	0.48
	50	0.43
	60	0.45
525	40	1.02
	50	1.03

	60	0.88
700	40	1.84
	50	1.78
	60	1.83
875	40	2.97
	50	2.73
	60	2.85
1050	40	4.20
	50	4.23
	60	4.18

4.1.7.3 Signature plots

Solids concentration is an important factor in stirred milling as it affects energy consumption. Figure 4-11 shows how the solids concentration affects the P80 and that there is no significant difference in the fineness of grind obtained for the same specific energy input with different solids concentrations when using 5 mm grinding media. This observation was in contradiction to the findings of Stenger et al. (2005), who observed that an increase in solids concentration resulted in a finer product at the same energy input. Stenger et al. (2005) attributed it to the fact that an increase in the solids fraction results in more ore particles being captured in the grinding zone and therefore leads to increased milling efficiency. Results obtained by Stenger et al. (2005) are shown in Figure 4-14. Jankovic (2003) tested 40%, 55% and 64% solids with a SAM mill and also noted that the higher solids concentration of 64% resulted in a finer product because the increased solids concentration minimised the media-to-media interactions. The results observed with the 5 mm grinding media could be because the particles have reached their limit of fineness with that grinding media size and thus changing the solids concentration has no effect. When using 3.5 mm grinding media, the solids concentrations behave similarly to observations made by Stenger et al. (2005) and Jankovic (2003).

The signature plot generated to observe the effect of solids concentration using a grinding media size of 3.5 mm showed that there is no significant difference between the efficiency of the mill at 40% and 50% solids concentration. However, using a solids concentration of 60% was more efficient for energy inputs above 2 kWh/t. The 60% solids concentration gave a finer product, as shown in Figure 4-12.

Using 2 mm grinding media showed that the 40% solids concentration was more energy efficient at producing fine material, whereas the 50% grinding media was the least efficient for energy inputs above 1.5 kWh/t, as shown in Figure 4-13. This may be due to the fact that the combination of the 2 mm grinding media and the high solids concentration does not result in

enough fluidization of the mill contents, so the breakage mechanisms are not in full effect. Whereas at 40% solids the media is fluidized adequately and break the particles.

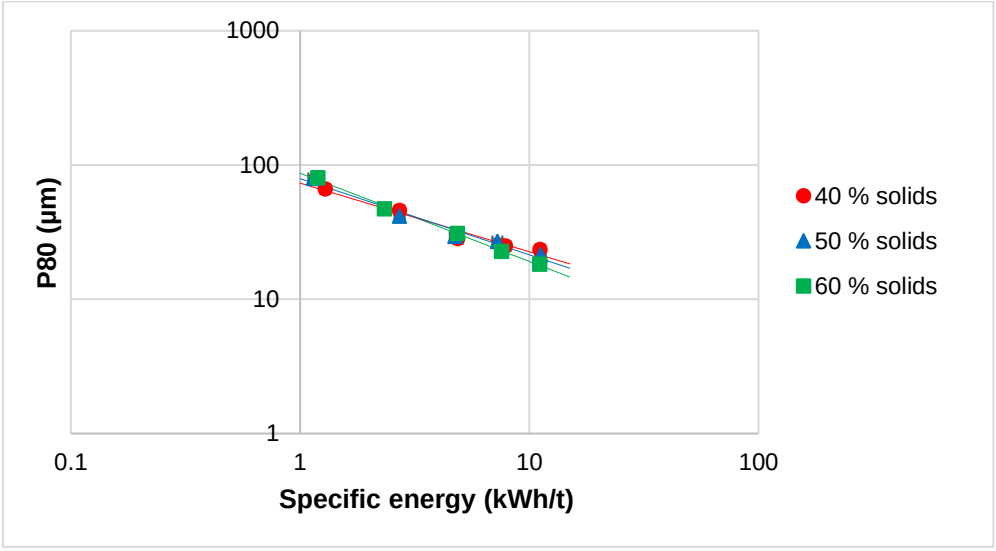

Figure 4-11: Signature plot to show the effect of solids concentration on specific energy and P80 for 5 mm grinding media

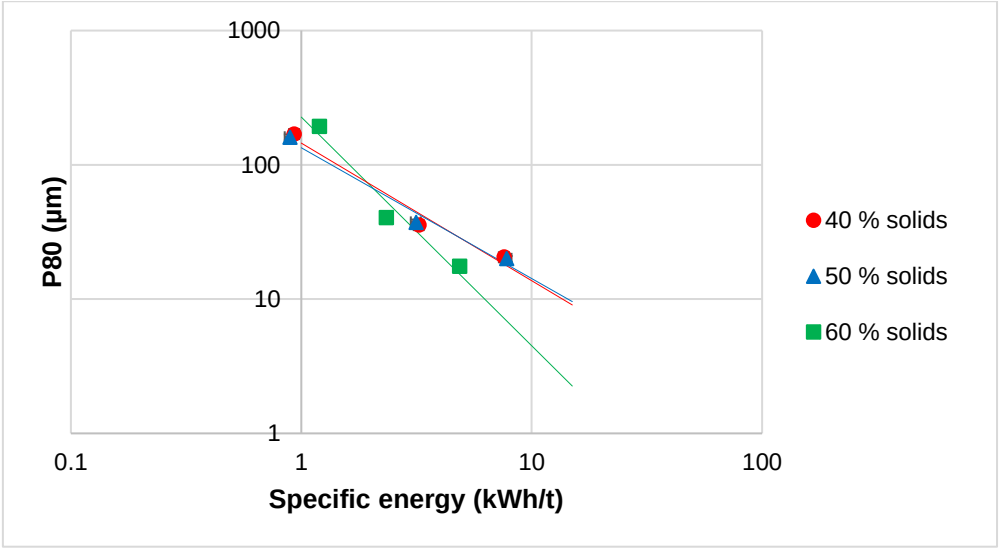

Figure 4-12: Signature plot to show the effect of solids concentration on specific energy and P80 for 3.5 mm grinding media

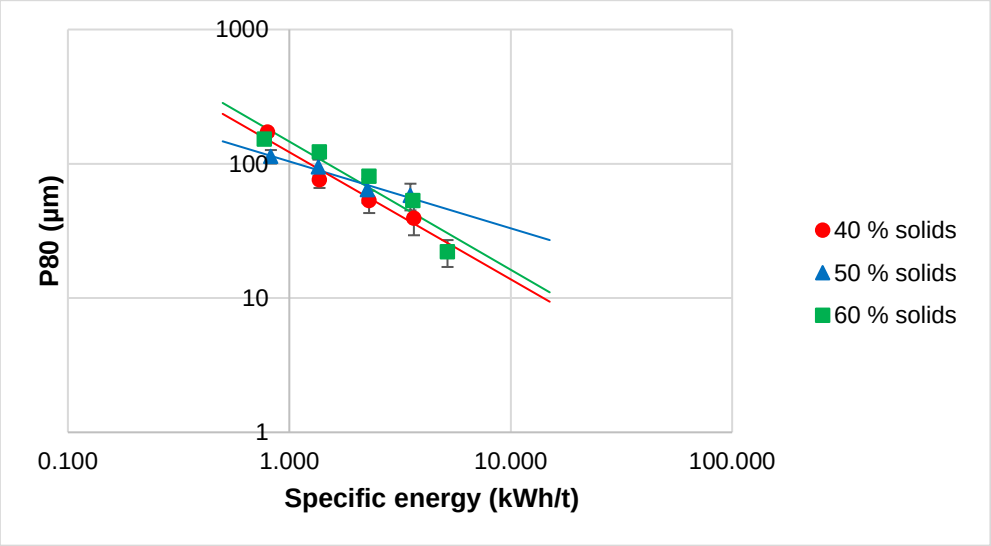

Figure 4-13: Signature plot to show the effect of solids concentration on specific energy and P80 for 2 mm grinding media

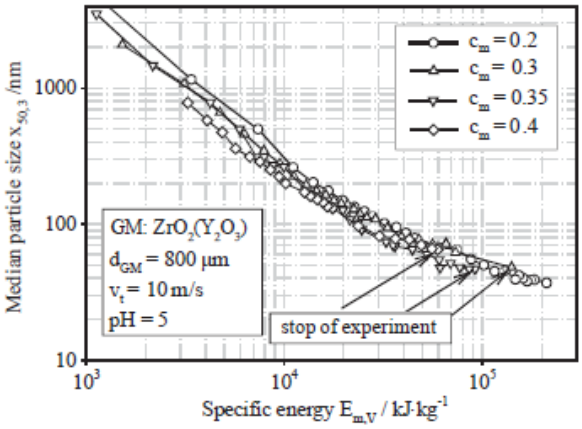

Figure 4-14: Effect of increase in solids fraction on median particle size (Stenger et al., 2005)

4.1.7.4 Effect of solids concentration on the size specific energy consumption

The effect of the solids concentration on the size specific energy was analysed for solids concentrations between 40% and 60% for the 5 mm grinding media. Data points for the size specific energy were plotted, along with their respective trendlines. The graph shows that, at specific energies greater than 10 kWh/t, a solids concentration of 60% gave a product with more sub 20 µm particles. As the specific energy increased, the 40% solids concentration gave less product with 20 µm particles than the 50% solids concentration and the 60% solids concentration. Figure 4-15 shows how the 40%, 50% and 60% solids concentrations performed at producing sub 20 µm material when using 5 mm grinding media. The results obtained with 3.5 mm grinding media are shown in the Appendix. The size specific energy

behaviour of the solids concentration using 3.5 mm grinding media behaved similarly to the solids concentration behaviour noted when using 5 mm grinding media. When using 2 mm grinding media, it was noted that the solids concentration 60% gave the least sub 20 µm product. This observation may be attributable to the fact that, at high solids concentrations, the grinding media motion is dampened by the increase in solids concentration, which reduces the stress intensities. At high solids concentrations, there are not enough media-to-particle spaces which also reduces the number of stress events in the mill, whereas the opposite is true for solids concentrations of 40%. The difference in the solids concentration behaviour shows that there is an optimum solids concentration and grinding media combination for efficiently grinding UG2 ore. The results observed for 2 mm grinding media are shown in Figure 4-16.

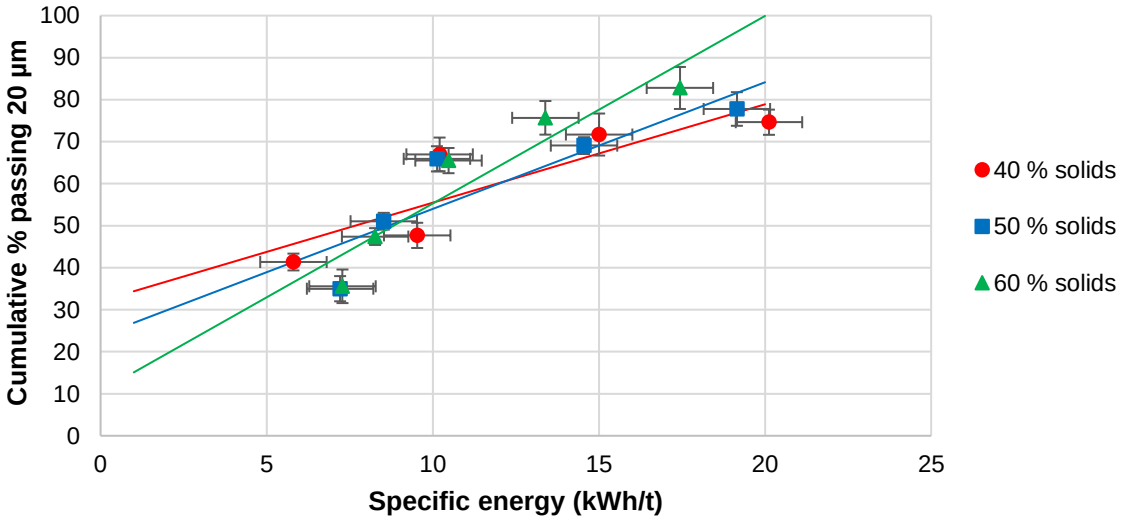

Figure 4-15: Size specific energy for 40%, 50% and 60% solids concentration using 5 mm grinding media

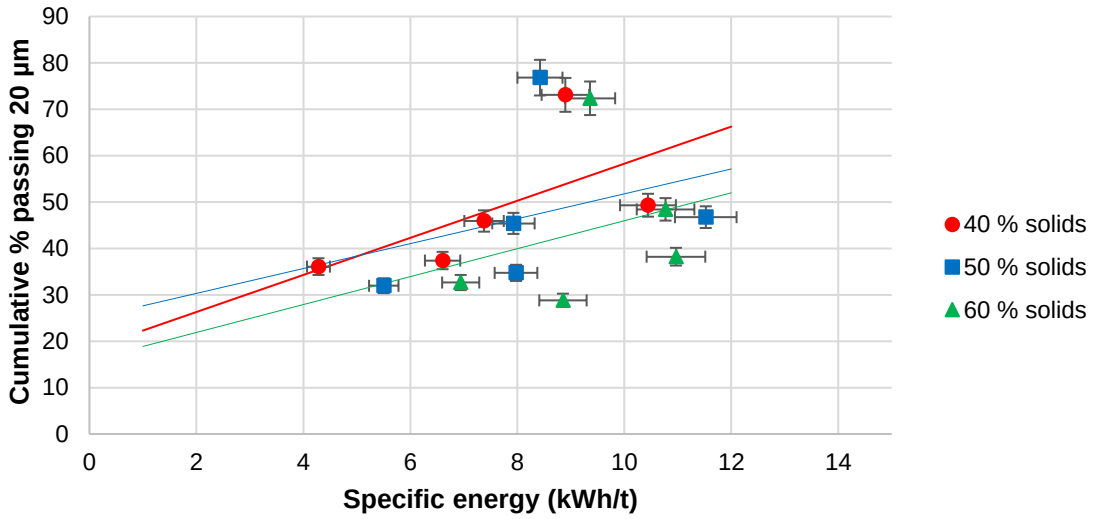

Figure 4-16: Size specific energy for 40%, 50% and 60% solids concentration using 2 mm grinding media

4.1.8 Grinding media

Grinding media is an important parameter in stirred milling because it affects the quality of the grind and it also affects the grinding energy consumption (Jankovic, 2003; Ouattara & Frances, 2014). The impact of grinding media was investigated using Keramax grinding media. The grinding media is one of the factors that affect the fluidisation of the mill. For efficient grinding to take place in the HIGmill, the grinding media has to be sufficiently fluidised (Scott & Gutsche, 1999). Three aspects of the grinding media were tested: grinding media size, grinding media size distribution and the grinding media volume.

The effect of the grinding media size was investigated using three media sizes at stirrer speeds of 350 rpm to 1050 rpm, and solids concentrations of 40% to 50% and the media filling was kept constant at a volume of 60%. The experiments were carried out to investigate the influence of media grinding, media filling and grinding media, and PSD tests were carried out at a solids concentration of 50%. The impact of grinding media size distribution was also tested by using different ratios of the 2 mm, 3.5 mm and 5 mm grinding media. These experiments were conducted to determine the optimal grinding media size, grinding media filling and grinding media PSD to be used in the comminution of UG2 ore.

4.1.8.1 Grinding media volume fill

Grinding media volume fill is an important factor in stirred milling because it affects the energy efficiency of the mill (He, Wang & Forssberg, 2006; Rahal, Erasmus & Major, 2011). The effect of the grinding media volume fill was tested using 5 mm grinding media at a solids concentration of 50%. The volume fillings degrees used in the study were 40%, 50%, 60%,

70%. The selection of the grinding media volumes was influenced by the volumes that were studied in literature and the recommended media filling range for the HIG5mill, which is 30%–75%.

4.1.8.1.1 Effect of grinding media volume fill on PSD and P80

The grinding media filling affects the fluidisation of the because increasing the grinding media fill decreases the porosity of the system and reduces the cavity size that is formed near the shaft when grinding media is fluidised. If the media filling is too high for the milling conditions, the grinding media may not be adequately fluidised, and it gives a coarse milled product. It was expected that increasing the media filling will result in a finer product because of increased grinding surfaces and the increase in compressive force that comes with increasing the media load (Yang et al., 2006). Figure 4-17 shows how the grinding media filling affected the PSD. The finest PSD was obtained with a grinding media fill of 60%. The coarsest PSD was obtained with a grinding media fill of 40%. This demonstrates that there is an optimal grinding media fill that the HIGmill should be operated at, which is in line with the observations made by Gao & Holmes (2008). The data indicates that the optimal media filling for the 5 mm grinding media at 700 rpm was 60%, which was the media fill that gave the finest product. The P80s for the different speeds in the range 350–1050 rpm were plotted, and they show that a 40% media fill gave a coarse P80 for all the speeds in the range. At 700 rpm and 525 rpm, a media filling of 60% gave the finest product, followed by 70% and then 50% media fill. There was no significant difference in the P80 product sizes that were observed for 50%, 60% and 70% media fillings when the mill was operated at speeds of 350 rpm, 825 rpm and 1050 rpm, as shown in Figure 4-18.

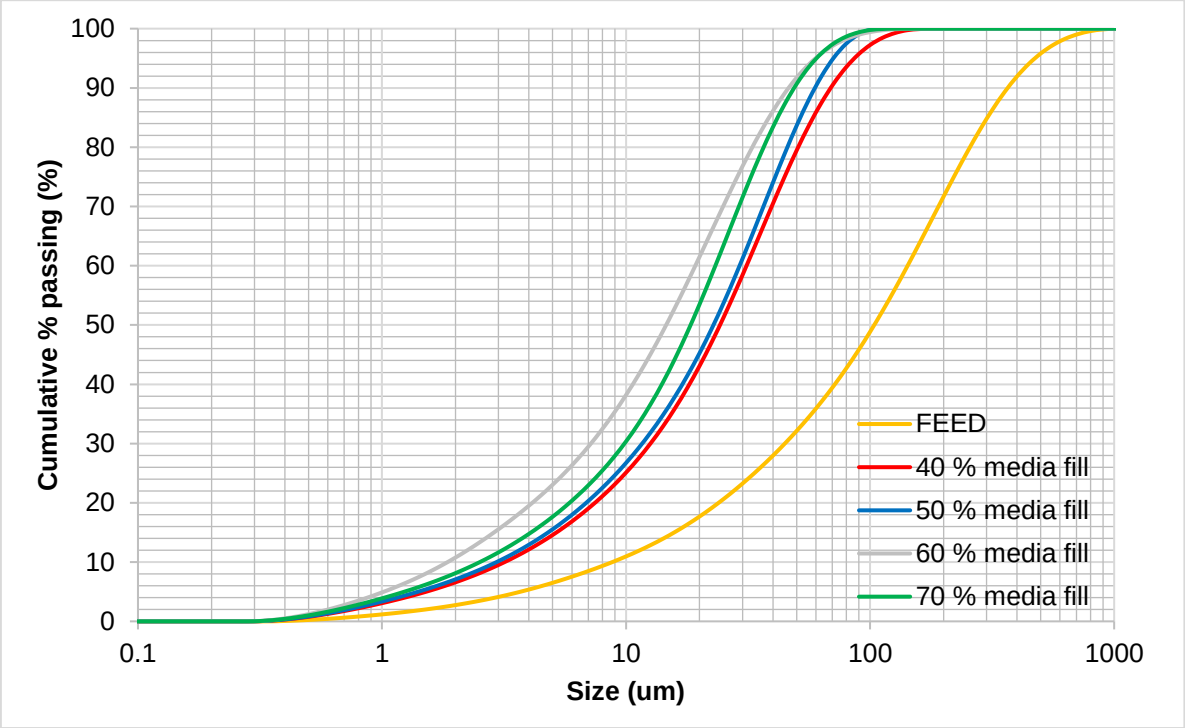

Figure 4-17: Effect of grinding media fill on PSD for 5 mm grinding media at 700 rpm

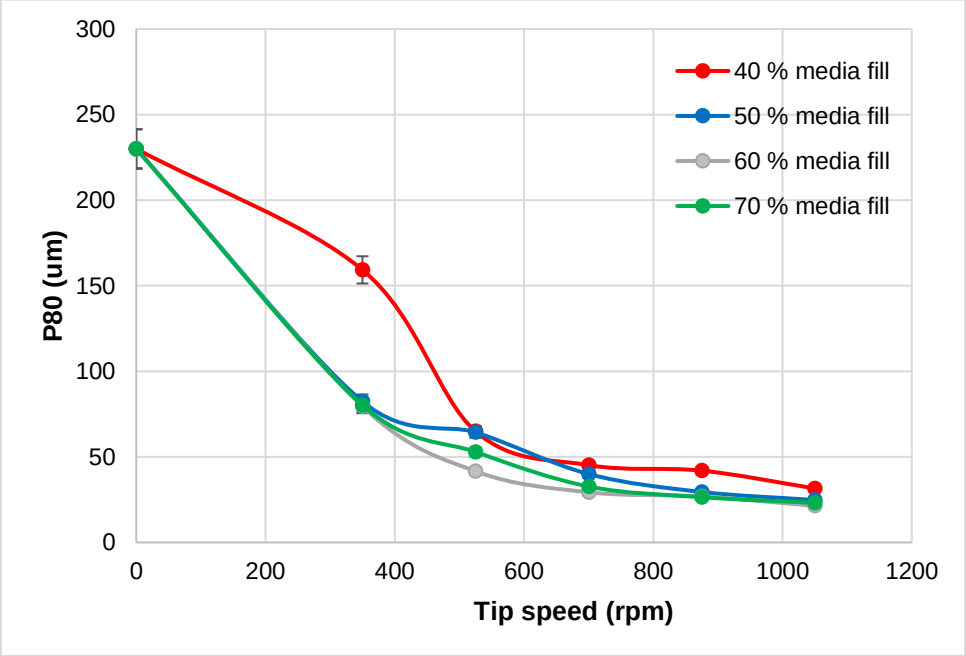

Figure 4-18: Effect of grinding media fill on the P80 using 5 mm grinding media at tip speeds in the range of 350–1050 rpm

4.1.8.1.2 Effect of grinding media volume on power draw

Increasing the grinding media filling results in an increase in power draw (Hasan, 2016). There is an increase in the power required to put the increased grinding media load in motion. Figure 4-19 shows that a media filling of 70% draws the most power at all the speeds tested in the experiments, and a media fill of 40% draws the least power.

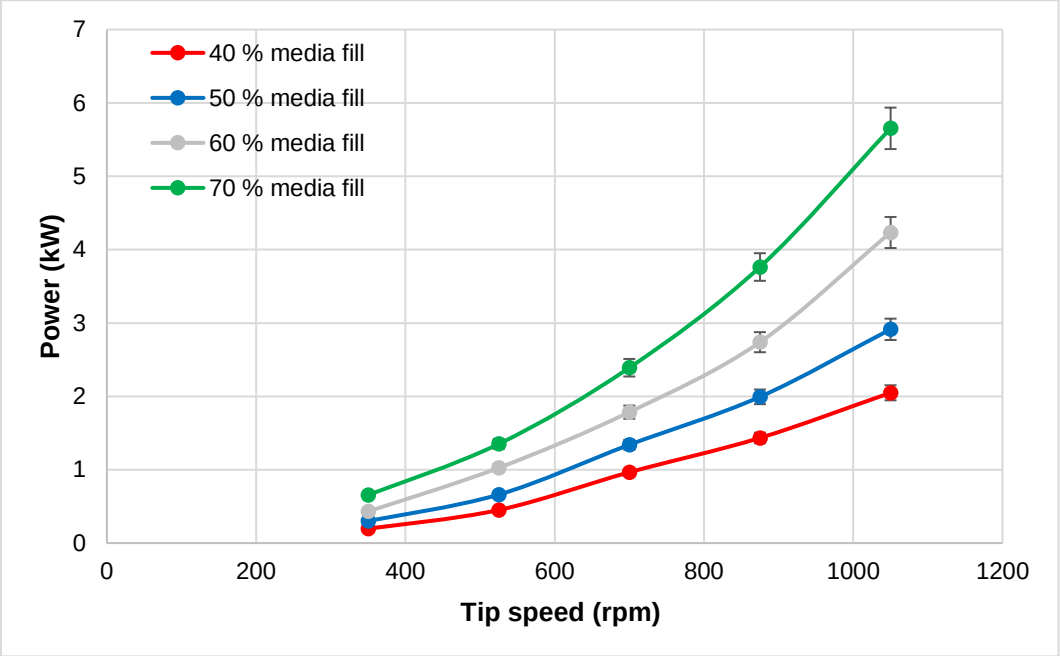

Figure 4-19: Effect of grinding media filling on the power draw for 5 mm grinding media

4.1.8.1.3 Signature plots

Signature plots were plotted for the media fillings tested to analyse the energy efficiency of the media filling. The trend lines show that a media filling of 70% is the least efficient because it needs more energy to achieve the same P80 values, as highlighted in Figure 4-20. To achieve a P80 of 50 µm, a media filling of 70% requires approximately 3.7 kWh/t of energy, whereas the 40%, 50% and 60% media fillings require approximately 2.5 kWh/t, 2.3 kWh/t and 2.3 kWh/t respectively. A media filling of 40% requires more energy to produce the same P80 size as the 50% and 60% for P80 values greater than 30 µm, after which the 40% media fill requires less energy to produce products with a P80 less than 30 µm. The data presented here show that, for 5 mm grinding media, a media filling of either 50% or 60% is the optimal choice.

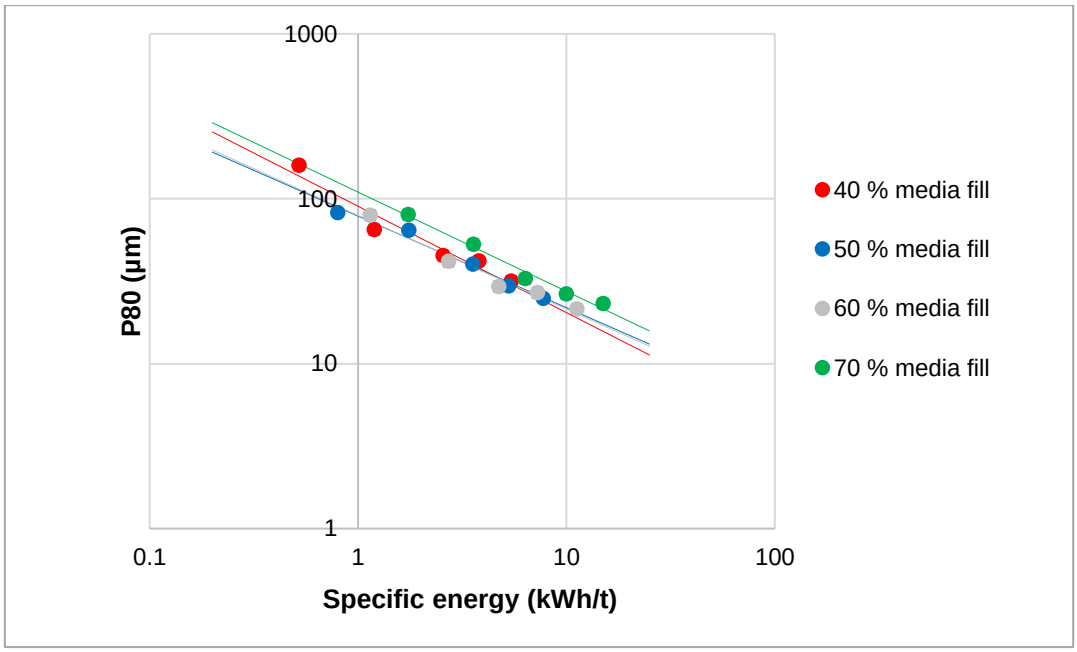

Figure 4-20: Signature plot for grinding media fill using 5 mm grinding media at 50% solids concentration

4.1.8.1.4 Effect of grinding media volume fill on size specific energy

The effect of grinding media volume fill was analysed using the size specific energy method to determine which grinding media fill efficiently produced sub 20 µm particles. For specific energy inputs below 15 kWh/t, a media filling of 60% gave more sub 20 µm particles and, thereafter, a media fill of 50% produced more sub 20 µm particles. This may be because, at higher energy inputs the grinding media is not adequately fluidised to produce sub 20 µm particles. The size specific energy for the different media fillings tested in the scope of work is shown in Figure 4-21.

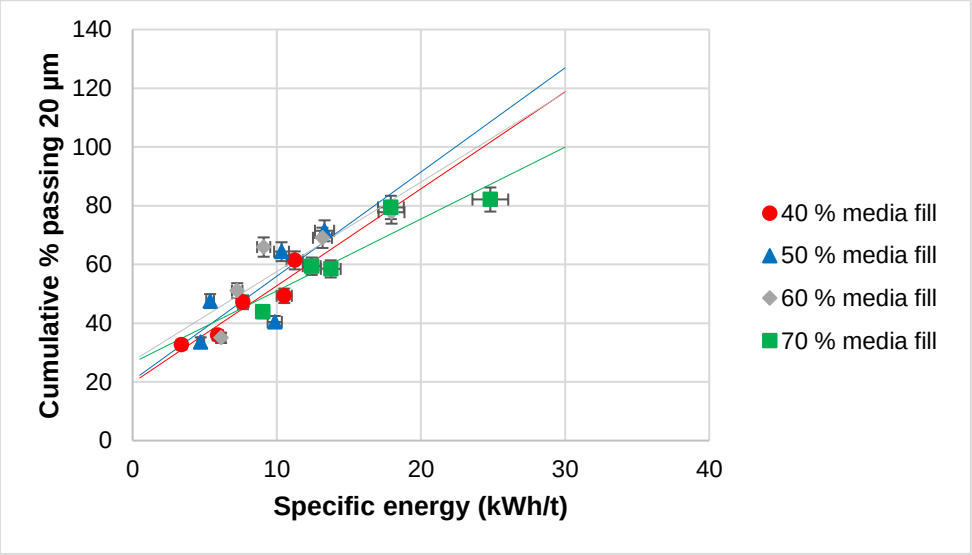

Figure 4-21: Effect of grinding media filling on the size specific energy using 5 mm grinding media

4.1.8.2 Grinding media size

Grinding media size is an important parameter in stirred milling as it affects both product fineness and energy consumption (Mankosa et al., 1986; Jankovic, 2003; de Bakker, 2014). For the scope of this thesis, three grinding media sizes were tested: 2 mm, 3.5 mm and 5 mm. The 2 mm and 3.5 mm were chosen because these sizes fall in the range of media sizes that can be tested using the HIGmill. Other scholars who have studied the effect of grinding media on stirred milling have also used media sizes between 2 mm and 5 mm (Mankosa et al., 1986; Jankovic, 2001; Chaponda, 2011; de Bakker, 2014), which is why the 5 mm grinding media size was also investigated in this thesis. The different sizes were tested to establish the optimal grinding media size for UG2 ore with a top feed size of 1 mm.

4.1.8.2.1 Effect of grinding media size on PSD and P80

The increase in grinding media size resulted in a finer PSD for the UG2 ore with a top size of 1.0 mm, as shown in Figure 4-22. The finer PSD was observed with an increased grinding media size because the larger grinding media provides higher stress intensities than the smaller grinding media (Becker et al., 2001).

The effect of the grinding media size was also studied for different solids concentrations, as shown in Figure 4-23, Figure 4-24, and Figure 4-25. At all the solids concentrations tested, the 5 mm grinding media constantly gave a finer product than the 3.5 mm and 2 mm grinding media because the larger media provides higher stress intensities. In the instances where the

2 mm grinding media gave a finer product, the surface area effect was greater than the stress intensity effect.

At low speeds (<525 rpm), the 2 mm grinding media gave a finer product than the 3 mm grinding media due to the higher frequency of media particle contact for the 2 mm grinding media. The size of the 2 mm grinding media means, at a constant fill of 60%, there is more grinding media than for the 3.5 mm grinding media. At high speeds (>700 rpm), the 3.5 mm grinding media and the 5 mm grinding media behaved similarly and produced similar PSDs and P80s.

The optimal grinding media to feed top size ratio for this study was 5:1. He & Forssberg (2007) experimented with quartzite for ultra-fine grinding and found that the optimal media size to feed was between 150 and 200, whereas Zheng et al. (1996) got a ratio of 12:1 using glass beads, and Mankosa, et al. (1986) recommended a ratio of 20:1 for steel beads. Chaponda (2011) experimented with a PGM ore of top with F80 of 212 µm and noted that the 2 mm grinding media gave a finer product than the 3.5 mm and 5 mm grinding media. The difference between the findings of this study and that of Chaponda (2011) is explained by the finding of Jankovic (2003) that a coarse feed requires larger grinding media than that required by a fine feed.

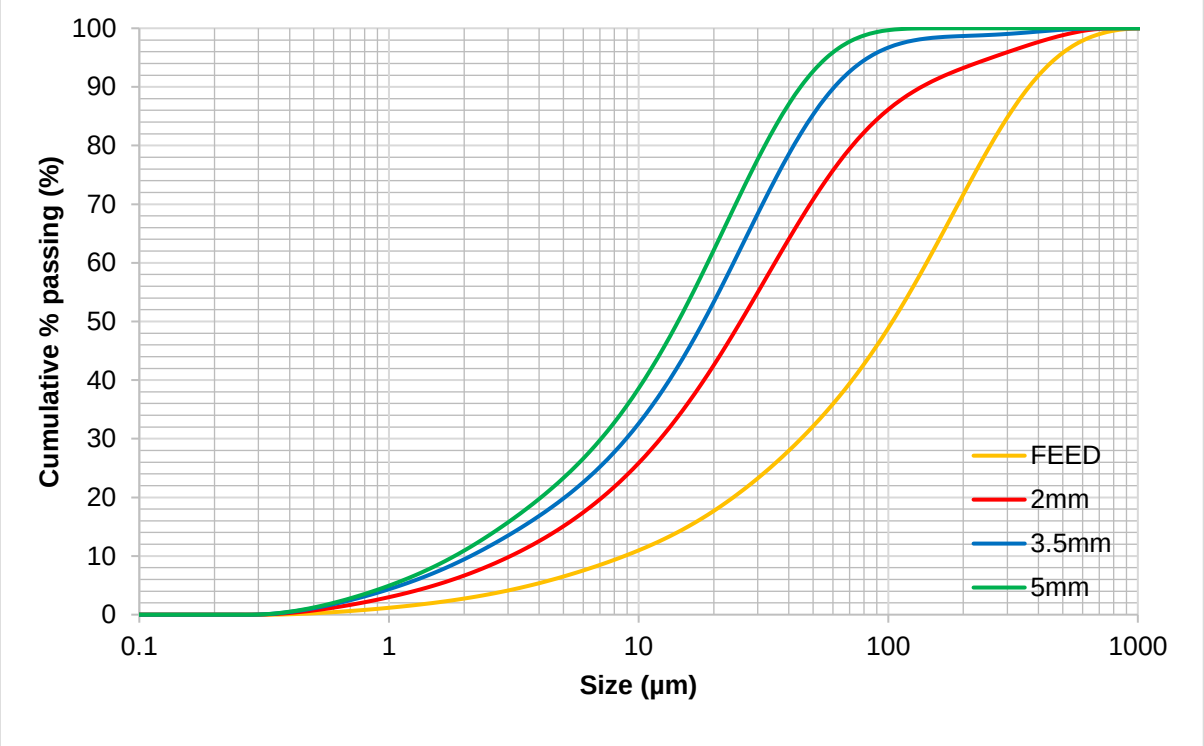

Figure 4-22: Effect of grinding media size on PSD for 2 mm, 3 mm and 5 mm grinding media at a solids concentration of 50% and a tip speed of 700 rpm

The effect of the grinding media size was also studied for different solids concentrations as shown in Figure 4-23, Figure 4-24, and Figure 4-25. At all the solids concentrations tested, the 5 mm grinding media constantly gave a finer product compared to 3.5 mm and 2 mm grinding median because the larger media has higher stress intensity. The 3.5 mm grinding media produced a coarser product at 50% and 60% solids up to a stirrer tip speed of 500 rpm, and thereafter the product was finer than that produced with the 2 mm grinding media. In the instances where the 2 mm grinding media gave a finer product, the surface area effect was greater than the stress intensity effect.

At low speeds (<525 rpm), the 2 mm grinding media gave a finer product than the 3 mm grinding media due to the higher frequency of media particle contact for the 2 mm grinding media. The size of the 2 mm grinding media means, at a constant fill of 60%, there are more grinding media beads than for the 3.5 mm grinding media. At high speeds (>700 rpm), the 3.5 mm grinding media and the 5 mm grinding media behaved similarly and produced similar PSDs and P80s.

He & Forssberg (2007) experimented with quartzite for ultra-fine grinding and found that the optimal media size to feed was between 150 and 200, whereas Zheng, et al. (1996) got a ratio of 12:1 using glass beads and Mankosa, et al. (1986) recommended a ratio on 20:1 for steel beads. Chaponda (2011) experimented with a PGM ore with F80 of 212 µm and noted that the 2 mm grinding media gave a finer product compared to the 3.5 mm and 5 mm grinding media. The difference in the findings of this study and that of Chaponda (2011) was explained by Jankovic (2003) when he discussed that a coarse feed requires larger grinding media than that required by a fine feed.

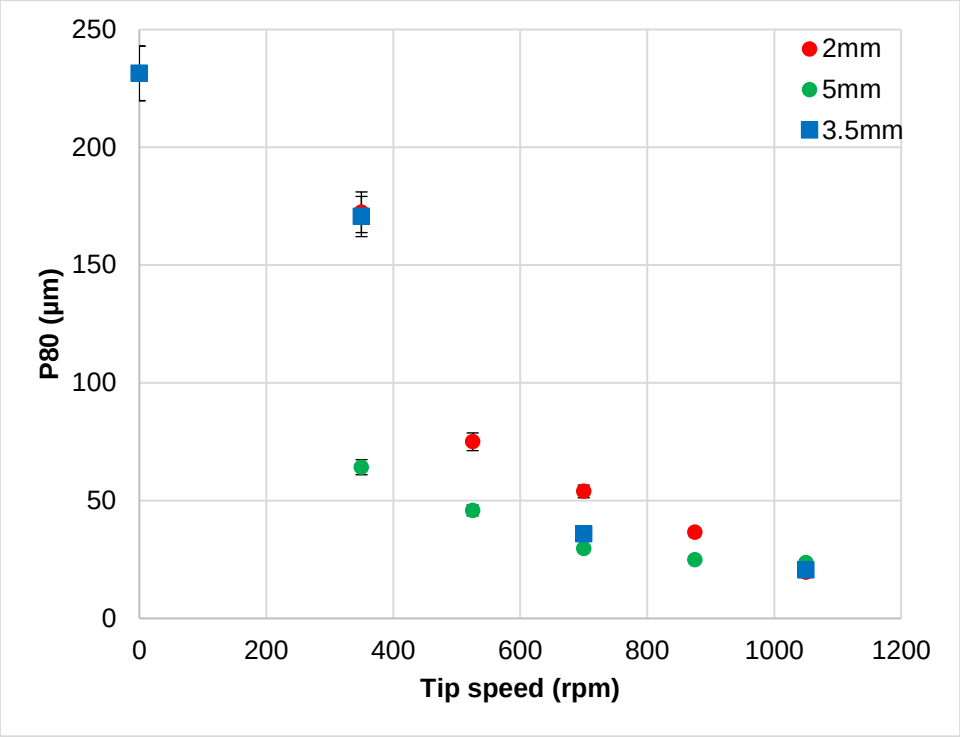

Figure 4-23: Effect of 2 mm, 3.5 mm and 5 mm grinding media size on P80 at 40% solids concentration using tip speeds in the range 350–1050 rpm

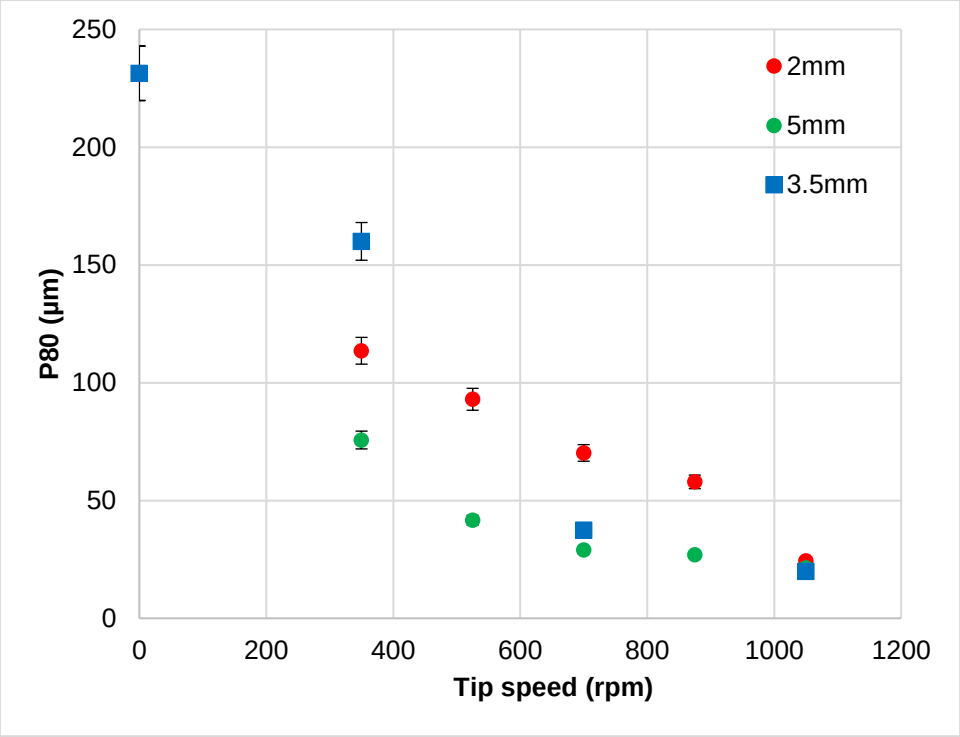

Figure 4-24: Effect of 2 mm, 3.5 mm and 5 mm grinding media size on P80 at 50% solids concentration using tip speeds in the range 350–1050 rpm

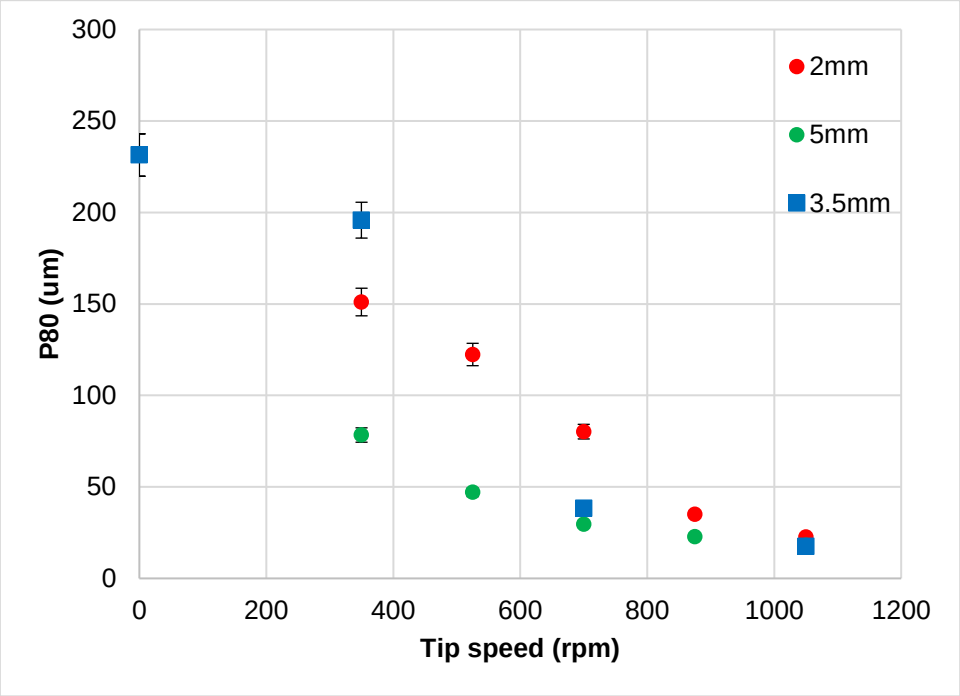

Figure 4-25: Effect of 2 mm, 3.5 mm and 5 mm grinding media size on P80 at 60% solids concentration using tip speeds in the range 350–1050 rpm

4.1.8.2.2 Effect of grinding media size on power draw

The effect of grinding media size on the power was observed. An increase in the grinding media size resulted in an increased power draw at all the tip speeds tested in the scope of work. Figure 4-26 shows the effect of the grinding media size on the power draw at a solids concentration of 50%. The trend noted at the solids concentration of 50% was consistent at solids concentrations of 40% and 60%. It was also observed that the power draw using 5 mm grinding media was double the power draw observed when using 2 mm grinding media. This demonstrates that it is more energy efficient to use a smaller grinding media in the HIGmill.

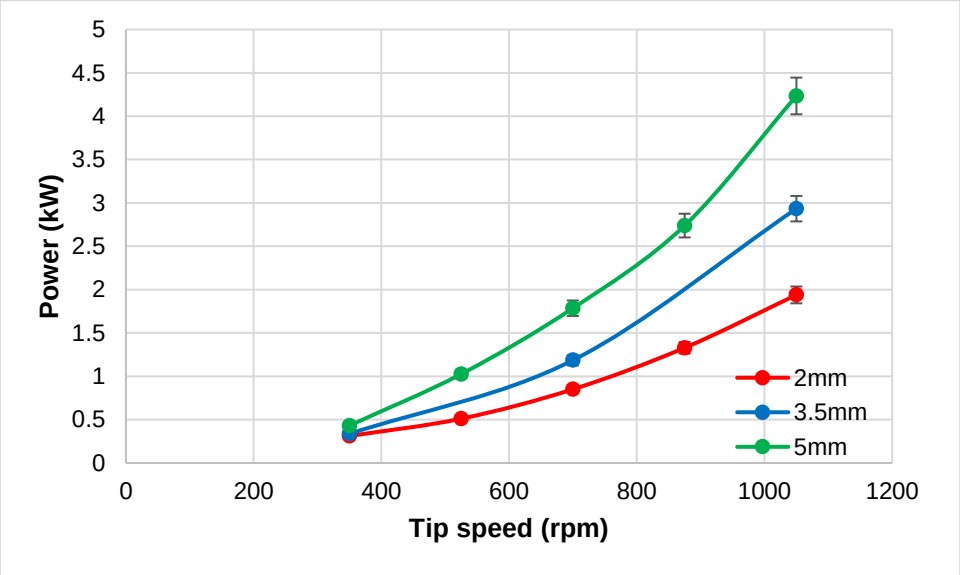

Figure 4-26: Effect of grinding media size on the power draw at a solids concentration of 50%

4.1.8.2.3 Signature plots

Signature plots were generated to analyse the effect of the grinding media size. The efficiency of the grinding media was determined by assessing which grinding media size produced a finer product at the same energy input. At a solids concentration of 50%, the 5 mm grinding media was more efficient for specific energy input less than 4 kWh/t, after which the 3.5 mm grinding media was more efficient. This trend was also noted at a solids concentration of 60% and can be found in the Appendix. At a solids concentration of 40%, the 5 mm grinding media produced a finer product at the same specific energy as the 2 mm and 3.5 mm grinding media up to a specific energy input of 4 kWh/t; thereafter the 2 mm grinding media produced a finer product. The results highlighted in this section suggest that, at low energy inputs, 5 mm grinding media is the best choice of grinding media size. At energy inputs above 4 kWh/t, the solids concentration also has to be considered when choosing the ideal grinding media size. Farber et al., (2011) ran experiments with the IsaMill to see the effects of grinding media size on the energy consumption and they noted that the smaller grinding medial size consumed less energy. Results obtained by Farber et al., (2011) can be seen in Figure 4-29 and it can also be noted that the energies observed by Farber et al., (2011) are similar to those observed in this scope of work.

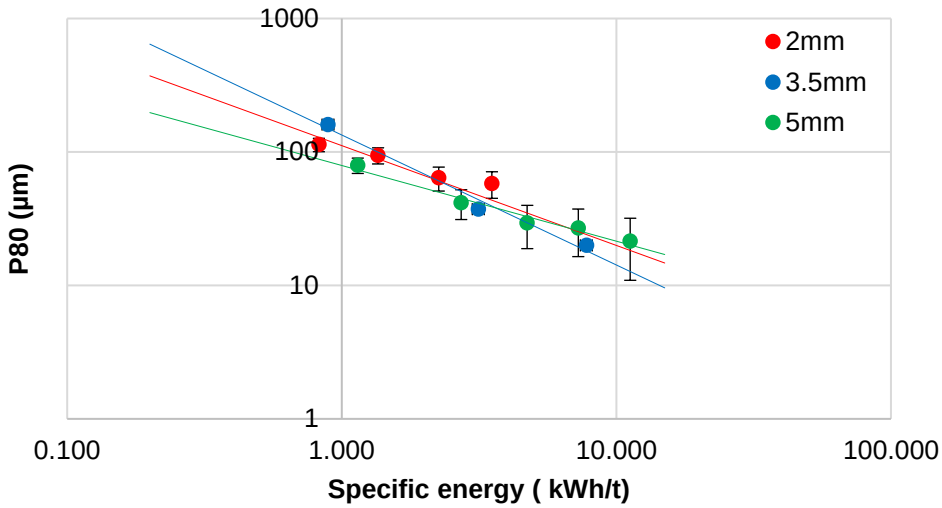

Figure 4-27: Signature plot for 2 mm, 3.5 mm and 5 mm grinding media with a solids concentration of 50%

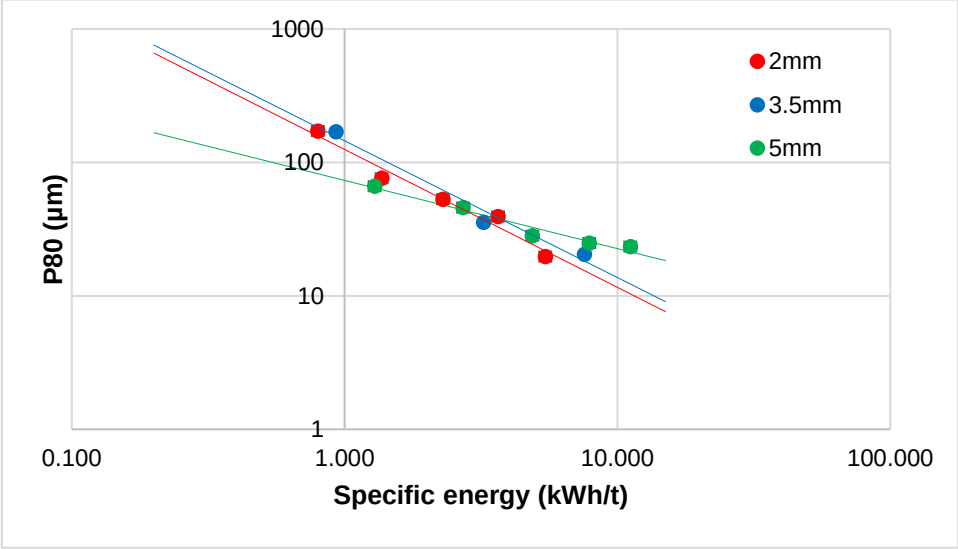

Figure 4-28: Signature plot for 2 mm, 3.5 mm and 5 mm grinding media with a solids concentration of 40%

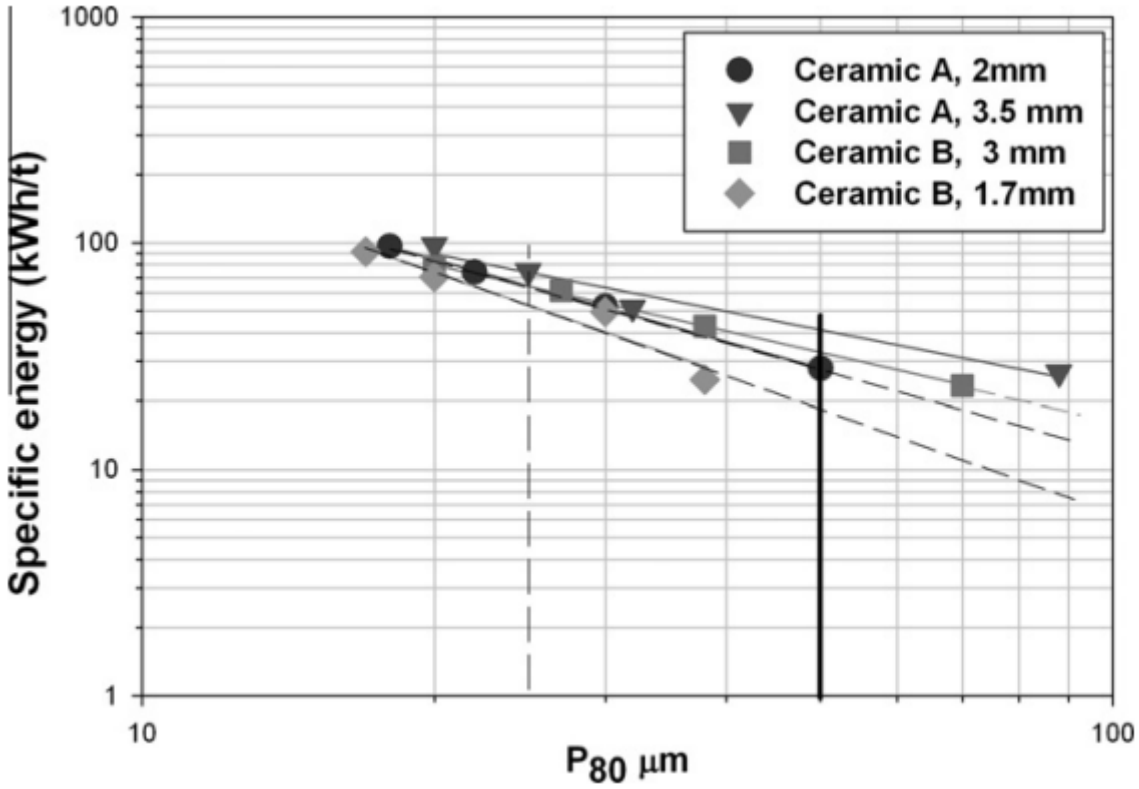

Figure 4-29:: IsaMill signature plots for ceramics grinding media Farber et al., (2011)

4.1.8.2.4 Effect of grinding media size on size specific energy consumption

To analyse the effect of the grinding media size on size energy consumption, the cumulative percent passing 20 µm was plotted against the size specific energy for each grinding media size. Figure 4-30 shows the efficiency of the different grinding media sizes at generating particles that are less than 20 µm at a solids concentration of 40%. The 2 mm grinding media was more efficient at generating −20 µm particles at energy inputs greater thar 7 kWh/t. Figure 4-31 shows that the 2 mm grinding media and 5 mm grinding media behave similarly when it comes to producing sub −20 µm particles. 3. 5 mm is more energy efficient at producing sub 20 µm for energy inputs greater than 9 kWh/t. Figure 4-32 shows the efficiency of the different grinding media sizes at generating particles that are less than 20 µm at a solids concentration of 60%. At energy inputs greater than 7 kWh/t the 3.5 mm grinding media produced the sub 20 µm more efficiently than the 2 mm grinding media and the 5 mm grinding media. The difference in the behaviour of the grinding media at the different solids concentration demonstrates that, when selecting the optimal grinding media size for a system, other parameters such as the solids concentration should be taken into consideration.

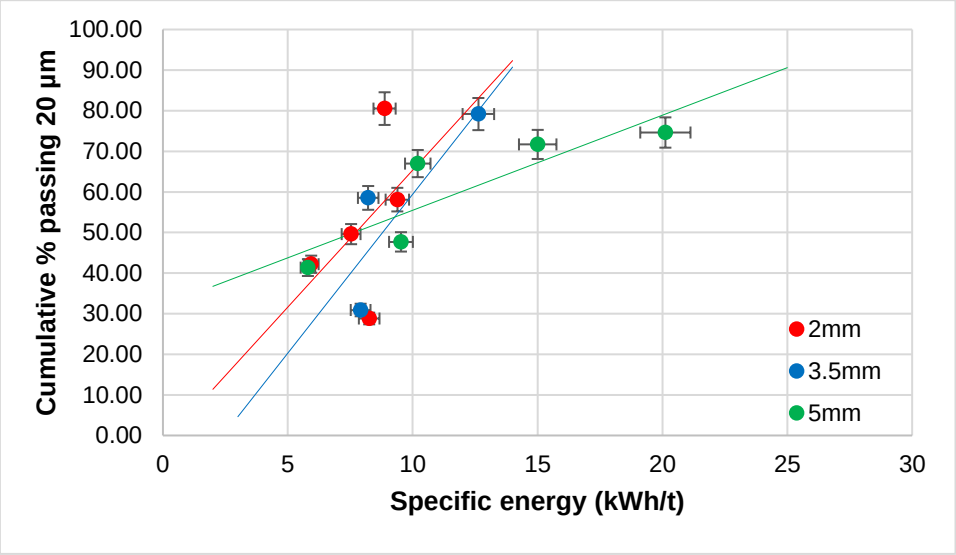

Figure 4-30: Effect of grinding media size on the size specific energy for a solids concentration of 40%

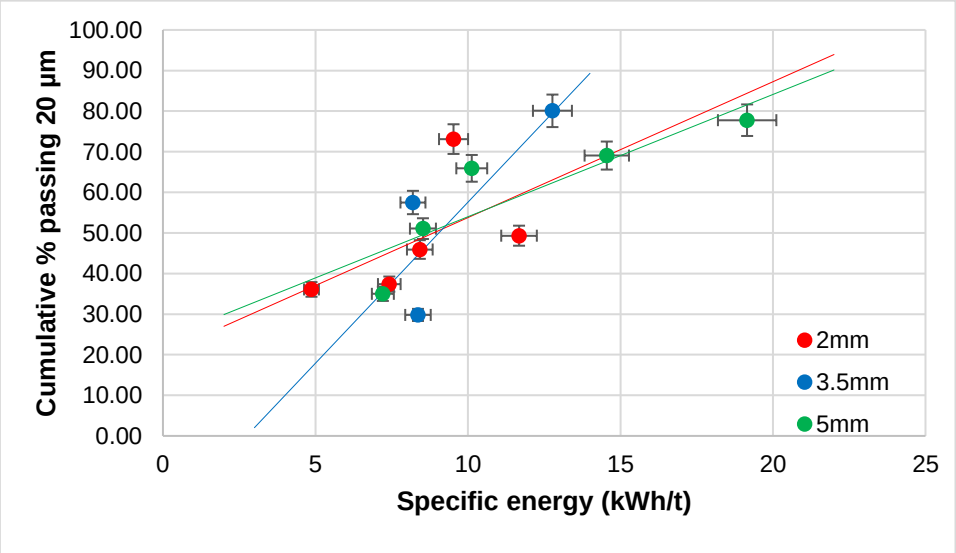

Figure 4-31: Effect of grinding media size on the size specific energy for a solids concentration of 50%

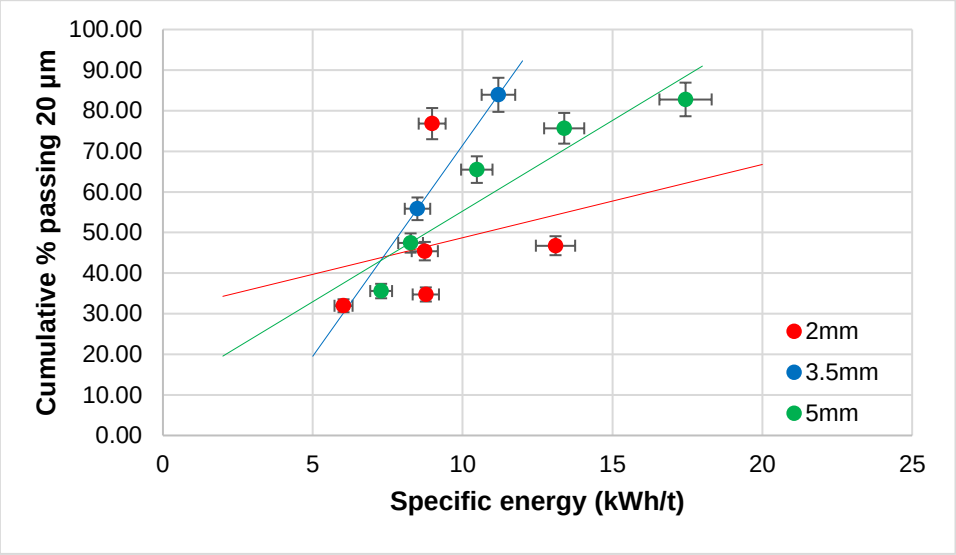

Figure 4-32: Effect of grinding media size on the size specific energy for a solids concentration of 60%

4.1.8.3 Effect of mixing grinding media sizes

There are only two instances when mills operate with monosized grinding media: when the mill is first operated and after the mill has been flushed, so it is valuable to investigate the effect of mixing grinding media sizes. Tests involving the mixing of grinding media sizes were carried out by combining 2 mm, 3.5 mm and 5 mm grinding media in the fractions presented in Table 4-2. Only two combinations were considered in the scope of work.

Table 4-2: Proportions of the media size used for each combination

Combination	2 mm	3.5 mm	5 mm
1	$\frac{1}{3}$	$\frac{1}{3}$	$\frac{1}{3}$
2	$\frac{1}{2}$	0	$\frac{1}{2}$

4.1.8.3.1 Effect of grinding media size distribution on PSD and P80

Test work conducted with monosized grinding media showed that an increase in grinding media size results in a finer PSD. Figure 4-33 shows the PSDs obtained from tests performed using media size combinations and individual media sizes at a tip speed of 700 rpm and a solids concentration of 50%. The tests with media combination 1 gave a product fineness similar to that obtained when using the 3.5 mm grinding media, and the tests conducted with media combination 2 gave a similar PSD to the distribution obtained with 5 mm grinding media.

At low speeds (i.e., speeds below 525 rpm), media combination 2 gave the finest product. In this combination, the 2 mm bead size increased the number of beads available for particle-to-media interaction to occur, and the 5 mm grinding media provided the high stress intensity required for particle breakage. The increase in media surface area and the high stress intensity resulted in finer products. Media combination 1, which had a third of 2 mm grinding media, a third of 5 mm grinding media and a third of 5 mm grinding media, provided a PSD similar to that produced by the 3.5 mm grinding media. This can be explained by the fact that the surface area available for grinding and media-to-particle interactions were similar. Figure 4-34 shows the effect of the media size combinations on the P80 at tip speeds in the range of 350–1050 rpm. At speeds above 700 rpm, all the media combinations give similar product sizes, except the 2 mm grinding media, which give the coarsest product size at all the tip speeds in the range.

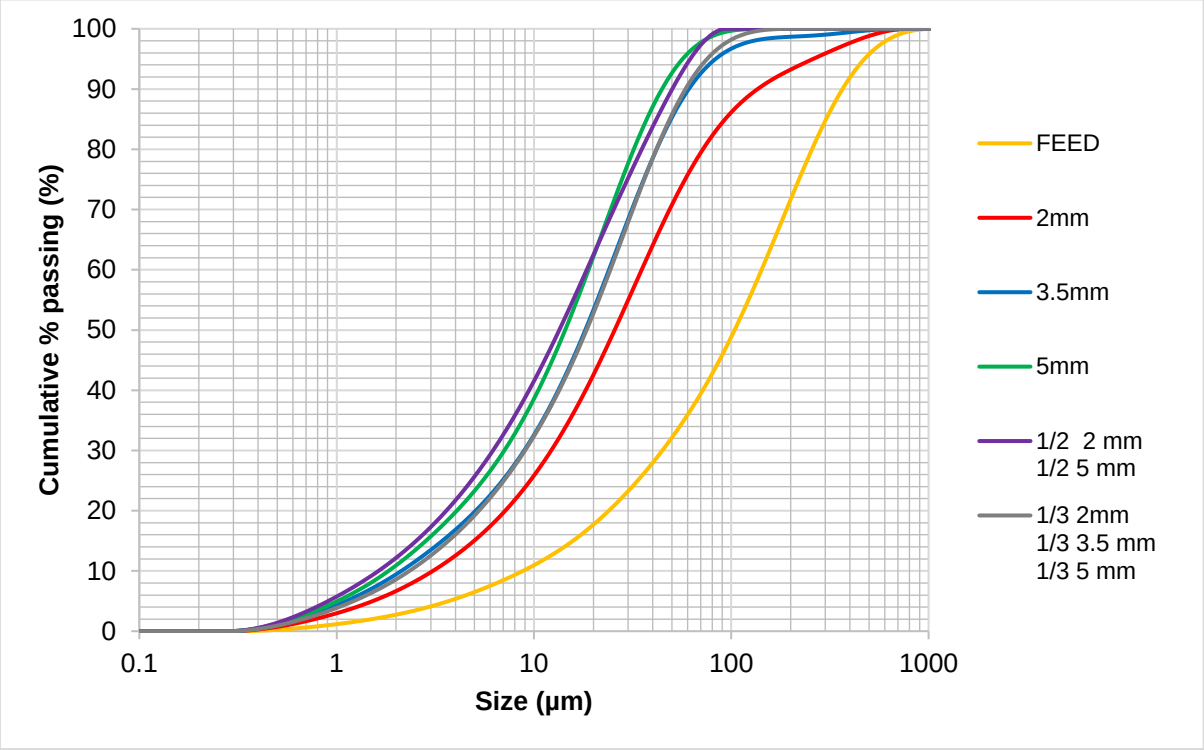

Figure 4-33: PSD of monosized media and mixing grinding media sizes (combination 1 & combination 2) at a tip speed of 700 rpm and a solids concentration of 50%

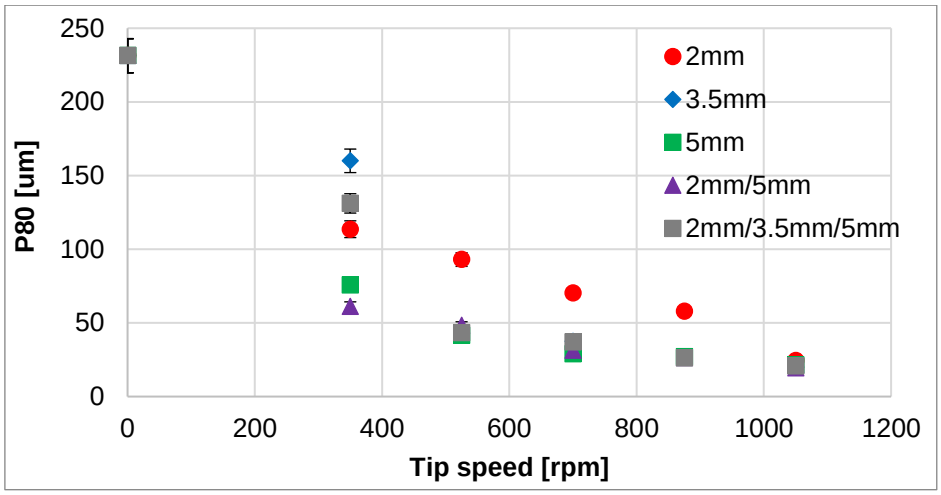

Figure 4-34: Effect of media size combinations on the product size (P80) compared to the product size obtained with 2 mm, 3.5 mm and 5 mm grinding media at a solids concentration of 50%

4.1.8.3.2 Effect of grinding media size distribution on power draw

The effect of grinding media combinations on the power draw was compared to the power draw of the 2 mm, 3.5 mm and 5 mm grinding media, and the results are highlighted in Figure 4-35. For all the speeds, there was no significant difference between the power draw of the media combinations and the power draw of the 3.5 mm grinding media, except at 525 rpm, where media combination 2 had a higher power draw than the 3.5 mm grinding media.

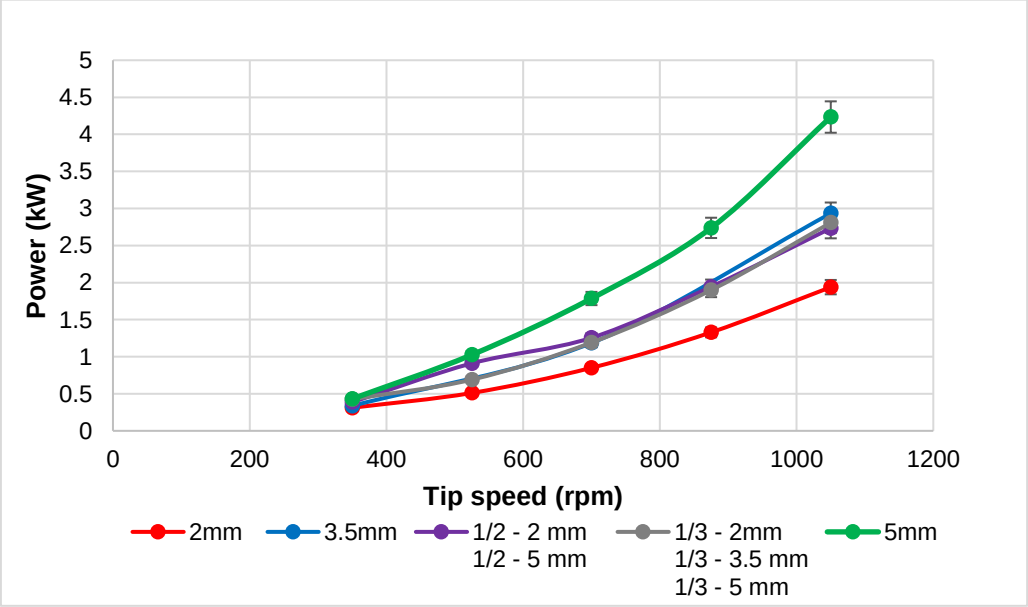

Figure 4-35: Effect of media size combinations on power compared to the power draw of 2 mm, 3.5 mm and 5 mm grinding media at a solids concentration of 50%

4.1.8.3.3 Signature plots

Signature plots for the tests conducted on the grinding media combinations were charted, along with the relevant plots for the 2 mm, 3.5 mm and 5 mm grinding media, as shown in Figure 4-36. The results show that, at specific energy inputs below 5 kWh/t, combination 2 grinding media is more energy efficient, giving a finer product for the same energy input as the other grinding media sizes and combinations. At energy inputs below 1.5 kWh/t, the 3.5 mm grinding media is the least energy efficient, giving a coarser product at the same energy input, thereafter the 2 mm grinding media is the least energy efficient.

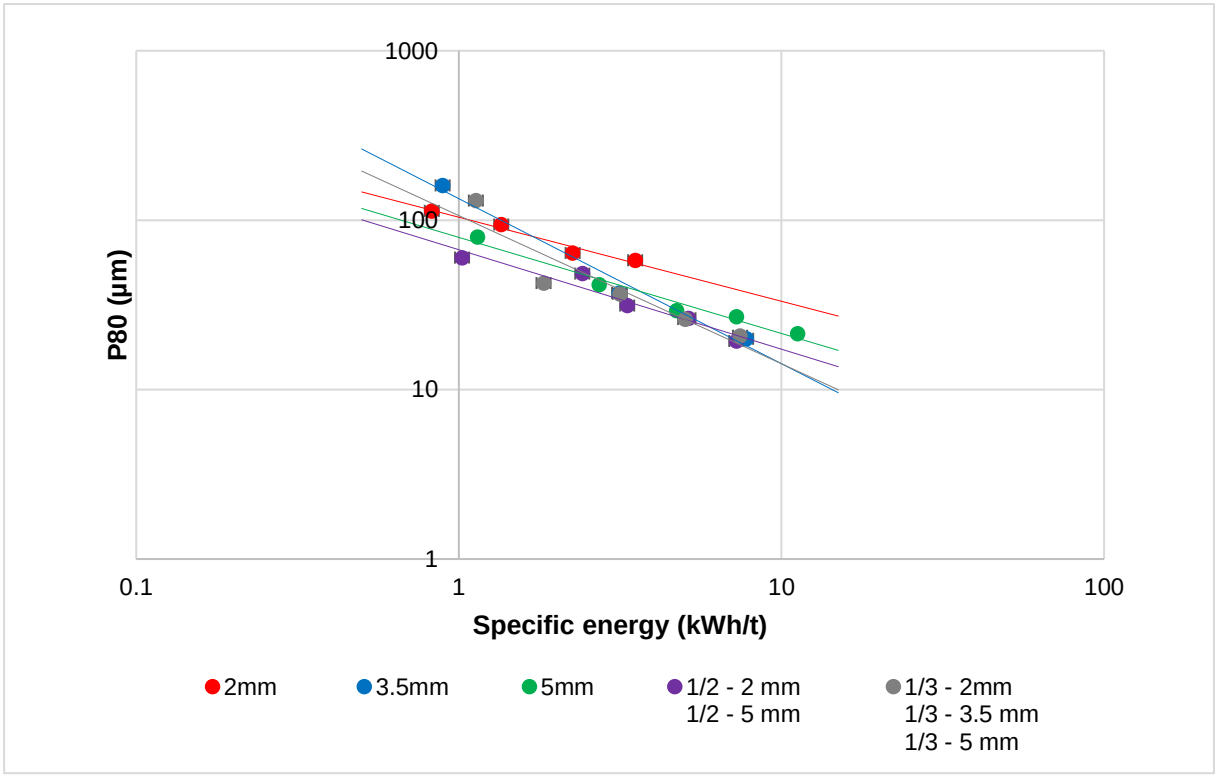

Figure 4-36: Signature plot for media size combinations, 2 mm, 3.5 mm and 5 mm grinding media at a solids concentration of 50%

4.1.8.3.4 Effect of grinding media on size specific energy

The size specific energy for the grinding media combinations was compared to the size specific energy for the 2 mm and 5 mm grinding media at a solids concentration of 50%, and results are shown in Figure 4-37. This analysis was done to determine which grinding media size or grinding media size combination was more efficient at producing sub 20 µm particles. The media size combinations were more efficient at producing sub 20 µm particles than the monosized media.

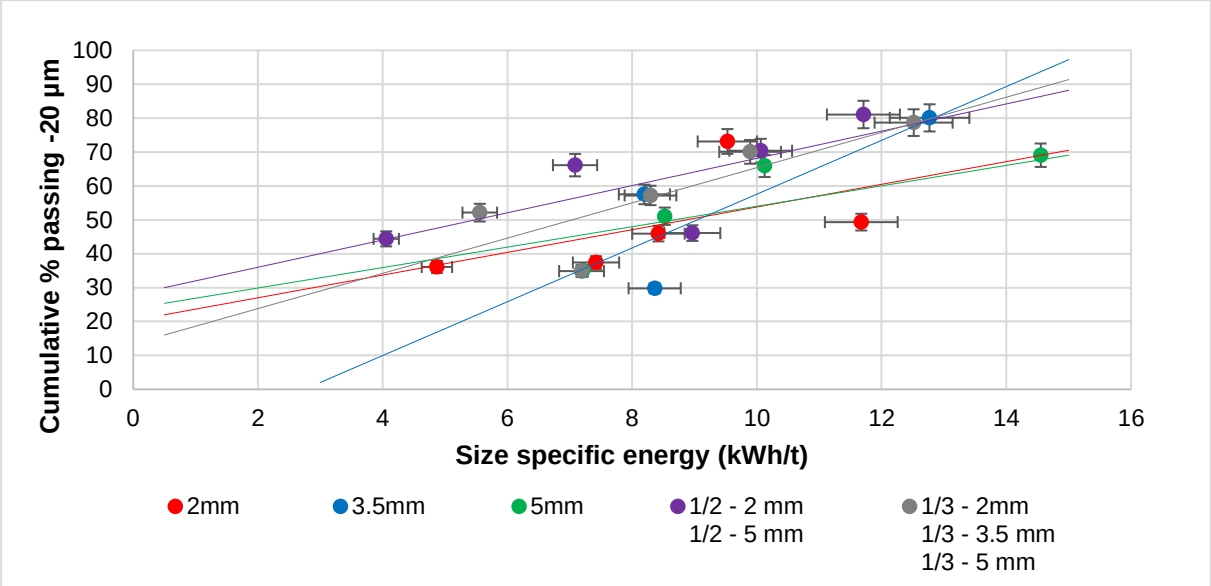

Figure 4-37: Size specific energy for media size combinations compared to the size specific energy for 2 mm, 3.5 mm and 5 mm grinding media at a solids concentration of 50%

4.1.9 Effect of Stress Intensity on P80

This section looks at the effect of the stress intensity on the product size and the energy efficiency. The stress intensity was calculated using Equation 4. For the experiments run in the scope of this work the range of the stress intensity was between 0.127 x 10^{-3} Nm and 17.8 x 10^{-3} Nm. The stress intensities obtained are comparable to those obtained by Jankovic (2003) when investigating the variables affecting the grind of zinc concentrate.

Figure 4-38 shows the effect of the stress intensity on the product size for a grinding media size of 5 mm at a solids concentration of 50%. As expected, the increase in the stress intensity results in a finer product with the product size decreasing to 20.3 µm from 79.5 µm when the stress intensity increased to 18.2 x 10^{-3} Nm from 1.98 x 10^{-3} Nm. However, between stress intensities of 7.00 x 10^{-3} Nm and 18.0 x 10^{-3} Nm the decrease in the P80 is gradual. Lisso (2012), also observed a similar stress intensity trend for the grinding of Merensky ore at solids concentration of 40% as shown in Figure 4-39.

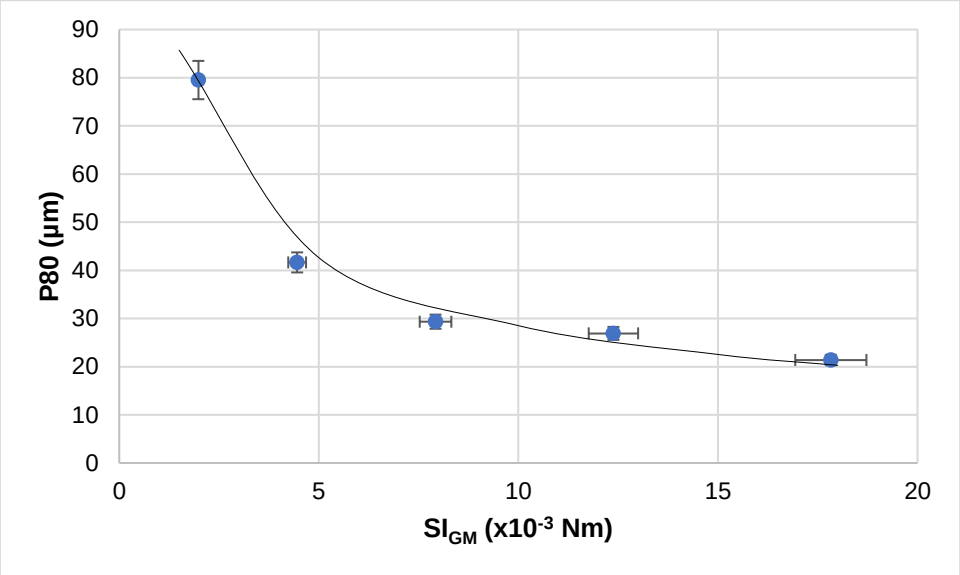

Figure 4-38: Effect of media stress intensity on the P80 at a solids concentration of 50% and grinding media size of 5 mm

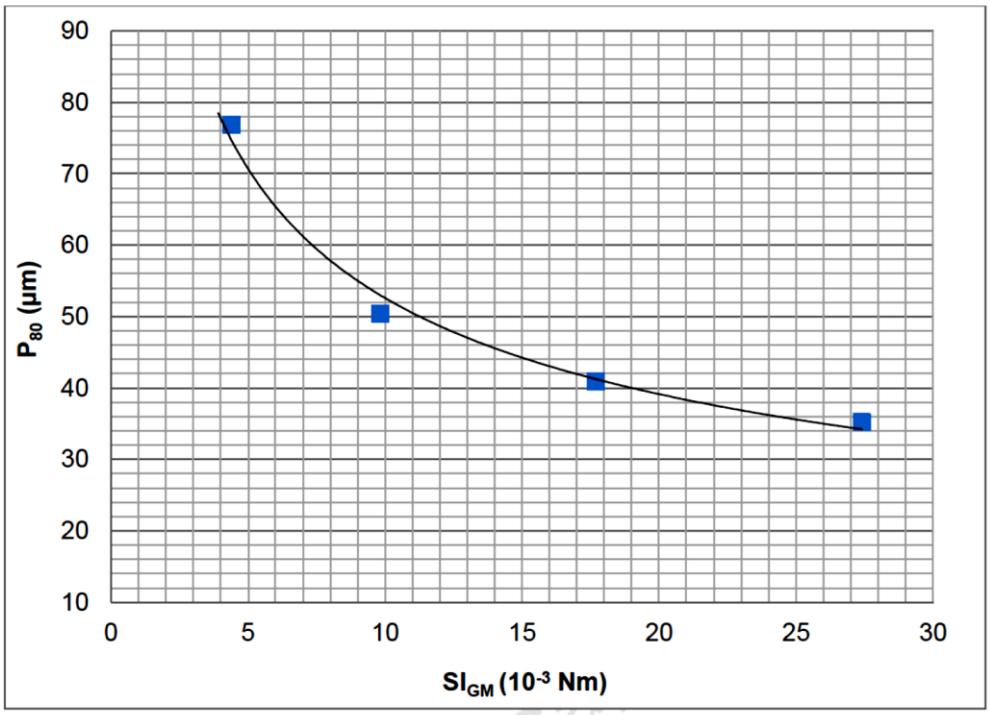

Figure 4-39: Effect of media stress intensity on the P80 at 40% solids concentration and 102 seconds milling time (Lisso,2012)

The stress intensities that were observed using 2 mm and 3.5 mm grinding media were comparable to those observed by Jankovic (2003) as shown in Figure 4-40 and Figure 4-41. The difference in the P80 numbers in the two graphs is attributed to the feed top size, where a top size of 100% passing 1000 µm was used for the experiments in the thesis and Jankovic

(2003) used a finer feed top size of 80% passing 47 µm. The work of Jankovic (2003) noted that there is an optimum stress intensity for a system and this was observed when a coarse product resulted as the stress intensity continued to increase as shown in Figure 4-41. Kwade et al. (1996) attributed this to the loss of energy utilization which is a result of energy losses. For the experiments run in this scope of work the optimal stress intensity was not observed. This indicates that the energy utilization in the scope of work did not reach a point where it started to decrease.

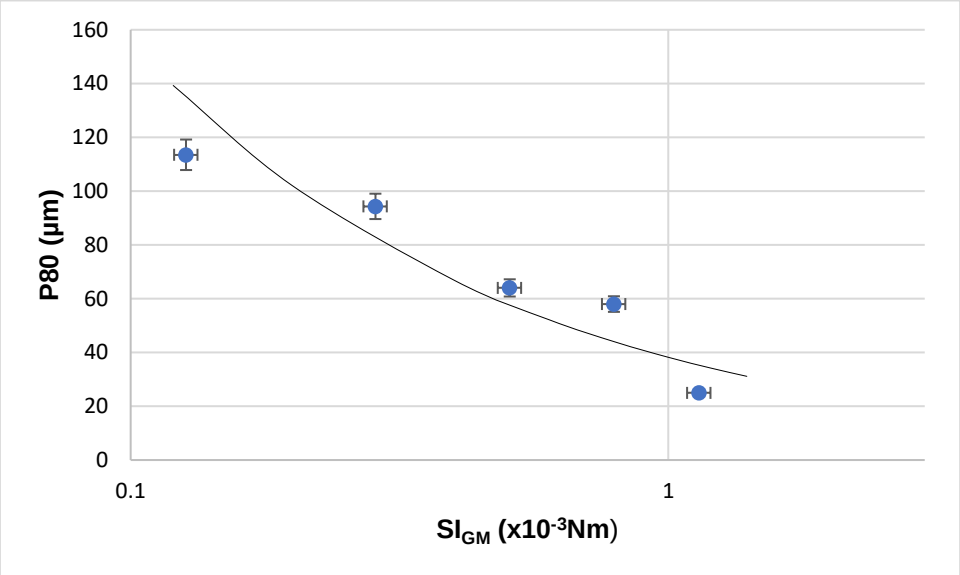

Figure 4-40: Stress intensity of 2mm grinding media at solids concentration of 50%

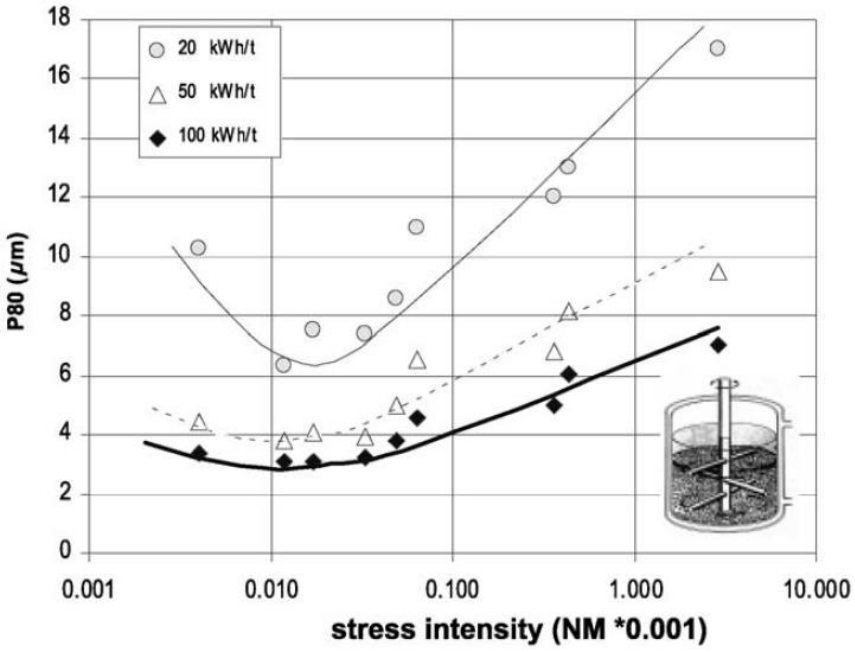

Figure 4-41: Stress intensity plot for mill of zinc concentrate in a pin mill (Jankovic, 2003)

4.1.10 Conclusion

This chapter has given an analysis of the results obtained from the test work that was conducted with the HIG5mill. The investigation conducted in this study was to assess the fine-grinding capabilities of the HIGmill on the UG2 ore. The parameters tested were solids concentration, tip speed, grinding media volume fill, grinding media size and grinding media size distribution. The tests conducted on the grinding media size volume fill and media size combinations were done to fully investigate the parameters associated with grinding media. The results from the experiments carried out can serve as a guide in selecting optimum parameter combinations to give the desired P80 size.

The different methods of analysis used in the interpretation of the data obtained from the experiments were used to deduce the best parameter combination to be used. Of the methods of analysis presented in this chapter three main methods were used to arrive at the optimum parameter. These methods were the PSD and P80 analysis, the signature plot, and the size specific energy analysis method. With the PSD and P80 method of analysis the optimum parameter was considered to be the one which gave the finest grind. With the signature plot the best parameter setting was concluded to be the one that gave a fine product in an energy efficient way. Using the size specific energy, the best parameter setting was considered to be the one that produced the most sub 20 µm particles whilst using the least energy.

The PSD and P80 method of analysis concluded that a speed of 1050 rpm gave the finest product for all grinding media sizes and solids concentrations tested. However, at a solids concentration of 50% and grinding media size of 5 mm both the signature plot and the size specific energy methods indicated that a tip speed of 700 rpm was the optimal speed. Running the mill at a speed of 700 rpm gave a fine product with less energy consumed and at a tip speed of 700 rpm more sub 20 µm particles were produced energy efficiently.

For solids concentrations tested at 700 rpm the PSD and P80 method indicated that for 3.5 mm and 5 mm grinding media either a solids concentration of 40% or 50% is optimal. For 2 mm grinding media, the running at 40% solids gives the finest product. The signature plots indicate that the effect of the grinding media size should be considered when selecting a solids concentration for a system. There was no significant difference in the energy consumption of the different solids concentrations tested when using a grinding media of 5mm. However, at energy inputs above 2 kWh/t, 60% solids concentration was more efficient. With 2 mm grinding media 40% solid was more efficient. The size specific energy indicated that the optimum solids concentration for a 5 mm and 3.5 mm grinding media at energy inputs greater than 9 kWh/t

was 60% solids. The optimum solids concentration when using the 2 mm grinding media at energy inputs above 5 kWh/t was 40% solids.

The tests conducted on the grinding media fill indicated that a grinding media fill of 60% was the optimal grinding media fill as it gave the finest product using the PSD analysis. The specific energy analysis showed that a grinding media fill of either 50% or 60% gave the finest product at the least energy input. Using the size specific energy showed that for energy inputs below 15 kWh/t, 60% grinding media fill gave the most sub 20 µm particles.

For the grinding media size, the 5 mm grinding media gave the finest product. However, using 5 mm grinding media proved to be energy intensive for the range of tip speeds tested. According to the signature plots 5 mm grinding media was the most energy efficient for energy inputs below 5 kWh/t. Above 5 kWh/t the 2 mm and 3.5 mm grinding media are the best media sizes to consider. The size specific energy analysis of the grinding media showed that when considering the optimal grinding media size the solids concentration should be considered.

Mixing grinding proved to have the most effect when considering the size specific energy as the grinding media mixture were efficient as producing sub 20 µm particles.

The effect of stress intensity was also investigated, and it was noted that increase in the media stress intensity resulted in a finer product size.

5. ASSESSMENT OF FLOTATION PERFORMANCE

This chapter details the results obtained from flotation tests conducted on the comminuted UG2 ore. Flotation tests were included to evaluate the downstream response to the particles prepared using the HIGmill for the standard UG2 flotation batch tests conducted.

Batch flotation tests were carried out on the products from the HIGmill to assess the flotation response after milling at different conditions. The aim of the floating of the HIGmill products was to investigate whether comminuting the ore using the HIGmill would change the flotation response of the specific UG2 ore used in the experiments. The work considered the ideal parameters that would allow the HIGmill products to respond better in the standard conditions used for UG2 batch flotation. The procedure used adopted the standard UG2 reagent suite at dosages used by the company that supplied the UG2 ore. The reagent dosages and conditioning times are reported in Chapter 3. The concentrate and tailings for the flotation tests were sent for assaying, and the analysis requested was for 4E PGMs. A total of 27 tests were performed that involved floating the HIGmill products. Of these 27 tests, four were selected for kinetics analysis, and assays of all concentrate fractions and the tailings were carried out. For the remainder of the flotation tests, the concentrate samples were composited to allow the final recovery and grade to be calculated. The flotation kinetics were used, along with important flotation efficiency parameters, such as the grade, recovery, and accountability, to assess the flotation response of the UG2 ore comminuted using the HIGmill under different operating conditions.

5.1 Flotation of HIGmill Products

The HIGmill products selected for the full assay analysis had P80 values of 29 µm, 37 µm, 52 µm and 64 µm. The particles size distributions of the four tests selected for the analysis of flotation kinetics are presented in Figure 5-1. It can be seen that the HIGmill operated at 700 rpm using different grinding media sizes and in-mill solids concentration gave products with different P80 values.

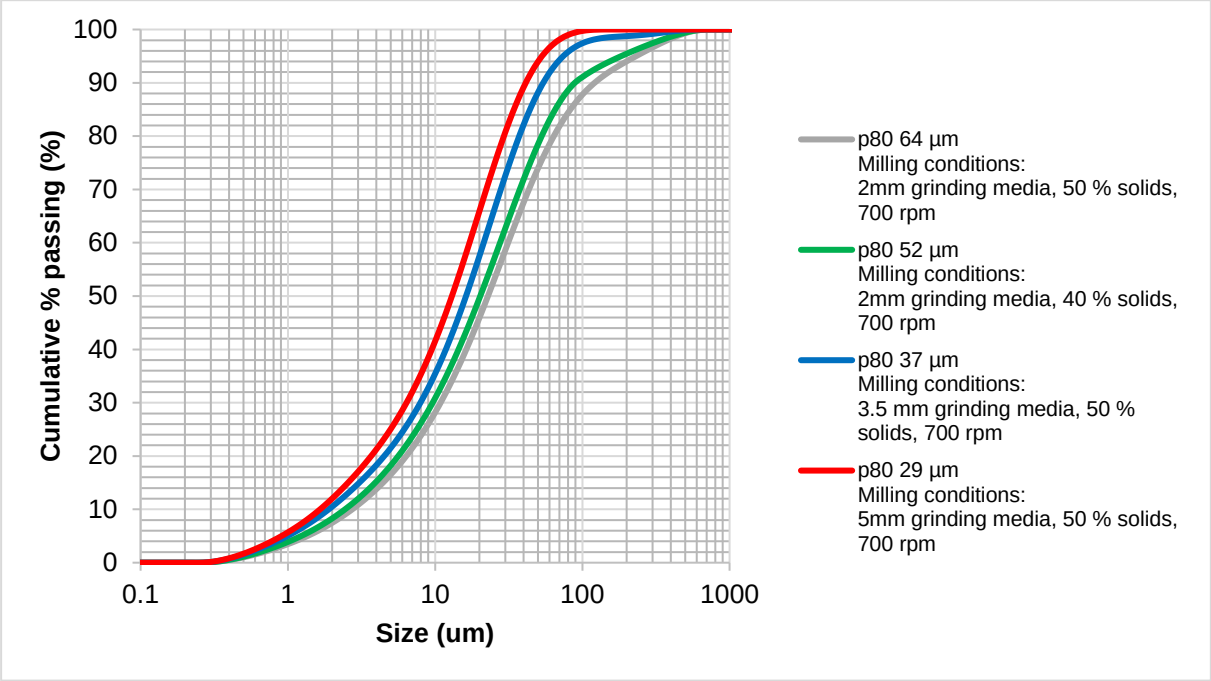

Figure 5-1: PSD for the flotation samples sent for full analysis.

5.2 Solids and Water Recovery

Recoveries of solids and water were calculated for each batch flotation test performed. Figure 5-2 shows the water and solids recovered in the flotation tests performed on particles prepared using the HIGmill to obtain products with different P80 values. The products at different P80 values were obtained by operating the HIGmill at 700 rpm and using monosized grinding media of 5 mm, 3.5 mm and 2 mm. It can be seen that the water recovery decreased as the product became finer. The solids recovery showed marginal increases with the flotation of finer HIGmill products. The HIGmill product with a P80 of 29 µm had the least water recovered and the most solids recovery. This indicates that this batch flotation had the least flotation by entrainment. This feed slurry responded well to the reagent dosages used in the test work.

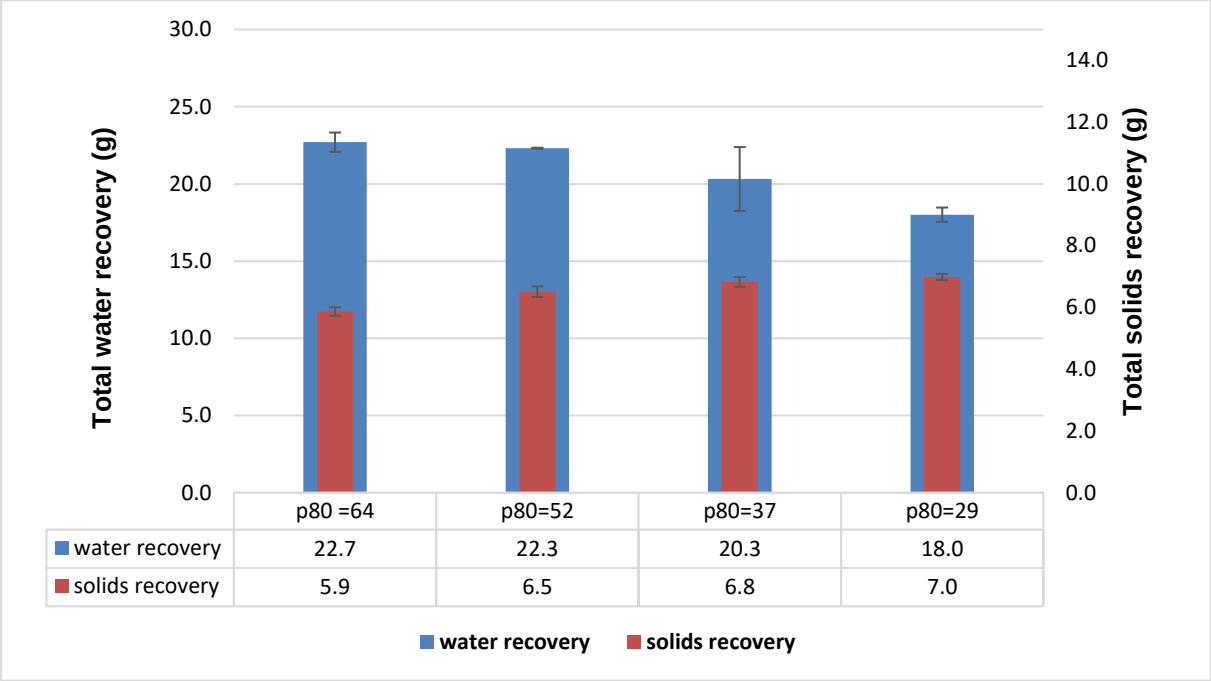

Figure 5-2: Solids and water recovery graph

5.3 Recovery Kinetics

The kinetic response of the material ground to different product size distributions was assessed using the assays from concentrate fractions and the tailings for the selected tests. Figure 5-3 and Figure 5-4 show the recovery time curve and recovery grade curves, respectively obtained by floating HIGmill products with different size distributions.

5.3.1 Effect of grind on recovery and grade

The grade-recovery curve for the 4E in Figure 5-3 shows no significant difference in the flotation response of P80 products prepared using the HIGmill. The results indicate that the product particle size distribution for this material did not have a significant impact on the flotation response. It was observed that the recovery attained from the tests was 81% at a grade of 18 g/t. The recovery and grade obtained from floating the feed was 73.2% at a grade of 42.4 g/t. Therefore, grinding the material in the HIGmill improved the recovery potential of the ore.

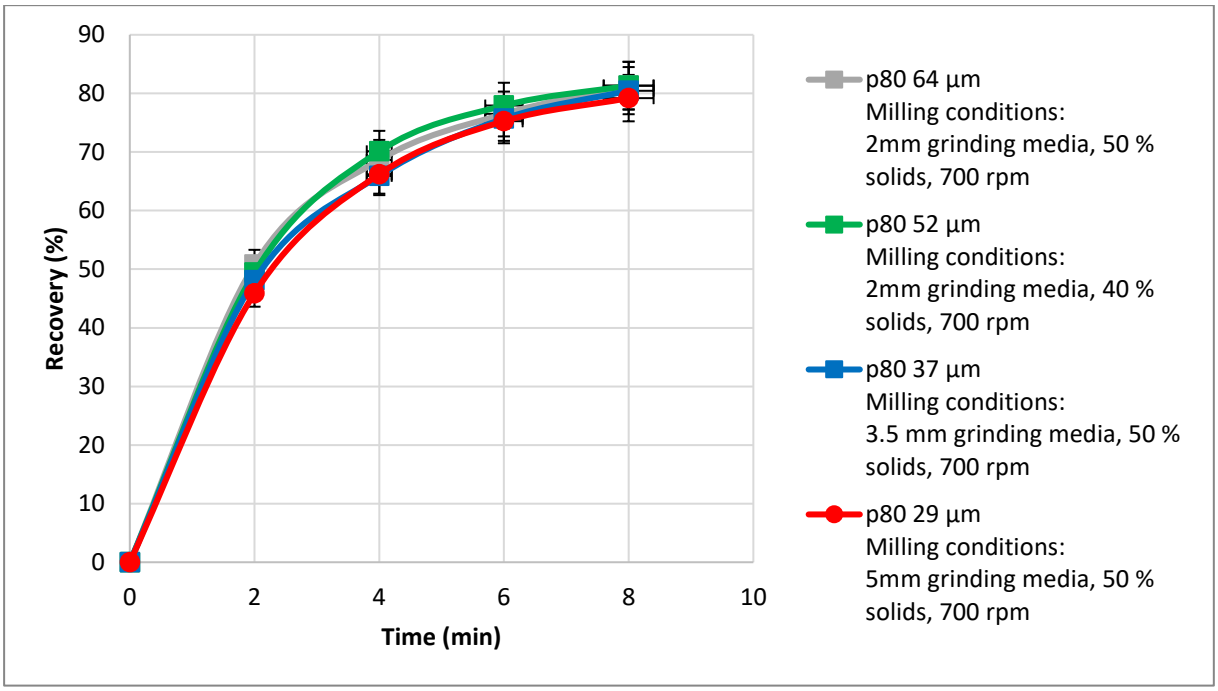

Figure 5-3: 4E recovery vs time

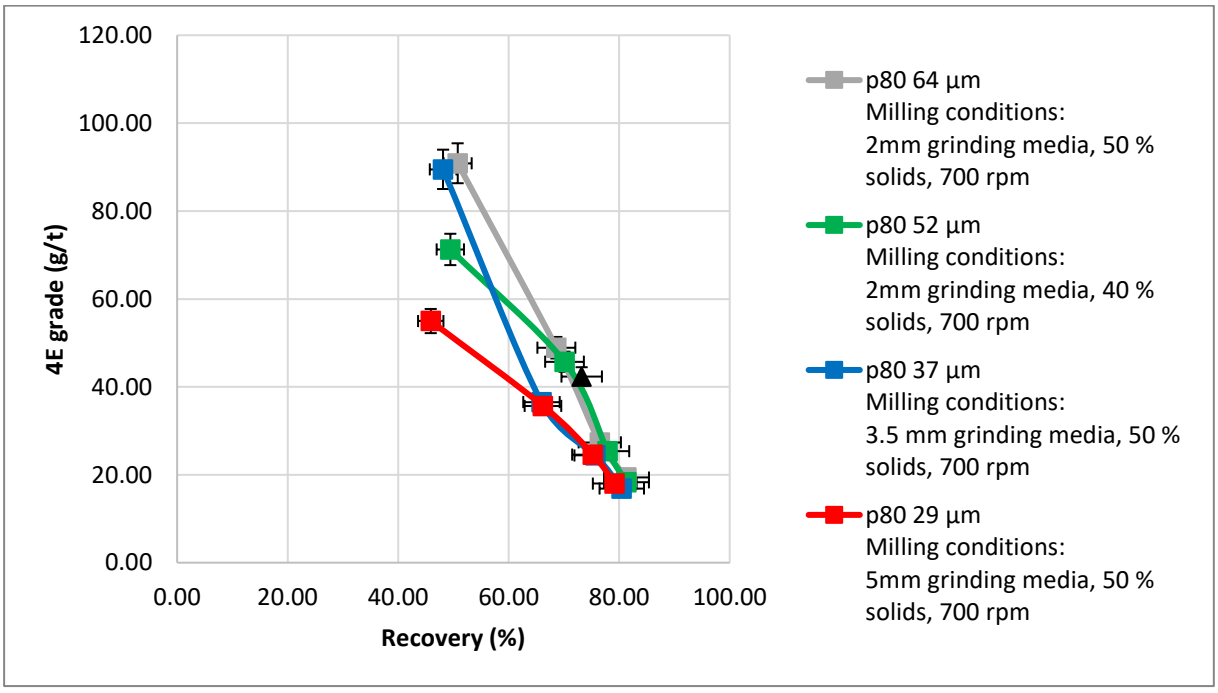

Figure 5-4: 4E grade recovery curve

5.3.2 Kinetic models

The recovery kinetics were studied further using the Klimpel model and the Kelsall model. The kinetics models helped to quantitatively combine the flotation response using model parameters that fitted the data.

5.3.2.1 Klimpel model

The Klimpel model was used to fit to the experimental data. Details of the model and the relevant equations are given in the literature review (section 2.6.4.2). According to the model, the maximum recovery achievable for the UG2 ore used in the experiments was 95.4%, and the rate constant for the flotation kinetics was 0.94. Figure 5-5 shows the comparison of the fitted and experimental data for the flotation results of HIGmill products with different P80 values. The model fitted the experimental data well in all cases, using the same parameters, which indicates that there were no significant differences in the responses. Ramlall & Loveday (2015) applied the Klimpel model to the UG2 ore, and they obtained a maximum recovery of 85.38% and a rate constant of 2.73 min^{-1}. The differences in maximum recoveries and the rate constants may be attributed to the differences in the sources of the UG2 ore.

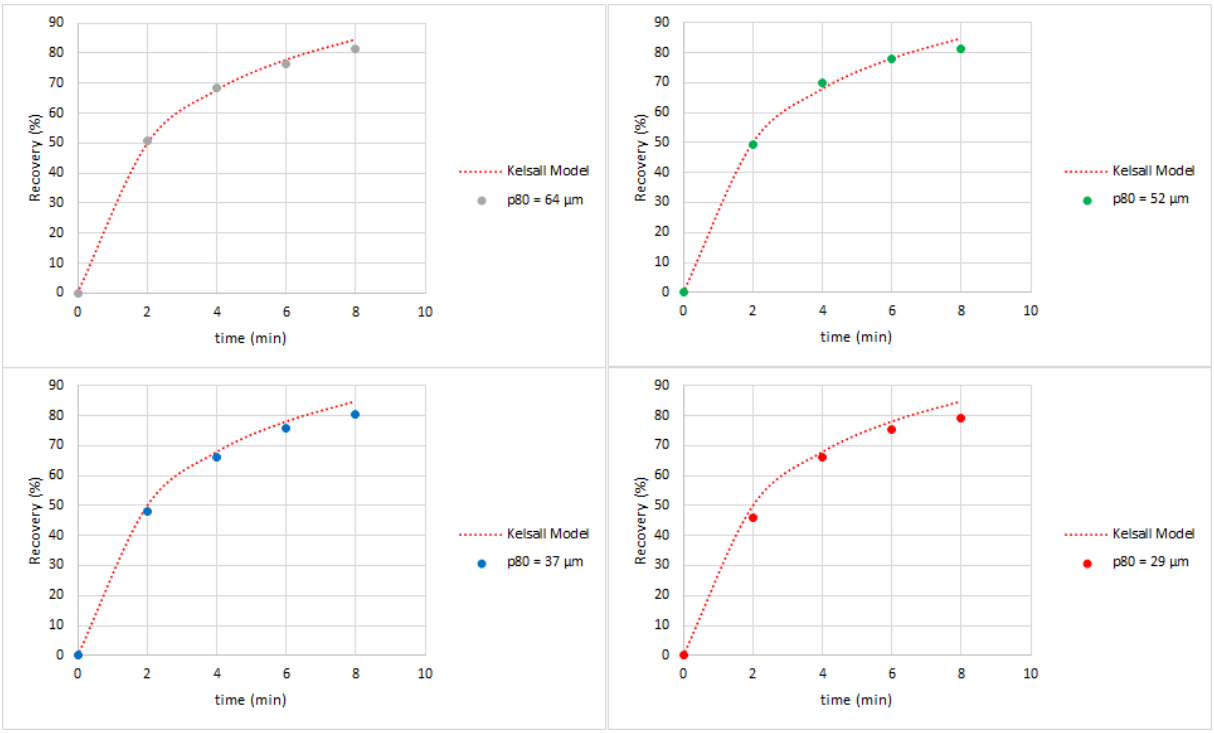

Figure 5-5: First order Klimpel model for PGM recovery from UG2 ore

5.3.2.2 Kelsall model

The Kelsall model was also used to fit the experimental data. Details of the Kelsall model can be found in the literature review (section 2.6.4.2). According to the Kelsall model of the experimental data, R_{fast} was 65.1% and R_{slow} was 34.9%, $-k_{fast}$ was 0.2 min^{-1} and k_{slow} was 1.0 min^{-1}. The fitting results using these parameters are given in Figure 5-6. The same parameters were used to fit the data from all four tests and a good fit was achieved in all cases, with minor deviations for the fit involved in the kinetics of the material milled to P80s of 29 µm and 37 µm. Ramlall & Loveday (2015) applied the Kelsall model to their experimental data for the flotation of UG2 ore, and their R_{fast} was 69.01% and R_{slow} was 30.99%; $-k_{fast}$ was 0.04 min^{-1} and k_{slow} was 1.77 min^{-1}. Achieving well-fitting results for the Kelsall model using the same parameters indicates that there was no significant difference in the kinetics of the four tests.

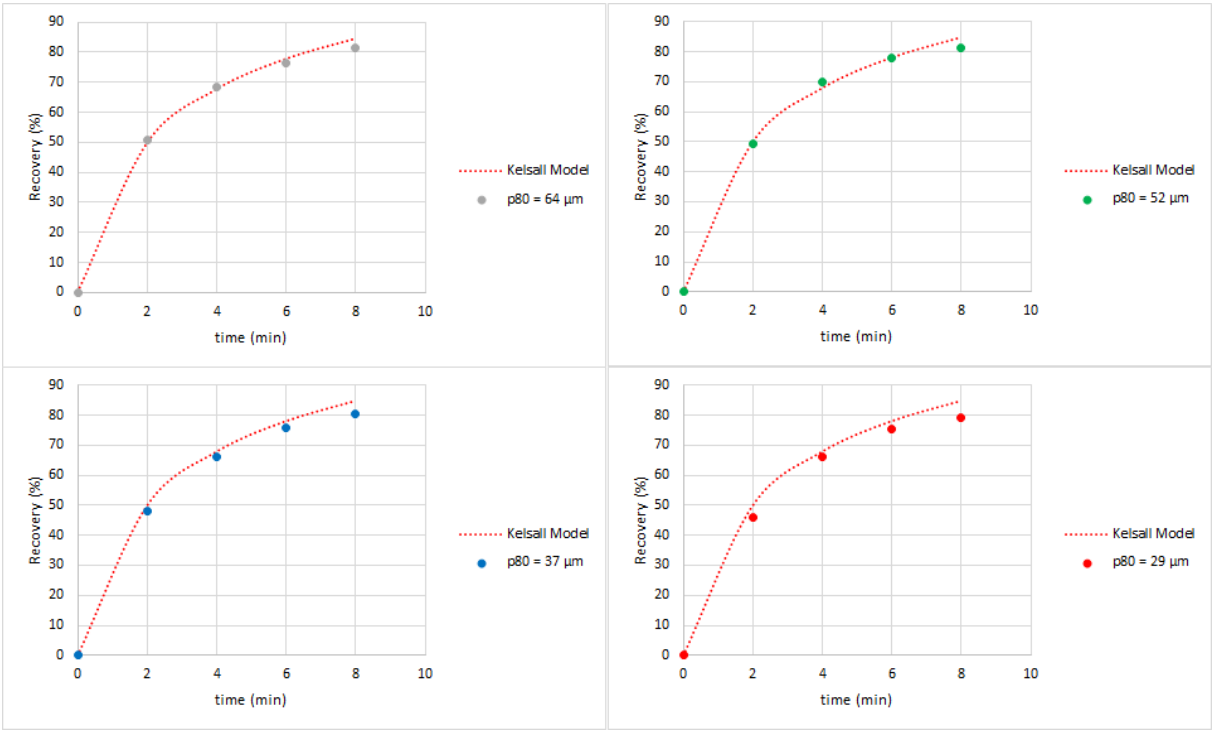

Figure 5-6: First-order Kelsall model for PGM recovery from UG2 ore

5.4 Effect of Parameters on Recoveries

5.4.1 Effect of tip speed

5.4.1.1.1 Effect of tip speed on solids and water recovery

To show the effect of the tip speed on the water and solids recovery, the individual data are shown in Figure 5-7. Table 8-13 highlights the solids and water recovery for each test. The effect of the tip speed on the solids and water recovery differed for each set of parameters run for the experiments. For example, a solids concentration of 40% and grinding media size of 2 mm resulted in an increase in both water and solids recovery when the speed was increased. For a solids concentration of 60% and grinding media size of 3.5 mm, the water recovery decreased with an increase in speed, and the solids recovery increased.

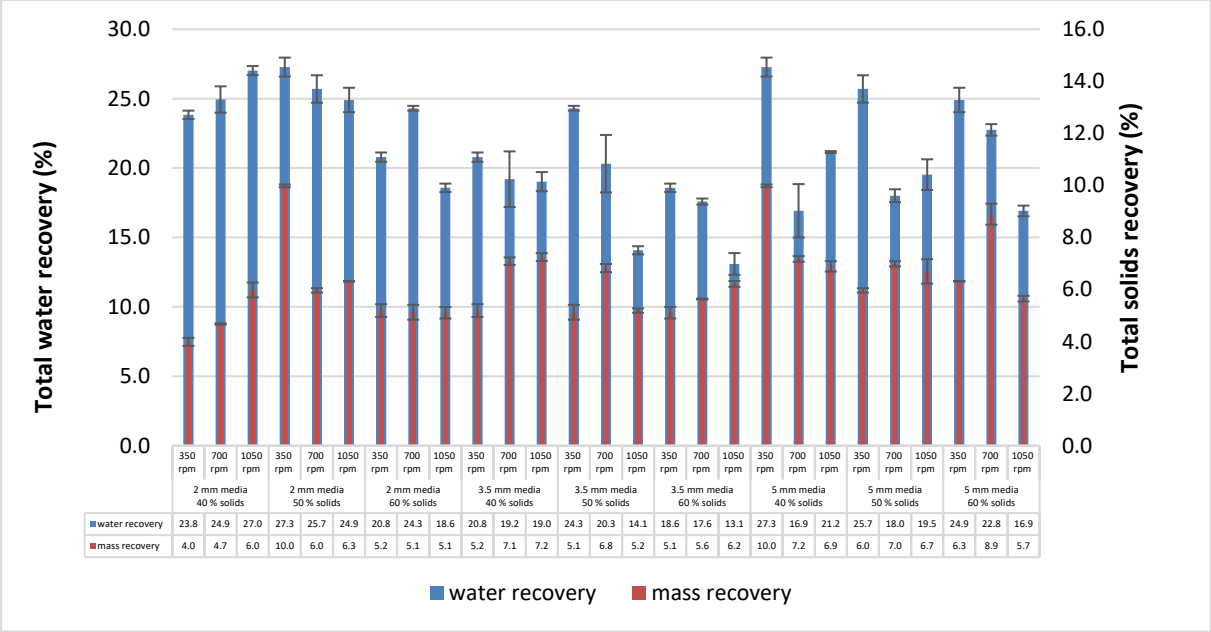

	350 rpm	700 rpm	1050 rpm	350 rpm	700 rpm	1050 rpm	350 rpm	700 rpm	1050 rpm	350 rpm	700 rpm	1050 rpm	350 rpm	700 rpm	1050 rpm	350 rpm	700 rpm	1050 rpm	350 rpm	700 rpm	1050 rpm	350 rpm	700 rpm	1050 rpm	350 rpm	700 rpm	1050 rpm
	2 mm media 40 % solids			2 mm media 50 % solids			2 mm media 60 % solids			3.5 mm media 40 % solids			3.5 mm media 50 % solids			3.5 mm media 60 % solids			5 mm media 40 % solids			5 mm media 50 % solids			5 mm media 60 % solids		
water recovery	23.8	24.9	27.0	27.3	25.7	24.9	20.8	24.3	18.6	20.8	19.2	19.0	24.3	20.3	14.1	18.6	17.6	13.1	27.3	16.9	21.2	25.7	18.0	19.5	24.9	22.8	16.9
mass recovery	4.0	4.7	6.0	10.0	6.0	6.3	5.2	5.1	5.1	5.2	7.1	7.2	5.1	6.8	5.2	5.1	5.6	6.2	10.0	7.2	6.9	6.0	7.0	6.7	6.3	8.9	5.7

Figure 5-7: Effect of tip speed on water and solids recovery

5.4.1.2 Effect of tip speed on PGM recovery

The PGM recovery was plotted against the P80, as shown in Figure 5-8. At high tip speeds and fine P80, the PGM recovery was less than 80%. At 700 rpm, the P80 range was between 25 µm and 85 µm, and the resultant PGM recoveries were above 80%. At low speeds of 350 rpm, both the P80 and the PGM recovery had a wide range. Figure 5-8 highlights that the speed of the mill has a significant impact on the P80.

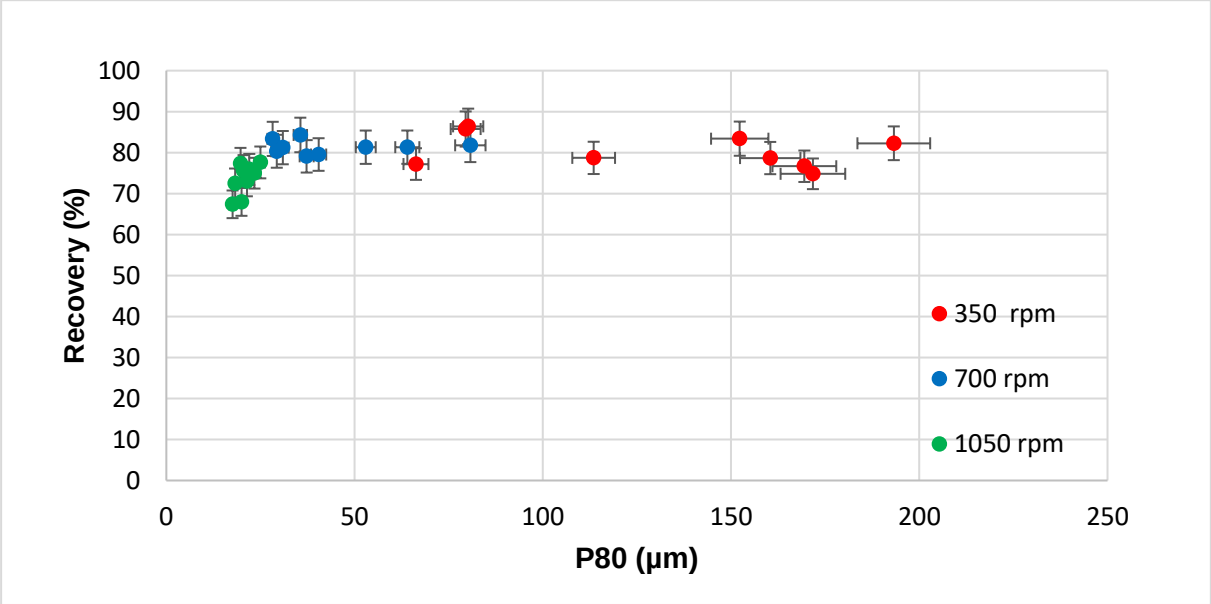

Figure 5-8: Effect of tip speed on PGM recovery

5.4.2 Effect of grinding media

5.4.2.1.1 Effect of grinding media size on water and solids recovery

The effect of the grinding media size on the water and solids recovery was studied by keeping the tip speed and solids concentration constant while changing the grinding media size. It was noted that a grinding media size of 5 mm gave the highest solids recovery for the whole run, except when the speed was at 1050 rpm. No significant trend was noted in the effect of the grinding media size on water recovery. Table 8-14 shows the values obtained for the water and solids recovery in the different combinations of parameters.

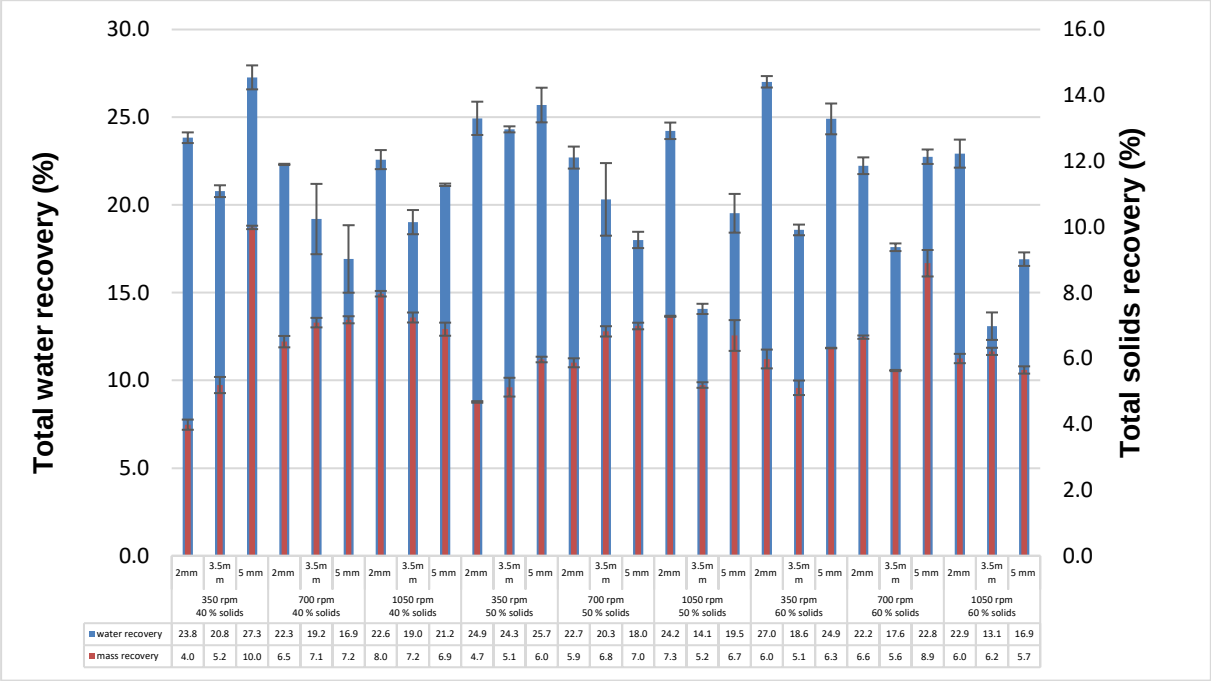

Figure 5-9: Effect of grinding media size on water and solids recovery

5.4.2.2 Effect of grinding media size on PGM recovery

Figure 5-10 shows the effect the grinding media size had on the P80 and the resultant recovery. The lowest recovery of 67.3% was observed at a P80 of 19 µm, which was achieved using a grinding media size of 3.5 mm. The highest recovery was achieved at a P80 of 80.1 µm using 5 mm grinding media. No significant trend was noted in the effect of grinding media size on the recovery, and the graph shows that the recovery is dependent on the P80.

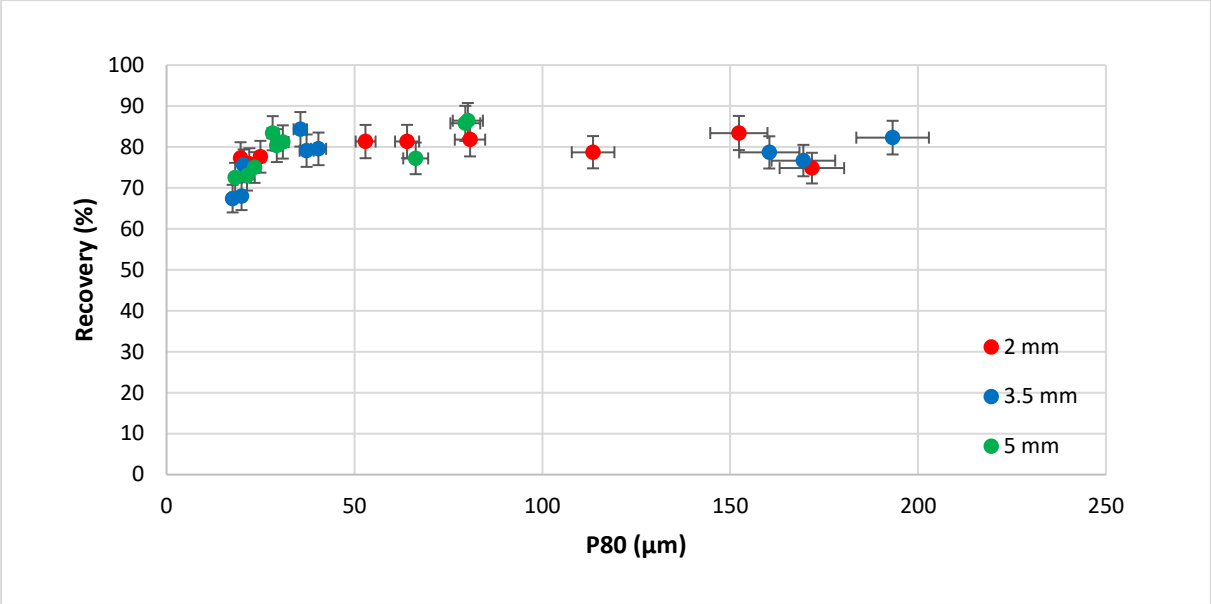

Figure 5-10: Effect of grinding media size on PGM recovery

5.4.3 Effect of solids concentration

5.4.3.1.1 Effect of solids concentration on water and solids recovery

The solids concentrations tested in the set of experiments were 40%, 50% and 60%. The effect of solids concentration on the water and solids recovery was studied by keeping the grinding media size and tip speed constant while changing the solids concentration. There was no significant trend in the water and solids recovery when the solids concentration was varied, as shown in Figure 5-11.

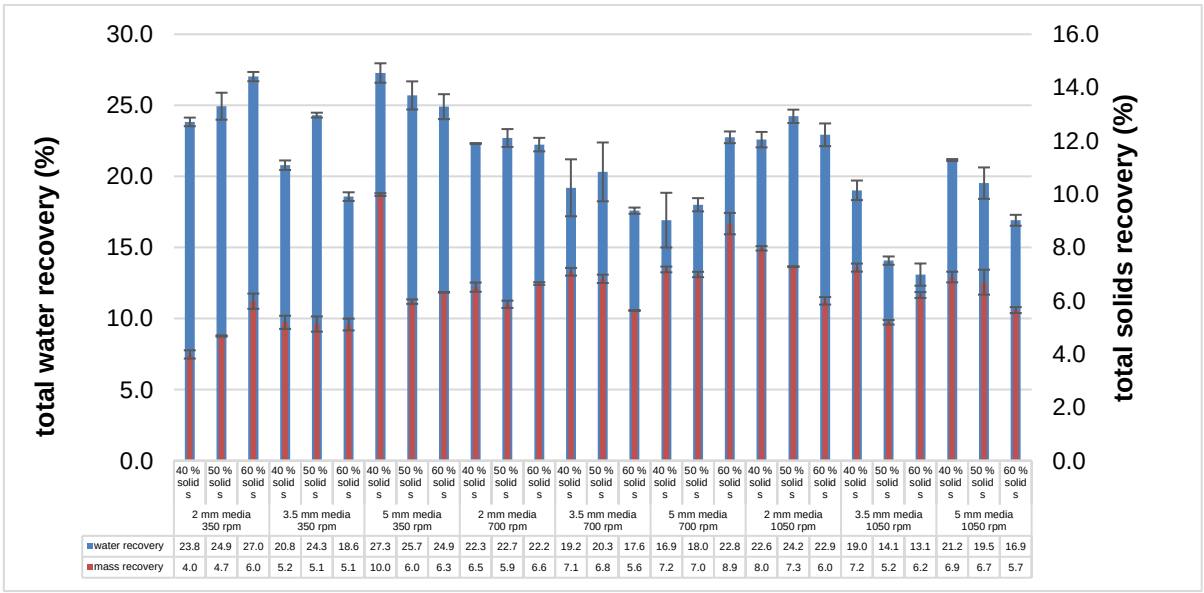

Figure 5-11: Effect of solids concentration on water and solids recovery

5.4.3.2 Effect of solids concentration on PGM recovery

Figure 5-12 shows the effect of the solids concentration on the PGM recovery. Varying the solids concentration has no significant impact on the P80 and the recovery. In Figure 5-12, the different solids concentrations give a wide distribution of P80s and recoveries. The recovery was dependent on the P80 value.

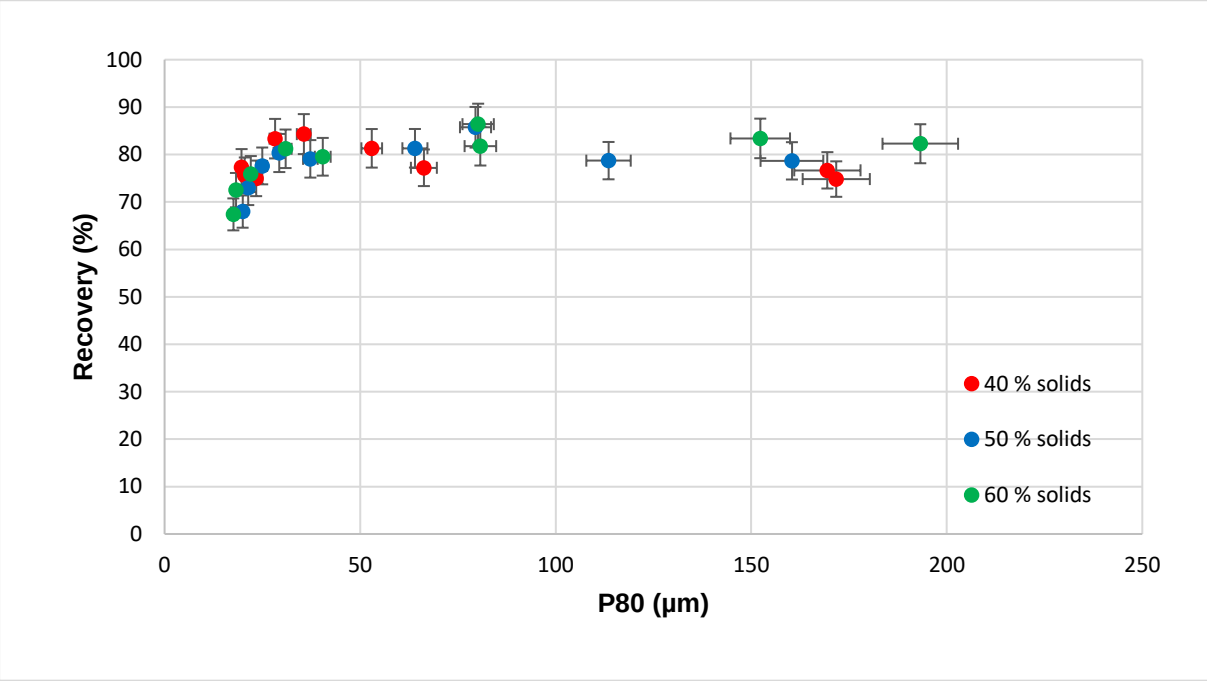

Figure 5-12: Effect of solids concentration on PGM recovery

5.5 Base Metal and Gangue Recovery

5.5.1 Nickel and copper recovery

In some instances, nickel recovery and copper recovery can be used as proxies for the PGM recovery. Figure 5-13 and Figure 5-14 show the recoveries for nickel and copper for the flotation tests that were done for the four different grinds. The nickel and copper recoveries behave similarly. For both copper and nickel, the highest recoveries were observed for the sample with a P80 of 52 µm and the lowest recoveries were observed for the sample with a P80 of 37 µm. Although the 4E recovery differences between the samples with different P80s, a similar trend was observed for the 4E recoveries, where the sample with a P80 of 52 µm had slightly higher recoveries and better kinetics than the other samples.

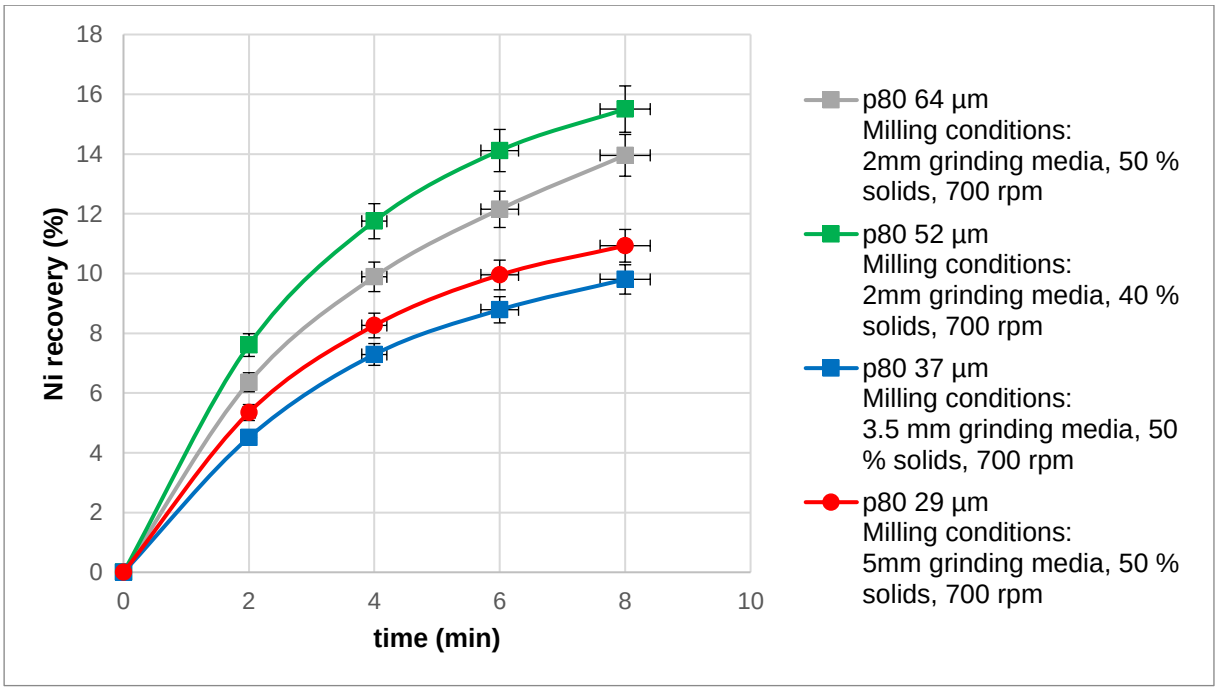

Figure 5-13: Ni recovery (%) vs flotation time

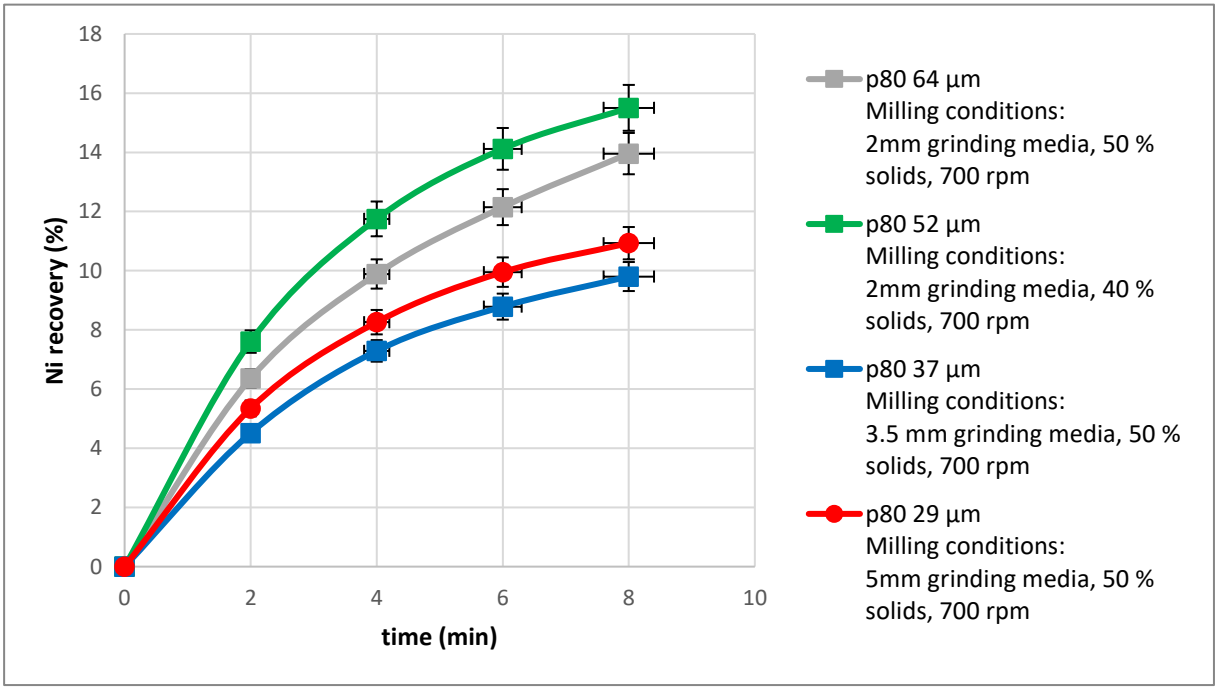

Figure 5-14: Cu recovery (%) vs flotation time

5.5.2 Nickel and copper recovery grade curves

Figure 5-15 and Figure 5-16 show the grade recovery curves for nickel and copper. The best grade recovery curves for both nickel and copper were observed for the samples with the coarser grinds i.e., a P80 of 64 µm and 52 µm. It is possible that optimizing the reagent doses could have resulted in improved the recoveries for the samples with finer grinds.

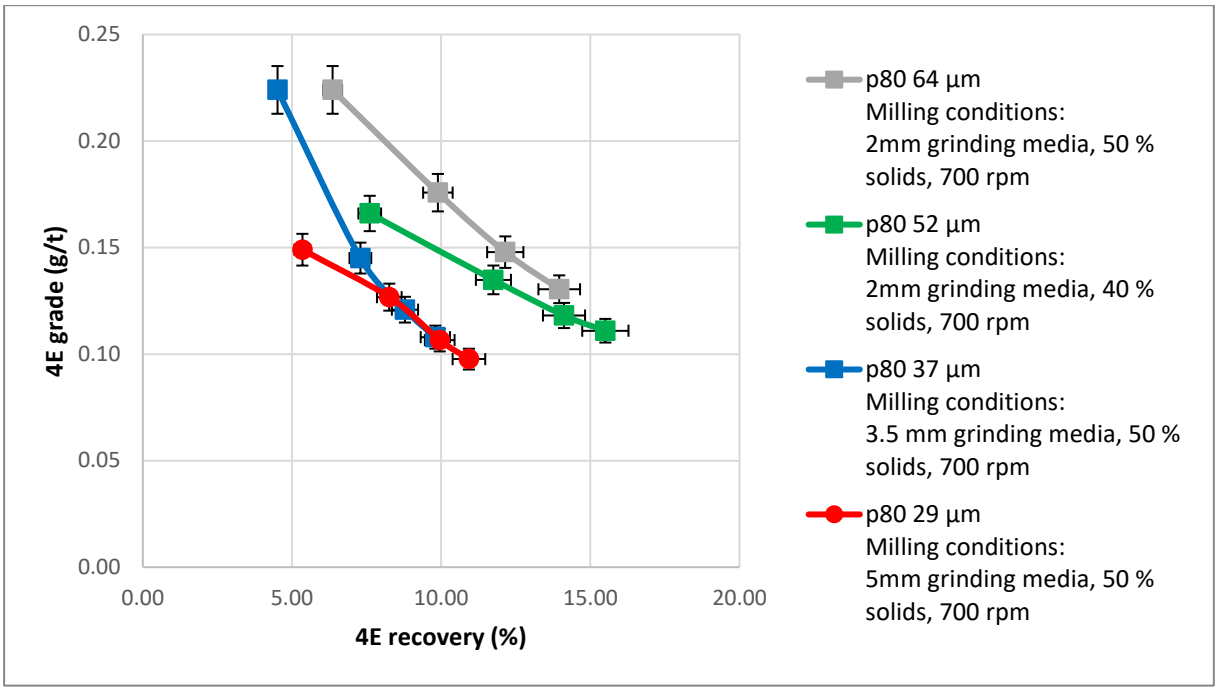

Figure 5-15: Ni grade recovery curves

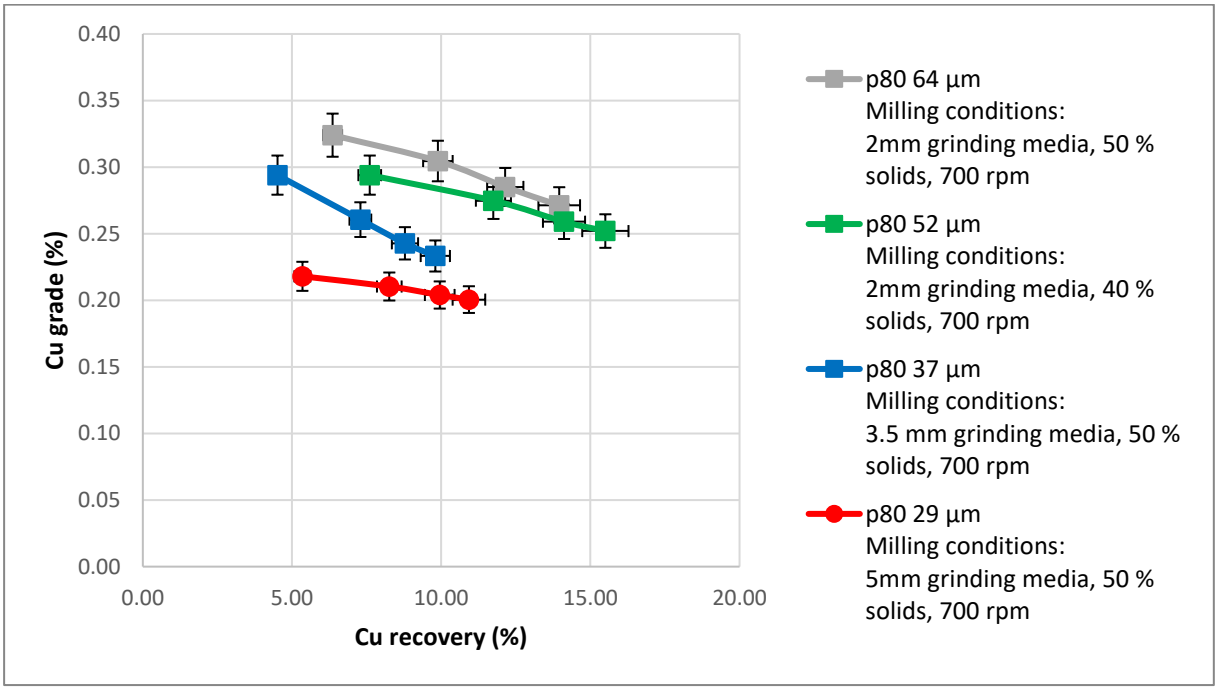

Figure 5-16: Cu grade recovery curves

5.5.3 Chrome and silica recovery

When considering the chrome and silica recoveries of a UG2 ore, the lower recoveries are favourable because of the adverse effects that chrome and silica have on the downstream processes in the PGM beneficiation chain such as smelting. Most processing plant target to

have chrome content of less than 3% (Wesseldijk et al., 1999). Figure 5-17 and Figure 5-18 show the chrome and silica recoveries for flotation tests conducted on the samples with varying P80s. The chrome and silica recoveries behaved similarly, in that the sample with the finer grind (P80 = 29 µm) gave the higher recoveries for both chrome and silica and the sample with the coarsest grind (P80 = 67 µm) gave the lowest recoveries for both chrome and silica. The high chrome and silica recoveries observed with the samples of finer grind may have been dues to high levels of entrainment since the reagent doses were not optimized.

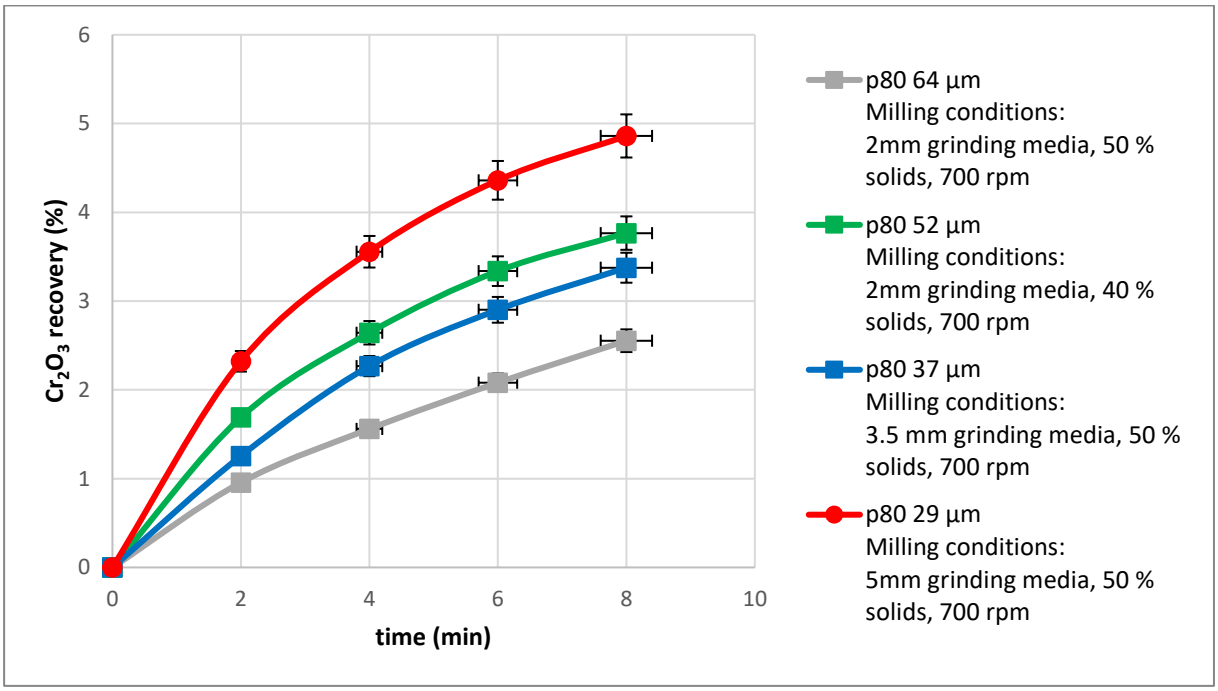

Figure 5-17: Cr2O3 recovery vs time

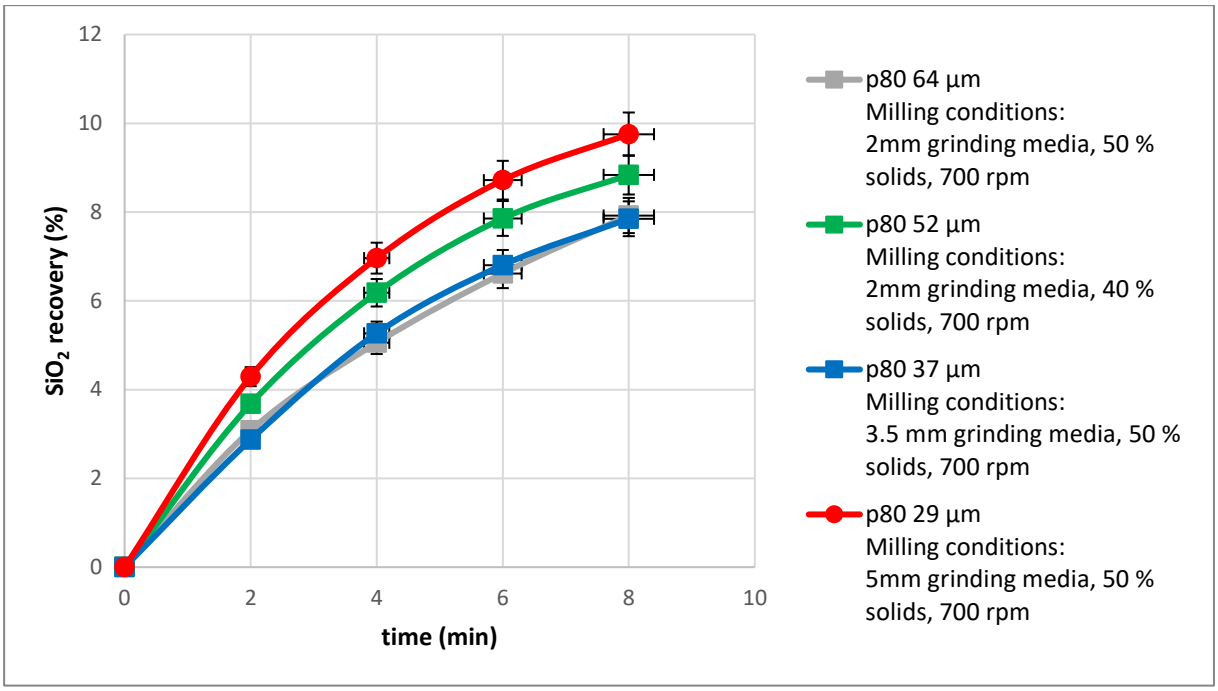

Figure 5-18: SiO_2 recovery vs time

5.5.4 Chrome and silica recovery grade curves

Figure 5-19 and Figure 5-20 show the recovery and grade curves for chrome and silica. For chrome, the sample that gave low recovery and low grade was the sample with a P80 67 µm. the results for the chrome sample indicate that sample would need to further flotation to decrease the chrome content. In the processing plant this would mean the samples would possibly need to be passed through a cleaning stage. The recovery grade curves for silica show that there is no significant change in the grade of silica for the different concentrates (C1, C2, C3, C4) and this may be due to the fact that silica makes up majority of the gangue material in the concentrates recovered

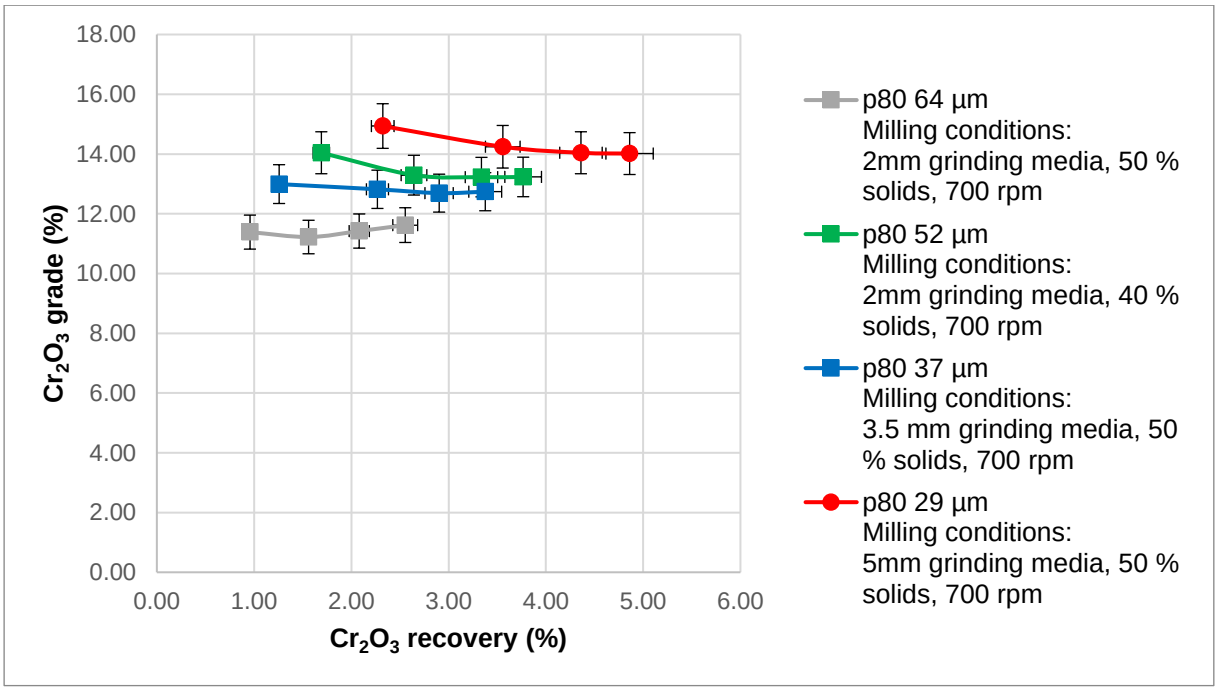

Figure 5-19: Grade recovery curve for Cr_2O_3

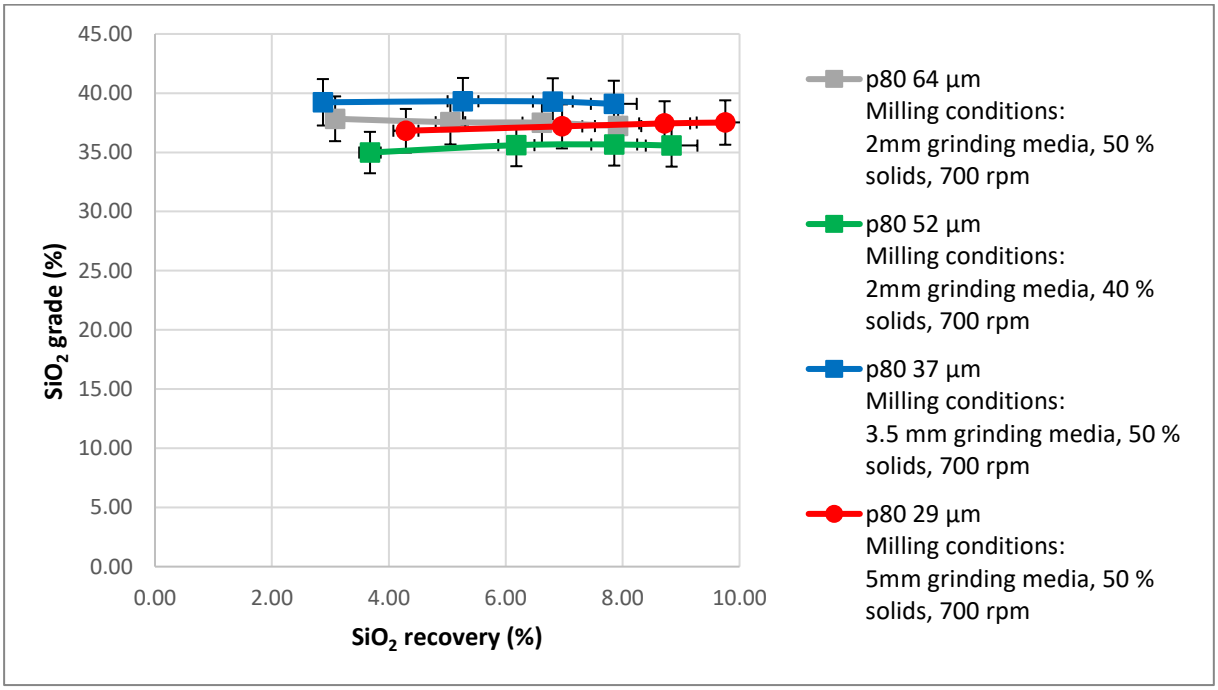

Figure 5-20: Grade recovery curve for SiO_2

5.5.5 Base metal and chrome size recovery plots

Size recovery plots for the base metals and chrome were plotted to assess if there is a noticeable trend as the particles get finer. Figure 5-21 and Figure 5-22 show the size recovery plots for copper and nickel. Both graphs indicate that there is an optimal size at which the high

recovery of the base metals can be achieved. Figure 5-23 shows the size recovery plot for chrome. It was observed the milled samples with a P80 of 20 µm and below had chrome recoveries that were higher than 3%. It can be noted that the flotation tested were conducted uses standard reagent doses for the treatment of UG2 ore and the reagents were not optimized to find the optimal dosages for the milled ore.

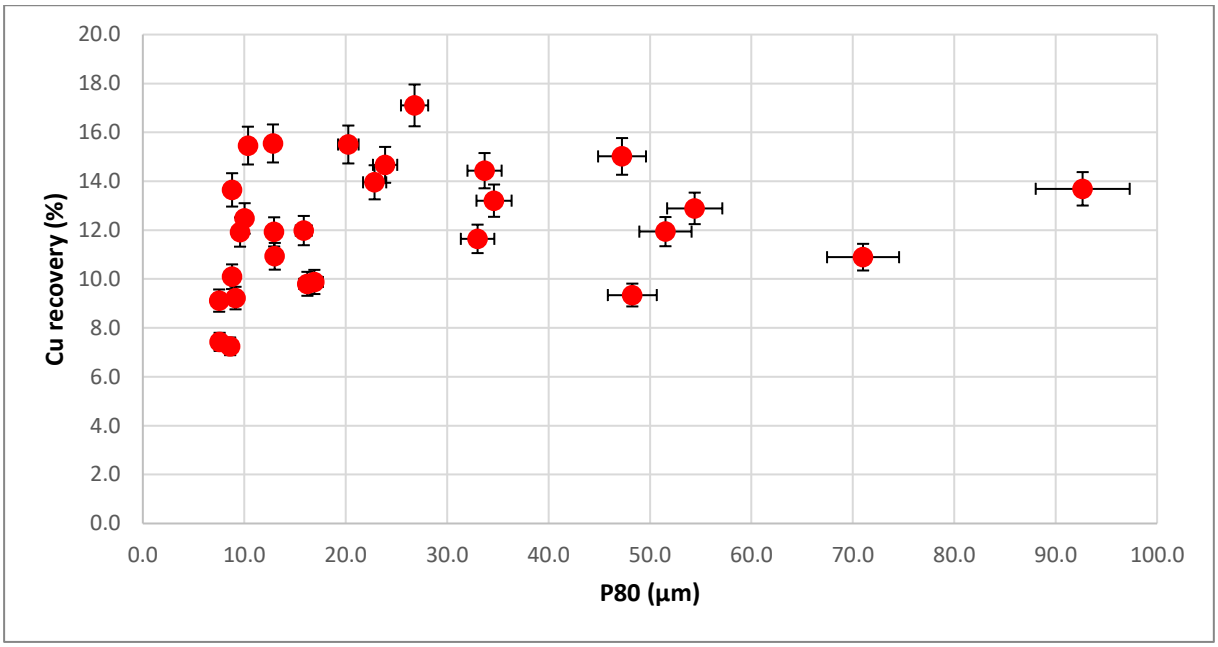

Figure 5-21: Copper size recovery plot

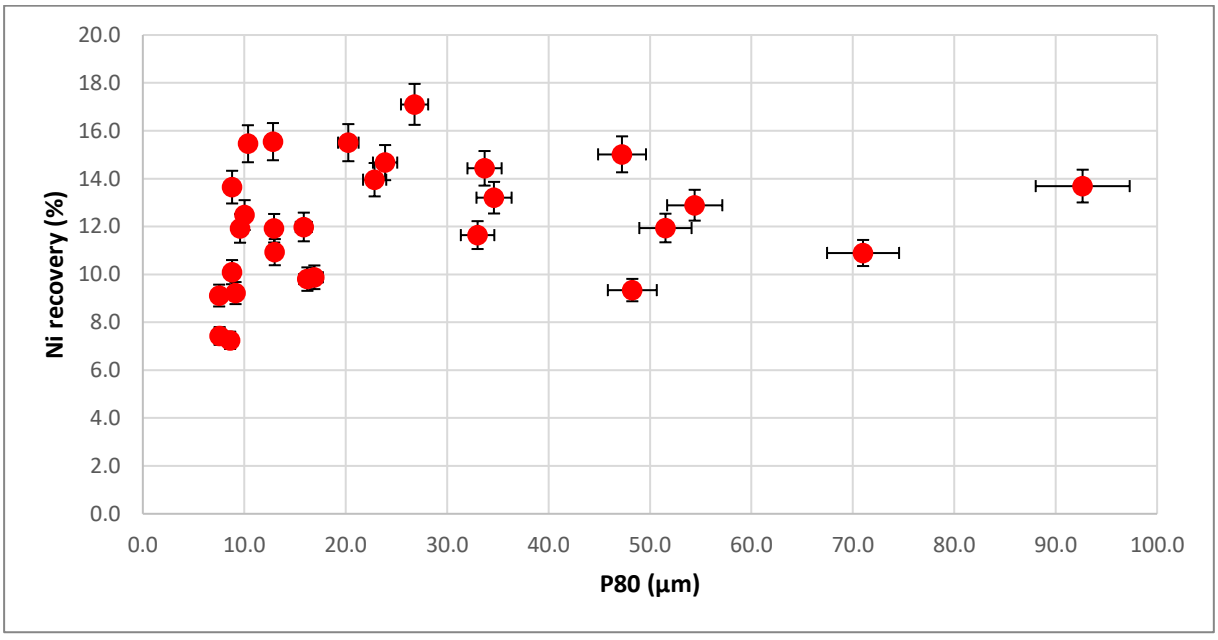

Figure 5-22: Nickel size recovery plot

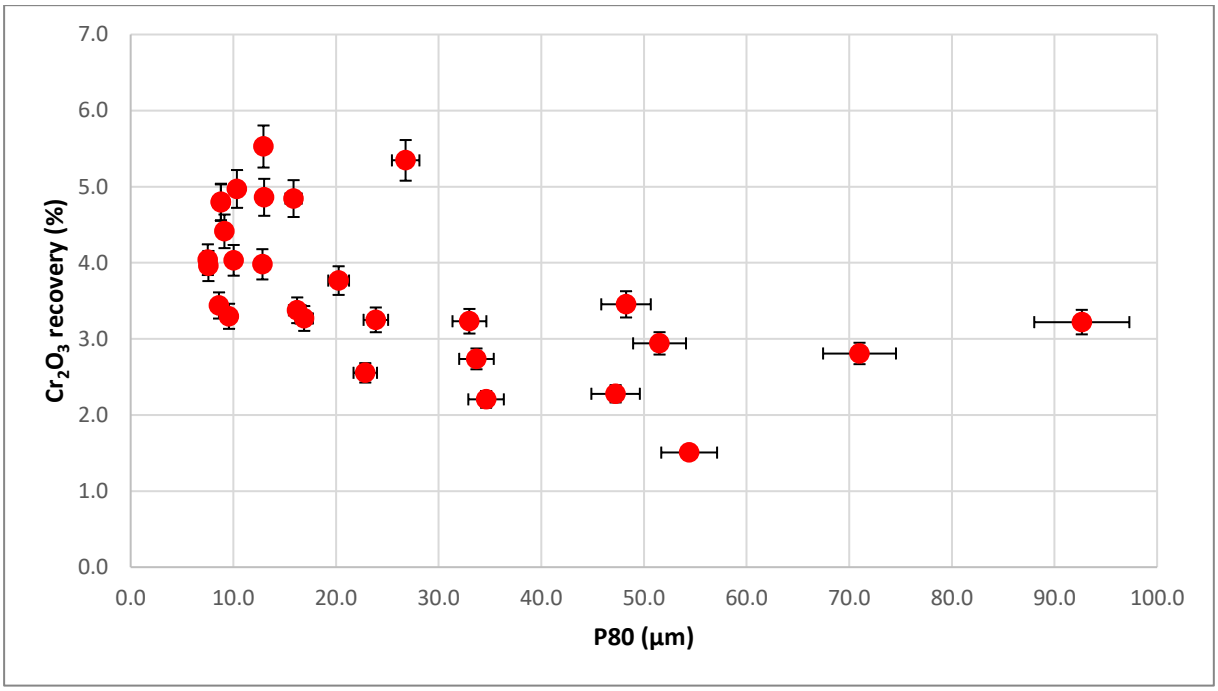

Figure 5-23: Chrome size recovery plot

5.6 Conclusion

This chapter analysed the results obtained from floating the milled UG2 ore. the water recovery decreased as the HIGmill product became finer. The result also showed that fine grinding increased the recovery potential of the ore. the increased in the recovery potential may be attributed to the increased liberation which results from fine grinding of the ore. Kinetic models used to fit the flotation tests showed that there is no significant difference in the recoveries of the finely ground material. It was also noted that the HIGmill P80 has the largest impact on the flotation result.

The flotation results were conducted using reagents at standard doses for the UG2 ore. Adjusting the reagent doses could potentially result in improved flotation efficiencies and reduce the chrome content in the concentrate.

6. CONCLUSION AND RECOMMENDATIONS

This chapter draws conclusions from the work done to test the hypotheses and answer the key questions. Results-based recommendations are detailed as part of the chapter.

This study was aimed at characterising fine grinding of UG2 ore by investigating the effects of HIGmill operating variables on the product fineness and energy efficiency. The parameters investigated in this project were the mill tip speed, the grinding media size, grinding media volume fill and the solids concentration. The study also investigated the flotation response of the comminuted UG2 by conducting batch flotation tests at standard conditions for the flotation of UG2 ores.

6.1 Conclusions

This section highlights the key questions posed in the literature review chapter and their respective answers.

6.1.1 Key questions and answers

1) What is the effect of tip speed, media size and solids concentration on the particle size distribution?

Tip speed

Increasing the tip speed resulted in a finer PSD for the speeds tested in the scope of work (350 rpm–1050 rpm). The increased speed resulted in higher media particle collision rates, which in turn resulted in higher grinding rates at high tip speeds.

Grinding media size

Increasing the grinding media size resulted in a finer PSD for the 2 mm, 3.5 mm and 5 mm grinding media size tested in the scope of work. This is because an increase in grinding media size results in high stress intensities.

Solids concentration

Increasing the solids concentration resulted in a coarser product when using grinding media sizes of 3.5 mm and 5 mm, although there was no significant difference between the 40% solids concentration and the 60% solids concentration. Using a grinding media size of 2 mm showed that.

2) What is the effect of tip speed, media size and solids concentration on the specific energy?

Tip speed

Increasing the tip speed resulted in a decrease in efficiency because of the increased power draw that is observed at high tip speeds.

Grinding media size

At solids concentrations of 50% and 60%, increasing the grinding media size was more energy efficient up to a certain specific energy, indicating that there is an optimum grinding media size that depends on the specific energy input of the system. At 40% solids, the 5 mm grinding media was the most efficient and 3.5 mm grinding media was the least efficient, up to an energy input of 5 kWh/t. Thereafter, the 2 mm grinding media was the most efficient and the 5 mm grinding media was the least efficient.

Solids concentration

There was no significant difference in the energy efficiency of the different solid concentrations when 5 mm grinding media was used. When 3.5 mm grinding media was used, the 40% and 50% solids concentrations were more efficient for energy inputs less than 2 kWh/t. Thereafter, the 60% solids concentration was more efficient. When using 2 mm grinding media, 40% solids concentration was more energy efficient, whereas the 50% grinding media was the least efficient for energy inputs above 2 kWh/t.

3) What is the effect of fine grinding on flotation recoveries?

Fine grinding helped to improve the recovery potential of the ore. The fine grinding did not significantly affect the recovery kinetics of the ore. When considering the UG2 ore the recovery of the chrome has to be observed as chrome negatively impacts the smelting process. Looking at the chrome recoveries observed in this scope of work it was noted that increase in milling product fineness resulted in an increase in the chrome recovery.

6.2 Recommendations

Based on the results and conclusions from this work, the following recommendations are made to gain a better understanding of stirred mill operation, and how stirred mills can be implemented in the mineral processing industry:

- The variables studied in the scope of work included tip speeds, grinding media sizes and solids concentrations at low, medium and high points. It is recommended that a wider range of variable settings and increased numbers of points should be studied to identify optimum points for the variables.
- It is recommended that studies that compare the HIGmill to other stirred mills on the market should be conducted to gain a better understanding of the HIGmill, since it is one of the newer stirred mills on the market.
- The feed top size in this study was 1000 µm. It is recommended that similar work be conducted with a finer feed top size because this is what has been used in other stirred mill studies.
- A similar study should be conducted that looks at the mineralogy of the milled product.
- It is recommended that a similar study be carried out, and the flotation reagents should be varied in order to assess the optimal flotation conditions for milled products. Optimizing the reagents would also help increase the flotation efficiencies and it could potentially decrease the recoveries of gangue material (chrome in particular)

7. REFERENCES

Amelunxen, P. & Meadows, D. 2011. Not another HPGR trade-off study! *Minerals and Metallurgical Processing*. 28(1):1–7. DOI: 10.1007/bf03402317.

Anderson, G.S. & Bandarian, P.A. 2019. Improving IsaMill™ energy efficiency through shaft spacer design. *Minerals Engineering*. 132(December 2018):211–219. DOI: 10.1016/j.mineng.2018.12.018.

Åstholm, M. 2015. Outotec HIGmill Outotec technology for fine and ultra-fine grinding in minerals processing.

de Bakker, J. 2014. Energy Use of Fine Grinding in Mineral Processing. *Metallurgical and Materials Transactions E*. 1(1):8–19. DOI: 10.1007/s40553-013-0001-6.

Ballantyne, G. & Giblett, A. 2019. Benchmarking comminution circuit performace for sustained improvement. *SAG Conference*. 1–16.

Ballantyne, G.R., Powell, M.S. & Tiang, M. 2012. Proportion of Energy Attributable to Comminution. (October):29–31.

Becker, M., Kwade, A. & Schwedes, J. 2001. Stress intensity in stirred media mills and its effect on specific energy requirement. *International Journal of Mineral Processing*. 61(3):189–208. DOI: 10.1016/S0301-7516(00)00037-5.

Becker, M., Mainza, A.N., Powell, M.S., Bradshaw, D.J. & Knopjes, B. 2008. Quantifying the influence of classification with the 3 product cyclone on liberation and recovery of PGMs in UG2 ore. *Minerals Engineering*. 21(7):549–558. DOI: 10.1016/j.mineng.2007.11.001.

Bel Fadhel, H. & Frances, C. 2001. Wet batch grinding of alumina hydrate in a stirred bead mill. 257–268.

Bergerman, M.G. & Delboni, H.J. 2014. Regrind of metallic ores with Vertical Mills : An overview of the existing plants in Brazil. *Impc 2014*. 1–10.

Bradshaw, D.J., Harris, P.J. & O'Connor, C.T. 1998. Synergistic interactions between reagents in sulphide flotation. *Journal of The South African Institute of Mining and Metallurgy*. 98(4):187–192.

Bu, X., Xie, G., Peng, Y., Ge, L. & Ni, C. 2017. Physicochemical Problems of Mineral Processing Kinetics Of Flotation. Order Of Process, Rate Constant Distribution And Ultimate Recovery. *Physicochem. Probl. Miner. Process*. 53(1):342–365.

Cayirli, S. & Gokcen, H.S. 2017. The Effect of Stirred Mill Orientation on Calcite Grinding The Effect of Stirred Mill Orientation on Calcite Grinding. (January):1–5.

Cayirli, S. & Serkan, H. 2017. The Effect of Stirred Mill Orientation on Calcite Grinding The Tests with Vertically Oriented Stirred. (January):5–8.

Celep, O., Aslan, N., Alp, I. & Taşdemir, G. 2011. Optimization of some parameters of stirred mill for ultra-fine grinding of refractory Au/Ag ores. *Powder Technology*. 208(1):121–127. DOI: 10.1016/j.powtec.2010.12.009.

Chaponda, B. 2011. Effect of operating variables on IsaMill™ performance using platinum bearing ores (MSc. Thesis). 19–21.

Cramer, L.A. 2001. The extractive metallurgy of South Africa's platinum ores. *Jom*. 53(10):14–18. DOI: 10.1007/s11837-001-0048-1.

Danielle, C.R., Erik, S., Patrick, T. & Hugh, M. 2017. Prediction of Product Size Distribution of a Vertical Stirred Mill Based on Breakage Kinetics. 11(11):1713–1717.

Ekmekçi, Z., Bradshaw, D.J., Allison, S.A. & Harris, P.J. 2003. Effects of frother type and froth height on the flotation behaviour of chromite in UG2 ore. *Minerals Engineering*. 16(10):941–949. DOI: 10.1016/j.mineng.2003.08.001.

Erb, H., van de Vijfeijken, M., Hanuman, Y., Rule, C., Swart, W.C.E., Lehto, H. & Keikkala, V. 2015. An initial review of the metallurgical performance of the HIGmillTM in a primary milling application in the hard rock mining industry. *SAG Conference*. 1–12.

Farber, B.Y., Durant, B. & Bedesi, N. 2011. Effect of media size and mechanical properties on milling efficiency and media consumption. *Minerals Engineering*. 24(3–4):367–372. DOI: 10.1016/j.mineng.2010.10.018.

Feng, D. & Aldrich, C. 1999. Effect of particle size on flotation performance of complex sulphide ores. *Minerals Engineering*. 12(7):721–731. DOI: 10.1016/S0892-6875(99)00059-X.

FLSmidth. 2018. *FLSmidth ® VXPmill*. Available: https://www.flsmidth.com/en-gb/products/milling-and-grinding/vxpmill.

Gao, M. & Forssberg, E. 1995. Prediction of product size distributions for a stirred ball mill. *Powder Technology*. 84:101–106.

Gao, M. & Holmes, R. 2008. Developments in fine and ultrafine grinding technologies for the minerals industry. *The Institute of Materials and Mining (IOM3) Mining, Feature, March, 1, p.20078.* 1–11.

Glencore Technology. 2015. IsaMill Breaking THE Boundaries.

Harris, T.. 2001. The Developmcnt of a Flotation Simulation Methodology Towards an Optimisation Study of UG2 Platinum Flotation Circuits. University of Cape Town.

Hasan, M.M. 2016. Process Modelling of Gravity Induced Stirred Mills. The University of Queensland.

Hasan, M., Palaniandy, S., Hilden, M. & Powell, M. 2016. Investigating internal classification within gravity induced stirred mills. *Minerals Engineering*. 95:5–13. DOI: 10.1016/j.mineng.2016.05.019.

Hasan, M., Palaniandy, S., Hilden, M. & Powell, M. 2017. Calculating breakage parameters of a batch vertical stirred mill. *Minerals Engineering*. 111(May):229–237. DOI: 10.1016/j.mineng.2017.06.024.

He, M. & Forssberg, E. 2007. Influence of slurry rheology on stirred media milling of quartzite. *International Journal of Mineral Processing*. 84(1–4):240–251. DOI: 10.1016/j.minpro.2006.08.001.

He, M., Wang, Y. & Forssberg, E. 2006. Parameter effects on wet ultrafine grinding of limestone through slurry rheology in a stirred media mill. *Powder Technology*. 161(1):10–21. DOI: 10.1016/j.powtec.2005.08.026.

Hogg, R. & Cho, H. 2000. A review of breakage behavior in fine grinding by stirred-media milling. *KONA Powder and Particle Journal*. 18(May):9–19. DOI: 10.14356/kona.2000007.

Howling Pixel. n.d. *IsaMill*. Available: https://howlingpixel.com/i-en/IsaMill.

Hu, W. 2014. Flotation Circuit Optimisation and Design. (September).

Jaiswal, S., Tripathy, S.K. & Banerjee, P.K. 2015. An overview of reverse flotation process for coal. *International Journal of Mineral Processing*. 134:97–110. DOI:

10.1016/j.minpro.2014.11.007.

Jankovic, A. 2001. MEDIA STRESS INTENSITY ANALYSIS FOR VERTICAL STIRRED MILLS *. 14(10):1177–1186.

Jankovic, A. 2003. Variables affecting the fine grinding of minerals using stirred mills. *Minerals Engineering*. 16(4):337–345. DOI: 10.1016/S0892-6875(03)00007-4.

Jankovic, A. 2008. A review of regrinding and fine grinding technology - the facts and myths. *Metso Minerals Process Technology Australia and Asia*.

Jankovic, A., Valery, W. & La Rosa, D. 2001. Fine grinding in the Austrilian mining industry. 1–11.

Jankovic, A., Valery, W., Maloney, K. & Markovic, Z.. 2006. Improving Overall Concentrator Performance with Stirred Milling. *Metsominerals.Nl*. (October):1–6.

Jayasundara, C.T., Yang, R.Y., Yu, A.B. & Rubenstein, J. 2010. Effects of disc rotation speed and media loading on particle flow and grinding performance in a horizontal stirred mill. *International Journal of Mineral Processing*. 96(1–4):27–35. DOI: 10.1016/j.minpro.2010.07.006.

Jeswiet, J. & Szekeres, A. 2016. Energy Consumption in Mining Comminution. *Procedia CIRP*. 48:140–145. DOI: 10.1016/j.procir.2016.03.250.

Junnola, J. 2013. Basic testwork with the Outotec pilot HIGmill TM. (December):88.

King, R.. 2001. *Modeling and Simulation of Mineral Processing Systems*. Utah: Butterworth-Heinemann.

Kwade, A. 1999a. Determination of the most important grinding mechanism in stirred media mills by calculating stress intensity and stress number. *Powder Technology*. 105(1–3):382–388. DOI: 10.1016/S0032-5910(99)00162-X.

Kwade, A. 1999b. Wet comminution in stirred media mills - Research and its practical application. *Powder Technology*. 105(1–3):14–20. DOI: 10.1016/S0032-5910(99)00113-8.

Kwade, A. 2003. A stressing model for the description and optimization of grinding processes. *Chemical Engineering and Technology*. 26(2):199–205. DOI: 10.1002/ceat.200390029.

Kwade, A. 2006. Specific Energy Consumption, Stress Energy and Power Draw of Stirred Media Mills and Their Effect on the Production Rate. In *Advances in Comminution*. S. Komar Kawatra, Ed. Colorado, USA: Society for Mining, Metallurgy and Exploration, Inc. 99–114.

Kwade, A. & Schwedes, J. 2002. Breaking characteristics of different materials and their effect on stress intensity and stress number in stirred media mills. *Powder Technology*. 122(2–3):109–121. DOI: 10.1016/S0032-5910(01)00406-5.

Kwade, A. & Schwedes, J. 2007. Wet Grinding in Stirred Media Mills. In *Handbook of Powder Technology*. Volume 12 ed. A.D. Salman, M. Ghadiri, & M.J. Hounslow, Eds. Els. 251–382.

Kwade, A., Blecher, L. & Schwedes, J. 1996. Motion and stress intensity of grinding beads in a stirred media mill. Part 2: Stress intensity and its effect on comminution. *Powder Technology*. 86(1):69–76. DOI: 10.1016/0032-5910(95)03039-5.

Laskowski, J.S. 2004. Testing flotation frothers. *2004 SME Annual Meeting Preprints*. (July):419–422.

Lehto, H. & Paz, A. 2013. Outotec HIGmills ; A Fine Grinding Technology. (April):245–250.

Lehto, H., Paz, A., Roitto, I. & Astholm, M. 2015. Outotec HIGmill TM Outotec technology for fine and ultra-fine grinding in minerals processing Outotec Comminution History.

Lichter, J.K.. & Davey, G. 2006. Selection and Sizing of Ultrafine and Stirred Grinding Mills. In *Advances in Comminution*. S. Komar Kawatra, Ed. Littleton, Colorado. 69–85.

Lisso, M. 2012. Evaluating the effect of operating variables on energy consumption in stirred mills. University of Cape Town.

Little, L. 2016. The Development And Demonstration Of A Practical Methodology For Fine Particle Shape Characterisation In Minerals Processing. University of Cape Town.

Little, L., Mainza, A.N., Becker, M. & Wiese, J. 2017. Fine grinding: How mill type affects particle shape characteristics and mineral liberation. *Minerals Engineering*. 111(May):148–157. DOI: 10.1016/j.mineng.2017.05.007.

Lofthouse, C.H. & Johns, F.E. 2002. The Svedala (ECC International) detritor and the metals industry. *Minerals Engineering*. 12(2):205–217. DOI: 10.1016/s0892-6875(98)00132-0.

Malvern Instruments. 2007.

Mankosa, M.., Adel, G.. & Yoon, R.. 1989. Effect of Operating Parameters in Stirred Ball Mill Grinding of Coal. 59:255–260.

Mankosa, M.J., Adel, G.T. & Yoon, R.H. 1986. Effect of media size in stirred ball mill grinding of coal. *Powder Technology*. 49(1):75–82. DOI: 10.1016/0032-5910(86)85008-2.

Metso. 2018. *Vertimill*. Available: https://www.metso.com/products/grinding-mills/stirred/vertimills/.

Metso. 2019. *VERTIMILL® Grinding Mills & Stirred Media Detritor*. Available: https://www.metso.com/globalassets/saleshub/documents---episerver/stirred_mills_brochure_en_lr.pdf.

Minerals, S. 2019. *User Manual HIG5 Mill*.

Mudd, G.M. 2010. Platinum group metals : a unique case study in the sustainability of mineral resources. 113–120.

Napier-munn, T. 2012. Comminution Energy and How to Reduce it. In *2012 CEEC Workshop,*. Australia.

Napier-Munn, T. & Wills, B.A. 2006. *Wills' Mineral Processing Technology*. DOI: 10.1016/B978-0-7506-4450-1.X5000-0.

Napier-Munn, T.., Morrell, S., Morrison, R.. & Kojovic, T. 2005. *Mineral Comminution Circuits: Their Operation and Optimization*. T. Napier-Munn, Ed. Queensland, Australia: Julius Kruttschnitt Mineral Research Center.

Ntsele, C. & Allen, J. 2012. Technology selection of stirred mills for energy efficiency in primary and regrinding applications for the platinum industry.

Ouattara, S. & Frances, C. 2014. Grinding of calcite suspensions in a stirred media mill : Effect of operational parameters on the product quality and the speci fi c energy. *Powder Technology*. 255:89–97. DOI: 10.1016/j.powtec.2013.11.025.

Outotec. 2016. *Grindforce - back to basics with higmill fine grinding physics*. Available: https://www.outotec.com/company/newsletters/minerva/minerva-issue-2--2016/grindforce---back-to-basics/.

Parsonage, P. 1988. Principles of mineral separation by selective magnetic coating.

International Journal of Mineral Processing. 24(3–4):269–293. DOI: 10.1016/0301-7516(88)90045-2.

Pease, J.D., Curry, D.C. & Young, M.F. 2006. Designing flotation circuits for high fines recovery. *Minerals Engineering*. 19(6–8):831–840. DOI: 10.1016/j.mineng.2005.09.056.

Peukert, W. 2004. Material properties in fine grinding. *International Journal of Mineral Processing*. 74(SUPPL.):3–17. DOI: 10.1016/j.minpro.2004.08.006.

Pitchumani, R., Zhupanska, O., Meesters, G.M.H. & Scarlett, B. 2004. Measurement and characterization of particle strength using a new robotic compression tester. *Powder Technology*. 143–144:56–64. DOI: 10.1016/j.powtec.2004.04.007.

Radziszewski, P. & Moore, A. 2017. Understanding the effect of pressure profile on stirred mill impeller wear. *Minerals Engineering*. 103–104:54–59. DOI: 10.1016/j.mineng.2016.08.013.

Rahal, D., Erasmus, D. & Major, K. 2011. Knelson-Deswik Milling Technology : Bridging the Gap between Low and High Speed Stirred Mills. *43rd Annual Meeting of the Canadian Mineral Processors*. 557–587.

Ramlall, N. V. 2013. An Investigation into The Effects Of UG2 Ore Variability On Froth Flotation. (January).

Ramlall, N. V. & Loveday, B.K. 2015. A comparison of models for the recovery of minerals in a UG2 platinum ore by batch flotation. *Journal of the Southern African Institute of Mining and Metallurgy*. 115(3):221–228. DOI: 10.17159/2411-9717/2015/v115n3a7.

Reddick, S., Rahal, D., Hines, B. & Shah, I. 2014. VXP2500 Stirred Mill Optimization at Casmyn Mining Turk Mine. In *46th Annual Canadian Mineral Processors Operators Conference*. 3–14.

Rocha, D., Spiller, E., Taylor, P. & Miller, H. 2018. Predicting the product particle size distribution from a laboratory vertical stirred mill. *Minerals Engineering*. 129(August):85–92. DOI: 10.1016/j.mineng.2018.09.016.

Roitto, I., Lehto, H., Paz, A. & Astholm, M. 2013. Stirred Milling Technology – A New Concept in Fine Grinding. (July):15–17.

Rule, C. 2010. Stirred milling — new comminution technology in the PGM industry. In *The 4th International Platinum Conference, Platinum in transition 'Boom or Bust'. The Southern African*

Institute of Mining and Metallurgy. 71–78.

Rule, C.M. 2009. Energy considerations in the current PGM processing flowsheet utilizing new technologies. *The Journal Of the Southern African Institute of Mining and Metallurgy*. (JANUARY):39–46.

Santosh, T., Soni, R.K., Eswaraiah, C., Rao, D.S. & Venugopal, R. 2020. Optimization of stirred mill parameters for fine grinding of PGE bearing chromite ore. *Particulate Science and Technology*. 0(0):1–13. DOI: 10.1080/02726351.2020.1795016.

Van Schoor, J.C.R. & Sandenbergh, R.F. 2012. Evaluation of the batch press as a laboratory tool to simulate medium-pressure roller crushers. *Journal of the Southern African Institute of Mining and Metallurgy*. 112(3):185–196.

Schouwstra, R.P., Kinloch, E.D. & Lee, C.A. 2000. A Short Geological Review of the Bushveld Complex. *Platinum Metals Review*. 44(1):33–39.

Scott, D.M. & Gutsche, O.W. 1999. ECT studies of bead fluidization in vertical mills. *1st World Congress on Industrial Process Tomography*. 90–95.

Sinnott, M., Cleary, P.W. & Morrison, R. 2006. Analysis of stirred mill performance using DEM simulation: Part 1- Media motion, energy consumption and collisional environment. *Minerals Engineering*. 19(15):1537–1550. DOI: 10.1016/j.mineng.2006.08.012.

Stenger, F., Mende, S., Schwedes, J. & Peukert, W. 2005. Nanomilling in stirred media mills. *Chemical Engineering Science*. 60(16):4557–4565. DOI: 10.1016/j.ces.2005.02.057.

Subrahmanyam, T. V. & Forssberg, K.S.E. 1990. Fine particles processing: shear-flocculation and carrier flotation - a review. *International Journal of Mineral Processing*. 30(3–4):265–286. DOI: 10.1016/0301-7516(90)90019-U.

Trahar, W.J. & Warren, L.J. 1976. The flotability of very fine particles - A review. *International Journal of Mineral Processing*. 3(2):103–131. DOI: 10.1016/0301-7516(76)90029-6.

Wang, Y. & Forssberg, E. 2000. Technical note product size distribution in stirred media mills. *Minerals Engineering*. 13(4):459–465. DOI: 10.1016/S0892-6875(00)00025-X.

Weber, U. & Langlois, D. 2010. The effect of grinding media performance on milling and operational behaviour. *Journal of the Southern African Institute of Mining and Metallurgy*. 110(3):147–152.

Weller, K.R., Spencer, S.J., Gao, M.W. & Liu, Y. 2000. Tracers studies and breakage testing in pilot-scale stirred mills. *Minerals Engineering*. 13(4):429–458. DOI: 10.1016/S0892-6875(00)00024-8.

Wesseldijk, Q.., Reuter, M.., Bradshaw, D.. & Harris, P.J. 1999. The Flotation Behaviour of Chromite With Respect to the Beneficiation of UG2 Ore. *Minerals Engineering*. 12(10):1177–1184.

Wills, B.A. 1997. Comminution. In *Mineral Processing Technology*. 6th ed. Butterworth-Heinemann. 110–116.

Wills, B.A. & Finch, J. 2015. *Wills' Mineral Processing Technology 8th Edition: An Introduction to the Practical Aspects of Ore Treatment and Mineral Recovery*.

Wills, B.A. & Finch, J.A. 2016. Grinding Mills. In *Wills' Mineral Processing Technology (Eighth Edition)*.

Yang, R.Y., Jayasundara, C.T., Yu, A.B. & Curry, D. 2006. DEM simulation of the flow of grinding media in IsaMill. *Minerals Engineering*. 19(10):984–994. DOI: 10.1016/j.mineng.2006.05.002.

Ye, X., Gredelj, S., Skinner, W. & Grano, S.R. 2010. Regrinding sulphide minerals - Breakage mechanisms in milling and their influence on surface properties and flotation behaviour. *Powder Technology*. 203(2):133–147. DOI: 10.1016/j.powtec.2010.05.002.

Yeu, J. & Klein, B. 2006. Effect of Bead Size on Ultra Fine Grinding in Stirred Bead Mill. In *Advances in Comminution*. S. Kawatra Komar, Ed. Littleton, Colorado: Society for Mining, Metallurgy and Exploration, Inc. 87–98.

Yianatos, J. & Contreras, F. 2010. Particle entrainment model for industrial flotation cells. *Powder Technology*. 197(3):260–267. DOI: 10.1016/j.powtec.2009.10.001.

Young, C.A. & Kawatra, K. 2019. *SME Mineral Processing and Extractive Metallurgy Handbook*. R. Dunne, C. Young, & K. Komar, Eds. United States Of America: Society for Mining, Metallurgy and Exploration, Inc.

Zheng, J., Harris, C.C. & Somasundaran, P. 1996. A study on grinding and energy input in stirred media mills. *Powder Technology*. 86(2):171–178. DOI: 10.1016/0032-5910(95)03051-4.

8. APPENDICES

Appendix A Literature Review

Table 8-1: FLSmidth VXPmill Ranges

Mill Class	Mill Type	Net Volume (L)	Installed Power (kW)
Lab	VXP2	3	3.7
	VXP10	10	15
Pilot	VXP25	27	30
	VXP50	50	56
Production	VXP100	110	110
	VXP250	290	132
	VXP500	480	224
	VXP1000	910	337
	VXP2500	2425	699
	VXP5000	5026	1475
	VXP10000	10273	3000

Table 8-2: The different mills available and their motor capacity (Young & Kawatra, 2019)

Installed Motor Capacity (Hp)	Vertimill	SMD	IsaMill	VXP Mill	HIGmill
0-499	VTM,15 VTM,20 VTM,40 VTM,60 VTM,75 VTM,125 VTM,150 VTM,200 VTM,250 VTM,300 VTM,400	SMD-0.75 SMD-7.5 SMD-18.5 SMD-90 SMD-185 SMD-355	M100 M500	VXP250 VXP500	HIG132 HIG300
500-999	VTM,500 VTM,650 VTM,800		M1000	VXP1000 VXP2000 VXP2500	HIG500 HIG700
1000-1999	VTM,1000 VTM,1250 VTM,1500	SMD-1100	M3000	VXP5000	HIG900 HIG1100
2000-2999			M5000		HIG1600
3000-3999	VTM,3000				HIG2300
4000-4999	VTM,4500		M10000		HIG3000 HIG3500
5000-9999			M15000 M50000		HIG4000 HIG5000

Appendix B Experimental Apparatus and Methodology

B.1 Milling Parameters Tested

The characterisation test work was conducted by varying different mill, ore and media parameters.

Table 8-3: Milling parameters tested

Feed Size [µm]	Mill Filling [v%]	Tip Speed [rpm]	Slurry% Solids [w/w]	Media Size [mm]
-1000	40	350	40	2
	50	525	50	3.5
	60	700	60	5
	70	875		
		1050		

B.1.1 Sample Preparation

Solids concentration preparation

Table 8-4: 40% solids concentration recipe

Mass of solids per test	3	kg
Target % solids (w/w)	40	%
Total mass (solids + water)	7.5	kg
Mass of water	4.5	kg
Volume of water	4.5	L
% Solids (v/v)	14.29	%
Density of the ore	4000	kg/m^3
Density of the ore	1000	kg/m^3
Volume of slurry	0.00525	m^3
Volume of slurry	5.25	L

Table 8-5: 50% solids concentration recipe

Mass of solids per test	3	kg
Target % solids (w/w)	50	%
Total mass (solids + water)	6	kg
Mass of water	3	kg
Volume of water	3	L
% Solids (v/v)	20.00	%
Density of the ore	4000	kg/m^3
Density of the ore	1000	kg/m^3
Volume of slurry	0.00375	m3
Volume of slurry	3.75	L

Table 8-6: 60% solids concentration recipe

Mass of solids per test	3	kg
Target% solids (w/w)	60	%
Total mass (solids + water)	5	kg
Mass of water	2	kg
Volume of water	2	L
% Solids (v/v)	27.27	%
Density of the ore	4000	kg/m^3
Density of the ore	1000	kg/m^3
Volume of slurry	0.00275	m3
Volume of slurry	2.75	L

B.1.2 Experimental Test Matrix

The experiment test matrix shows the milling runs with the products that were further processed using batch flotation.

Table 8-7: Core experimental test matrix

Experiment Number	Media Size [mm]	Slurry Density [% solids]	Tip Speed [m/s]
1	-1	-1	-1
2	-1	-1	0
3	-1	-1	1
4	-1	0	-1
5	-1	0	0
6	-1	0	1
7	-1	1	-1
8	-1	1	0
9	-1	1	1
10	1	-1	-1
11	1	-1	0
12	1	-1	1
13	1	0	-1
14	1	0	0
15	1	0	1
16	1	1	-1
17	1	1	0
18	1	1	1
19	0	-1	-1
20	0	-1	0
21	0	-1	1
22	0	0	-1
23	0	0	0
24	0	0	1
25	0	1	-1
26	0	1	0
27	0	1	1

B.1.3 HIGmill calibration

Test HIG5 Mill

Total number of Discs	9	#
Number of Castellated Discs	9	#
Disc Diameter	0.11	m
Bead density	4	kg/dm^3
Bead Size	3-4	mm

University of Cape Town

Verder VF15 Pump	
240 L/h	1142.6 rpm Pump Motor Speed on VSD Display
120 L/h	576.2 Pump Motor Speed on VSD Display
60 l/h	294.8 Pump Motor Speed on VSD Display

HIG5 mill power Calibration (Water; Grinding Media)

Bead Mass (kg)	Bead Volume (dm^3)	Bead Bulk Density (kg/dm^3)
4.65	1.86	2.5
6.97	2.788	2.5
9.3	3.72	2.5

Control Room SP	Motor Speed	Disc/Shaft Speed		Tip Speed	Media Filling	Bead Depth	No Discs Covered	Feed Rate	Solids Density	Liquid Density	% Solids	Water only Flowrate	Flowrate Selection	VSD Motor Power	Motor Power from Torque	Measured Torque	Motor Power from Torque (Display)					
Hz	%	rpm	rpm	m/s	%	m		kg/h	kg/m^3	kg/m^3	%	l/h			kg/h	A			%	W	Nm	W
8	20	238	240	1.38	30	0.174	2.7	0	3360	1000	0	240			240		12.3	49.8466	2	51	5	157
12	30	358	360	2.07	30	0.174	2.7	0	3360	1000	0	240			240	8.4		97.47315	2.6	97	6.1	284
16	40	477	480	2.76	30	0.174	2.7	0	3360	1000	0	240			240	8.25		164.8394	3.3	166	7.3	460
20	50	596	600	3.46	30	0.174	2.7	0	3360	1000	0	240			240	8.05		262.1345	4.2	261	9	706
24	60	718	720	4.15	30	0.174	2.7	0	3360	1000	0	240			240	8.05		375.9439	5	367	10.5	980
28.2	70	842	840	4.84	30	0.174	2.7	0	3360	1000	0	240			240	8.02		520.2268	5.9	518	12.4	1357
32.2	80	961	960	5.53	30	0.174	2.7	0	3360	1000	0	240			240	8.11		684.3227	6.8	681	14.3	1785
36.2	90	1081	1080	6.22	30	0.174	2.7	0	3360	1000	0	240			240	8.16		837.6952	7.4	840	15.6	2188
49.9	100	1491	1493	8.6	30	0.174	2.7	0	3360	1000	0	240			240	8.4	20.5	1483.303	9.5	1479	17.2	2686
7.9	20	236	240	1.38	30	0.174	2.7	0	3360	1000	0	120			120	8	12	49.42772	2	50	4.5	114
12	30	351	360	2.07	30	0.174	2.7	0	3360	1000	0	120			120	8.39	6	102.9186	2.8	104	5.7	213
16	40	477	480	2.76	30	0.174	2.7	0	3360	1000	0	120			120	8.2	0.8	179.8248	3.6	179	6.6	330
20	50	596	600	3.46	30	0.174	2.7	0	3360	1000	0	120			120	8.11	4.3	274.6171	4.4	276	7.6	477
24	60	716	720	4.15	30	0.174	2.7	0	3360	1000	0	120			120	8	10.2	389.8926	5.2	392	8.7	660
28	70	836	840	4.84	30	0.174	2.7	0	3360	1000	0	120			120	8.05	14.6	516.5197	5.9	517	10	878
32.2	80	961	960	5.53	30	0.174	2.7	0	3360	1000	0	120			120	8.09	16	674.2591	6.7	673	11.4	1139
36.2	90	1080	1080	6.22	30	0.174	2.7	0	3360	1000	0	120			120	8.15	17	836.9203	7.4	831	12.9	1450

Control Room SP	Motor Speed	Disc/Shaft Speed		Tip Speed	Media Filling	Bead Depth	No Discs Covered	Feed Rate	Solids Density	Liquid Density	% Solids	Water only Flowrate	Flowrate Selection	VSD Motor Power	Motor Power from Torque	Measured Torque	Motor Power from Torque (Display)				
Hz	%	rpm	rpm	m/s	%	m		kg/h	kg/m³	kg/m³	%	l/h			kg/h	A			%	W	Nm	W
40.2	100	1200	1200	6.91	30	0.174	2.7	0	3360	1000	0	120			120	8.23	18.4	1017.876	8.1	1022	14.4	1792
8	20	248	240	1.38	30	0.174	2.7	0	3360	1000	0	60			60	8.86	11.5	59.73215	2.3	56	5	126
12	30	358	360	2.07	30	0.174	2.7	0	3360	1000	0	60			60	8.4	6.1	104.9711	2.8	104	5.9	224
16	40	477	480	2.76	30	0.174	2.7	0	3360	1000	0	60			60	8.16	0.9	174.8296	3.5	175	6.8	340
20	50	596	600	3.46	30	0.174	2.7	0	3360	1000	0	60			60	8.05	4.2	268.3758	4.3	271	7.8	489
24	60	716	720	4.15	30	0.174	2.7	0	3360	1000	0	60			60	8.3	10.1	389.8926	5.2	388	8.9	674
28.1	70	838	840	4.84	30	0.174	2.7	0	3360	1000	0	60			60	8.05	14.9	526.5309	6	524	10.2	895

Parameters with 4.65 kg grinding media

Control Room SP		Motor Speed	Disc/Shaft Speed	Tip Speed	Media Filling	Bead Depth	No Discs Covered	Feed Rate	Solids Density	Liquid Density	% Solids	Water only Flowrate	Flowrate Selection	VSD Motor Power				Motor Power from Torque (calc)	Measured Torque (Display)	Motor Power from Torque (Display)
Hz	%	rpm	rpm	m/s	%	m		kg/h	kg/m³	kg/m³	%	l/h	kg/h	A			%	W	Nm	W
10.1	20	301	240	1.73	45	0.2608	4	0	3360	1000	0	240	240	8.6			4.2	157.6032	5	157
15.1	30	448	360	2.59	45	0.2608	4	0	3360	1000	0	240	240	8.3			2.9	286.1781	6.1	284
20.1	40	597	480	3.46	45	0.2608	4	0	3360	1000	0	240	240	8.19			9.6	456.3792	7.3	460
25.1	50	750	600	4.32	45	0.2608	4	0	3360	1000	0	240	240	8.23			20.5	706.8583	9	706
30.1	60	896	720	5.18	45	0.2608	4	0	3360	1000	0	240	240	8.4			23.1	985.2035	10.5	980
35.1	70	1051	840	6.05	45	0.2608	4	0	3360	1000	0	240	240	8.6			26.4	1364.75	12.4	1357
40.3	80	1200	960	6.91	45	0.2608	4	0	3360	1000	0	240	240	8.86			29.8	1796.991	14.3	1785
45.3	90	1349	1080	7.78	45	0.2608	4	0	3360	1000	0	240	240	9.05			32.2	2203.764	15.6	2188

Control Room SP		Motor Speed	Disc/Shaft Speed	Tip Speed	Media Filling	Bead Depth	No Discs Covered	Feed Rate	Solids Density	Liquid Density	% Solids	Water only Flowrate	Flowrate Selection	VSD Motor Power				Motor Power from Torque(calc)	Measured Torque (Display)	Motor Power from Torque (Display)
Hz	%	rpm	rpm	m/s	%	m		kg/h	kg/m³	kg/m³	%	l/h	kg/h	A			%	W	Nm	W
49.9	100	1486	1493	8.56	45	0.2608	4	0	3360	1000	0	240	240	9.02			35.1	2676.553	17.2	2686
8	20	237	240	1.38	45	0.2608	4	0	3360	1000	0	120	120	8.86			7.5	111.6836	4.5	114
12	30	356	360	2.07	45	0.2608	4	0	3360	1000	0	120	120	8.4			0.8	212.4973	5.7	213
16.1	40	478	480	2.76	45	0.2608	4	0	3360	1000	0	120	120	8.2			5	330.3699	6.6	330
20.1	50	597	600	3.46	45	0.2608	4	0	3360	1000	0	120	120	8.2			10.3	475.1345	7.6	477
24.2	60	720	720	4.15	45	0.2608	4	0	3360	1000	0	120	120	8.2			17.2	655.9645	8.7	660
28.2	70	839	840	4.84	45	0.2608	4	0	3360	1000	0	120	120	8.3			22.2	878.5987	10	878
32.2	80	961	960	5.53	45	0.2608	4	0	3360	1000	0	120	120	8.5			24.6	1147.247	11.4	1139
36.3	90	1080	1080	6.22	45	0.2608	4	0	3360	1000	0	120	120	8.6			27.4	1458.956	12.9	1450
40.2	100	1197	1200	6.91	45	0.2608	4	0	3360	1000	0	120	120	8.8			29.9	1805.033	14.4	1792
8.1	20	240	240	1.38	45	0.2608	4	0	3360	1000	0	60	60	8.7			6.3	125.6637	5	126
12.1	30	359	360	2.07	45	0.2608	4	0	3360	1000	0	60	60	8.3			0.4	221.8069	5.9	224
16.2	40	480	480	2.76	45	0.2608	4	0	3360	1000	0	60	60	8.2			5.3	341.8053	6.8	340
20.2	50	600	600	3.46	45	0.2608	4	0	3360	1000	0	60	60	8.2			10.6	490.0885	7.8	489
24.3	60	722	720	4.15	45	0.2608	4	0	3360	1000	0	60	60	8.2			17.7	672.9082	8.9	674
28.3	70	842	840	4.84	45	0.2608	4	0	3360	1000	0	60	60	8.3			22.5	899.3751	10.2	895

Parameters with 9.3 kg grinding media

Control Room SP		MotorSpeed	Disc/Shaft Speed	Tip Speed	Media Filling	Bead Depth	No Discs Covered	Feed Rate	Solids Density	Liquid Density	% Solids	Water only Flowrate	Flowrate Selection	VSD Motor Power				Motor Power from Torque (calc)	Measured Torque (Display)	Motor Power from Torque (Display)
Hz	%	rpm	rpm	m/s	%	m		kg/h	kg/m³	kg/m³	%	l/h	kg/h	A			%	W	Nm	W
10.1	20	297	300	1.73	60	0.348	5.4	0	3360	1000	0	240	240	8.5	2	261.2548	8.4	263	5	157
15.2	30	449	450	2.59	60	0.348	5.4	0	3360	1000	0	240	240	8.4	10	465.4898	9.9	466	6.1	284
20.2	40	597	699	3.46	60	0.348	5.4	0	3360	1000	0	240	240	8.5	18.4	743.9606	11.9	745	7.3	460
25.3	50	749	750	4.32	60	0.348	5.4	0	3360	1000	0	240	240	8.7	31.1	1137.309	14.5	1128	9	706
30.3	60	898	900	5.18	60	0.348	5.4	0	3360	1000	0	240	240	9	35.2	1485.806	15.8	1575	10.5	980
35.3	70	1047	1050	6.05	60	0.348	5.4	0	3360	1000	0	240	240	9.4	38.2	2039.333	18.6	2029	12.4	1357
40.4	80	1197	1200	6.91	60	0.348	5.4	0	3360	1000	0	240	240	9.9	45	2782.76	22.2	2785	14.3	1785
45.5	90	1349	1350	7.78	60	0.348	5.4	0	3360	1000	0	240	240	10.44	50.1	3531.674	25	3520	15.6	2188
50	100	1480	1482	8.56	60	0.348	5.4	0	3360	1000	0	240	240	10.7	55.1	4277.593	27.6	4282	17.2	2686
8.2	20	240	240	1.38	60	0.348	5.4	0	3360	1000	0	120	120	8.76	0.7	208.6018	8.3	209	4.5	114
12.2	30	359	360	2.07	60	0.348	5.4	0	3360	1000	0	120	120	8.56	7	357.1467	9.5	397	5.7	213
16.3	40	481	480	2.76	60	0.348	5.4	0	3360	1000	0	120	120	8.46	13.3	549.0352	10.9	548	6.6	330
20.2	50	597	600	3.46	60	0.348	5.4	0	3360	1000	0	120	120	8.56	19.3	775.2194	12.4	776	7.6	477
24.3	60	719	720	4.15	60	0.348	5.4	0	3360	1000	0	120	120	8.75	28.2	1084.226	14.4	1079	8.7	660
28.3	70	838	840	4.84	60	0.348	5.4	0	3360	1000	0	120	120	9.03	34.7	1439.185	16.4	1432	10	878
32.4	80	960	960	5.53	60	0.348	5.4	0	3360	1000	0	120	120	9.27	37.1	1799.504	17.9	1797	11.4	1139
36.4	90	1079	1080	6.22	60	0.348	5.4	0	3360	1000	0	120	120	9.73	43.5	2395.443	21.2	2388	12.9	1450
40.5	100	1200	1200	6.91	60	0.348	5.4	0	3360	1000	0	120	120	10.1	47.7	2978.23	23.7	2974	14.4	1792
8.2	20	240	240	1.38	60	0.348	5.4	0	3360	1000	0	60	60	8.71	0.3	213.6283	8.5	214	5	126

Control Room SP		Motor Speed	Disc/Shaft Speed	Tip Speed	Media Filling	Bead Depth	No Discs Covered	Feed Rate	Solids Density	Liquid Density	% Solids	Water only Flowrate	Flowrate Selection	VSD Motor Power				Motor Power from Torque (calc)	Measured Torque (Display)	Motor Power from Torque (Display)
Hz	%	rpm	rpm	m/s	%	m		kg/h	kg/m^3	kg/m^3	%	l/h	kg/h	A			%	W	Nm	W
12.3	30	362	360	2.07	60	0.348	5.4	0	3360	1000	0	60	60	8.5	7.1	367.7129	9.7	369	5.9	224
16.2	40	478	480	2.76	60	0.348	5.4	0	3360	1000	0	60	60	8.4	13.2	545.6109	10.9	547	6.8	340
20.3	50	600	600	3.46	60	0.348	5.4	0	3360	1000	0	60	60	8.5	20	797.9645	12.7	794	7.8	489
24.4	60	722	720	4.15	60	0.348	5.4	0	3360	1000	0	60	60	8.7	28	1103.872	14.6	1103	8.9	674
28.4	70	840	840	4.84	60	0.348	5.4	0	3360	1000	0	60	60	9	34.9	1451.416	16.5	1455	10.2	895

Note

Check mill for gearbox and shell vibration at each speed input, starting from minimum to maximum data useful to determine the power input to the material

For each speed hold for 30 s to stabilise power

Test HIGmill = 100% torque at 50 Hz (1500 rpm)

Test HIGmill tip speed: min 2 m/s; nom 3 m/s; max 7 m/s Test HIGmill max flow (design) 240 l/h

B.2 Assessment of Milling Performance

B.2.1 Product Size Distribution

Effect of mill tip speed

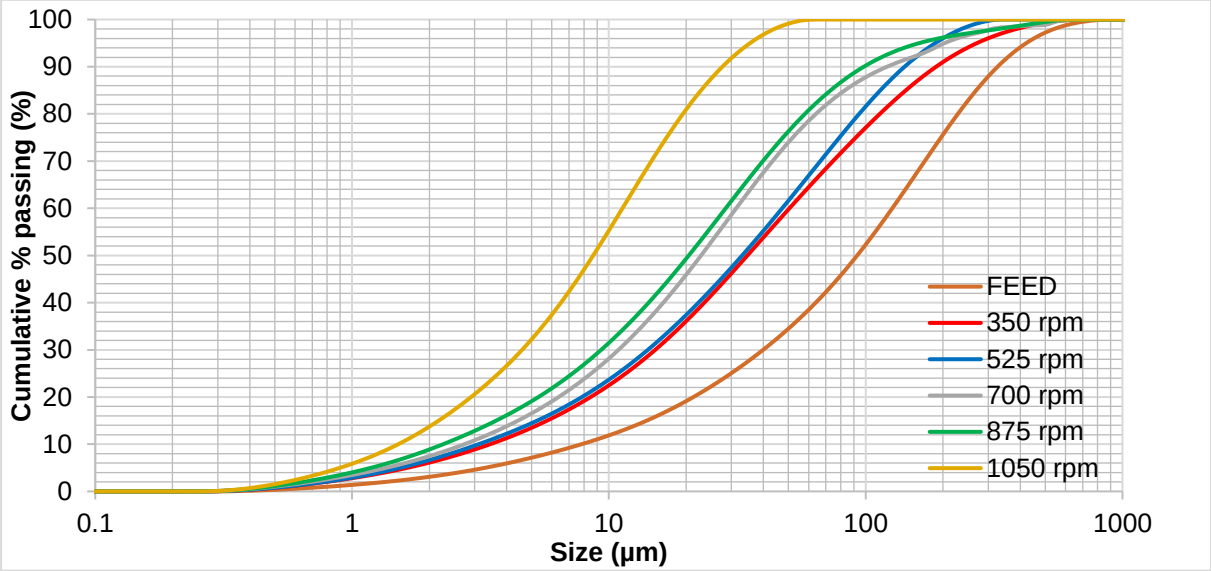

Figure 8-1: Effect of mill speed on product PSD at 3 min grinding time, 50% solids concentration, and a grinding media size of 2 mm

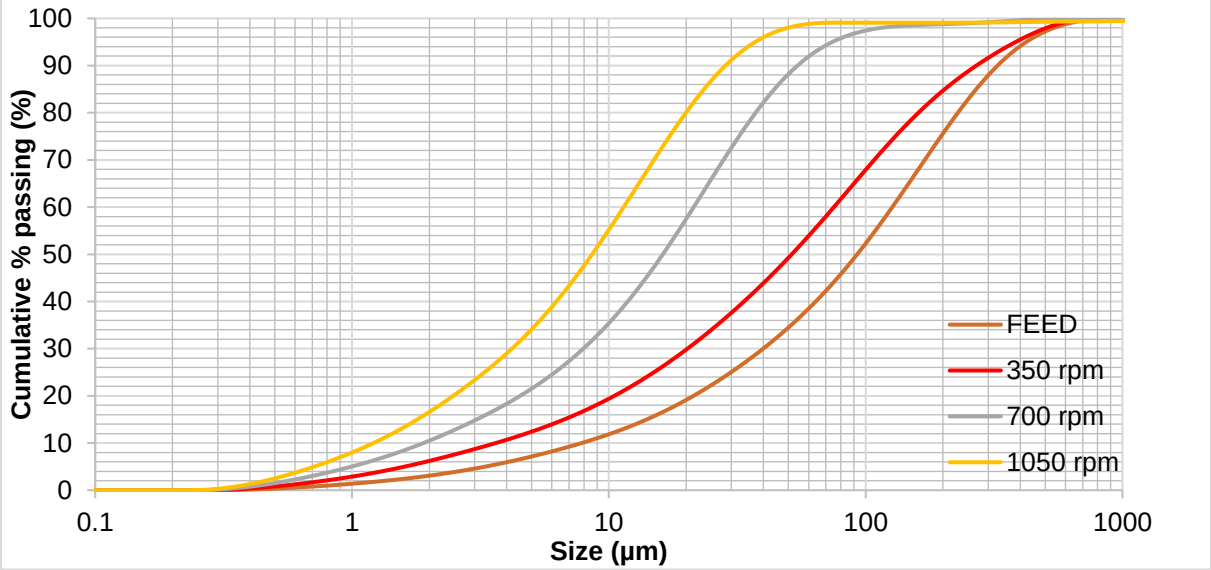

Figure 8-2: Effect of mill speed on product PSD at 3 min grinding time, 50% solids concentration, and a grinding media size of 3.5 mm

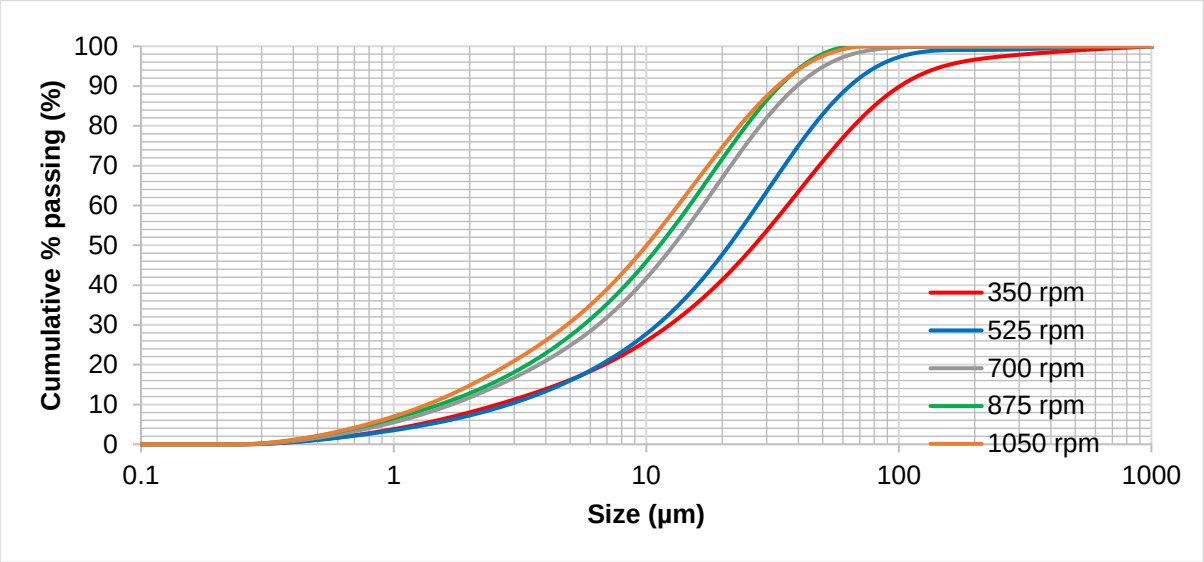

Figure 8-3 Effect of tip speed on the PSD using 5 mm grinding media at a solids concentration of 40%

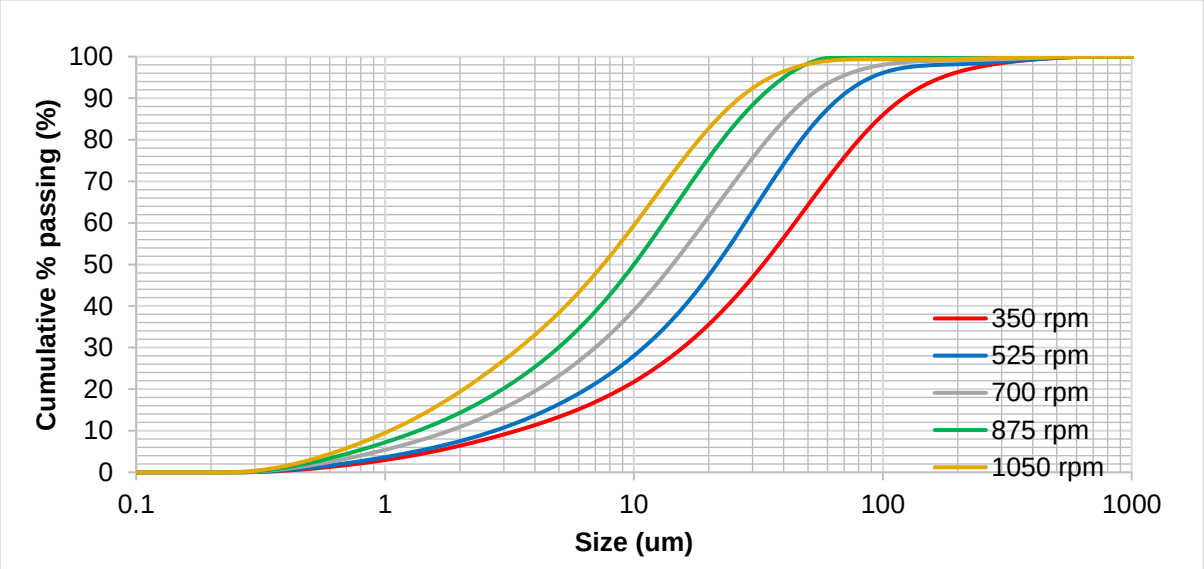

Figure 8-4: Effect of tip speed on the PSD using 5 mm grinding media at a solids concentration of 60%

Effect of solids concentration

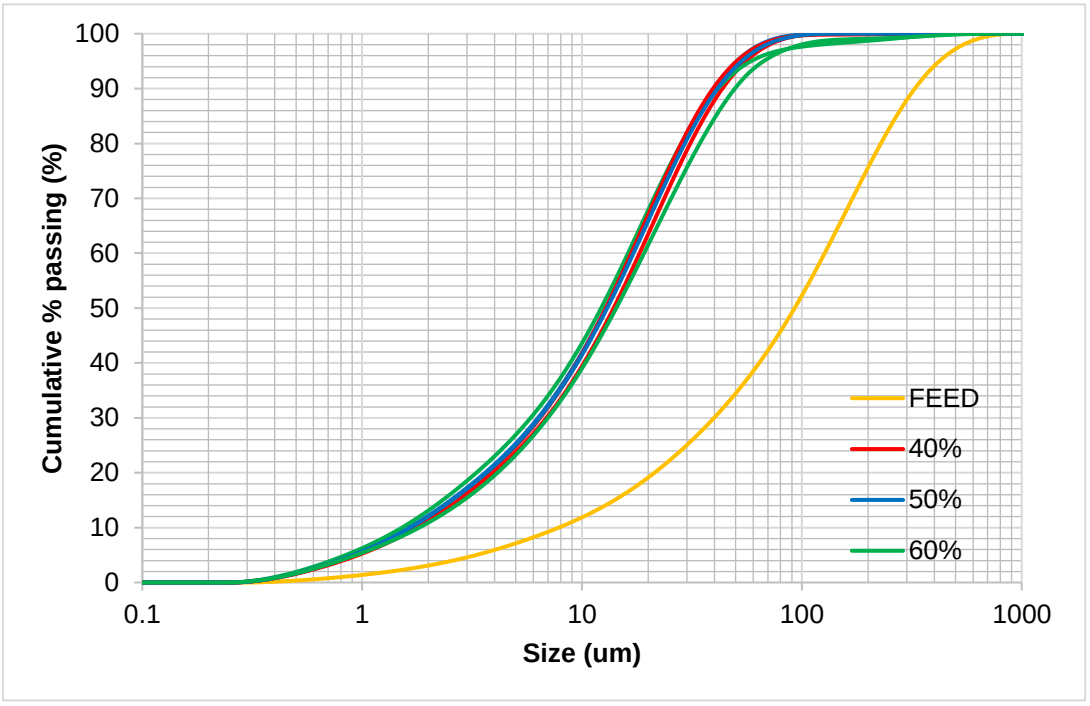

Figure 8-5: Repeat run of effect of solids concentration on PSDs for 5 mm grinding media at 700 rpm

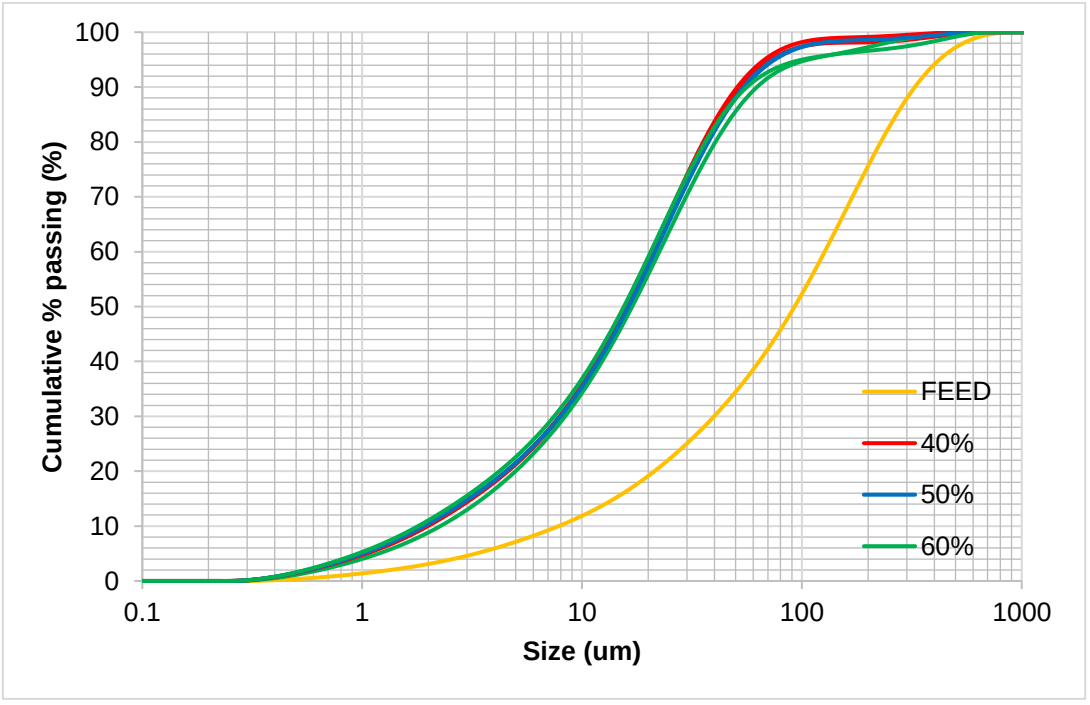

Figure 8-6: Repeat run of effect of solids concentration on PSDs for 3.5 mm grinding media at 700 rpm

Effect of grinding media volume filling

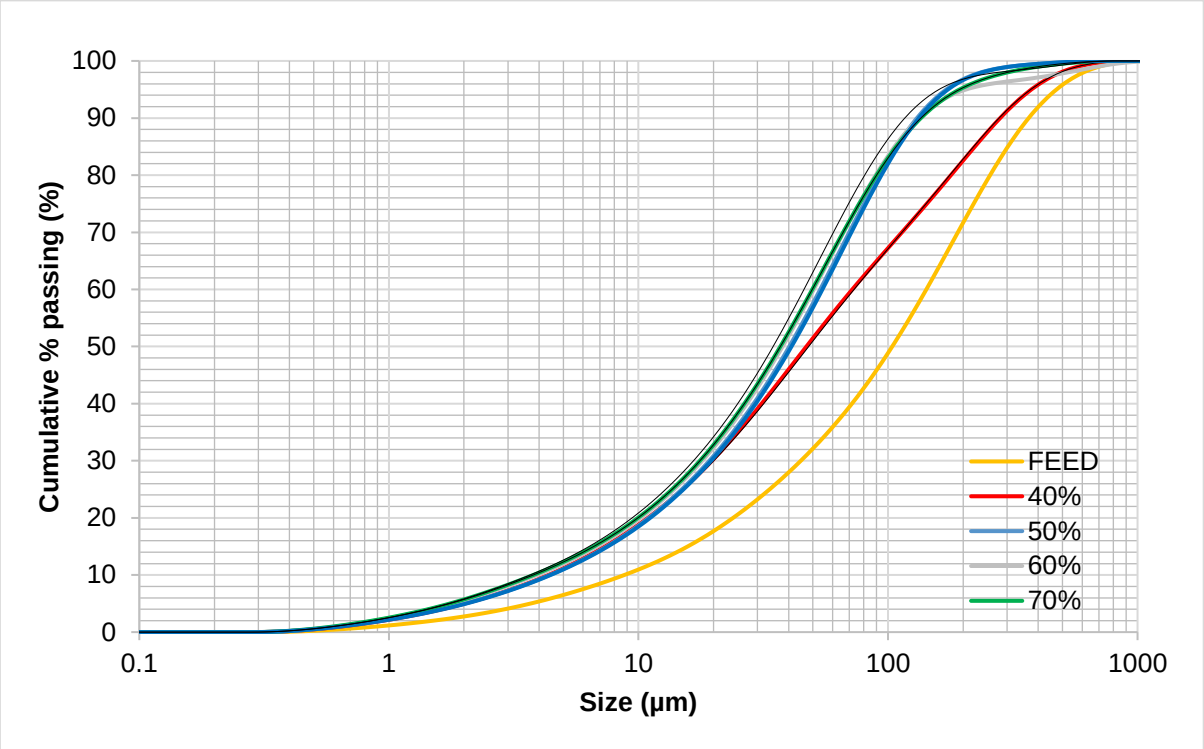

Figure 8-7: Effect of grinding media volume fill on the PSD for 5 mm grinding media at a tip speed of 350 rpm

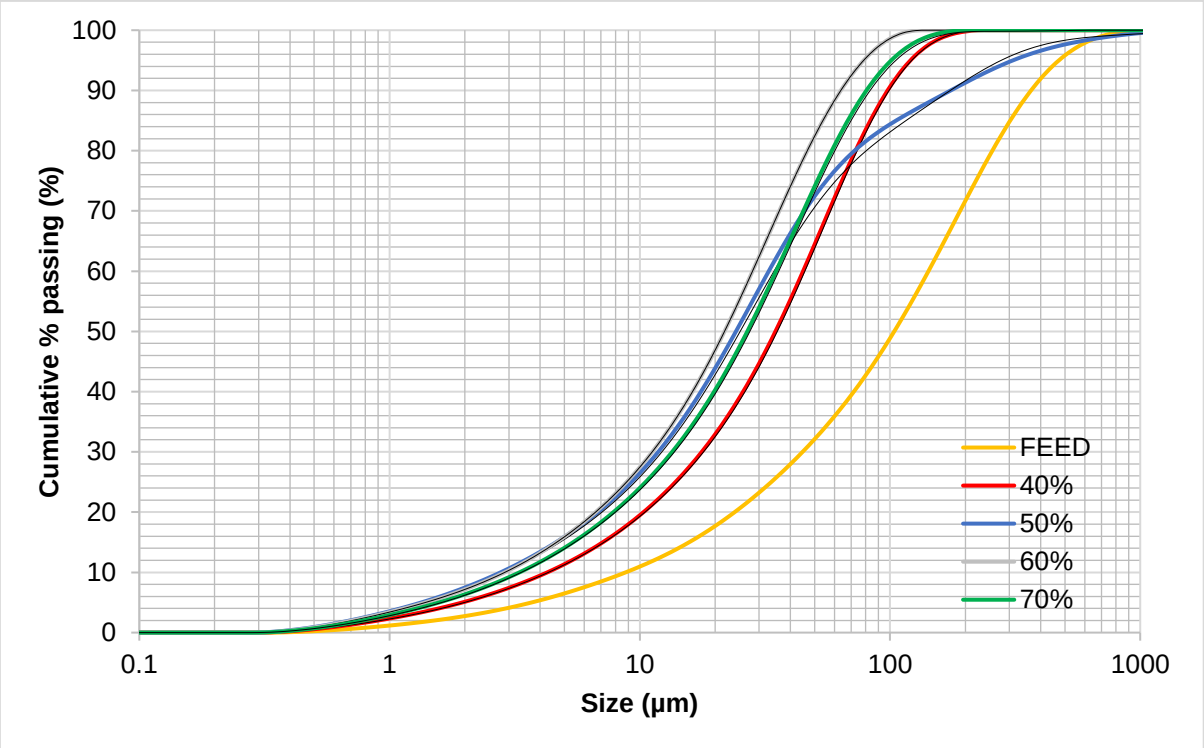

Figure 8-8: Effect of grinding media volume fill on the PSD for 5 mm grinding media at a tip speed of 525 rpm

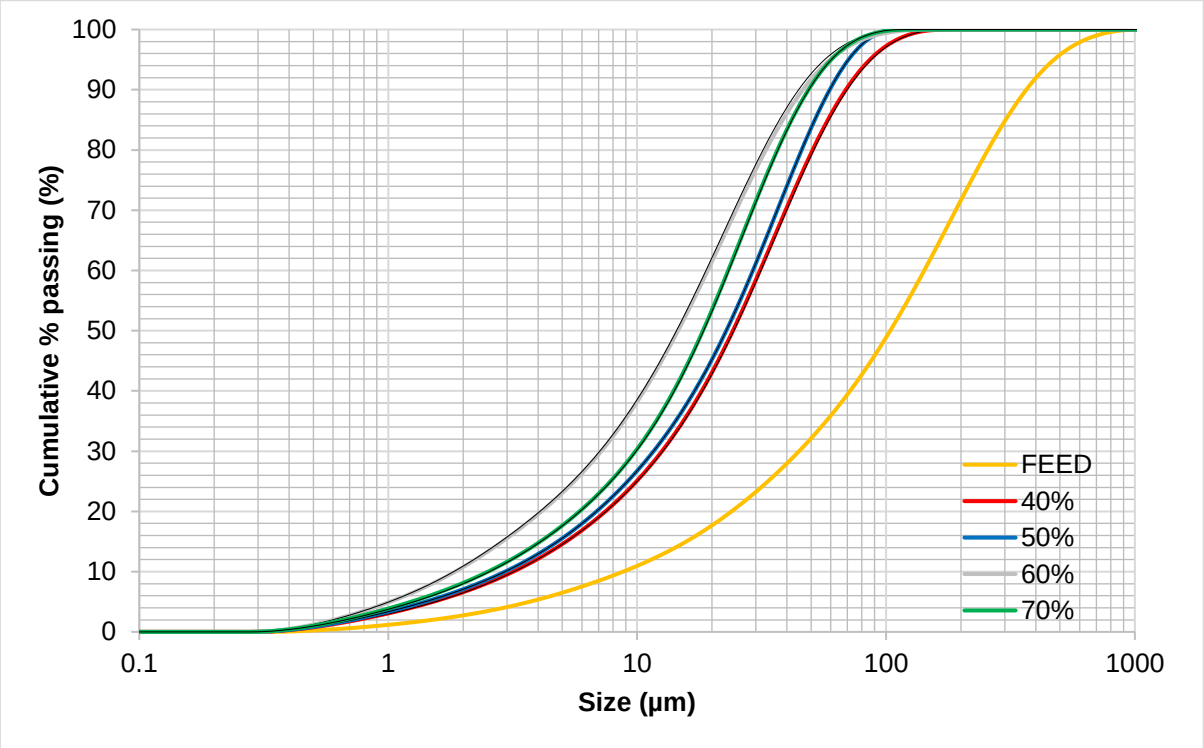

Figure 8-9: Effect of grinding media volume fill on the PSD for 5 mm grinding media at a tip speed of 700 rpm

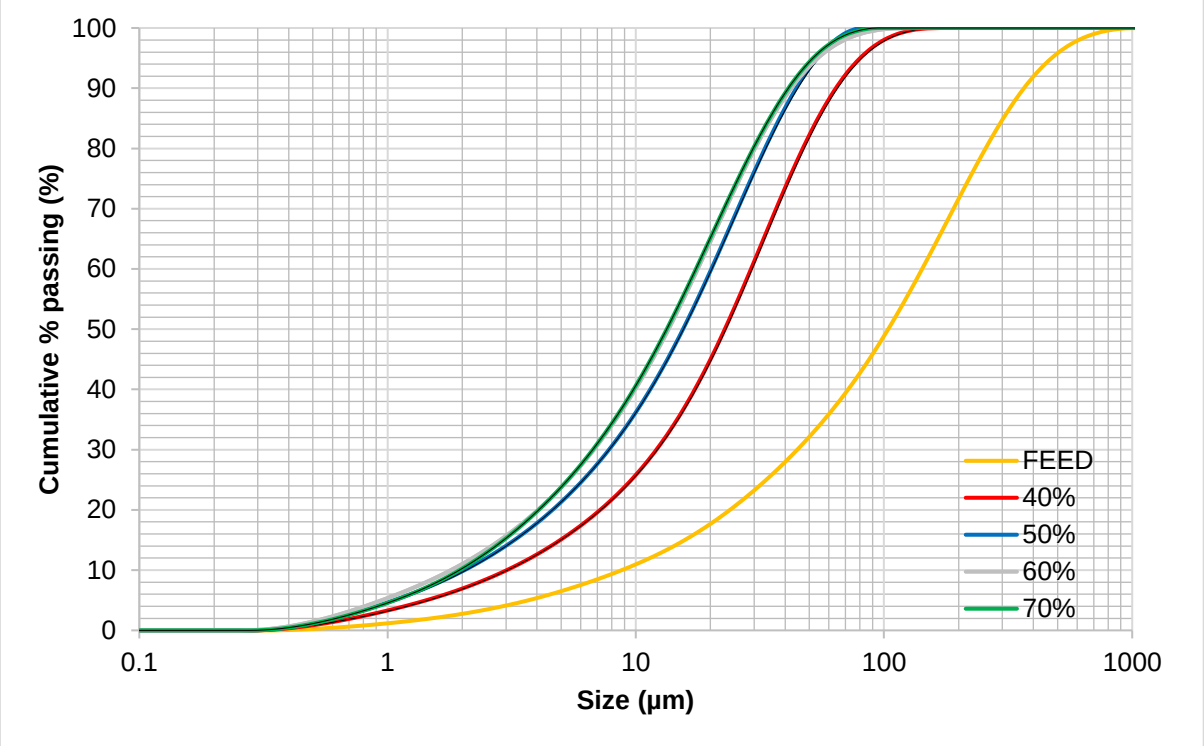

Figure 8-10: Effect of grinding media volume fill on the PSD for 5 mm grinding media at a tip speed of 875 rpm

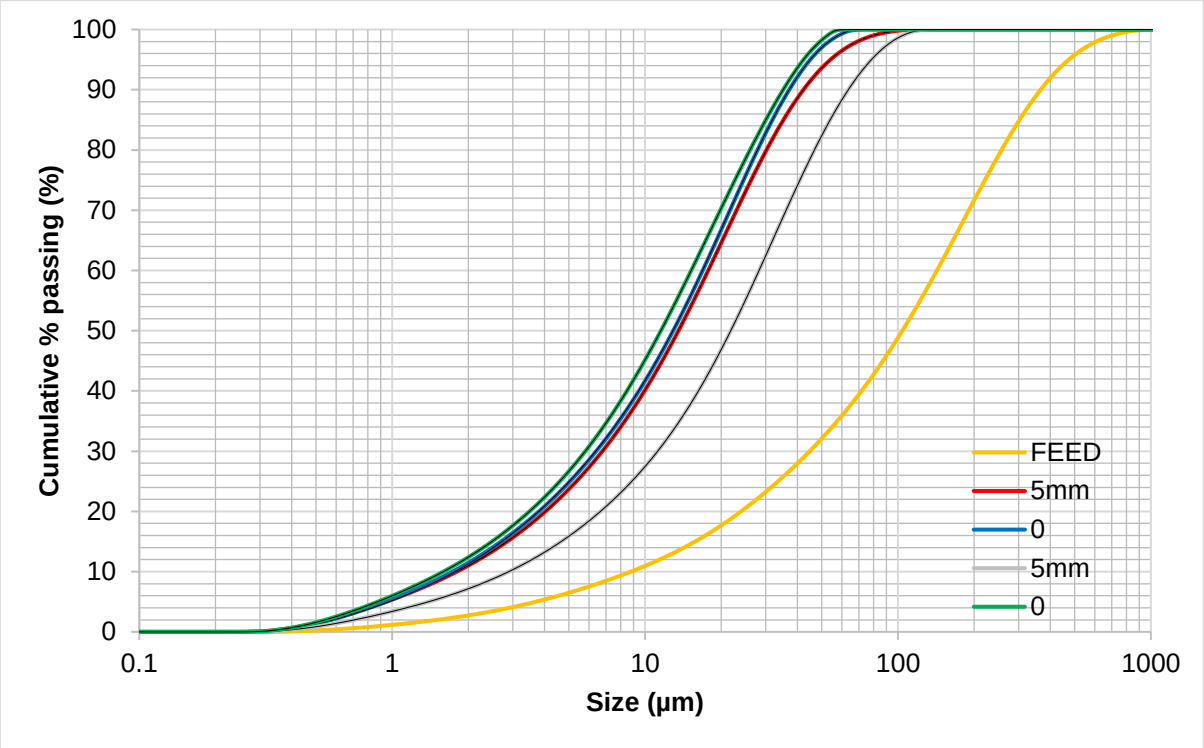

Figure 8-11: Effect of grinding media volume fill on the PSD for 5 mm grinding media at a tip speed of 1050 rpm

Effect of grinding media size

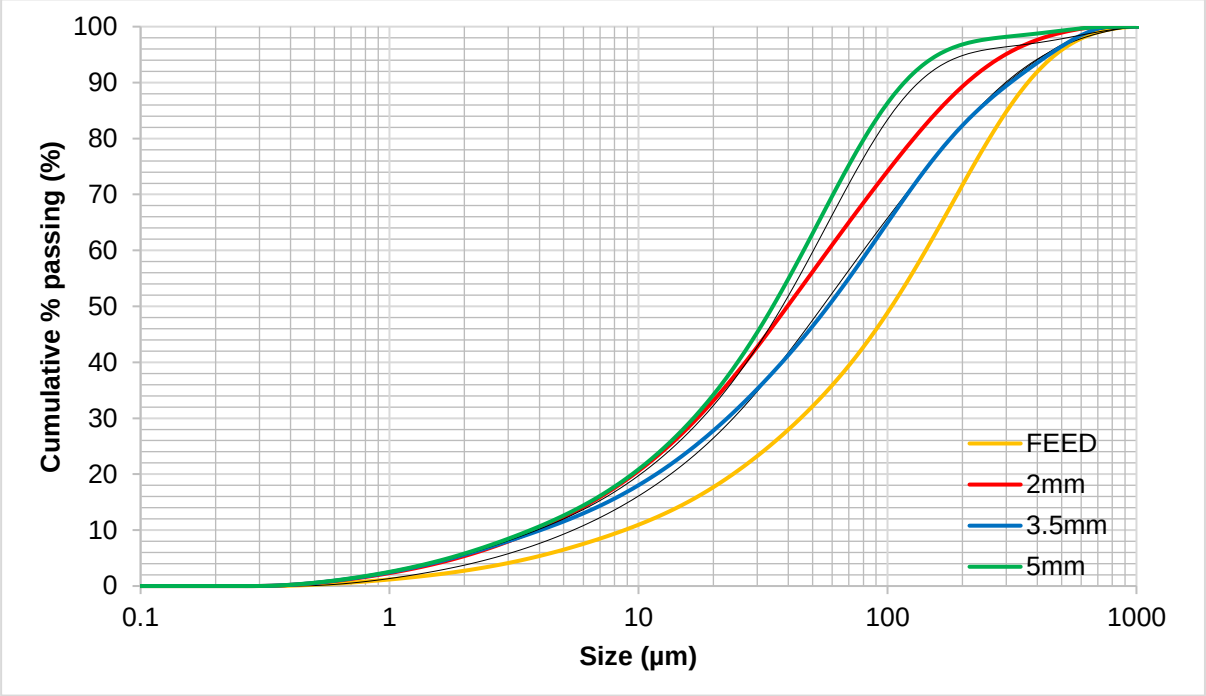

Figure 8-12: Effect of grinding media size on PSD for 2 mm, 3 mm and 5 mm grinding media at a solids concentration of 50% and a tip speed of 350 rpm

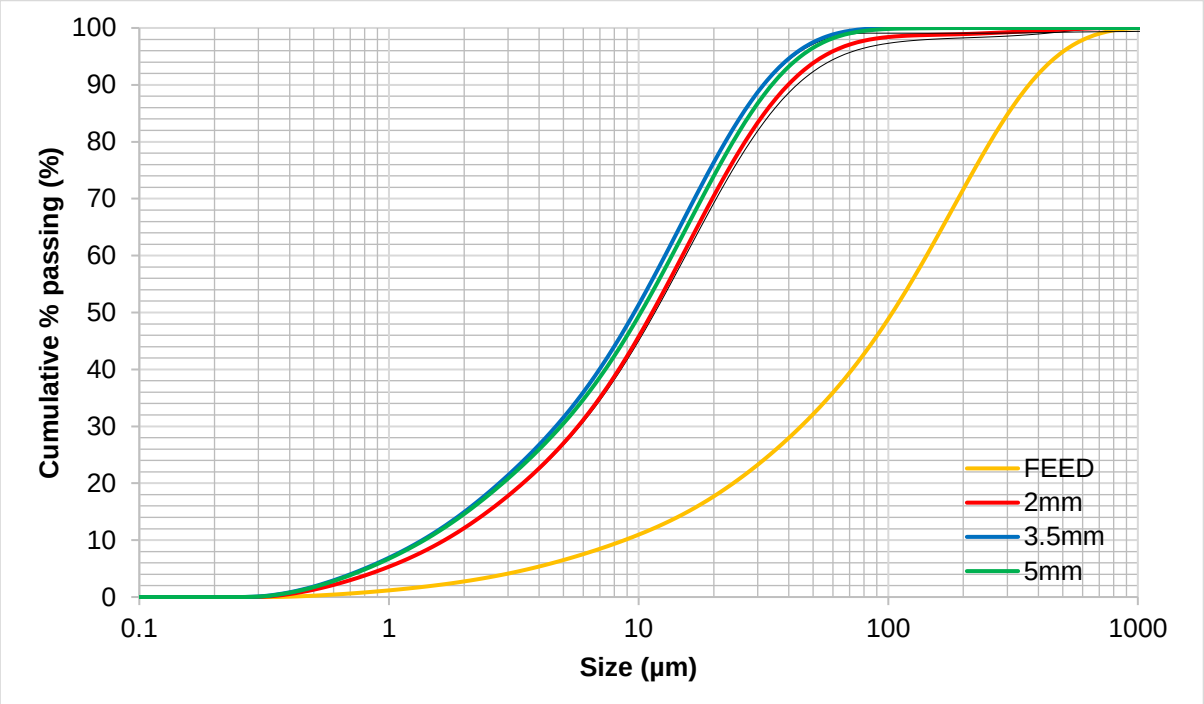

Figure 8-13: Effect of grinding media size on PSD for 2 mm, 3 mm and 5 mm grinding media at a solids concentration of 50% and a tip speed of 1050 rpm

B.2.2 Power plots

Effect of mill tip speed

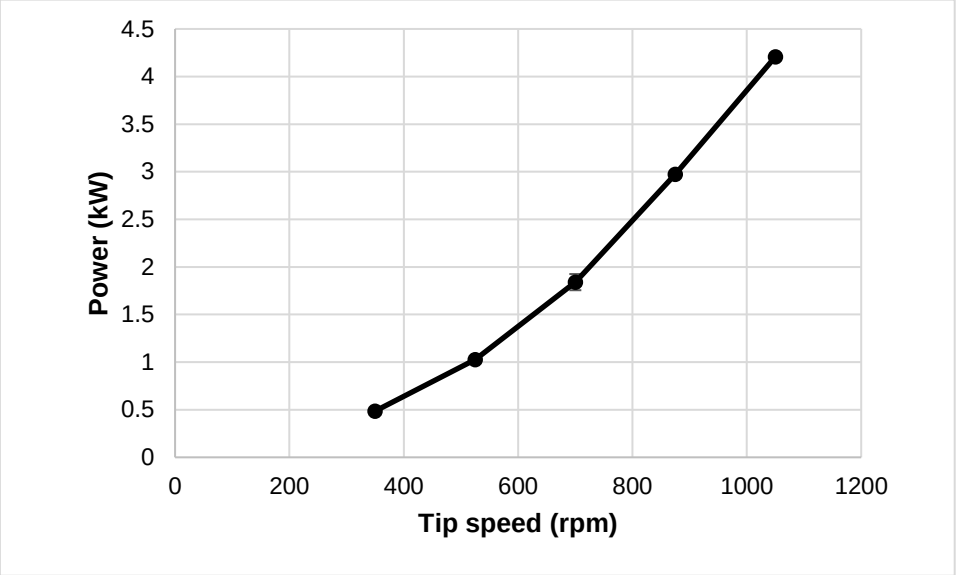

Figure 8-14: Effect of tip speed on power for 5 mm grinding media at a solids concentration of 40%

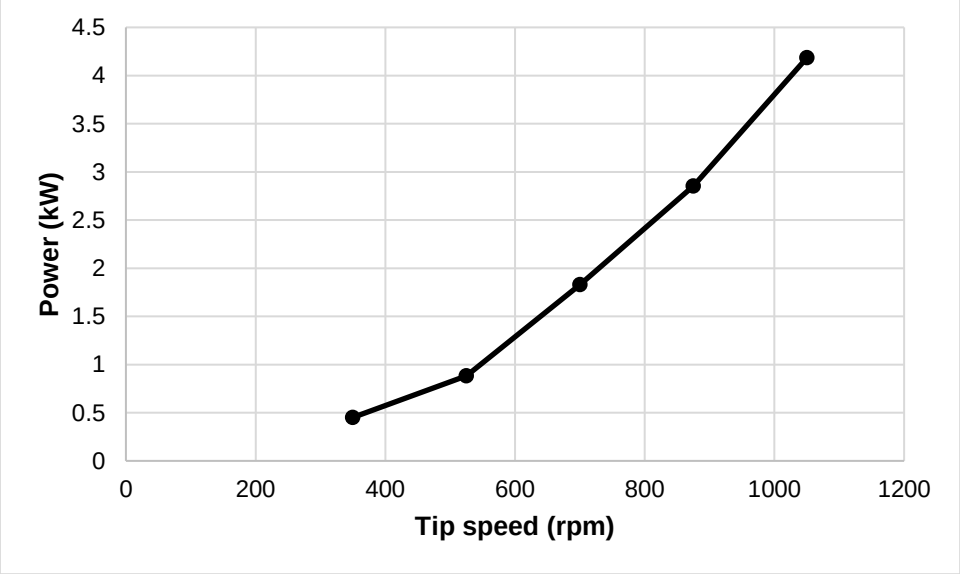

Figure 8-15: Effect of tip speed on power for 5 mm grinding media at a solids concentration of 60%

Effect of solids concentration

Table 8-8: The effect of solids concentration on power for 3.5 mm grinding media

2 mm		
Speed (rpm)	**Solids Concentration' (%)**	**Power (kW)**
350	40	0.30
	50	0.31
	60	0.29
525	40	0.52
	50	0.51
	60	0.52
700	40	0.87
	50	0.85
	60	0.87
875	40	1.38
	50	1.33
	60	1.36
1050	40	2.05
	50	1.94
	60	1.95

Table 8-9: The effect of solids concentration on power for 3.5 mm grinding media

3.5 mm		
Speed (rpm)	**Solids Concentration' (%)**	**Power (kW)**
350	40	0.35
	50	1.22
	60	2.86
700	40	0.34
	50	1.19
	60	2.93
1050	40	0.33
	50	1.18
	60	2.73

B.2.3 Signature plots

Effect of mill tip speed

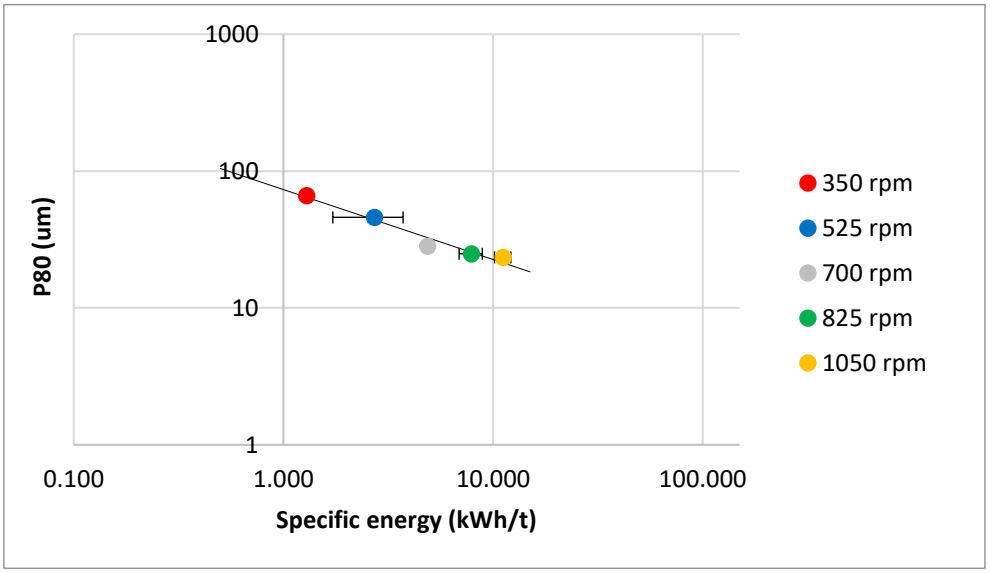

Figure 8-16: Signature plot showing the effect of tip speed on the specific energy using 5 mm grinding media at solids concentration of 40%

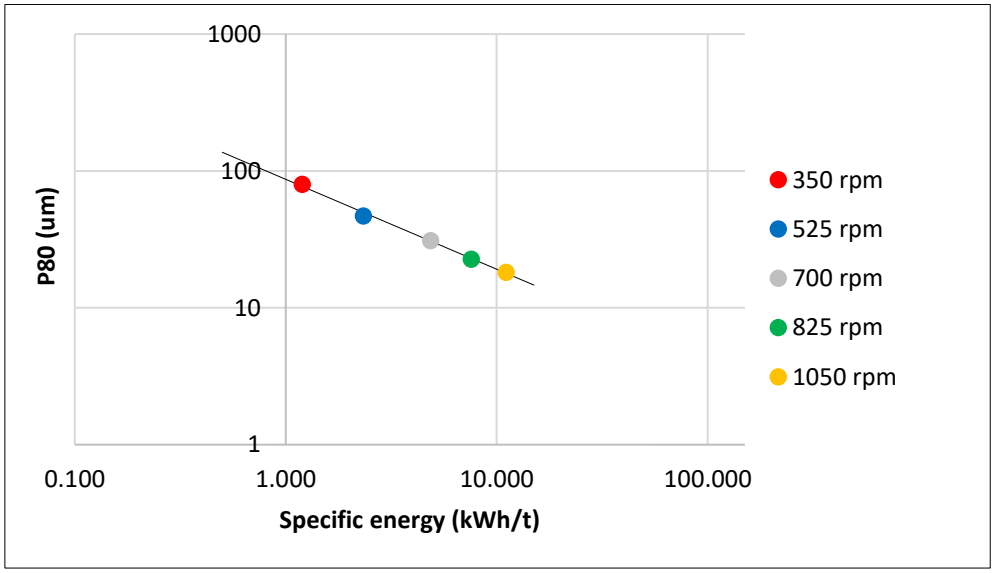

Figure 8-17: Signature plot showing the effect of tip speed on the specific energy using 5 mm grinding media at solids concentration of 60%

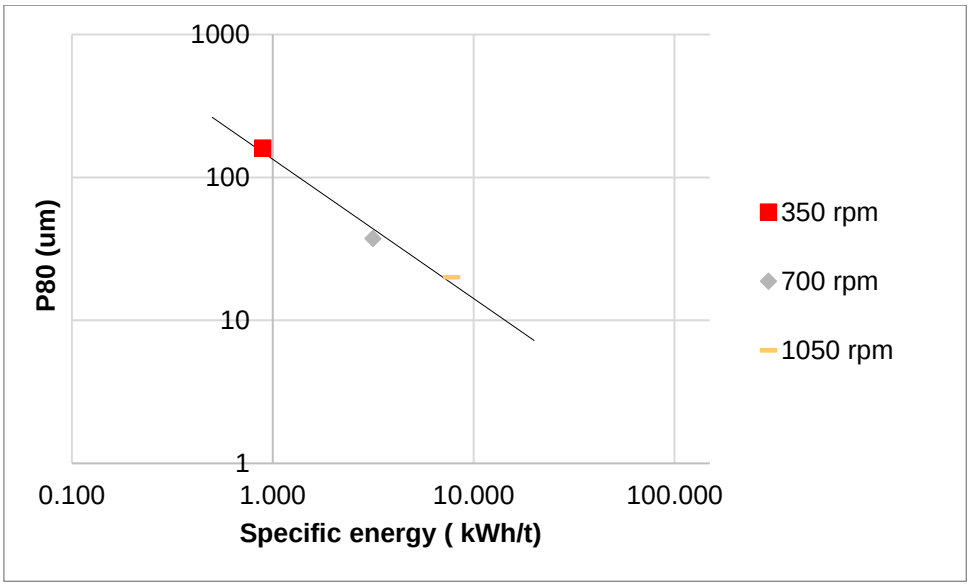

Figure 8-18: Signature plot showing the effect of tip speed on the specific energy using 3.5 mm grinding media at solids concentration of 50%

Effect of solids concentration

Table 8-10: Specific energy and P80 data for 40%, 50%, 60% solids concentration using 2 mm grinding media

2 mm Grinding Media		
Solids Concentration (%)	**Specific Energy (kWh/t)**	**Average P80 (um)**
40	0.80	171.7
	1.37	76.0
	2.30	53.0
	3.66	39.4
	5.45	19.7
50	0.83	113.5
	1.36	94.3
	2.26	64.0
	3.52	58.0
	5.14	25.0
60	0.77	152.3
	1.37	122.1
	2.30	80.8
	3.62	53.2
	5.18	22.0

Table 8-11: Specific energy and P80 data for 40%, 50%, 60% solids concentration using 2 mm grinding media

3.5 Grinding Media		
Solids Concentration (%)	**Specific Energy (kWh/t)**	**Average P80 (um)**
40	0.93	169.5
	3.24	35.6
	7.58	20.5
50	0.89	160.4
	3.14	37.3
	7.78	20.0
60	0.87	193.2
	3.12	40.4
	7.25	17.6

Table 8-12: Specific energy and P80 data for 40%, 50%, 60% solids concentration using 5 mm grinding media

5 mm Grinding Media		
Solids Concentration (%)	**Specific Energy (kWh/t)**	**Average P80 (um)**
40	1.29	66.3
	2.72	45.9
	4.88	28.3
	7.89	24.9
	11.16	23.4
50	1.14	79.5
	2.72	41.6
	4.74	29.3
	7.26	26.9
	11.23	21.4
60	1.20	80.2
	2.34	47.0
	4.85	30.9
	7.57	22.7
	11.10	18.2

Effect of grinding media size

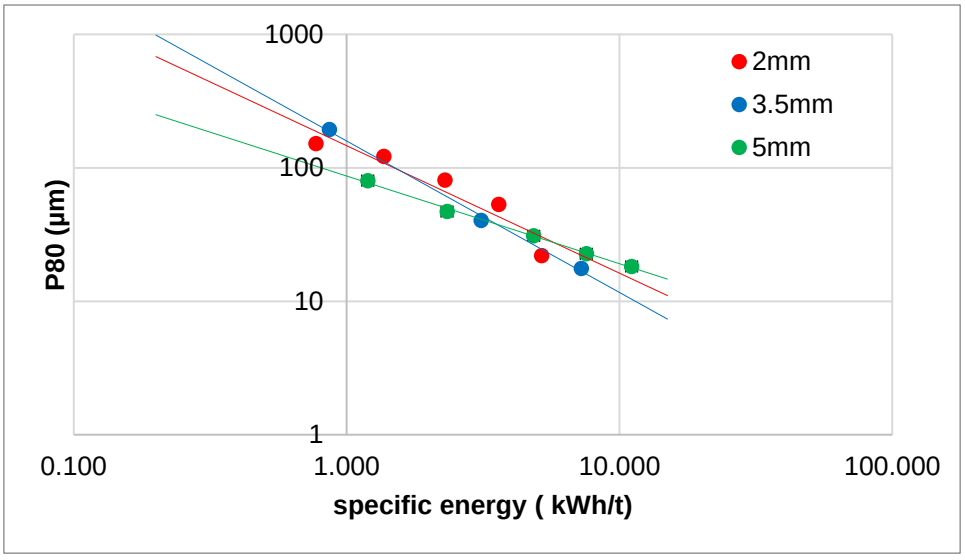

Figure 8-19: Signature plot for 2 mm, 3.5 mm and 5 mm grinding media for a solids concentration of 60%

B.2.4 Size Specific Energy

Effect of tip speed

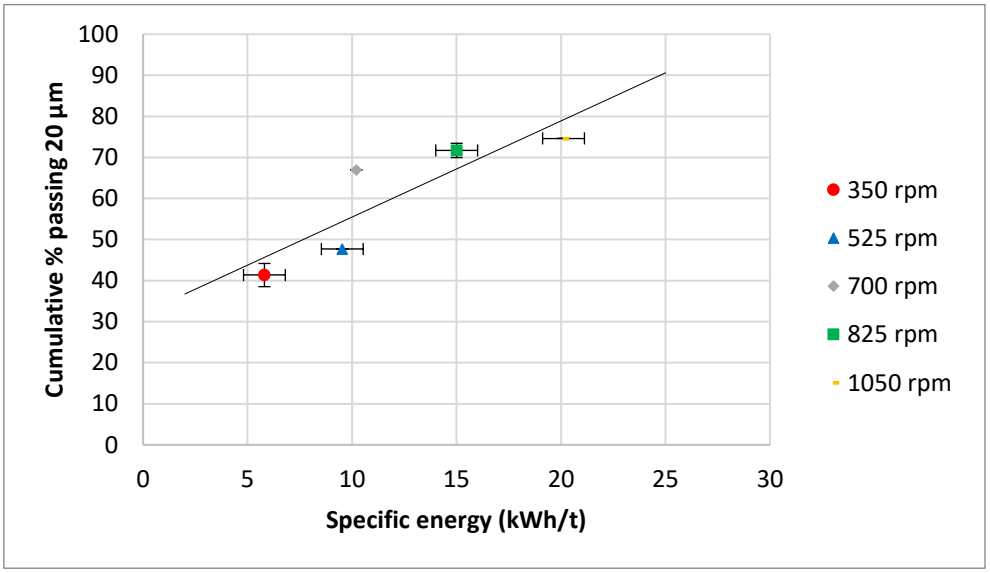

Figure 8-20: Size specific energy of different tip speeds at 5 mm grinding media and solids concentration of 40%

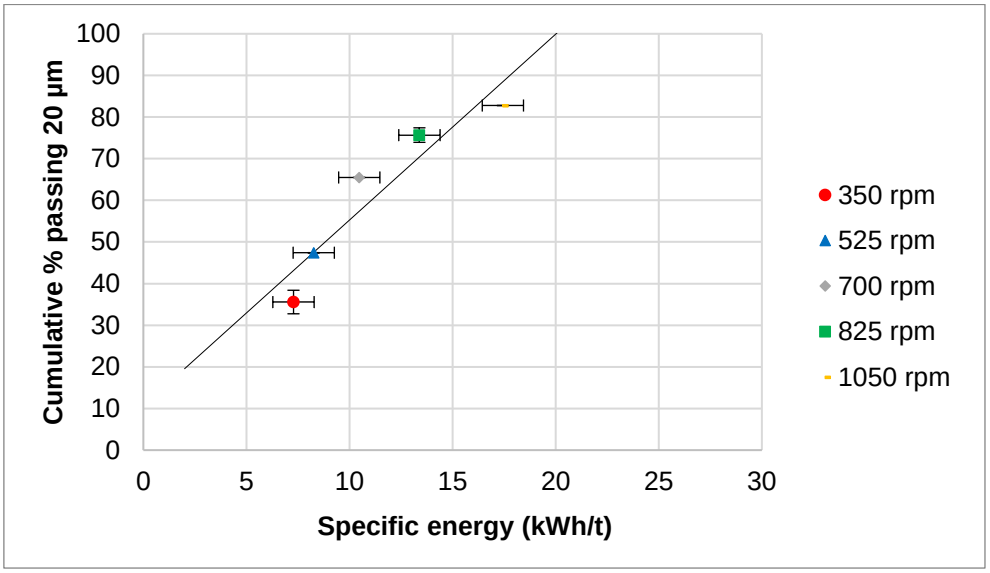

Figure 8-21: Size specific energy of different tip speeds at 5 mm grinding media and solids concentration of 60%

Effect of solids concentration

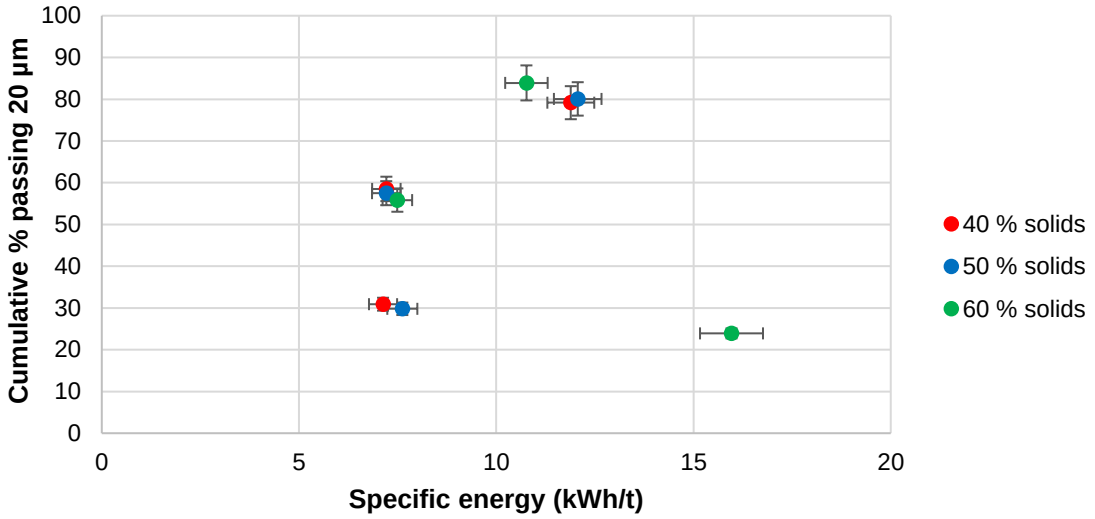

Figure 8-22: Size specific energy for 40%, 50% and 60% solids concentration using 3.5 mm grinding media

B.2.5 Stress Intensity

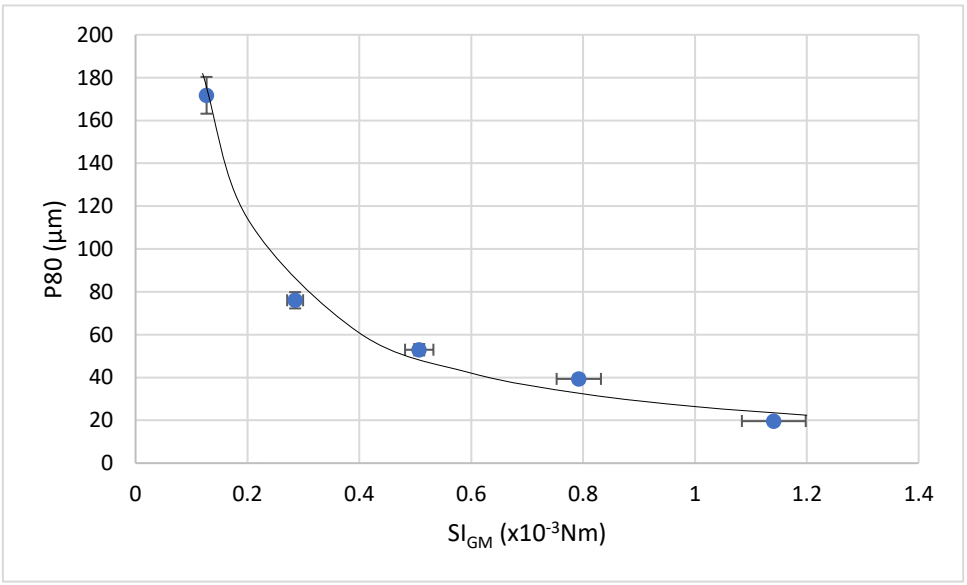

Figure 8-23: Stress intensity graph for 2 mm grinding media at a solids concentration of 40%

B.3 Assessment of Flotation Performance

B.3.1 Effect of tip speed on water and solids recovery

Table 8-13: Effect of tip speed on water and solids recovery

Media and Solids	Tip Speed (rpm)	Average Solids Recovery (%)	Average Water Recovery (%)
2 mm media 40% solids	350 rpm	4.88	25.26
2 mm media 50% solids	700 rpm	7.42	25.96
2 mm media 60% solids	1050 rpm	5.14	21.22
3.5 mm media 40% solids	350 rpm	6.51	19.67
3.5 mm media 50% solids	700 rpm	5.7	19.6
3.5 mm media 60% solids	1050 rpm	5.7	16.4
5 mm media 40% solids	350 rpm	8.0	21.8
5 mm media 50% solids	700 rpm	6.6	21.1
5 mm media 60% solids	1050 rpm	7.0	21.5

B.3.2 Effect of grinding media size on water and solids recovery

Table 8-14: Effect of grinding media size on water and solids recovery

	Grinding Media Size (mm)	Average Solids Recovery (%)	Average Water Recovery (%)
350 rpm 40% solids	2 mm	6.39	23.96
700 rpm 40% solids	3.5 mm	6.93	19.48
1050 rpm 40% solids	5 mm	7.37	20.92
350 rpm 50% solids	2 mm	5.26	24.98
700 rpm 50% solids	3.5 mm	6.6	20.3
1050 rpm 50% solids	5 mm	6.4	19.3
350 rpm 60% solids	2 mm	5.8	23.5

700 rpm 60% solids	3.5 mm	7.1	20.9
1050 rpm 60% solids	5 mm	6.0	17.6

B.3.3 Effect of solids concentration on water and solids recovery

Table 8-15: Effect of solids concentration on water and solids recovery

	Solids Concentration (%)	Average Solids Recovery (%)	Average Water Recovery (%)
2 mm media 350 rpm	40% solids	4.88	25.26
3.5 mm media 350 rpm	50% solids	5.14	21.22
5 mm media 350 rpm	60% solids	7.42	25.96
2 mm media 700 rpm	40% solids	6.34	22.42
3.5 mm media 700 rpm	50% solids	6.5	19.0
5 mm media 700 rpm	60% solids	7.7	19.2
2 mm media 1050 rpm	40% solids	7.1	23.2
3.5 mm media 1050 rpm	50% solids	6.2	15.4
5 mm media 1050 rpm	60% solids	6.4	19.2